

https://dspace.org/

Using Zooarchaeology by Mass Spectrometry and stable carbon and nitrogen isotopes to infer palaeoenvironment conditions at Grassridge Rockshelter during the Late Pleistocene and Early to mid-Holocene

Spruit, Bacara Ashleigh

2022
https://hdl.handle.net/10539/37056

Downloaded from a DSpace repository. https://dspace.org/

Using Zooarchaeology by Mass Spectrometry and stable carbon and nitrogen isotopes to infer palaeoenvironment conditions at Grassridge Rockshelter during the Late Pleistocene and Early to mid-Holocene



UNIVERSITY OF THE
WITWATERSRAND,
JOHANNESBURG

Bacara Ashleigh Spruit (820310)

A dissertation submitted to the Faculty of Science, University of the Witwatersrand, in fulfilment of the requirements for the degree of Master of Science

DIVISION OF ARCHAEOLOGY

SCHOOL OF GEOGRAPHY, ARCHAEOLOGY, AND ENVIRONMENTAL SCIENCES

Dr Jerome Reynard, Dr Benjamin Collins, and Dr Michael Buckley

27 July 2022

STATEMENT OF ORIGINALITY

I declare that this dissertation is my own, unaided work. It is being submitted for the Degree of Master of Science at the University of the Witwatersrand, Johannesburg. It has not been submitted before for any degree or examination at any other University.



_____

(Signature of candidate)

27 July 2022, Johannesburg

ABSTRACT

The adoption of Zooarchaeology by Mass Spectrometry (ZooMS) provides an alternative approach to traditional morphological and ancient DNA (aDNA) analysis, allowing previously unidentifiable and morphologically ambiguous remains to be identified. Dietary preferences are reflected in the stable carbon and nitrogen isotope ratios, with variations indicating behavioural, physiological, and/or environmental change. Together, fauna identified by ZooMS and stable carbon and nitrogen isotopes has the potential to provide more information about vegetation and palaeoenvironmental change than either dataset alone.

This study focuses on the morphologically unidentifiable faunal assemblage from Grassridge Rockshelter (GRS), South Africa. Ten samples were selected from the late Pleistocene (LP; ca. 43–28 ka), 20 from the terminal Pleistocene (TP; ca. 13.5–11.6 ka), and 70 from the mid-Holocene (MH; ca. 7.3–6.8 ka) layers. Here, fauna identified by ZooMS and stable carbon and nitrogen isotopes from bone collagen is used to infer the palaeoenvironmental conditions at GRS during each occupation.

Eighty-five percent (n = 85) of the GRS sample was successfully identified to at least tribe using ZooMS. Success increased through time, but not significantly, suggesting that ZooMS can be used on older assemblages, up to ca. 40 ka, and in warm environments. Faunal and stable isotope shifts are documented and are indicative of changing vegetation and palaeoenvironment through time. At GRS, results indicate a cool and dry grassland environment dominated by open-habitat grazers during the LP, transitioning to a warmer and mesic mosaic environment dominated by browsers during the MH. Broad taxonomic resolutions and the misidentification of a suni antelope (*Neotragus moschatus*) indicate a need for the development of novel ZooMS peptide markers, the expansion of the reference database, and emphasise the need to incorporate multiple proxies when undertaking palaeoenvironmental research. Furthermore, the identification of a blue duiker (*Philantomba monticola*) and ostrich (*Struthio camelus*) was unexpected, highlighting the potential of ZooMS to identify rare or unexpected taxa.

In loving memory of

Gordon Whitlow (Pop)

1932–2022

ACKNOWLEDGEMENTS

Throughout the writing of this dissertation, I have received a great deal of support and assistance.

To begin, I would like to thank my supervisors Drs Jerome Reynard, Benjamin Collins, and Michael Buckley. They have offered invaluable advice, continuous support, and guidance throughout this project. Specific thanks to Dr Reynard for giving me access to his lab, providing sound advice when I was overwhelmed, and pushing me to ask questions and stay on task; to Dr Collins for providing encouragement, motivation, and thought-provoking comments; to Dr Buckley for answering all of my ZooMS questions and for your help in getting the samples sorted in the United Kingdom.

In addition to my supervisors, many thanks go to Dr Christopher Ames for his continued support and help, Dr Emma Loftus for her invigorating comments, suggestions, and feedback, Dr Stephan Woodborne and Moshabi Silidi at iThemba Labs for making me feel welcome, accommodating me during my research, and answering all of the questions I had, and Finlay Thomas for not only processing and identifying my ZooMS samples but also answering my questions and helping me with the ZooMS materials and methods section as I was unable to travel due to Covid-19 restrictions.

This work is based on the research supported wholly by the National Research Foundation (NRF) of South Africa through the GENUS grant (132877). Opinions, findings, and conclusions or recommendations expressed are those of the author and are not necessarily to be attributed to the NRF. Additionally, I would like to thank Dr Benjamin Collins and Dr Christopher Ames for their financial contribution to this project.

I would also like to thank my mom for always supporting me. I am grateful for her sacrifices that have allowed me to follow my dreams. To my grandparents who were a little apprehensive when I first told them I was going to be studying Archaeology but have become one of my greatest supporters. To my partner Richard Whitlow, thank you for your continued support and encouraging words, you have pushed me to challenge myself and kept me motivated during these past two years.

TABLE OF CONTENTS

Statement of Originality i

Abstract ii

Acknowledgements iv

Table of Contents v

List of Figures viii

List of Tables xii

List of Appendices xiv

Abbreviations xvi

List of Naming and Style Conventions xviii

Chapter 1 : Introduction 1

1.1 Rationale 2

1.2 Aim 3

1.3 Objectives 3

1.4 Research Questions 3

1.5 Outline of Dissertation 3

Chapter 2 : Literature Review 5

2.1 Site Background 5

2.1.1 Previous Work at Grassridge 8

2.1.2 Archaeological Background 14

2.2 Faunal Theory and Methods 18

2.2.1 Zooarchaeological Methods 19

2.2.2 Morphological Methods 19

2.2.3 Biomolecular Methods 20

2.2.4 Zooarchaeology by Mass Spectrometry 22

2.3 Stable Isotopes 27

2.3.1 Isotopes, Isotope Notation, and Measurements 27

2.3.2 Stable Carbon Isotopes 28
2.3.3 Stable Nitrogen Isotopes 34
2.3.4 ZooMS and Stable Carbon and Nitrogen Isotopes 40
2.4 Palaeoenvironment 41
2.4.1 The Palaeoenvironment of southern Africa 42
2.4.2 Marine Isotope Stage 3 (57–29 ka) 45
2.4.3 Marine Isotope Stage 2 (29–14 ka) 46
2.4.4 Marine Isotope Stage 1 (14–5 ka) 51
Chapter 3 : Materials and Methods 58
3.1 Sample Collection 58
3.2 Sample Selection 58
3.3 ZooMS Analysis 59
3.3.1 Bone Preparation 59
3.3.2 Collagen Peptide Isolation 59
3.3.3 Maldi-MS Analysis 60
3.4 Isotopic Analysis 60
3.4.1 Bone Preparation 60
3.4.2 Pretreatment 60
3.4.3 Determination of Stable Carbon and Nitrogen Isotope Ratios 60
3.4.4 Quality Indicators 61
3.5 Statistical Analysis 61
Chapter 4 : Results 63
4.1 The Success of ZooMS at GRS 66
4.2 Faunal Remains 66
4.3 Stable Carbon and Nitrogen Isotopes 67
4.3.1 Water Dependency 73
4.3.2 Individual Taxa 74

Chapter 5 : Discussion 76
5.1 ZooMS 76
5.1.1 Unexpected Taxa 78
5.2 Variability in Faunal Abundance and Stable Isotope Ratios 82
5.2.1 Faunal Change 82
5.2.2 Stable Isotope Change 86
5.2.3 ZooMS and Stable Isotopes 93
5.3 The Palaeoenvironment 95
5.3.1 Late Pleistocene Occupation (43–28 ka) 97
5.3.2 Terminal Pleistocene Occupation (13.5–11.6 ka) 98
5.3.3 Mid-Holocene Occupation (7.3–6.8 ka) 101
5.4 Summary 103
Chapter 6 : Conclusion 105
6.1 Limitations 106
6.2 Future Avenues of Research 107
References 109
Appendix 1 174
Appendix 2 180
Appendix 3 183
Appendix 4 187
Appendix 5 189
Appendix 6 193
Appendix 7 195

LIST OF FIGURES

Figure 2.1: Grassridge Rockshelter (star) and other relevant archaeological sites within modern vegetation bioregions as described by Mucina & Rutherford (2006) (In Ames *et al.* 2020: 2). 5
Figure 2.2: Weather station data for the Stormberg/Drakensberg region, Eastern Cape collected from the South African Weather Bureau. An example diagram is given on the bottom right. a: mean rainfall curve, b: mean temperature curve, TEMP: mean annual temperature, and MAP is mean annual precipitation (In Hoare & Bredenkamp 2001: 597). 8
Figure 2.3: Plan view of GRS, indicating when and where the site was excavated (In Collins *et al.* 2020: 3). 9
Figure 2.4: Occupational layers identified by Opperman at GRS (In Opperman 1988: 3). .. 9
Figure 2.5: Photograph of Opperman's excavation with an overlay of the 1979 stratigraphic sequence and the GAPP lithostratigraphic zones (red segments = 100 mm) (In Collins *et al.* 2017: 165). 12
Figure 2.6: Flow chart showing the process of ZooMS (In Brandt *et al.* 2018: 4)..... 23
Figure 2.7: Leaf anatomy and photosynthetic biochemistry of C_3 plants (Adapted from Ehleringer & Cerling 2002: 2). 29
Figure 2.8: Leaf anatomy and photosynthetic biochemistry of C_4 plants (Adapted from Ehleringer & Cerling 2002: 2). 30
Figure 2.9: The relationship between growing season temperature and pCO_2 showing the modelled crossover favouring C_3 and the different C_4 plants (In Ehleringer *et al.* 1997: 292). 32
Figure 2.10: Approximate fractionation factors for modern terrestrial food chain (Adapted from Lee-Thorp *et al.* 1989). 33
Figure 2.11: Simplified diagram of the nitrogen cycle with average fractionation for each process included (In Sharp 2017: 243). 34
Figure 2.12: The relationship between precipitation and $\delta^{15}N_{collagen}$ faunal values from several studies. The data was compiled and extracted from southern Africa (Heaton *et al.* 1986a [blue diamond]; Sealy *et al.* 1987 [green triangle]), North America (Cormie & Schwarcz 1996 [red square]), and Australia (Pate & Anson 2008 [purple circle]) (In Luyt 2017: 43). 37
Figure 2.13: Plant-herbivore dynamics with reference to environmental parameters (In Faith 2011b: 1678). 39

Figure 2.14: Map of southern Africa with locations of caves and rock shelter sites with published dates and palaeoenvironmental data from Marine Isotope Stage 6 to 1. Sites and abbreviations are listed in Table 1 in Stratford *et al.* (2021: 882-889) (In Stratford *et al.* 2021: 881). 42
Figure 2.15: Modern oceanic and atmospheric circulation systems. Mean monthly precipitation is included from 1981-2010 across southern Africa during (a) austral summer and (b) austral winter. The three rainfall zones (i.e., SRZ, YRZ, and WRZ) are shown as well as the South Atlantic Anticyclone, South Indian Anticyclone, Benguela Current, and Agulhas Current (Tyson & Preston-Whyte 2000) (In Zhao *et al.* 2016b: 844). 43
Figure 2.16: An evaluation of modern southern African rainfall zones. Conceptual models have been proposed (see Engelbrecht *et al.* 2019) to elucidate the rainfall seasonality and distribution during glacial periods (In Chase & Meadows 2007: 109). 44
Figure 3.1: Scatter plot showing the elevation and easting position of the GRS plotted finds which are categorised by time period. 58
Figure 4.1: Cluster diagram showing the taxonomic resolution for each period and the overall sample. Number of samples for each category is given on the graph. 66
Figure 4.2: Cluster diagram showing the proportion (%) of bovid browsers and grazers for each occupational period at GRS with n-values included. 67
Figure 4.3: Violin plot with box plot included for the $\delta^{13}C$ values of TP and MH taxa. Taxa include browsers and grazers. A third violin plot with a box plot excluding MH grey rhebok is presented to investigate the effect of their large sample size (n =33) on the MH distribution. 68
Figure 4.4: Scatter plot containing the $\delta^{13}C$ and $\delta^{15}N$ values of TP (orange) and MH (blue) taxa. The dotted grey lines represent the mean $\delta^{13}C$ values for C_3 and C_4 consumers which were adjusted by 1.5‰ from modern means. 69
Figure 4.5: $\delta^{13}C$ vs $\delta^{15}N$ values for individual taxa from the TP. The dotted grey lines represent the mean $\delta^{13}C$ values for C_3 and C_4 consumers which were adjusted by 1.5‰ from modern means. 70
Figure 4.6: $\delta^{13}C$ vs $\delta^{15}N$ values for individual taxa from the MH. The dotted grey lines represent the mean $\delta^{13}C$ values for C_3 and C_4 consumers which were adjusted by 1.5‰ from modern means. 70
Figure 4.7: Box and jitter plots showing the $\delta^{13}C$ and $\delta^{15}N$ values of TP and MH browsers and grazers. 71

Figure 4.8: Violin plots with box plots for the $\delta^{13}C$ values of the remaining MH browsers, MH grey rhebok, and MH browsers. 72
Figure 4.9: Box and jitter plots showing the $\delta^{13}C$ and $\delta^{15}N$ values of TP and MH WD and WI taxa. 73
Figure 5.1: Clustered column showing an increase in successful ZooMS identifications (to at least tribe) and decrease in unsuccessful ZooMS identifications through time. The n-values are included. 76
Figure 5.2: The current distribution of ostrich in southern Africa (In Sinclair *et al.* 2020: 158). 78
Figure 5.3: Photograph of specimen 066 which has been identified as ostrich using ZooMS. 79
Figure 5.4: A painting with five ostriches showing curiosity behaviour when approached by a bushman disguised as an ostrich. Found in the Hershel District (In Thackeray 1983: 39). 80
Figure 5.5: Current distribution of blue duiker in Africa (In Skinner & Chimimba 2005: 670). 80
Figure 5.6: Phylogenetic tree showing southern African representatives from various tribes and sub-families of the Bovidae family (In Bradfield *et al.* 2021: 14). 81
Figure 5.7: Proportion (%) of bovid browsers (incl. springbok), grazers, and intermediate feeders for each occupational period at GRS with n-values included. (a) This study, (b) Opperman (1984, 1987, 1988), and (c) Beard (2018). A decline in grazers and increase in browsers from the LP to MH layers are documented in this study and Opperman's. While Beard's (2018) shows a slight increase in grazers and decline in browsers from the TP to MH. No significant difference ($\chi 2$ (1) = 0.60, p = 0.44) was found between Beard's TP and MH browsers and grazers. 84
Figure 5.8: (a) Beard (2018) bovid size classes in the TP and MH, bovid size class 3 and 4 were combined by Beard to increase the sample size of the category. (b) Opperman (1984, 1987, 1988) bovid size classes in the LP, TP, and MH, bovid size class 3 and 4 were combined to allow for comparison with Beard (2018). 85
Figure 5.9: Histograms of the carbon isotope ratios of modern plants and modern tooth enamel (In Ehleringer & Cerling 2002: 188). 87
Figure 5.10: The mean $\delta^{13}C$ values with one standard deviation for (1) browsers and (2) grazers across a range of biomes and time periods. Any $\delta^{13}C$ enamel values have been adjusted -9‰ so that they can be compared with $\delta^{13}C$ collagen values. Modern values have

been adjusted by 1.5‰ to account for the 'fossil fuel' effect and are represented by a circle. Mid-Holocene samples are represented by a square, early Holocene by a diamond, and TP by a triangle. These values come from (a) Luyt 2017, (b) This study, (c) Ambrose & DeNiro 1986a, and (d) Ecker *et al.* 2018 (Wonderwerk Cave, WWC). 89
Figure 5.11: Comparison of $\delta^{15}N$ values of modern (a) browsers and (b) grazers from different biomes (Luyt 2017: 258–265) and TP and MH GRS browsers and grazers (Adapted from Luyt 2017: 119). 90
Figure 5.12: $\delta^{15}N$ (‰) values for modern (a) WD and (b) WI taxa from various biomes (Luyt 2017: 258–265) and TP and MH GRS taxa (Adapted from Luyt 2017: 136–137). ..92
Figure 5.13: Current distribution of suni (In Skinner & Chimimba 2005: 712). 94
Figure 5.14: The taphonomic indicators, phytolith ratios, and proportion of recovered sponge spicules and diatoms in a stratigraphic presentation. Each Lithostratigraphic Zone is matched with the LP, TP, or MH occupation (Adapted from Ames *et al.* 2020: 11). 97
Figure 5.15: The mean $\delta^{15}N$ values with one standard deviation from fauna inhabiting mesic and arid regions. (a) This study, (b) Luyt 2017, (c) Kelly 2000, (d) Ambrose & DeNiro 1986a, and (e) Schoeninger 1989. 100

LIST OF TABLES

Table 2.1: Taxonomic resolution of faunal identifications using ZooMS from various sites and time periods in Africa. Most common taxonomic identification highlighted in green, this does not include failed samples which are shown in grey. 25

Table 4.1: Table of fauna identified using ZooMS and their stable carbon and nitrogen isotopes. Diet based on life history (Skinner & Chimimba 2005) unless the faunal resolution is low then stable carbon isotope ratios (italics) are used to infer diet. C_3 browser (B) between -29.5‰ and -17.5‰, C_4 grazer (G) between -10.5‰ and -2.5‰, intermediate (M) falls between -17.5‰ and -10.5‰ (Adapted from Lee-Thorp 2008). Water-dependent (WD) and water-independent (WI). *Springbok $\delta^{13}C$ values not significantly different from browsers. **Reduncini (browser) most likely grey rhebok, inferred from C_3 signature. Heated: ✓ = bone was heated, × = bone was not heated. Surface preservation: 1 = < ¼ of total cortical surface is well preserved, 2 = ¼ - ½, 3 = ½ - ¾, 4 = ≥ ¾ (Fernandez-Jalvo & Andrews 2016). Diet of suni and carbon signature differ, likely misidentification of suni. 63

Table 5.1: Success of ZooMS on faunal remains from several sites with varying ages. Results are ordered from most successful to least successful. Success is determined by the level of taxonomic resolution, with successful samples identified to at least tribe. 78

Table 5.2: List of identified peptide markers found in Bradfield *et al.* (2021) and Janzen *et al.* (2021). Collagen peptide markers of blue duiker and other small antelope that have previously been identified at GRS (Opperman 1984, 1987, 1988). Differences are highlighted in green. No peptide markers have been reported for grysbok. 82

Table 5.3: Ungulate faunal assemblage in the LP, TP, and MH from this study and Opperman's (1984, 1987, 1988). 82

Table 5.4: Mean $\delta^{13}C$ values for TP and MH browsers and grazers showing a trend to more negative values from the TP to MH. Significance between TP and MH is shown. 88

Table 5.5: Comparison of modern browser and grazer $\delta^{15}N$ medians across biomes (Luyt 2017: 258–265) and $\delta^{15}N$ medians from GRS TP and MH taxa with significance (Adapted from Luyt 2017: 171). 91

Table 5.6: Mean $\delta^{15}N$ values for TP and MH browsers and grazers showing a trend to more negative values from the TP to MH. Significance between TP and MH is shown for each. 92

Table 5.7: Collagen peptide markers for Unknown Antilopinae 1 and 2. Colours in sample indicate what occupation samples came from: yellow is LP, orange is TP, and green is MH. 94
Table 5.8: Habitat selection matrix for each taxon based on their selection for preferred (green) and marginal (yellow) habitats using current literature (Gagnon & Chew 2000; Skinner & Chimimba 2005; Faith & Beherensmeyer 2013; Sinclair *et al.* 2020; Venter *et al.* 2020). Three habit categories exist, including open (O; grassland), intermediate (I; bushland, ecotone, shrubland, woodland), and closed (C; continuous tree cover) and species were assigned following Plummer & Bishop (1994). Diet is separated into three guilds, namely browser (B), intermediate feeder (M), and grazer (G). 96
Table 5.9: Summary of palaeoenvironmental data from microbotanical, faunal, and stable isotope proxies (Data found in Opperman (1984, 1987, 1988), Ames *et al.* 2020, and this study). 104

LIST OF APPENDICES

Appendix 1.A: Taphonomic data from GRS faunal remains, abbreviations and scoring found below. Fauna from the MH are highlighted in green, TP are orange, and LP are yellow.....174
Appendix 2.A: $\delta^{13}C$ and $\delta^{15}N$ values with collagen quality indicators including %N, %C and C:N ratio elemental. 180
Appendix 3.A: Summary statistics for $\delta^{13}C$ and $\delta^{15}N$ values from browser, grazer, intermediate feeder, water-dependent, and water-independent taxa in the TP and MH....183
Appendix 3.B: Outcome of Shapiro-Wilk tests for normality, significant results in green. 183
Appendix 3.C: Outcome of chi-square test for success of ZooMS at GRS. Expected values smaller than five in orange.....184
Appendix 3.D: Outcome of chi-square test for success of ZooMS vs surface preservation and heating at GRS. Expected values smaller than five in orange. 184
Appendix 3.E: Outcome of chi-square test for browsers vs grazers through time. Expected values and adjusted residuals are included when necessary. Expected values smaller than five are highlighted in orange, significant values in green. 184
Appendix 3.F: Outcome of chi-square test for water-dependent vs water-independent through time. Expected values and adjusted residuals are included when necessary. Expected values smaller than five are highlighted in orange, significant values in green.185
Appendix 3.G: Outcome of Mann-Whitney U-Test, significant differences in green. 186
Appendix 4.A: Opperman's fauna were combined with the fauna from this study. Outcome of chi-square test for browsers vs grazers through time. Expected values and adjusted residuals are included when necessary. Expected values smaller than five in orange, significant values in green. 187
Appendix 4.B: Opperman's fauna were combined with the fauna from this study. Outcome of chi-square test for water-dependent vs water-independent through time. Expected values and adjusted residuals are included when necessary. Expected values smaller than five in orange, significant values in green. 188
Appendix 5.A: ZooMS results for GRS fauna. Collagen peptide markers included. Collagen markers from Bradfield et al. (2021) used to identify fauna. 189

Appendix 6.A: Outcome of chi-square test for browsers vs grazers through time. Expected values and adjusted residuals are included when necessary. Expected values smaller than five in orange, significant values in green. 193
Appendix 6.B: Outcome of chi-square test for water-dependent vs water-independent through time. Expected values and adjusted residuals are included when necessary. Expected values smaller than five in orange, significant values in green. 194
Appendix 7.A: Outcome of chi-square test for browsers vs grazers through time. Expected values and adjusted residuals are included when necessary. Expected values smaller than five in orange, significant values in green. 195
Appendix 7.B: Outcome of chi-square tests for bovid size classes through time. This was done for both Beard's and Opperman's faunal assemblages. Expected values and adjusted residuals are included when necessary. Expected values smaller than five in orange, significant values in green. 195

ABBREVIATIONS

Given the length of this dissertation, abbreviations will be repeated in each chapter

ABC: ammonium bicarbonate

ACR: Antarctic Cold Reversal

aDNA: ancient deoxyribonucleic acid

AIR: atmospheric nitrogen

CAM: Crassulacean acid metabolism

CO_2: carbon dioxide

COL1: Collagen type 1

GAPP: Grassridge Archaeological and Palaeoenvironmental Project

GRS: Grassridge Rockshelter

HCl: hydrochloric acid

ITCZ: Intertropical Convergence Zone

LGM: Last Glacial Maximum

LP: late Pleistocene

LSA: Later Stone Age

LZ: Lithostratigraphic Zone

MALDI-MS: Matrix-assisted laser desorption/ionisation-mass spectrometry

MALDI-ToF: Matrix-assisted laser desorption/ionisation time of flight

MAP: Mean Annual Precipitation

MAT: Mean Annual Temperature

MH: mid-Holocene

MIS: Marine Isotope Stage

MSA: Middle Stone Age

MW: Mann Whitney U-test

N_2: dinitrogen

NH_{4+}: ammonium

NO_{3-}: nitrate

O_2: oxygen

OES: ostrich eggshell

PEP: Phosphoenolpyruvate

Rubisco: Ribulose-1,5-bisphosphate carboxylase-oxygenase

SRZ: Summer rainfall zone

SST: sea surface temperature

TFA: trifluoroacetic acid

TP: terminal Pleistocene

V-PDB: Vienna Pee Dee Belemnite

WD: Water-dependent

WI: Water-independent

WRZ: Winter rainfall zone

YD: Younger Dryas

YRZ: Year-round rainfall zone

ZooMS: Zooarchaeology by Mass Spectrometry

LIST OF NAMING AND STYLE CONVENTIONS

± cal. kBP: measured, calibrated radiocarbon dates; thousand years before present

‰: parts per mille

^{14}C, ^{13}C, ^{12}C: 14-Carbon, 13-Carbon, 12-Carbon

^{15}N, ^{14}N: 15-Nitrogen, 14-Nitrogen

ca.: circa

ka: thousand years ago

kBP: un-calibrated dates age-dates presented in publication; thousand years before present

m/z: mass-to-charge ratios

masl: meters above sea level

pCO_2: atmospheric carbon dioxide

pH: potential Hydrogen

ppm: parts per million

rpm: revolutions per minute

CHAPTER 1: INTRODUCTION

Southern Africa has a rich palaeoenvironmental history, but it is impeded by large spatial and temporal gaps which lead to broad reconstructions that overlook regional differences (Meadows & Baxter 1999; Stone 2014). Palaeoenvironmental reconstructions provide invaluable insight into the archaeological record as the environment provides the context in which organisms live, interact, and adapt (Lyman 2017). A wide range of palaeoenvironmental proxies are available but not all of them are widely applicable due to chronological and preservation constraints (Chase & Meadows 2007; Stone 2014; Stratford *et al.* 2021). In South Africa, faunal assemblages are the most utilised palaeoenvironmental proxy, comprising 52% of the utilised proxies (Stratford *et al.* 2021). However, their use as a palaeoenvironmental proxy is dependent on secure taxonomic identifications (Wolverton 2013). Faunal remains are traditionally identified through osteomorphological analysis; however, this method is inherently subjective and unable to identify highly fragmented bones that lack diagnostic markers (Klein & Cruz-Uribe 1984; Driver 1992; O'Connor 2000; Reitz & Wing 2008; Wolverton 2013; Buckley *et al.* 2009; Buckley 2018). Archaeofaunal assemblages often contain a large number of unidentifiable bones. These are typically neglected, introducing bias and limiting archaeological and environmental information (Klein & Cruz-Uribe 1984; Plug 1997; Outram 2001; Badenhorst & Plug 2011; Buckley & Collins 2011; Buckley 2018).

Stable isotope analysis on fauna constitutes ~5% of published proxies in southern Africa (Stratford *et al.* 2021). Stable isotopes provide palaeoenvironmental information and insight into faunal dietary preferences (Lee-Thorp 2008). The combination of faunal and stable isotope data may enhance palaeoenvironmental reconstructions and be used to improve and validate taxonomic identifications, ultimately providing more information than either dataset alone.

This study will use faunal remains identified by Zooarchaeology by Mass Spectrometry (ZooMS) and stable carbon and nitrogen isotopes to infer the palaeoenvironmental conditions at Grassridge Rockshelter (GRS) during the late Pleistocene (LP; ca. 43–28 ka), terminal Pleistocene (TP; ca. 13.5–11.6 ka), and mid-Holocene (MH; ca. 7.3–6.8 ka) occupations. Notably, the occupations at GRS will be referred to as the LP, TP, and MH. This allows this study to reconcile with time categories used in previous GRS publications (see Opperman 1984, 1987, 1988; Collins *et al.* 2017). However, it does not disregard the

Marine Isotope Stages (MIS) and recognises that the LP is not confined to ca. 43–28 ka. Zooarchaeology by Mass Spectrometry enables unidentifiable faunal remains to be indirectly identified by comparing the collagen type I (COL1) protein sequence of an unknown sample with known samples in the collagen peptide marker reference database (Buckley *et al.* 2009; Bradfield *et al.* 2021; Janzen *et al.* 2021). Overall, this research contributes palaeoenvironmental information to this relatively understudied interior region of southern Africa. It is also the first to use both ZooMS and stable carbon and nitrogen isotopes on South African faunal remains predating 2000 years.

1.1 RATIONALE

Archaeological and palaeoenvironmental studies, excluding rock art, are relatively limited in the area surrounding GRS (Collins *et al.* 2017; Ames *et al.* 2020). Palaeoenvironmental reconstructions predominately come from the northern, southern, and western regions of southern Africa. Many of these records are limited by sparse, low-resolution data, providing general regional and temporal variations, and are incapable of detecting rapid climate change (Smith *et al.* 2002: 683). This study will complement the microbotanical (Ames *et al.* 2020) and faunal data (Opperman 1984, 1987, 1988) from Grassridge, thus increasing the local and regional palaeoenvironmental data. Furthermore, this study may elucidate the factors influencing faunal and floral change and provide invaluable insight into human-environment interactions in the eastern interior of southern Africa (Ames *et al.* 2020).

So far, two honours projects have examined the newly excavated GRS faunal assemblage (Beard 2018; Geoghegan 2019). Beard (2018) attempted to infer the TP and MH palaeoenvironmental conditions at GRS from morphologically identifiable bovid remains. This is potentially problematic as many of the GRS faunal remains are highly fragmented and unidentifiable, possibly introducing bias and limiting archaeological and environmental data. This project utilises ZooMS to examine a subset of the unidentifiable GRS faunal remains. Zooarchaeology by Mass Spectrometry was selected over ancient DNA (aDNA) to reduce issues of contamination, cost and time-constraints, degradation, destructiveness, and low-success rates (Smith *et al.* 2003; Kistler *et al.* 2017; Lebrasseur *et al.* 2018). To date, four South African studies (see Coutu *et al.* 2016, 2021; Bradfield *et al.* 2019, 2021) have utilised ZooMS with studies focusing on worked bone or ivory and domestic taxa, mostly dating to the last 2000 years.

Furthermore, this project utilises stable carbon and nitrogen isotopes to track the proportion of C_3 and C_4 vegetation and changes in mean annual temperature (MAT) and mean annual precipitation (MAP) (O'Leary 1981; Handley *et al.* 1999; Lee-Thorp 2008; Pate & Anson 2008; Szpak *et al.* 2013; Makarewicz & Sealy 2015; Loftus *et al.* 2016a). Stable isotope data complements the faunal and microbotanical data, providing further palaeoenvironmental information and insight into faunal dietary choices over time.

1.2 AIM

This study aims to infer the palaeoenvironmental conditions at GRS during the LP, TP, and MH. Palaeoenvironmental conditions will be inferred from faunal remains identified by ZooMS and stable carbon and nitrogen isotopes.

1.3 OBJECTIVES

1) Construct a bone selection protocol and select ten LP, 20 TP, and 70 MH faunal bone fragments from the GRS faunal assemblage
2) Identify the LP, TP, and MH faunal remains using ZooMS
3) Determine the stable carbon and nitrogen isotope ratios from the TP and MH faunal remains
4) Use the faunal remains identified by ZooMS and stable isotope data to infer the palaeoenvironmental conditions at GRS during the LP, TP, and MH

1.4 RESEARCH QUESTIONS

1) Can GRS taxa be successfully identified using ZooMS?
2) Does the faunal assemblage change between the LP, TP, and MH?
3) Do the stable carbon and nitrogen isotope ratios change between the TP and MH?
4) What were the palaeoenvironmental conditions at GRS during the LP, TP, and MH?

1.5 OUTLINE OF DISSERTATION

Each chapter begins with an introduction that describes the chapters' layout and structure. Where appropriate, each chapter will be organised following the four research questions outlined above. This thesis contains six chapters. The first is an introductory chapter that covers a general overview of this field, the rationale, and presents the aims, objectives, and research questions. The second chapter delves into the current literature and expands on the site background at GRS and the surrounding region, faunal theory and methods, and the southern African palaeoenvironment. The third chapter describes the materials and

methods used to obtain these data. The fourth chapter contains the results from this study and the fifth chapter discusses and interprets the results. Finally, the sixth chapter is a conclusion.

CHAPTER 2: LITERATURE REVIEW

The following chapter includes a review of the current literature which comprises the site background, faunal theory and methods, stable isotopes, and the palaeoenvironment.

2.1 SITE BACKGROUND

Grassridge Rockshelter (GRS) is located approximately 1500 masl at the base of the Stormberg Mountains in the Eastern Cape province of South Africa (Fig. 2.1) (Opperman 1984, 1987, 1988; Collins *et al.* 2017; Ames *et al.* 2020). Grassridge is located near the top of a small steep-sided valley and faces southeast. The shelter is large and curved, approximately 40 m wide, 10 m deep, and 7 m high at the dripline narrowing to less than 1 m high towards the back wall (Opperman 1984, 1987, 1988; Collins *et al.* 2017: 162; Ames *et al.* 2020: 3).

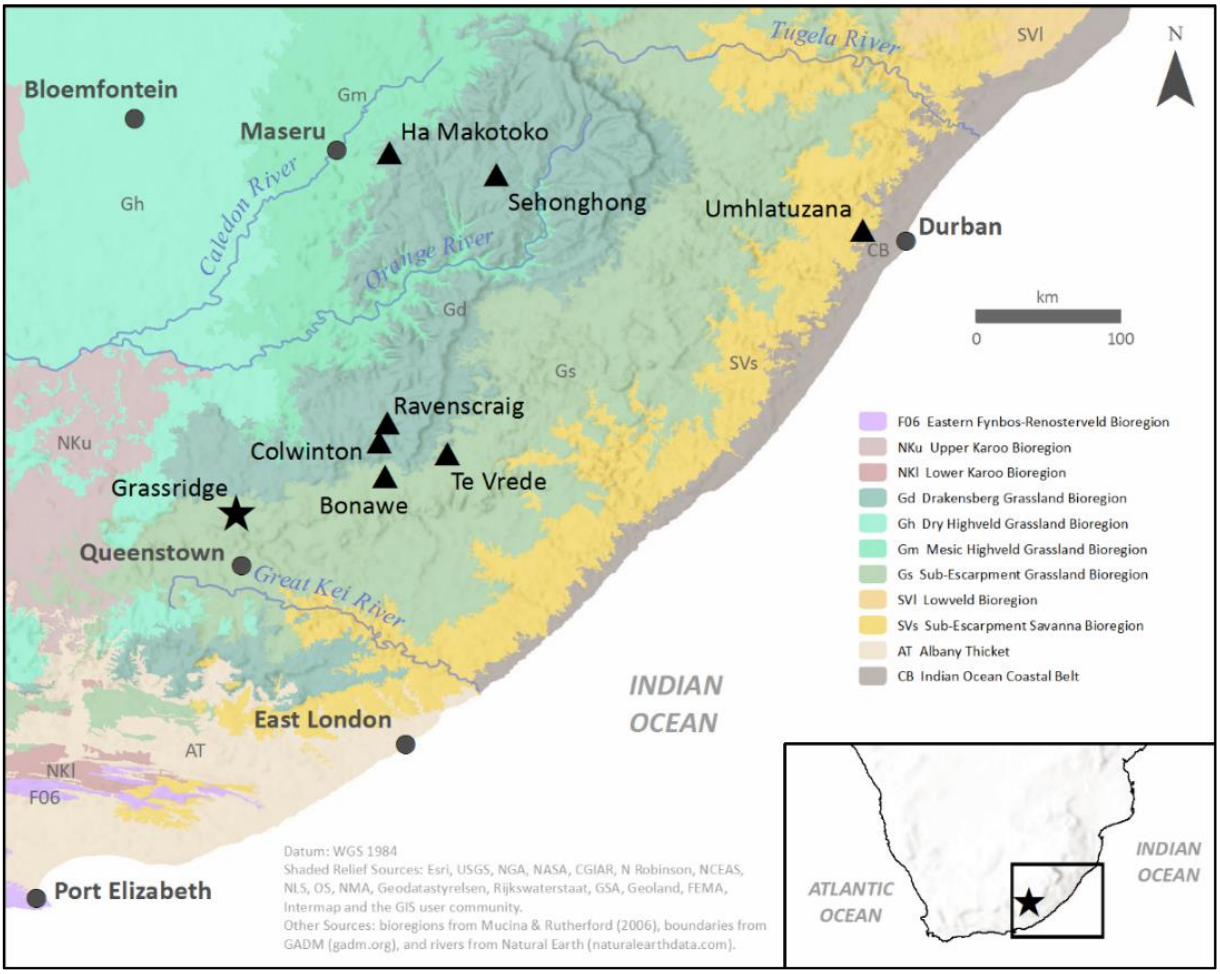


Figure 2.1: Grassridge Rockshelter (star) and other relevant archaeological sites within modern vegetation bioregions as described by Mucina & Rutherford (2006) (In Ames et al. 2020: 2).

Extensive erosion has exposed a rich-artefact palimpsest along the dripline. Rock art is present on a small overhang in front of and below the shelter opening and on the northeastern back wall (Collins *et al.* 2017: 162). A stone-lined drainage channel is present in the middle of the shelter and the remains of a stone wall are found near the northeast entrance (Collins *et al.* 2017: 162).

The curved appearance of the shelter likely resulted from water scouring which removed the weaker strata from the Clarens Formation, a Triassic sandstone (Kitching & Raath 1984; Castro & Bell 1995; Grab 2015; Ames *et al.* 2020). The Clarens Formation and the underlying Molteno and Elliot Formations form the Stormberg Group which comprises alternating bands of shale, mudstone, fine-grained sandstone, and intrusive dolerite sills and dykes (Smith 1990; Hoare & Bredenkamp 2001; Bordy & Catuneanu 2002; Bordy & Eriksson 2015). This intrusion is archaeologically significant as it led to the creation of large quantities of hornfels through contact metamorphism (Hoare & Bredenkamp 2001; Aarnes *et al.* 2011). Hornfels is the primary raw material source for stone tool manufacture at GRS (Opperman 1984, 1987; Collins *et al.* 2017; Ames *et al.* 2020).

The Stormberg region (Fig. 2.1) is divided into the Drakensberg Grassland bioregion in the north and the Sub-Escarpment Grassland bioregion in the south (Mucina & Rutherford 2006; Ames *et al.* 2020). The Drakensberg Grassland bioregion is dominated by the Stormberg Plateau Grassland and is interspersed with Southern Drakensberg Highland Grassland which becomes more prevalent to the east with increasing rainfall and elevation (Mucina & Rutherford 2006; Ames *et al.* 2020). Vegetation from the Stormberg Plateau Grassland includes grasses with a strong dwarf shrub component occurring on flat to undulating plains above 1500 masl, and shrubland vegetation sometimes occurring on rocky outcrops (Mucina & Rutherford 2006: 365). In contrast, vegetation from the Southern Drakensberg Highland Grassland is characterised by dense tussock grasslands occurring on steep mountain slopes at high altitudes with some dwarf shrublands on exposed rocky areas (Mucina & Rutherford 2006: 366). C_4 grasses are dominant in this region, but many C_3 grasses are sustained at higher elevations, including *Pentaschistis microphylla, Helictotrichon turgidulum, Merxmuellera disticha, M. drakensbergensis,* and *Koeleria capensis* (Ames *et al.* 2020: 4).

The Sub-Escarpment Grassland bioregion consists of the Tsomo Grassland and the Tarkastad Montane Shrubland (Mucina & Rutherford 2006: 43–45; Ames *et al.* 2020). The Tsomo Grassland occurs in flat or gently undulating plains between 760–1580 masl (Mucina & Rutherford 2006: 427; Ames *et al.* 2020). The vegetation is characterised by grassland to

open thornveld with *Aristida, Elionurus, Cymbopogon, Eragrostis*, and *Themeda* dominating the grass genera (Mucina & Rutherford 2006: 427; Ames *et al.* 2020). Non-grass vegetation includes several shrubs (e.g., *Senecio burchellii, Felicia muricata, Euryops floribundus*) and herbs of the Asteraceae family (e.g., *Berkheya onoparioides, Aster bakerianus*) (Ames *et al.* 2020: 4). The Tarkastad Montane Shrubland occurs on ridges, hills, and mountain slopes, especially those intruded by dolerite, between 1020–1780 masl (Mucina & Rutherford 2006: 428; Ames *et al.* 2020: 4). Low, semi-open mixed shrubland characterises the vegetation (Mucina & Rutherford 2006: 428). Small trees and dwarf shrubs are prevalent (e.g., *Acacia karroo, Cadaba aphylla, Diospyros austro-africana, Rhus burchellii, Tarchonanthus minor*), as well as several succulents (e.g., *Aloe ferox*) and C_4 grasses (Mucina & Rutherford 2006; Ames *et al.* 2020: 4). Grassridge Rockshelter is located within the Tarkastad Montane Shrubland and is near the Tsomo Grassland which prevails on undulating plains and valley bottoms (Ames *et al.* 2020: 4). Furthermore, Grassridge is located at the biogeoclimatic intersection (Fig. 2.1) of the Nama-Karoo biome, several coastal biomes to the south and southeast, and the Drakensberg Grassland bioregion in the northeast. Its location makes local vegetation susceptible to palaeoenvironmental change (Hoare & Bredenkamp 2001; Mucina & Rutherford 2006; Ames *et al.* 2020: 3–4).

Precipitation predominately falls in the austral summer (October to May) with Mean Annual Precipitation (MAP) ranging between 400–600 mm, increasing along a west to east rainfall gradient (Fig. 2.2) (Hoare & Bredenkamp 2001: 596; Mucina & Rutherford 2006; Ames *et al.* 2020: 3). Mean Annual Temperature (MAT) is approximately 13 °C with summer temperatures often exceeding 30 °C and winters regularly experiencing temperatures below freezing with frequent frosts (Fig. 2.2) (Sampson 1970; Opperman 1987; Hoare & Bredenkamp 2001; Mucina & Rutherford 2006). Elevation ranges from 1200 masl in the southeast to 1800 masl in the northwest and is negatively correlated with temperature and positively correlated with precipitation (Hoare & Bredenkamp 2001; Ames *et al.* 2020).

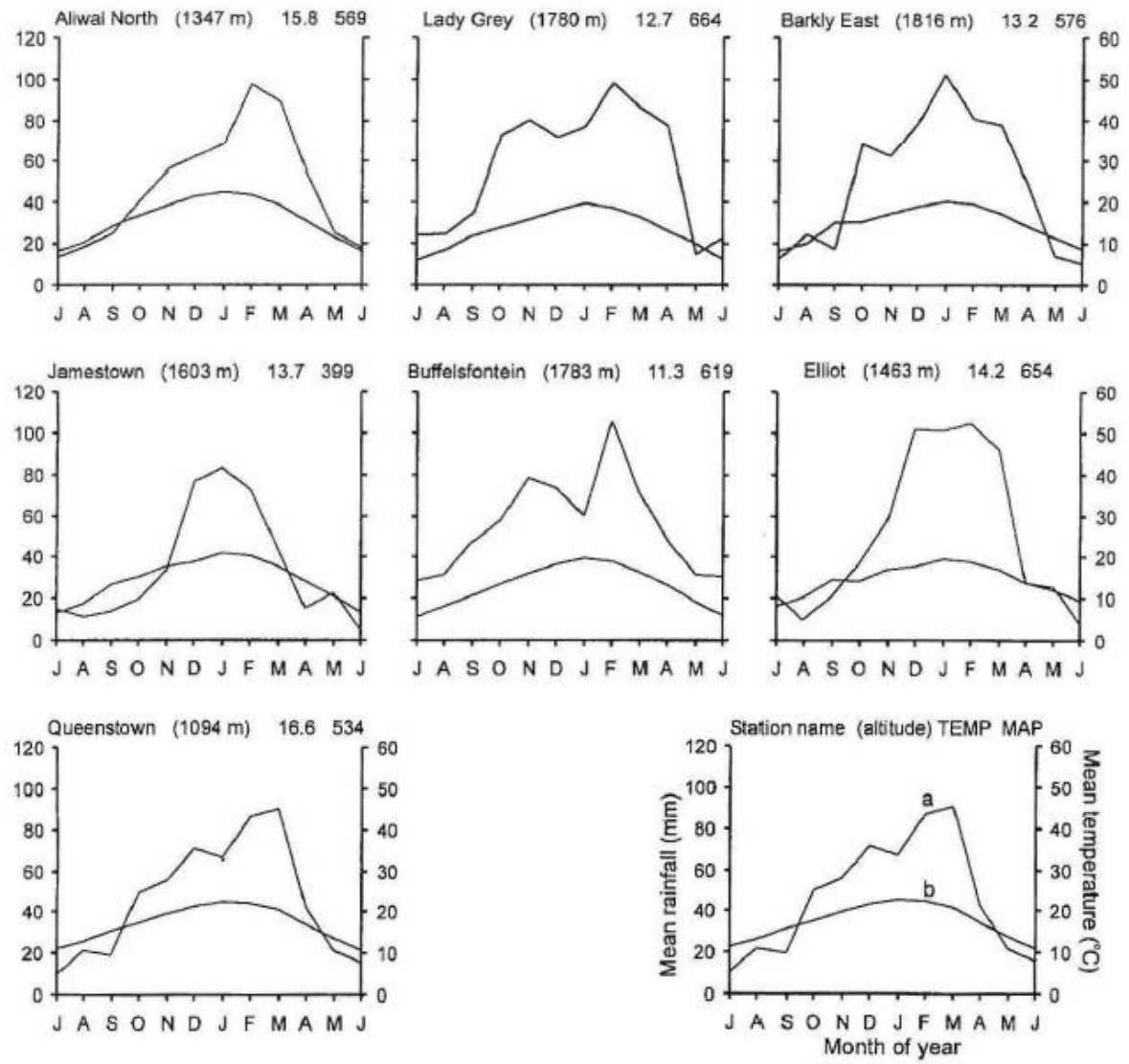


Figure 2.2: Weather station data for the Stormberg/Drakensberg region, Eastern Cape collected from the South African Weather Bureau. An example diagram is given on the bottom right. a: mean rainfall curve, b: mean temperature curve, TEMP: mean annual temperature, and MAP is mean annual precipitation (In Hoare & Bredenkamp 2001: 597).

2.1.1 PREVIOUS WORK AT GRASSRIDGE

Grassridge was first excavated by Dr Hermanus Opperman in 1979 as part of a larger project, designed to investigate Later Stone Age (LSA) occupations in the southern foothills of the Drakensberg Mountains (Opperman 1984, 1987, 1988; Collins *et al.* 2017; Ames *et al.* 2020). Colwinton, Bonawe, Te Vrede, and Ravenscraig Rockshelter were the primary focus of this project and GRS was included as a comparative control sample located in a different environment (Opperman 1984, 1987; Collins *et al.* 2017; Ames *et al.* 2020). Opperman's original excavation comprised a 2×3 m trench located in the southwest portion of the shelter close to the back wall (Fig. 2.3).

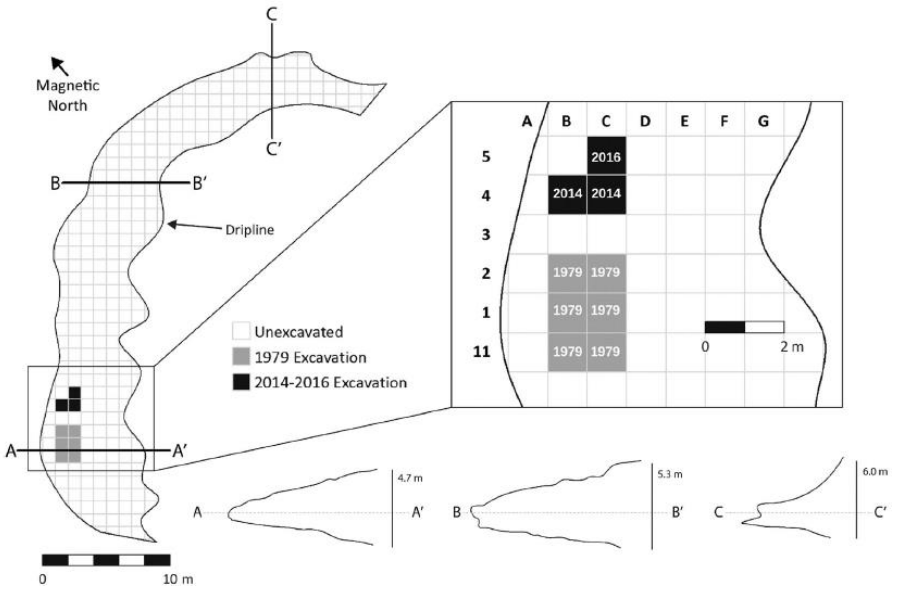


Figure 2.3: Plan view of GRS, indicating when and where the site was excavated (In Collins et al. 2020: 3).

Opperman (1984, 1987, 1988) identified three Middle Stone Age (MSA) occupation layers (KGS, VGS, and GS) dated to ca. 36 ka and five artefact-rich LSA occupation layers (LBS, AS, HSK, BR, and VB) dated from 7–6 ka (Fig. 2.4).

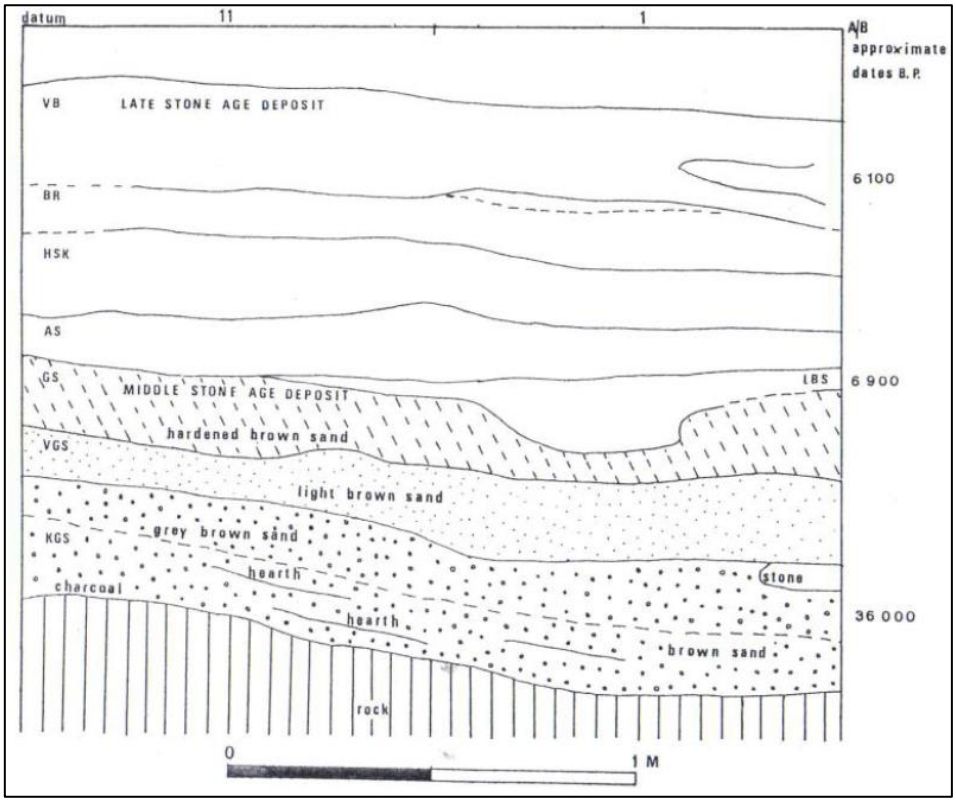


Figure 2.4: Occupational layers identified by Opperman at GRS (In Opperman 1988: 3).

Opperman recorded an occupational hiatus between the late Pleistocene (LP) and mid-Holocene (MH) occupations. This is indicated by a transition from hard sediment in the MSA layers to relatively loose and soft sediment with high ash content in the LSA layers. An extremely slow build-up of natural deposition during the occupational hiatus suggests that mixing of MSA and LSA artefacts occurred at the interface of these layers (Opperman 1984, 1988).

The LSA layers contained large quantities of stone artefacts and faunal remains, as well as two freshwater mussel pendants and some modified bone (Opperman 1984, 1987; Ames *et al.* 2020). Additionally, 4707 ostrich eggshell (OES) fragments, 151 complete OES beads, and 575 incomplete or broken OES beads were recovered (Opperman 1984, 1987; Collins *et al.* 2017). The number of OES beads at Grassridge is relatively high compared to other grassland sites in the region. However, this is not unusual as Grassridge is located near the Nama-Karoo biome and ostrich are currently found in the Grassridge region (Opperman 1987: 166; Ames *et al.* 2020: 5; Collins *et al.* 2020; Sinclair *et al.* 2020; Stewart *et al.* 2020). Scraper size and form change in the LSA, with larger, elongated side and end scrapers in the older layers (LBS and AS) and shorter, broader end scrapers in the younger layers (HSK, BR, and VB). This is consistent with the transition from Early to MH technocomplexes documented at other southern African sites (Opperman 1984, 1987: 167–168; Lombard *et al.* 2012; Ames *et al.* 2020). The Grassridge taxa are relatively diverse, consisting of carnivores, browsers, and grazers (Opperman 1984: 403). A shift in subsistence activity is documented during the LSA with GRS inhabitants shifting focus from large and medium sized bovids to browsers and small territorial species (Opperman 1984, 1987). This trend likely resulted from changing palaeoenvironmental conditions (Opperman 1984).

Approximately 10 000 stone artefacts, a small well-preserved faunal assemblage, and some OES fragments were recovered from the LP layers (Opperman 1988). The stone artefacts from the three layers are metrically and typologically similar, predominately consisting of plain platform, unmodified hornfels flakes, and blades. Roughly 0.5% of the lithic assemblage is retouched, including points, flakes, laterally retouched blades, and scrapers. Twelve cores were retrieved; however, no technological detail was provided (Opperman 1988; Ames *et al.* 2020: 4). The faunal assemblage is small and comprises 15 identified specimens. The data suggest that the LP occupants focused on medium to large bovids which included hartebeest (*Alcelaphus* sp.), wildebeest (*Connochaetes* sp.), and a southern reedbuck (*Redunca arundinum*) (Opperman 1988: 9).

In 2014, the Grassridge Archaeological and Palaeoenvironmental Project (GAPP) was launched to relocate Opperman's original excavation, reanalyse and re-date the stratigraphic sequence, and initiate new excavations at the site (Collins *et al.* 2017; Ames *et al.* 2020). The GAPP aims to examine the role of the palaeoenvironment on mobility, subsistence, and adaptation in the highland grasslands from Marine Isotope Stage (MIS) 3 (57–29 ka) through to the recent past (Ames *et al.* 2020: 2). New excavations were initiated 1 m north of Opperman's trench (Fig. 2.3) and comprise three 1×1 m squares (B4, C4, and C5) (Collins *et al.* 2017). Many of the broad LSA patterns reported by Opperman were substantiated by the new excavation (Collins *et al.* 2017). In addition, a previously unknown TP occupation and a perforated *Nassarius* marine shell were discovered (Collins *et al.* 2017, 2020; Ames *et al.* 2020).

Additional dates were obtained for the GRS sequence, including 16 radiocarbon age estimates from intact charcoal fragments and eight single-grain Optically Stimulated Luminescence dates. Three occupational pulses are recorded at Grassridge, namely the LP (ca. 45–28 ka), TP (ca. 13.5–11.6 ka), and the MH (ca. 7.3–6.8 ka) (Collins *et al.* 2017; Ames *et al.* 2020). Similar, pulsed occupational sequences are recorded at sites across southern Africa (Lewis 2008, 2011; Stewart & Mitchell 2018), implying a complex relationship between rapid palaeoenvironmental change and mobility within this biogeoclimatically diverse region (Ames *et al.* 2020: 15).

The LP (Lithostratigraphic Zone [LZ] II) layer (Fig. 2.5) contains 500–800 mm of yellowish-brown to brown sand that accumulated gradually during MIS 3 and is primarily of geogenic origin (Collins *et al.* 2017: 164; Ames *et al.* 2020). Occupation of the site is relatively consistent, until immediately above the carbonate crust (Fig. 2.5) where bulk sediments indicate an increase in occupational intensity. Lithostratigraphic Zone II and I are separated by a thin (10–30 mm) carbonate crust (Collins *et al.* 2017: 164; Ames *et al.* 2020). This feature is located below the recently identified TP layer and is found within the upper portion of Opperman's LBS layer (Fig. 2.5). Therefore, Opperman's LBS layer should be considered mixed as it contains both Pleistocene and Holocene sediments (Collins *et al.* 2017: 164–165).

The carbonate crust development is unusual as calcium carbonate is relatively scarce in this sandstone-dominant landscape. It may be the remnant of a microbial mat that lithified into calcium carbonate (Ames *et al.* 2020). Its presence may explain the depositional gap between the LP and TP layers as this hardened surface promoted surface runoff and erosion (Chafetz

& Buczynski 1992; Freytet & Verrecchia 1995; Riding 2000; Northup & Lavoie 2001; Morley *et al.* 2017; Ames *et al.* 2020). Alternatively, regional records suggest that conditions were dry and cool during MIS 2 (29–14 ka) which could explain the occupational gap at GRS (Lewis 2008; Ames *et al.* 2020). However, the microbial mat's presence suggests that some water was available at the end of MIS 3 and possibly some of MIS 2 (Ames *et al.* 2020: 13).

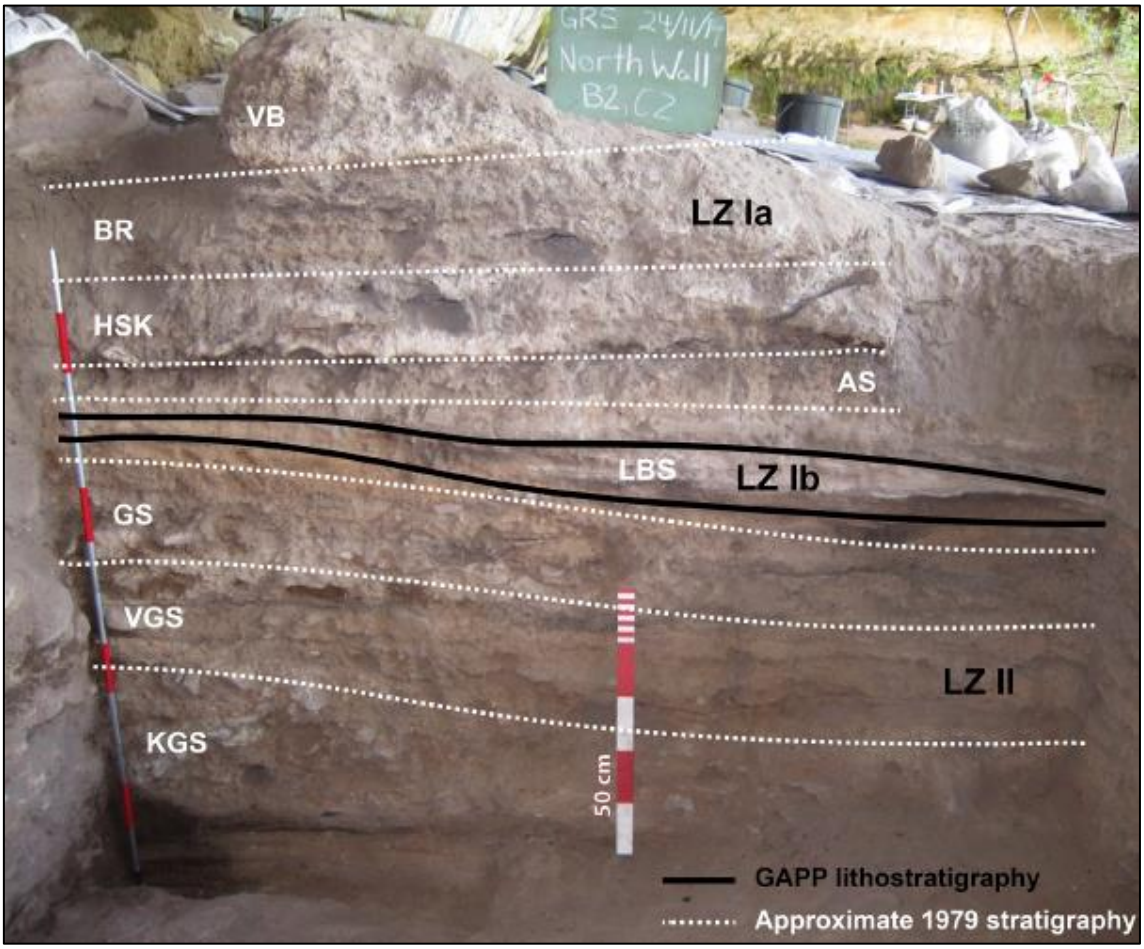


Figure 2.5: Photograph of Opperman's excavation with an overlay of the 1979 stratigraphic sequence and the GAPP lithostratigraphic zones (red segments = 100 mm) (In Collins et al. 2017: 165).

Lithostratigraphic Zone I contains the TP (LZ Ib) and MH (LZ Ia) layers which consist of 500–700 mm of grey, ashy, predominately silty sediments rich in lithics, OES fragments and beads, marine shell beads, fauna, worked bone, ochre, and charcoal (Collins *et al.* 2017, 2020; Ames *et al.* 2020). The site was reoccupied during the TP from ca. 13.5 to 11.6 ka, which roughly corresponds with the Younger Dryas (YD; 13–11.5 ka) chronozone. This occupation is represented by a thin layer that accumulated at a similar rate to the deposits from MIS 3. High artefact density and the presence of a large diameter combustion feature suggest that the shelter was used intensely during this period (Ames *et al.* 2020: 13). The

lithic assemblage is consistent with the Albany/Oakhurst technocomplex and comprises large side and end scrapers, but lacks backed segments (Deacon 1978, 1984; Opperman 1984, 1988; Lombard *et al.* 2012; Collins *et al.* 2017, 2020). The site is abruptly abandoned around 11.6 ka; however, the abruptness of this sedimentary transition warrants caution as LZ Ia may truncate LZ Ib. Some of the TP (LZ Ib) occupation was possibly removed, perhaps through hearth construction and maintenance by the MH occupants or by erosion (Ames *et al.* 2020: 13).

The MH occupation (LZ Ia) is brief and intense. Chronostratigraphic results reveal that the MH inhabitants constructed and maintained hearths throughout the sequence (Ames *et al.* 2020: 13). Intact combustion features are present as well as triplets of stratified ash, rubified sediment, and charcoal, intertwined with thick ashy sediment deposits (Goldberg & Bar-Yosef 2002; Meignen *et al.* 2007; Ames *et al.* 2020: 13). This is further supported by the presence of many woody-plant phytoliths and calcined and burnt bones (Collins *et al.* 2017; Ames *et al.* 2020: 13). The lithic assemblage includes backed segments, single platform cores, and small convex scrapers, most likely associated with the Wilton technocomplex (Deacon 1984; Opperman 1987; Lombard *et al.* 2012; Collins *et al.* 2017; Ames *et al.* 2020).

Additional work on the faunal remains, marine shell, and OES has been done by Beard (2018), Geoghegan (2019), Craig *et al.* (2020), and Collins *et al.* (2020). Beard (2018) used morphologically identified bovid remains to infer the palaeoenvironmental conditions at GRS during the Early Holocene (now TP) and MH. He found no significant difference between the number of browsers, grazers, and intermediate feeders during the TP and MH suggesting that there was no vegetation change, and thus no palaeoenvironmental change. He did, however, document a shift in bovid size class and concluded that there was a shift in subsistence strategy through time. These results are inconsistent with the palaeoenvironmental study conducted by Ames *et al.* (2020) which documents palaeoenvironmental change at GRS from the TP to the MH. Geoghegan (2019) analysed the taphonomy and skeletal element representation of bovids to examine changes in subsistence behaviour at GRS during the TP and MH. Her study documents change in subsistence behaviour and suggests that changing environmental conditions resulted in these changes as opposed to overexploitation or resource stress (Geoghegan 2019: 42).

Craig *et al.* (2020: 1) analysed the effects of heating OES on bead manufacturing. An experimental sample of OES fragments were heated and manufactured into beads and then compared with the worked OES assemblage from GRS (Craig *et al.* 2020: 1). The results

from this study suggest that deliberate heat-treatment of OES did not aid bead manufacture and that colour change most likely occurred after the beads were discarded, broken, or finished (Craig *et al.* 2020: 8). Collins *et al.* (2020) examined MIS 1 gastropod and OES bead assemblages from GRS. Results from this study emphasised the importance of bead manufacture at GRS during the TP and MH (Collins *et al.* 2020: 18). Variation is found in the bead size, aperture, and diameter, possibly indicating changes in stylistic preferences and/or different bead manufacturing traditions (Collins *et al.* 2020: 17). Similar trends are documented at other sites in Africa (Miller 2019; d'Errico *et al.* 2020) and have been associated with changing lithic technocomplexes, (Ames *et al.* 2020; Collins *et al.* 2020), and other broad cultural changes (Collins *et al.* 2020: 17). Use-wear and residue analysis suggest that these beads were used as ornaments or jewellery which came into contact with ochred surfaces, such as hide or skin (Collins *et al.* 2020: 17–18).

To date, only one other major archaeological project (published and excluding rock art) has taken place in the Stormberg region. This project was undertaken by Dr Garth Sampson (1968, 1970, 1972) at Merino Walk in response to the construction of the Gariep and Vanderkloof dams along the Orange River. Both MSA and LSA occupations were identified (Sampson 1968, 1970, 1972).

2.1.2 ARCHAEOLOGICAL BACKGROUND

Further investigation into the pulsed occupations at GRS and other southern African sites could provide critical insight into socio-cultural networks across southern Africa and their relationship to fluctuating palaeoenvironments through time (Ames *et al.* 2020: 2). The following section will discuss the occupational sequences and material culture from several southern African sites from MIS 3 to 1. Notably, MIS 1 will not include the last 5000 years and this section will not discuss the palaeoenvironment as it is discussed later.

Marine Isotope Stage 3 (57–29 ka)

This period is marked by the abandonment of sites in the southern Cape with continued or increased occupation in the interior and near the eastern coast of southern Africa (Deacon & Thackeray 1984; Wadley 2015; Wurz 2019). Sites include Border Cave (d'Errico *et al.* 2012; Villa *et al.* 2012), Boomplaas Cave (Mitchell 2008; Pargeter *et al.* 2018), GRS (Opperman 1984, 1987, 1988; Collins *et al.* 2017; Ames *et al.* 2020), Ha Makotoko (Mitchell & Arthur 2014), Melikane (Stewart *et al.* 2012; Stewart *et al.* 2016), Ntloana Tšoana (Mitchell & Steinberg 1992; Jacobs *et al.* 2008), Rose Cottage Cave (Wadley 1997, 2004), Sehonghong (Mitchell 1994; Pargeter *et al.* 2017), Sibudu Cave (Wadley *et al.* 2011; Conard *et al.* 2012),

Strathalan B (Opperman & Heydenrych 1990; Opperman 1992, 1996), and Waterfall Bluff (Fisher *et al.* 2020). Occupational shifts likely occurred due to the onset of hyperarid conditions in the southern Cape, however, rising sea levels may have resulted in flooding at these sites (Deacon & Thackeray 1984; Wurz 2019).

Faunal assemblages were dominated by grazers and large to very large bovids, some small animals were present (Clark & Kandel 2013; Wurz 2019). Lithic assemblages from the beginning of MIS 3 mostly comprise unifacial retouched points such as those found at Border Cave, Sibudu Cave, and Rose Cottage Cave (Wurz 2013). Tool forms and techniques changed at Border Cave between ca. 49–45 cal. kBP, a period marked by a decline in both the production of blades and conventional retouched pieces, the absence of unifacial points, and an increase in bipolar knapping (Villa *et al.* 2012: 13209). This is paralleled at Rose Cottage Cave at 47.1 ± 10.2 ka (Soriano *et al.* 2007) and may suggest that populations interacted with one another and encouraged the transmission of cultural information within and between different regions (Villa *et al.* 2012; Mackay *et al.* 2014). The 'Early Later Stone Age' assemblage first appears at Border Cave around 46 to 43 kBP and is characterised by unstandardised microliths and bipolar artefacts (Lombard *et al.* 2012; d'Errico *et al.* 2012; Villa *et al.* 2012; Bousman & Brink 2018; Wurz 2019). This pattern of simplification is not observed in other aspects of material culture which include well-preserved bone artefacts, bored stones, a digging stick, OES beads, and engraved and decorated bone. This may provide "early evidence of San material culture" (d'Errico *et al.* 2012: 1; Villa *et al.* 2012: 13210). However, this implies that ethnic groups have survived largely unchanged since the LP and has arisen from a fundamental misunderstanding of the nature of archaeological and cultural taxonomies, and ultimately misuses analogical reasoning (Pargeter *et al.* 2016: 1072). Early LSA assemblages gradually appear throughout southern Africa and coincide with late MSA industries, persisting until 22–21 kBP in the interior region (Opperman & Heydenrych 1990; Wurz 2019).

Marine Isotope Stage 2 (29–14 ka)

Marked cultural changes are documented across southern Africa from MIS 3 to 2 (Loftus *et al.* 2019). During MIS 2, only a few archaeological sites are occupied in the southern African interior (Mitchell 2013; Ames *et al.* 2020), including Boomplaas Cave (Deacon 1995; Pargeter *et al.* 2018), Strathalan B (Opperman & Heydenrych 1990; Opperman 1992, 1996), Ha Makotoko (Mitchell & Arthur 2014), Melikane (Stewart *et al.* 2016), Sehonghong (Mitchell 1996a; Pargeter *et al.* 2017; Loftus *et al.* 2019), and Rose Cottage Cave (Wadley

1997; Loftus *et al.* 2019). Occupational and population trends were drastically affected by the onset of the Last Glacial Maximum (LGM; 24–18 cal. kBP) (Chase & Meadows 2007; Wurz 2019).

Microlithic technology and compound hafted tools appeared, and symbolic material culture became widely adopted and used more regularly (Loftus *et al.* 2019). Both final MSA and Robberg-like lithic assemblages were present (Opperman 1992, 1996; Mitchell 1995; Clark 1997). The Robberg technocomplex is characterised by microlithic technologies with an emphasis on small, unretouched bladelets (Wurz 2019) and occurs at most southern African sites from 22–12 kBP (Lombard *et al.* 2012). It was first documented in the Lesotho highlands, at Melikane (20 200 ± 150 BP; Pta-1407) and Sehonghong (19 400 ± 200 BP; Pta-6281), and in the southern Cape at Nelson Bay Cave (19 110 ± 110 BP) (Klein 1974; Deacon 1978; Mitchell 1996a; Loftus *et al.* 2016b) and spread rapidly through southern Africa.

Lithic data pre-dating the LGM in and around the Maloti-Drakensberg Mountains (i.e., Rose Cottage Cave, Sehonghong, Ha Makotoko, Ntloana Tšoana, and Strathalan) record lower core to retouch ratios, lower lithic discard intensity, and higher retouched tool frequencies. These data indicate an increase in mobility across the region and individual provisioning systems. Conversely, lithic data from the LGM record higher core to retouch ratios, higher lithic discard intensity, and lower retouched tool frequencies, suggesting a reduction in regional mobility and place provisioning strategies (Loftus *et al.* 2019: 13).

Interior occupations post-dating the LGM (19–14 ka) are recorded at Ha Makotoko (Mitchell & Arthur 2014), Rose Cottage Cave (Wadley 1995, 1996), Sehonghong (Mitchell 1995; Pargeter *et al.* 2017; Loftus *et al.* 2019), and Boomplaas Cave (Deacon 1979; Deacon 1984; Pargeter *et al.* 2018). Lithic data in and around the Maloti-Drakensberg Mountains is variable with a wide range of lithic discard intensities at all four sites (i.e., Ntloana Tšoana, Ha Makotoko, Rose Cottage Cave, and Sehonghong); these values are significantly higher than those pre-dating the LGM (Loftus *et al.* 2019: 14). The core to retouch ratios at Sehonghong are significantly higher than the other three sites, suggesting some continuation of provisioning systems in the highlands. Furthermore, low core to retouch ratios and increased retouched tool frequencies are recorded at these sites suggesting that regional mobility and individual provisioning systems increased. The frequency of retouched tools from Sehonghong is low (Loftus *et al.* 2019: 14).

Boomplaas Cave records its highest occupational intensity at 17–13 cal. kBP (Member CL). Marine shell was found in member CL suggesting that there was a link to the coast, either through group movement or exchange networks (Deacon 1984). Moreover, the number of bone tools, tortoise shell bowls, and OES fragments in member CL increases drastically (Deacon 1984), indicating a complex process of social and technological change during a period of fluctuating palaeoenvironmental conditions and landscape reorganisation (Pargeter *et al.* 2018: 3). Marine/estuarine shell ornaments are also found at Sehonghong around 24–23 cal. kBP and 15–14 cal. kBP, indicating a relationship between the interior and the coastal regions (Loftus *et al.* 2019: 14).

Marine Isotope Stage 1 (14–5 ka)

The shift from MIS 2 to 1 is accompanied by increasing environmental productivity and expanding populations (Mitchell 1997). A brief cold event, namely the YD (ca. 13–11.5 cal. kBP), interrupted post-glacial warming (Alley *et al.* 1993; Andres *et al.* 2003; Thackeray & Scott 2006), during which only a few interior sites were occupied (Mitchell & Arthur 2014; Collins *et al.* 2017; Fitchett *et al.* 2017a; Loftus *et al.* 2019; Ames *et al.* 2020). The Robberg technocomplex is replaced by the Oakhurst and appears at most sites between 12–8 kBP. It is characterised by large macrolithic scrapers and flakes, lacking microlithic technology (Sampson 1974; Deacon 1978, 1984; Lombard *et al.* 2012). This transition is accompanied by an increase in the number of interior sites and population expansion (Wadley 1993). As the number of sites increases, there is a tendency toward more homogenous flakes and symbolic material culture such as bone and shell beads, engraved OES, and bone artefacts, especially after 10 ka (Wadley 1993; Mitchell 1997, 2002; Lombard *et al.* 2012; Dayet *et al.* 2017; Ryano *et al.* 2017). During the TP, Robberg-like assemblages occur at Blydefontein Rockshelter (Bousman 2005), Sehonghong (Mitchell 1996b; Pargeter *et al.* 2017), Rose Cottage Cave (Wadley 1997), and Ravenscraig (Opperman 1987) with Oakhurst-like assemblages occurring at GRS (Collins *et al.* 2017; Ames *et al.* 2020), Ha Makotoko (Mitchell & Arthur 2014), Tloutle Rockshelter (Mitchell 1993), Rose Cottage Cave (Wadley 2000a), Nelson Bay Cave (Loftus *et al.* 2016b), Boomplaas Cave (Deacon 1979), and Te Vrede (Opperman 1987). Furthermore, a regional variant of the Oakhurst technocomplex, the Lockshoek, dated to 8541 ± 471 BP (SMU-1823) was identified in the eastern Karoo surrounding Blydefontein and is characterised by large unifacial scrapers, large flakes, and a few cores (Sampson 1974; Bousman 2005).

There is a notable shift in subsistence activity and diet from the TP to MH, with focus shifting from large bovids to small bovids and territorial animals (Klein 1972, 1974, 1978; Opperman 1984, 1987; Plug & Engela 1992; Bousman 2005; Barham & Mitchell 2008). This trend is less noticeable at coastal sites (e.g., Nelson Bay Cave) where there are massive accumulations of shellfish (Klein 1972, 1974). At GRS there is an increase in small bovids such as grey rhebok (*Pelea capreolus*), mountain reedbuck (*R. fulvorufula*), steenbok/grysbok (*Raphicerus* sp.), and klipspringer (*Oreotragus oreotragus*) (Opperman 1984: 403). A similar trend is found at sites above the escarpment, namely Colwinton (Opperman 1982, 1987) while a contrasting trend is found at sites below the escarpment, namely Te Vrede and Bonawe, where equids and alcelaphines occur throughout the Holocene (Opperman 1984, 1987).

An interesting yet complex relationship exists between beads, pigments, and residues at GRS (Collins *et al.* 2020) and Bushman Rockshelter (Dayet *et al.* 2017). At Bushman Rockshelter beads are manufactured from OES, marine shell (*N. kraussianus*), and giant land snail shell (*Achatina* sp.). Residue and pigment were found on some of the beads suggesting that they encountered ochred surfaces (i.e., skin), and may have been used to convey complex social messages (Dayet *et al.* 2017; Collins *et al.* 2020). The presence of marine shell beads at GRS and Bushman Rockshelter is interesting as both sites are located approximately 200 km away from the coast. Thus, indicating the existence of a long-distance relationship between the interior regions and the coast (Collins *et al.* 2017, 2020; Dayet *et al.* 2017).

The Oakhurst technocomplex is replaced by the Wilton around 8 kBP. It is characterised by microlithic tools and includes thumbnail scrapers, straight-backed bladelets, and segments (Sampson 1974; Deacon 1984; Wadley 1993; Mitchell 1997, 2002). The MH Wilton occupation at GRS is contemporaneous with other sites in the high elevation grasslands, like Colwinton (Opperman 1987), Rose Cottage Cave (Wadley 2000b), Tloutle Rockshelter (Mitchell 1990; Mitchell 1993), and Sehonghong (Mitchell & Vogel 1994).

2.2 FAUNAL THEORY AND METHODS

Zooarchaeology is the identification, analysis, and interpretation of faunal remains from archaeological sites to gain insight into the relationship between humans, animals, and their environment (Reitz & Wing 2008; Brandt *et al.* 2018). Zooarchaeological studies comprise several qualitative and quantitative methodologies and theoretical frameworks, enabling the study of several topics, including resource exploitation, animal domestication and husbandry, diet, palaeoenvironment, cultural identities, trade networks, and economy across a range of

periods, geographical regions, and settlement types (Reitz & Wing 2008; Steele 2015; Makarewicz 2016; Brandt *et al.* 2018). This section will examine some of the methods used to examine and interpret faunal remains from archaeological sites.

Current zooarchaeological research is composed of anthropological, methodological, and biological research (Reitz & Wing 2008). It is best contextualised within the wider scope of environmental archaeology which examines the efficient relationship between humans and their environment (Reitz *et al.* 2012; LeFebvre & Sharpe 2018). The ontological foundation of environmental archaeology is the understanding that we are working with zoological remains that can be defined objectively and understood within an environmental and biological context (LeFebvre & Sharpe 2018: 38). Therefore, we accept the principles and uses of analogical reasoning and uniformitarian approaches within zooarchaeological studies, especially those used to identify species and serve as palaeoenvironmental proxies (LeFebvre & Sharpe 2018: 38).

2.2.1 ZOOARCHAEOLOGICAL METHODS

Faunal remains are commonly found at archaeological and palaeontological sites. Zooarchaeological studies are reliant on secure taxonomic identifications. It is a central goal of most faunal analyses and constitutes the primary source of data for almost all other zooarchaeological quantification and interpretation (Wolverton 2013; Janzen *et al.* 2021). This section will discuss the morphological and biomolecular methods used to identify faunal remains and will highlight the advantages and limitations of each.

2.2.2 MORPHOLOGICAL METHODS

Faunal remains are traditionally identified by osteomorphological analysis by comparing the diagnostic morphological features on archaeological bone to identified bones in modern reference collections (Klein & Cruz-Uribe 1984; O'Connor 2000; Reitz & Wing 2008; Chowdhury *et al.* 2021). This method relies on analogical inferences and uniformitarian principles and assumes that archaeological specimens share similar morphological characteristics with their contemporary counterparts (Lyman 2010; Brandt *et al.* 2018; LeFebvre & Sharpe 2018).

Osteomorphological analysis may provide vital information about age at death, bone element, bone preservation, pathology, sex, and traces of wear, but suffer from certain limitations. The most notable limitation is the inability to identify highly fragmented remains, which often lack diagnostic features (Lyman 1994; Buckley *et al.* 2009; Steele 2015; Buckley *et al.* 2017; Brandt *et al.* 2018; Buckley 2018; Chowdhury *et al.* 2021). As a result, a large portion of the

sample may be neglected, introducing bias, and limiting archaeological and environmental data (Badenhorst & Plug 2011; Buckley & Collins 2011; Buckley 2018). Marean *et al.* (2001, 2004) attempted to mitigate these issues by refitting long bone fragments. This method, however, time-consuming and requires specialist knowledge. Additional factors impacting the success of osteomorphological analysis include analyst experience, access to and quality of reference collections, and an implicit understanding of standard zooarchaeological procedures, methods, and theories (White 1992; Reitz & Wing 2008; Buckley *et al.* 2010; Buckley & Kansa 2011; Gifford-Gonzalez 2018). Several methods are proposed to overcome these issues, ranging from histology (Harsanyi 1993; Hillier & Bell 2007; Cuijpers & Lauwerier 2008; Greenlee & Dunnell 2010) to biomolecular methods (Lowenstein *et al.* 2006; Blow *et al.* 2008; Buckley *et al.* 2009; Coutu *et al.* 2016; Janzen *et al.* 2021).

2.2.3 BIOMOLECULAR METHODS

Biomolecular methods, such as ancient DNA (aDNA) (Campana *et al.* 2013; Matisoo-Smith 2018), protein-based methods (Fletcher *et al.* 1984; Kang'ethe & Gathuma 1987; Hollemeyer *et al.* 2002; Buckley *et al.* 2009), and stable isotopes (Makarewicz & Sealy 2015; Loftus *et al.* 2016a) have revolutionised zooarchaeological studies in the 21st century. These approaches may expand the scope of zooarchaeological studies, improve taxonomic resolution and identification rates, provide access to previously neglected unidentifiable bone fragments, and reduce bias introduced by analysts (Horsburgh *et al.* 2016; Janzen *et al.* 2021). However, these approaches do not replace morphological analysis but rather aim to revise and complement them.

Ancient DNA

Ancient DNA is widely used to identify archaeological specimens as the molecule is predominant and provides a pre-eminent level of genetic information (Fiddyment *et al.* 2015; Brown *et al.* 2016; Buckley 2016; O'Sullivan *et al.* 2016; Buckley *et al.* 2017; Cassidy *et al.* 2017; Librado *et al.* 2017; Welker 2017; Matisoo-Smith 2018). This approach is objectively superior to morphological approaches and has been used to confirm or revise morphological identifications, such as those from Blydefontein Rockshelter, South Africa where aDNA showed that five out of the six specimens were incorrectly identified as domestic stock using morphological analysis (Horsburgh & Moreno-Mayar 2015; but see Scott & Plug 2016).

Unfortunately, aDNA studies are expensive, have contamination issues, require specialist facilities and knowledge, are destructive, and they have a low rate of success (Brown & Brown 1992; Nielsen-Marsh & Hedges 2000; Haile *et al.* 2007; Leonard *et al.* 2007;

Campana *et al.* 2013; Buckley 2018; Gifford-Gonzalez 2018; Matisoo-Smith 2018). The success rate of aDNA decreases with age and in torrid or temperate environments (Nielsen-Marsh & Hedges 2000; Kahila Bar-Gel *et al.* 2002; Campana *et al.* 2013); these environments often contain the largest range of wild and domestic fauna (Buckley 2018: 227).

Proteins are generally more robust than aDNA and have often been detected in samples that fail to yield usable aDNA (Buckley 2013, 2015; Hendy 2021). However, the relationship between aDNA and protein survival in the same samples is still poorly understood (Buckley *et al.* 2008a). Several alternatives are proposed to overcome these issues (Cattaneo *et al.* 1992; Collins *et al.* 1998; Ostrom *et al.* 2000; Ostrom *et al.* 2006; Buckley 2016).

Protein-based Methods: Collagen

Bone contains many taxonomically informative proteins, including the abundant and persistent collagen type 1 (COL1) protein (Buckley *et al.* 2008b, 2010; Buckley & Kansa 2011; Buckley & Wadsworth 2014). Type I collagen is a large heterotrimeric molecule, consisting of two identical alpha-1 chains and one genetically distinct alpha-2 chain (Termine 1993; Buckley *et al.* 2008b; Buckley 2018). The chain structure is formed by glycine, which is very flexible and allows the alpha chains to bend and create a helix that connects with hydroxylysine cross-linkages and creates fibrils that are closely organised with bone apatite (Shoulders & Raines 2009). The chain structure is highly conserved but significant variation in the alpha-2 chain allows it to be used for species identification (Chu *et al.* 1984; Buckley *et al.* 2009; Shoulders & Raines 2009; Henriksen & Karsdal 2016; Buckley 2018).

Collagen is selectively enriched when non-collagenous proteins degrade (Wadsworth & Buckley 2014). Under optimal conditions measurable amounts of collagen can survive for well over 100 ka (Jones *et al.* 2001; Lee-Thorp 2008). However, collagen survival is subject to certain biological, chemical, and environmental factors (i.e., moisture, pH, weathering, and temperature) but its survival is intimately linked with the preservation of hydroxyapatite, the mineral component of bone (Richter 1986; Stiner *et al.* 1995; Taylor *et al.* 1995; Nielsen-Marsh *et al.* 2000; Collins *et al.* 2002; Lee-Thorp 2008; Gifford-Gonzalez 2018; Kendall *et al.* 2018). Preservation of the mineral component (antler, bone, or dentine) regulates collagen biodegradation, making collagen more resistant to high temperatures and the deleterious effects of long-term burial (Collins *et al.* 2002, 2010: 6; Buckley *et al.* 2009; Buckley & Kansa 2011; San Antonio *et al.* 2011; Harvey *et al.* 2016; Brandt *et al.* 2018: 3; Desmond *et al.* 2018).

Thus, in the absence of mineral dissolution, collagen should not significantly degrade over time as seen in temperate environments (Nielsen-Marsh *et al.* 2000: 442). Collagen, however, deteriorates more rapidly in tropical and warm environments (Lee-Thorp 1989; Ambrose 1990; Klinken 1991; Holmes *et al.* 2005; Lee-Thorp & Sponheimer 2006; Pestle & Colvard 2012). Notably, collagen degradation is significant at most African sites by ca. 10-20 ka (Lee-Thorp 1989; Lee-Thorp & Sponheimer 2006). Mineral dissolution is promoted by low pH which makes collagen more susceptible to degradation (Nielsen-Marsh *et al.* 2000). Hydroxyapatite is less likely to dissolve and is most stable when pH is above 7.5 (Lindsay 1979; Gordon & Buikstra 1981; White & Hannus 1983). The sediments from GRS have a pH value ranging between 7.9 and 8.8 (Ames *et al.* 2020). These values are high when compared to the pH values of sandstone rockshelters from around the globe. For example, pH ranges from 5.0 to 5.5 at Gledwood Shelter 1, Australia (Lowe *et al.* 2018), 4.5 to 5.5 at Nonda Rock Rockshelter, Australia (David *et al.* 2007), 3.7 to 5.8 at Loberia I Rockshelter, Argentina (Martinez *et al.* 2013), 4.4 to 6.4 at Santana do Riacho Rockshelter, Brazil (de Sousa *et al.* 2017), and 4.9 to 8.9 at Umhlatuzana Rockshelter, South Africa (Reidsma *et al.* 2021).

Despite a range of taphonomic processes, collagen protein sequences are known to survive in deep time and under sub-optimal conditions (Asara *et al.* 2007; Buckley *et al.* 2008b; Buckley *et al.* 2011; Cappellini *et al.* 2012; Wang *et al.* 2012; Rybczynski *et al.* 2013; Le Meillour *et al.* 2018). Collagen is abundant and resilient and is utilised for stable isotope, radiocarbon dating, and Zooarchaeology by Mass Spectrometry (ZooMS) analyses (Longin 1971; Vogel & van der Merwe 1977; Jones *et al.* 2001; Buckley *et al.* 2008b; Lee-Thorp 2008; Buckley *et al.* 2015).

2.2.4 ZOOARCHAEOLOGY BY MASS SPECTROMETRY

Taxonomic identification using ZooMS is facilitated by peptide mass fingerprinting of proteins (i.e., COL1) (Buckley *et al.* 2008b, 2009; Buckley 2018; Culley 2021). This method (Fig. 2.6) does not directly identify the amino acid sequence but rather compares the distribution of peptide masses (i.e., the mass spectra) of an unknown sample with known samples in the reference database (Hendy 2021). Early studies isolated the collagen α2(I) carboxytelopeptide using solid-phase extraction after being digested by bacterial collagenase (Buckley *et al.* 2008b; Buckley 2018). A single 18 amino acid peptide was produced but could not sufficiently separate some of the major domesticates, such as goat (*Capra hircus*) and sheep (*Ovis aries*), prompting further methodological developments (Buckley & Kansa 2011; Buckley 2018). Buckley *et al.* (2010) produced a single 33 amino acid peptide by

isolating the collagen α2(I) using a similar solid phase extraction method following digestion with trypsin and was later verified by aDNA (Campana *et al.* 2013). This method has been further simplified and the adoption of a specialised C18 pipette tip has allowed samples to be separated into two fractions (Buckley *et al.* 2009; Buckley 2018).

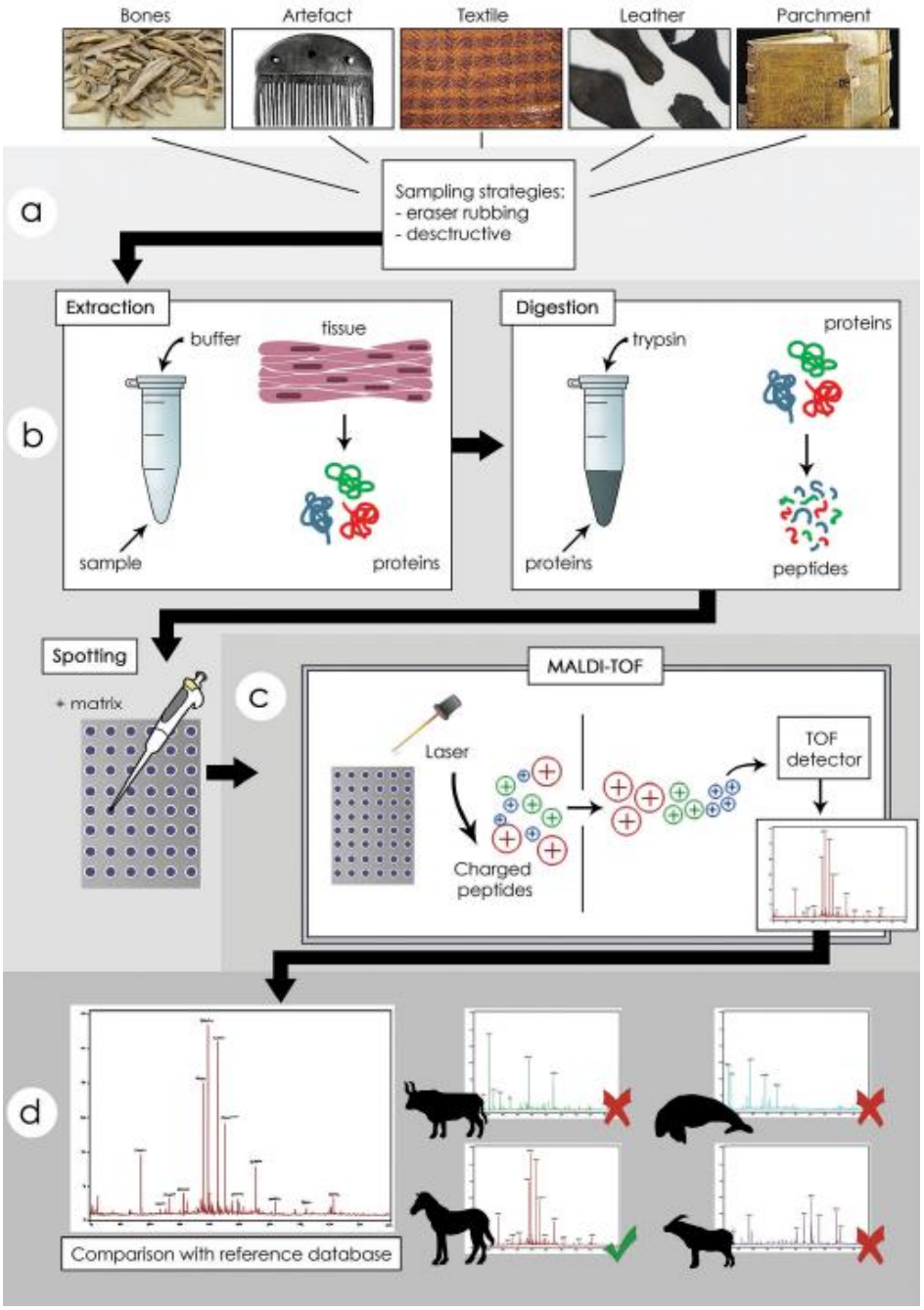


Figure 2.6: Flow chart showing the process of ZooMS (In Brandt et al. 2018: 4).

There are several advantages to using ZooMS; however, it must be noted that this method does not attempt to replace aDNA or traditional morphological approaches but rather aims to revise and complement them. Advantages of ZooMS include (1) collagen's dominance in

bone and the ability to collagen fingerprint bones with limited amounts of collagen (Buckley *et al.* 2011), (2) the persistence of collagen in bone for long periods and warmer environments (Asara *et al.* 2007; Schweitzer *et al.* 2009; Buckley *et al.* 2009, 2010; Rybczynski *et al.* 2013; but see Buckley *et al.* 2008c; Kaye *et al.* 2008; Bern *et al.* 2009 for comments on dinosaur collagen), (3) low cost of analysis (Buckley *et al.* 2009, 2010), (4) significant reduction in contamination issues (Buckley *et al.* 2009, 2010), (5) rapid results from otherwise unidentifiable specimens (Buckley *et al.* 2009, 2010), (6) minimal to non-destructive sampling (Fiddyment *et al.* 2015; Coutu *et al.* 2016; Brandt *et al.* 2018), (7) excellent screening method for large assemblages (Brown *et al.* 2016; Welker *et al.* 2016), (8) can be successfully used by non-specialists (Kirby *et al.* 2013; Fiddyment *et al.* 2015).

The most notable limitation is the taxonomic resolution of ZooMS compared to aDNA. Zooarchaeology by Mass Spectrometry identifications are, however, significantly better than those achieved by other molecular and non-molecular approaches (Buckley *et al.* 2010, 2017). Genus-level identifications are often achieved by ZooMS, although there are notable exceptions (Buckley *et al.* 2011, 2016, 2018; Rybczynski *et al.* 2013; Coutu *et al.* 2016; Bradfield *et al.* 2019, 2021; Buckley & Cheylan 2020; Janzen *et al.* 2021). Some taxa may not be taxonomically consistent with their phylogenetic expectations, so the extent of molecular diversity and thus collagen fingerprint specificity may vary between taxa (Buckley 2018). For example, *Alces* is difficult to separate from *Cervus/Dama*, whereas *Rangifer* and *Capreolus* are easier to separate, even though *Rangifer* should be closer to *Alces* than *Capreolus* is to *Cervus/Dama* (Welker *et al.* 2015; Buckley 2018). Another limitation of ZooMS is the lack of a robust peptide marker reference database outside of Eurasia (Brandt *et al.* 2018; McGrath *et al.* 2019; Janzen *et al.* 2021).

African bovids are often coarsely identified to family or bovid size class using traditional methods (Klein 1976; Brain 1981). While bovids are osteologically similar their diets and habitat preferences are extremely diverse making them an ideal palaeoenvironmental proxy (Vrba 1980; Gagnon & Chew 2000; Skinner & Chimimba 2005; Jousse & Escarguel 2006; Faith 2011a; Roberts *et al.* 2020). Collagen peptide mass fingerprints are highly conserved in African bovids, often resulting in sub-family or tribal-level identifications when using ZooMS (Table 2.1). Despite lower resolutions than aDNA, tribal identifications are useful as bovid tribes have diverse dietary and habitat requirements. For example, members of the Alcelaphini tribe are water-dependent (WD) open grassland grazers while members of the Cephalophini tribe are water-independent (WI) closed forest or canopy browsers (Skinner &

Chimimba 2005; Hempson *et al.* 2015). The level of taxonomic resolution is likely related to collagen turnover rates. A divergence time of approximately four to five million years is required for identifiable discriminatory markers to develop in mammals with slow rates of collagen sequence evolution, mostly medium-large sized mammals (Buckley & Collins 2011; Buckley *et al.* 2011, 2017). Less divergence time is required in small mammals which have higher rates of amino acid substitution (Gu & Li 1992; Buckley *et al.* 2016). However, the effect of the peptides' chemical properties on species identification cannot be discounted (Buckley *et al.* 2017: 408).

Table 2.1: Taxonomic resolution of faunal identifications using ZooMS from various sites and time periods in Africa. Most common taxonomic identification highlighted in green, this does not include failed samples which are shown in grey.

Location	n	Approximate age (BP)	Taxonomic Resolution						Reference
			≥Sub-Family	Tribe	Genus	Species	Unknown	No ID	
North interior region, South Africa	77	< 2000	33	1	11	0	0	32	Bradfield *et al.* 2019
Zambia	192	500–4000	58	41	5	0	3	85	Janzen *et al.* 2021
Taforalt, Morocco	13	13500–15000	0	0	8	5	0	0	Desmond *et al.* 2018
Kwa-Zulu Natal, South Africa	83	150–8500	2	35	6	1	0	39	Bradfield *et al.* 2021
Panga ya Saidi, Kenya	105	320-1180	20	2	0	61	3	19	Culley *et al.* 2021a

Recent work by Bradfield *et al.* (2021) and Janzen *et al.* (2021) has significantly expanded the African bovid peptide marker reference database, however, a lot more work is required here. Modern specimens should be submitted along with archaeological specimens (M. Buckley, personal communication, 2021).

Applications of ZooMS: Beyond Species Identification

ZooMS has been used on an array of archaeological materials, including bone (Buckley *et al.* 2009; Janzen *et al.* 2021), hair (Solazzo *et al.* 2011), antler (von Holstein *et al.* 2014), skin (Kirby *et al.* 2013; Brandt *et al.* 2014; Fiddyment *et al.* 2015), eggshell (Stewart *et al.* 2013; Presslee *et al.* 2018), and mollusc shell (Sakalauskaite *et al.* 2020). It can discriminate between closely related domesticates, like sheep and goat (Buckley *et al.* 2009, 2010; Buckley & Kansa 2011), wild fauna (Buckley & Collins 2011; Buckley & Kansa 2011; Buckley *et al.* 2016, 2017; Buckley & Herman 2019; Janzen *et al.* 2021; Peters *et al.* 2021), marine animals (Buckley *et al.* 2014; van der Sluis *et al.* 2014; Harvey *et al.* 2019; Wagner *et*

al. 2020; Winter *et al.* 2021), amphibians (Buckley & Cheylan 2020), molluscs (Sakalauskaite *et al.* 2020), and fish (Richter *et al.* 2011, 2020; Harvey *et al.* 2018, 2019).

The combination of ZooMS with other methods is beneficial and may reduce bias. It provides identifications for rare artefacts like worked bone and leather, allows ambiguous isotopic identifications to be refined, increases sample size, and tests the reliability and accuracy of morphological methods. Importantly, ZooMS provides an affordable screening method for palaeoproteomics and radiocarbon dating (Buckley *et al.* 2010, 2017; Buckley & Kansa 2011; van Doorn *et al.* 2011; Kirby *et al.* 2013; van der Sluis *et al.* 2014; Welker *et al.* 2015; Harvey *et al.* 2016; Brandt *et al.* 2018; Bradfield *et al.* 2019, 2021; McGrath *et al.* 2019; Pilaar Birch *et al.* 2019; Prendergast *et al.* 2019; Sinet-Mathiot *et al.* 2019; Kontopoulos *et al.* 2020; Bouchard *et al.* 2020; Janzen *et al.* 2021). For example, Buckley *et al.* (2010) found a strong correlation (19/20 correctly identified) between the morphological and ZooMS identifications of sheep and goat at Domuztepe, Turkey, suggesting that the morphological criteria used to identify these species were reliable. Buckley and Kansa (2011), however, documented a higher number of misidentifications (two of seven incorrectly identified) when a wider range of taxa was examined, reducing our confidence in the morphological criteria. Sites containing a diverse faunal assemblage will benefit from ZooMS as it has the potential to reduce bias and increase palaeoenvironmental, symbolic, subsistence, and taphonomic information (Buckley *et al.* 2017). Additionally, ZooMS provides a cost-effective method to screen for aDNA analysis (Brown *et al.* 2016, Welker *et al.* 2016; Brandt *et al.* 2018; McGrath *et al.* 2019) and increases the chance of identifying unexpected or exotic species providing invaluable insight into prehistoric lifeways and relationships (Solazzo *et al.* 2011; Brown *et al.* 2016; Buckley *et al.* 2017; Brandt *et al.* 2018). For instance, Brandt *et al.* (2018) found evidence of long-distance trade networks and the pursuit of luxury items by some inhabitants at Odense as indicated by a gaming piece made from walrus (*Odobenus rosmarus*) tusk and combs made from local resources.

In recent years, non-destructive peptide mass fingerprinting has been used on unique or rare artefacts (van Doorn *et al.* 2011; Fiddyment *et al.* 2015; McGrath *et al.* 2019; Kirby *et al.* 2020; Martisius *et al.* 2020). Three non-destructive methods have been proposed, the first uses an ammonium bicarbonate (ABC) buffer to extract collagen from well-preserved bones (van Doorn *et al.* 2011), the second extracts collagen using the triboelectric effect which generates an electrostatic charge using a PVC eraser (Fiddyment *et al.* 2015) or a plastic storage bag (McGrath *et al.* 2019), and the third abrades and removes a small amount of

surface material using a very fine polishing film (Kirby *et al.* 2020). The success rates of these analyses are variable and inconsistent, occasionally providing partial collagen peptide fingerprints favouring low-molecular-weight peptides (Fiddyment *et al.* 2015; Brandt *et al.* 2018; Martisius *et al.* 2020). However, these methods have allowed researchers to access previously inaccessible information from unique artefacts such as bone tools, parchment, and photographs (Fiddyment *et al.* 2015; Bradfield *et al.* 2019, 2021; McGrath *et al.* 2019; Kirby *et al.* 2020).

In Africa, ZooMS studies are limited (Coutu *et al.* 2016, 2021; Prendergast *et al.* 2017, 2019; Desmond *et al.* 2018; Bradfield *et al.* 2019, 2021; Le Meillour *et al.* 2020; Culley 2021; Culley *et al.* 2021a, b; Janzen *et al.* 2021). These studies tackle similar issues and research questions as those described above but their applicability in African environments has only recently been explored. Of these studies, only four are from South Africa (Coutu *et al.* 2016, 2021; Bradfield *et al.* 2019, 2021). These studies focus on worked bone or ivory dating to the last 2000 years. Older samples (3000–8700 BP) were examined by Bradfield *et al.* (2021) but only 16.67% (n = 18) were successfully identified to tribe.

2.3 STABLE ISOTOPES

Stable isotope analysis emerged in the 1970s. Initial studies focused on human diet and later included faunal and environmental studies (van der Merwe & Vogel 1978; Gifford-Gonzalez 2018). Two fundamental characteristics underlie stable isotope studies, namely, that dietary sources have distinct isotopic compositions that allow them to be distinguished from one another and that these distinct isotope ratios are integrated into consumer tissue (Kelly 2000: 4). Notably, stable isotope studies are reliant on middle-range theory, analogy, and uniformitarian principles and may suffer from issues of equifinality and cannot determine the dietary contribution of each dietary source (Bogaard & Outram 2013; Makarewicz & Sealy 2015).

2.3.1 ISOTOPES, ISOTOPE NOTATION, AND MEASUREMENTS

Isotopes are atoms of the same chemical element that have the same number of electrons and protons, but a differing number of neutrons (Faure 1986; Fry 2006; Sulzman 2007; Katzenberg 2008). The atomic mass is affected by the number of neutrons which cause subtle differences in the physical properties of isotopologues and elements, affecting the isotopic ratio (Farquhar *et al.* 1989; Hayes 1993; Dawson & Siegwolf 2007; Katzenberg 2008). There are two properties or ‘isotope effects’, namely, equilibrium (reversible) or kinetic (occur in one direction). The ratio of light to heavy isotopes varies because lighter isotopes have a

higher vibration frequency and weaker bonds than heavier isotopes, thus less energy is needed to break them, resulting in higher rates of reaction and 'isotopic fractionation' (Dawson & Siegwolf 2007; Katzenberg 2008). Isotopic fractionation occurs during chemical reactions and the diffusion of a substance along a concentration gradient (Dawson & Siegwolf 2007: 7). These biological or physiochemically mediated reactions result in isotopic discrimination. Isotopic ratios are measured using an Isotope Ratio Mass Spectrometer. (Dawson & Siegwolf 2007; Sulzman 2007).

2.3.2 STABLE CARBON ISOTOPES

Carbon has three naturally occurring isotopes, specifically, carbon-14 (^{14}C), carbon-13 (^{13}C), and carbon-12 (^{12}C). Stable carbon isotopes, ^{13}C and ^{12}C, occur at 1.1% and 98.9% in the atmosphere, respectively. They are dynamically interchanged between the atmosphere, marine, and terrestrial environments (Peterson & Fry 1987; Fry 2006: 45). In recent times, atmospheric carbon dioxide (CO_2) has been progressively depleted in ^{13}C due to fossil fuel combustion (Marino & McElroy 1991; Keeling *et al.* 2017: 10361). Overall, the global atmospheric $\delta^{13}C$ average has declined from -6.4‰ in pre-industrial times to -8.4‰ at present; this must be considered when measuring stable carbon isotope ratios (Marino & McElroy 1991; Keeling *et al.* 2017: 10361).

Stable carbon isotope studies trace the flow of carbon through foodwebs. Atmospheric CO_2 is incorporated into plants during photosynthesis, during which ^{13}C is discriminated against relative to ^{12}C assimilation (O'Leary 1981; Ambrose & DeNiro 1986a, b; DeNiro 1987; Farquhar *et al.* 1989). Discrimination of ^{13}C differs between C_3 and C_4 plants and was realised when the radiocarbon dates of C_4 plants were constantly underestimated compared to C_3. This underlies the foundation of stable carbon isotope studies (Bender 1968; O'Leary 1981; van der Merwe 1982; Balasse 2003; Fry 2006; Makarewicz & Sealy 2015). Three major photosynthetic pathways exist, namely, the Calvin-Benson cycle or C_3 pathway, the Hatch-Slack cycle or C_4 pathway, and the Crassulacean Acid Metabolism (CAM) pathway (Smith & Epstein 1971; Lee-Thorp 2008; Loftus *et al.* 2016a). Variation in the $\delta^{13}C$ values of plants mostly results from the utilisation of different photosynthetic pathways, although variation may occur due to fluctuating environmental conditions and CO_2 sources (Smith & Epstein 1971; O'Leary 1981; Ehleringer & Cerling 2002; Lee-Thorp 2008; Loftus *et al.* 2016a; Lightfoot *et al.* 2020; Sanborn *et al.* 2021). Stronger discrimination against the heavy ^{13}C isotope is found in C_3 plants, resulting in lower ^{13}C:^{12}C ratios in C_3 compared to C_4 plants (Bender 1968; Smith & Epstein 1971; Vogel *et al.* 1978).

The C_3 photosynthetic pathway (Fig. 2.7) is the oldest and most energy-efficient. It comprises approximately 95% of terrestrial plants (Cerling *et al.* 1997; Fry 2006; Sharp 2017). Plants utilising this pathway often occur in temperate environments and include trees, woody shrubs, aquatic plants, most herbs, and temperate grasses (Ehleringer & Monson 1993; Still *et al.* 2003; Fry 2006; Sharp 2017).

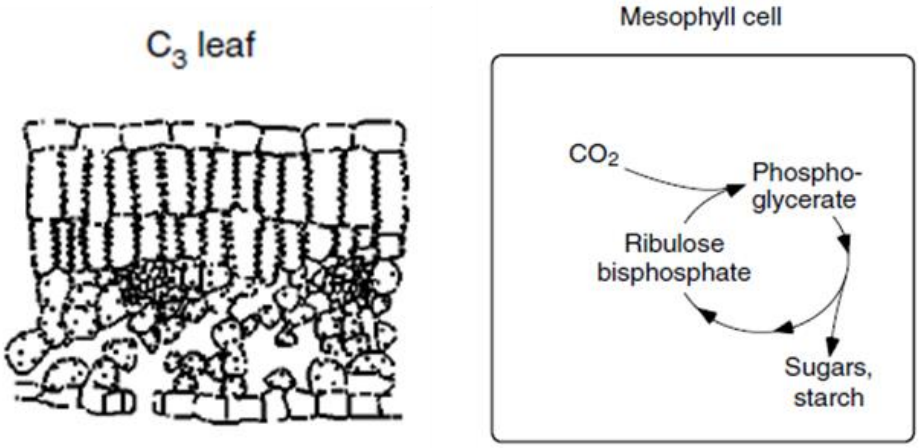


Figure 2.7: Leaf anatomy and photosynthetic biochemistry of C_3 plants (Adapted from Ehleringer & Cerling 2002: 2).

C_3 plants have $\delta^{13}C$ values ranging from -36‰ to -24‰, with a mean of -26.5‰ (Smith 1972; Lee-Thorp 2008; Loftus *et al.* 2016a). This pathway begins with the uptake and transfer of atmospheric CO_2 across the stomata and into the internal gas space of leaves, resulting in an apparent fractionation of roughly 4.4‰ (O'Leary 1988: 398; Diefendorf *et al.* 2010: 5738). Kinetic isotope effects are responsible for this as $^{12}CO_2$ is selectively diffused over $^{13}CO_2$ (Farquhar *et al.* 1989: 505). Carbon dioxide dissolves and diffuses to the chloroplast, where the enzyme ribulose-1.5-biphosphate carboxylase/oxygenase (Rubisco) combines CO_2 with ribulose bisphosphate to form two three-carbon molecules of phosphoglycerate (Ehleringer & Cerling 2002). This reaction results in further discrimination of ^{13}C because differences in the kinetic constants of each reaction lead to the preferential absorption of $^{12}CO_2$ (Farquhar *et al.* 1989: 505). Furthermore, a second discrete reaction is catalysed by Rubisco and occurs when oxygen (O_2) is the substrate. A phosphoglycolate (two-carbon sugar) and a phosphoglycerate molecule are produced (Ehleringer & Cerling 2002). This oxygenase reaction is known as photorespiration and occurs when O_2, light, and temperature are high, and CO_2 and water are low. This results in reduced net carbon fixation as a CO_2 molecule is formed and then lost through the stomata (Wingler *et al.* 2000; Ehleringer & Cerling 2002; Edwards *et al.* 2010). The efficiency of the C_3 pathway is,

therefore inhibited by Rubisco's sensitivity to O_2 (Ehleringer & Cerling 2002). Nevertheless, photorespiration may protect against certain stresses that can cause structural changes in chloroplast, reduce the rate of photosynthetic CO_2 assimilation, and impede plant growth (Wingler *et al.* 2000: 1517). The C_3 pathway evolved over 2800 million years ago in a CO_2-rich atmosphere. Atmospheric CO_2 began to decline 30 million years ago reducing the efficacy of the C_3 pathway and creating a niche for the development of two other photosynthetic pathways, specifically C_4 and CAM (Edwards *et al.* 2010).

C_4 grasslands emerged globally as an important ecosystem roughly six to eight million years ago (Ehleringer & Cerling 2002: 187). Plants utilising this pathway include maize, sorghum, sugarcane, and tropical grasses (Sharp 2017: 189). They have $\delta^{13}C$ values ranging from -17‰ to -9‰, with a mean of -12.5‰ (Smith 1972; Lee-Thorp *et al.* 2007; Lee-Thorp 2008). This pathway (Fig. 2.8) begins with the absorption of atmospheric CO_2 through the stomata which is subsequently fixed by phosphoenolpyruvate (PEP) carboxylase enzyme in the mesophyll cells, producing oxaloacetate, a four-carbon sugar, which is transferred to the bundle sheath cells where a phosphoglycerate molecule and CO_2 are formed (O'Leary 1988: 330; Marshall *et al.* 2007: 23). The CO_2 formed during photosynthesis is concentrated in the bundle sheath cells, where it is resorbed and refixed by Rubisco, allowing CO_2 to be retained (Ehleringer & Cerling 2002; Marshall *et al.* 2007; Sharp 2017).

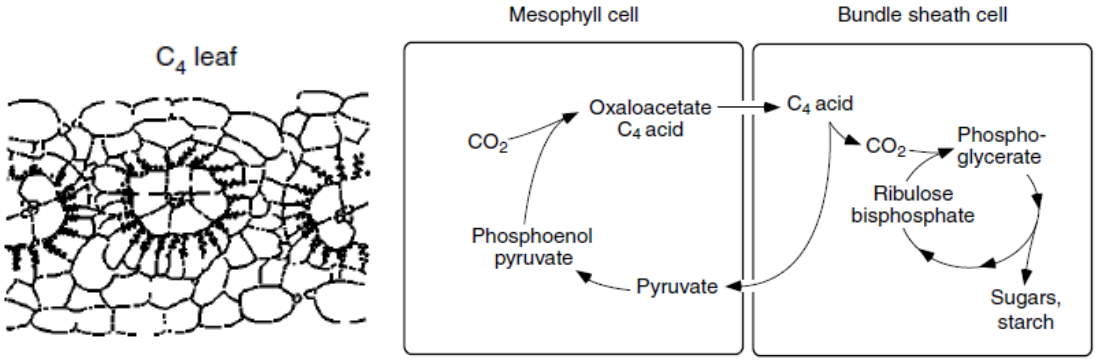


Figure 2.8: Leaf anatomy and photosynthetic biochemistry of C_4 plants (Adapted from Ehleringer & Cerling 2002: 2).

The adverse effects of photorespiration are minimised in C_4 photosynthesis making it more efficient than C_3 photosynthesis in hot and dry environments, when insolation is strong and direct, and atmospheric CO_2 is low (e.g., during the LGM) (Vogel *et al.* 1978; Ehleringer *et al.* 1997; Ehleringer & Cerling 2002; Sharp 2017). However, under elevated atmospheric CO_2, cool temperatures, shade cover, and increased moisture availability, photorespiration is

minimised in C_3 plants and the efficiency of C_4 photosynthesis is offset by the additional adenosine triphosphate cost involved (Ehleringer & Cerling 2002: 186; Sharp 2017: 188). A third photosynthetic pathway, CAM, developed in some plants growing in arid conditions (Sponheimer & Cerling 2014).

Plants utilising the CAM pathway are usually succulents like agave, bromeliads, cacti, and euphorbia. These plants are adapted to arid environments with low atmospheric moisture and high temperatures (Sponheimer & Cerling 2014). Two types of CAM plants exist, namely, obligate and facultative. Obligate CAM plants use the C_4 photosynthetic pathway and carboxylating enzymes but split enzyme activity between day and night (DeNiro 1987; Marshall *et al.* 2007). Carbon dioxide diffuses through the stomata and is fixed by the enzyme PEP carboxylase into oxaloacetate at night. It is then reduced to and stored as malate in the vacuoles of bulky leaves and stems (O'Leary 1988; Farquhar *et al.* 1989; Marshall *et al.* 2007). The stomata close at dawn and malate is decarboxylated, releasing CO_2 which is refixed by Rubisco (O'Leary 1988; Farquhar *et al.* 1989; Marshall *et al.* 2007). Carbon-13 is similarly discriminated against in both C_4 and obligate CAM plants, thus obligate CAM plants have $\delta^{13}C$ values ranging from -14‰ to -10‰, with a mean of -11‰ (Luyt 2001; Marshall *et al.* 2007). Alternatively, facultative CAM plants, fluctuate between C_3 photosynthesis during favourable conditions and CAM photosynthesis during unfavourable conditions, thus their $\delta^{13}C$ values range between C_3 plants (-26.5‰) and obligate CAM plants (-11‰) (Marshall *et al.* 2007; Britton 2010).

The distribution (Fig. 2.9) of C_4 plants is strongly influenced by growing season temperature (Ehleringer *et al.* 1997). In southern Africa, C_4 plants dominate (>50%) areas with maximum summer temperatures exceeding 25 °C. C_3 plants typically replace C_4 plants in the Winter Rainfall Zone (WRZ), shaded and moist habitats like forests, and at higher altitudes and latitudes (Vogel *et al.* 1978; Tieszen *et al.* 1979a; Livingstone & Clayton 1980; Smith *et al.* 2002). While CAM plants are mostly found in desert, high-salinity, and semi-arid environments (Sponheimer & Cerling 2014). The isotopic composition of plants is affected by several factors including edaphic factors, minor physiological adaptations, partial pressure, and environmental conditions (Ehleringer *et al.* 1997; Diefendorf *et al.* 2010; Sponheimer & Cerling 2014; Loftus *et al.* 2016a). Environmental conditions such as moisture availability, canopy effects, CO_2 concentration, and temperature affect $\delta^{13}C$ values (Tieszen 1991, van der Merwe & Medina 1991; Heaton 1999; Diefendorf *et al.* 2010; Kohn 2010).

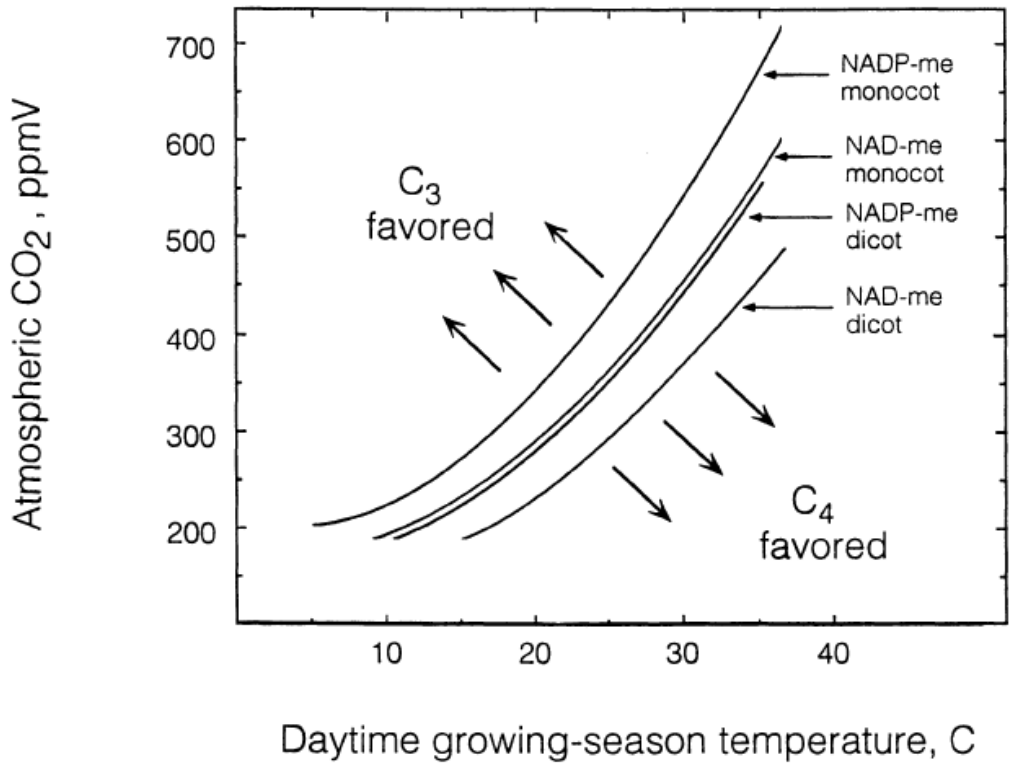


Figure 2.9: The relationship between growing season temperature and pCO_2 showing the modelled crossover favouring C_3 and the different C_4 plants (In Ehleringer et al. 1997: 292).

An inverse relationship was found between $\delta^{13}C$ and water availability (Swap *et al.* 2004; Murphy & Bowman 2009). Swap *et al.* (2004) found a weak inverse relationship ($r^2 = 0.2$) between water-stress and the $\delta^{13}C$ values of C_3 plants from southern Africa; however, this was not found in C_4 plants. In Australia, Murphy and Bowman (2009) report a similar relationship between water availability and the $\delta^{13}C$ values of C_3 grasses ($r^2 = 0.21$), and a weak relationship in C_4 grasses. Generally, C_3 plants tend to have more positive $\delta^{13}C$ values in arid environments due to the partial closure of their stomata to conserve water, resulting in decreased discrimination of ^{13}C by Rubisco during photosynthesis. C_4 plants, however, are thought to be relatively insensitive to changes in water availability, exhibiting less isotopic variability than C_3 plants (Farquhar *et al.* 1989; Ambrose 1993; Swap *et al.* 2004). Both positive (Peisker & Henderson 1992; Schulze *et al.* 1996; Dercon *et al.* 2006; Murphy & Bowman 2009; Cernusak *et al.* 2013; An *et al.* 2015; Lightfoot *et al.* 2016, 2020; Sanborn *et al.* 2021) and negative (Peisker & Henderson 1992; Ghannoum *et al.* 2002; Weiguo *et al.* 2005; Cernusak *et al.* 2013) correlations are found between $\delta^{13}C$ and water availability in C_4 plants and has been associated with the amount of CO_2 leakage out the bundle-sheath cells (Farquhar *et al.* 1989; Lightfoot *et al.* 2016, 2020).

Murphy and Bowman (2009) also examined the relationship between $\delta^{13}C$ and temperature in C_3 and C_4 grasses. This relationship was less significant than the one described above, although increases in photorespiration and decreases in net carbon fixation are observed in C_3 plants. C_4 plants become more efficient at high temperatures (Vogel *et al.* 1978; Ehleringer *et al.* 1997; Luyt 2017). Variations in the isotopic signatures of plants are transferred to consumers through diet with some additional fractionation (Fig. 2.10) (Vogel 1978; van der Merwe & Vogel 1983; Lee-Thorp *et al.* 1989; Ambrose & Norr 1993; Cerling & Harris 1999; Hoefs 2004; Passey *et al.* 2005; Codron *et al.* 2006, 2012; Codron & Brink 2007; Lee-Thorp 2008).

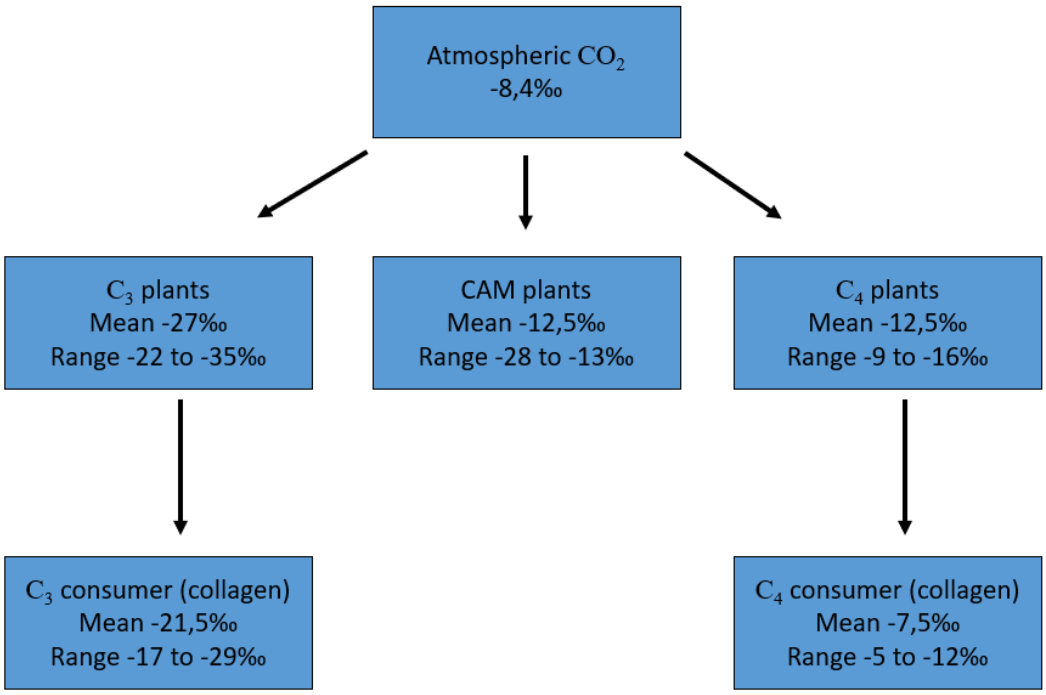


Figure 2.10: Approximate fractionation factors for modern terrestrial food chain (Adapted from Lee-Thorp et al. 1989).

This was first documented by DeNiro and Epstein (1978) who fed mice (*Mus musculus*) and eight species of invertebrate diets of known isotopic compositions and found marginal enrichments of approximately 1‰ in their tissues relative to diet (DeNiro & Epstein 1978: 495). Further experimental studies revealed that collagen is typically enriched in ^{13}C by 3.7‰ to 6.0‰, averaging 5.0‰ relative to diet (Ambrose & Norr 1993; Bocherens & Drucker 2003; Kellner & Schoeninger 2007). Tieszen *et al.* (1979b) showed that the $\delta^{13}C$ values of eight ungulate species rumen contents provided an estimate of the proportion of C_3 to C_4 plants consumed. This was strongly correlated with visual identifications of plant fragments. Importantly, differences in the isotopic composition of C_3 and C_4 plants, as well as the

widespread occurrence of C_4 grasses in South Africa, allow grazers (C_4) and browsers (C_3) to be distinguished from one another (Vogel 1978). Thus, animals consuming predominately C_4 grass have higher $\delta^{13}C$ values than C_3 browsers (Sponheimer *et al.* 2003a). Although environmental factors contribute to variations in $\delta^{13}C$, mean $\delta^{13}C_{collagen}$ values for modern C_3 and C_4 consumers are approximately -21‰ and -6‰, respectively, with intermediate feeders falling between these values (Vogel 1978).

2.3.3 STABLE NITROGEN ISOTOPES

There are two stable nitrogen isotopes, namely, nitrogen-15 (^{15}N) and nitrogen-14 (^{14}N) (Faure 1986: 513; Sharp 2017: 242). Nitrogen mostly occurs as atmospheric dinitrogen gas (N_2) and has a $\delta^{15}N$ value of 0‰ and serves as an extensive, well-combined reservoir that propels the nitrogen cycle (Peterson & Fry 1987; Ambrose 1991: 295; Fry 2006: 46). A diverse range of biogeochemical processes affects the $\delta^{15}N$ value of plant-soil systems and an understanding of these processes are essential for the assessment of isotopic variation in consumer tissues (Szpak 2014: 1).

The nitrogen cycle (Fig. 2.11) comprises several complex processes resulting in isotope fractionation (Sharp 2017: 248). These processes are difficult to quantify because most of them are the result of kinetic not equilibrium isotope effects. Ambient conditions, nutrient availability, and reaction rates influence the degree of fractionation (Sharp 2017: 244). For example, biological nitrogen fixation of N_2 leads to lower $\delta^{15}N$ values in soils while higher $\delta^{15}N$ soil values result from denitrification (Heaton 1986; Ambrose 1991).

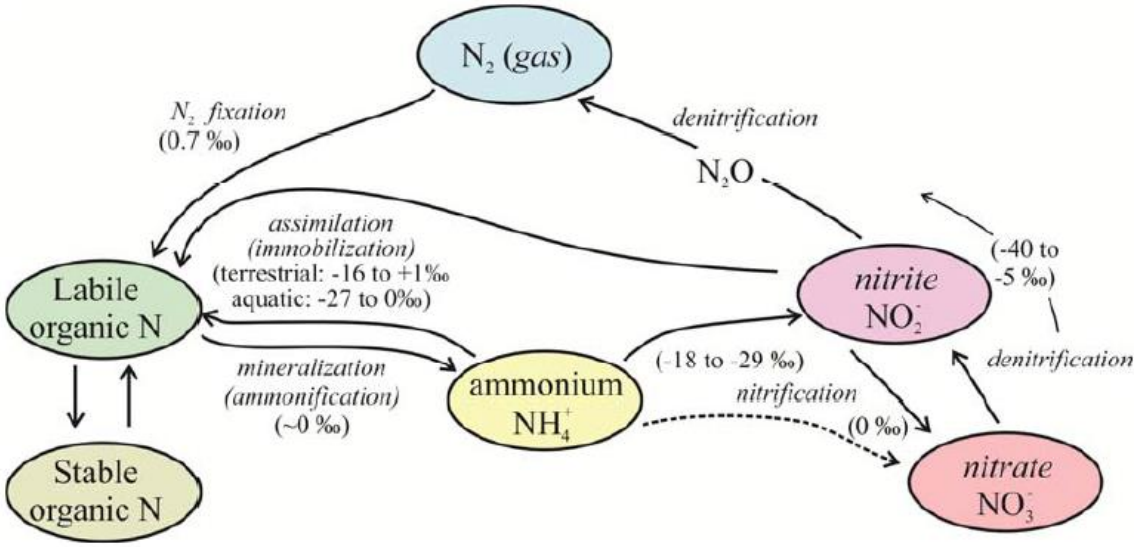


Figure 2.11: Simplified diagram of the nitrogen cycle with average fractionation for each process included (In Sharp 2017: 243).

In hot and arid conditions, nitrogen fixation is inhibited, resulting in higher $\delta^{15}N$ (Ambrose 1991: 296; Handley *et al.* 1999; Hedges *et al.* 2004; Koch 2007; Szpak 2014). Similarly, higher $\delta^{15}N$ soil values occur from the volatilisation of ammonia which is depleted by approximately 34‰ compared to its ammonium substrate (Kreitler 1975; Ambrose 1991). Ammonia volatilisation significantly increases at high temperatures, high pH, and in dry soils (Ambrose 1991: 296). Soil from cool and moist environments tends to have lower $\delta^{15}N$ values and increased rates of mineralisation and nitrogen fixation (Ambrose 1991; Handley *et al.* 1999; Amundson *et al.* 2003; Hedges *et al.* 2004; Koch 2007; Murphy & Bowman 2009; Szpak 2014).

The $\delta^{15}N$ values of soils range from -10‰ to +15‰, averaging between 2‰ and 5‰ (Sharp 2017: 248). Several factors influence these values including the physical composition of soils, soil maturity, ammonium (NH_{4+}) and nitrate (NO_{3-}) dispersion, pH, moisture availability in soils, salinity, oxygen content, relationship with nitrogen-fixing bacteria or mycorrhizal fungi, and temperature, likely resulting in intra-habitat differences in the $\delta^{15}N$ values of plants (Heaton 1987; Ambrose 1991; Koch 2007; Pate & Anson 2008; Makarewicz 2014; Szpak 2014). Leguminous plants may incorporate nitrogen through a mutualistic relationship with N_2-fixing bacteria while non-leguminous plants incorporate nitrogen through the assimilation of inorganic NH_{4+} or NO_{3-} from the soil (Virginia & Delwiche 1982; DeNiro 1987: 184; Sharp 2017: 248). The $\delta^{15}N$ values of leguminous plants differ from non-leguminous plants and are more depleted in ^{15}N (Heaton 1987; Craine *et al.* 2009; Spriggs & Dakora 2009; Hobbie & Högberg 2012; Szpak 2014). For example, Spriggs and Dakora (2009) documented $\delta^{15}N$ values between -3.6‰ and -0.1‰ in leguminous plants (e.g., *Cyclopia*) growing in the Fynbos biome in South Africa.

Global variations in the $\delta^{15}N$ values of soils and plants are related to differences in MAP and MAT (Heaton 1987; Sharp 2017: 248). An inverse relationship (-0.39‰/100 mm rain per year) exists between $\delta^{15}N$ plant values and precipitation while a direct relationship exists between $\delta^{15}N$ plant values and temperature (>0.5 °C) (Heaton *et al.* 1986a; Heaton 1987; Handley *et al.* 1999; Hartman & Danin 2010; Szpak *et al.* 2013: 8). This is likely related to the relative 'openness' of the nitrogen cycle which leads to the loss of nitrogen in hot, dry environments and the conservation and recycling of nitrogen in cool, moist environments (Handley *et al.* 1999; Pate & Anson 2008; Szpak *et al.* 2013: 9). Swap *et al.* (2004) examined the relationship between $\delta^{15}N$ and rainfall in southern African plants and discovered a stronger relationship in C_3 plants ($r^2 = 0.54$) compared to C_4 plants ($r^2 = 0.04$). A similar

study was conducted in Australia by Murphy and Bowman (2009). An inverse relationship (r^2 = 0.40) was found between $\delta^{15}N$ and moisture availability for C_3 and C_4 grasses suggesting that moisture availability regulated $\delta^{15}N$ (Murphy & Bowman 2009). Codron *et al.* (2013) examined the effects of rainfall (300–700 mm per annum) and temperature on the $\delta^{15}N$ values of C_3 foliage and C_4 grasses from the Kruger National Park, South Africa. They found no correlation between the $\delta^{15}N$ values of C_4 grasses or C_3 foliage and rainfall or temperature ($0.01< r^2 <0.08$) and suggested that these results were constrained by the limited range of rainfall.

Nitrogen is incorporated into animal tissue through diet. Consumer tissue is systematically enriched in ^{15}N relative to diet and is used to determine trophic level and dietary sources (DeNiro & Epstein 1981; Schoeninger *et al.* 1983; Minagawa & Wada 1984; Schoeninger & DeNiro 1984; Peterson & Fry 1987; Sealy *et al.* 1987; Ambrose 1991; Bocherens & Drucker 2003; Sponheimer *et al.* 2003*b*; Caut *et al.* 2008, 2009; O'Connell *et al.* 2012; Szpak *et al.* 2012). Early studies (DeNiro & Epstein 1981; Schoeninger *et al.* 1983; Minagawa & Wada 1984; Peterson & Fry 1987) suggest that tissue was typically enriched by 3‰ to 4‰ relative to diet, with higher values of ~6‰ being reported in later studies (Drucker & Bocherens 2004; O'Connell *et al.* 2012). Several factors influence the $\delta^{15}N$ values of animals, including diet composition, water and nutritional stress, environmental conditions, and digestive physiology (see review in McCue & Pollock 2008).

The $\delta^{15}N$ values of plants and animals vary along regional and global aridity gradients (Gröcke *et al.* 1997; Schulze *et al.* 1998; Kelly 2000; Hedges *et al.* 2004; Murphy & Bowman 2006). Figure 2.12 shows the relationship between precipitation and $\delta^{15}N$ in fauna from different regions. Kelly (2000) compiled meta-data from 60 global mammal studies, revealing a relationship between MAT, MAP, and the $\delta^{15}N_{collagen}$ values of mammals. Herbivores inhabiting arid environments had mean $\delta^{15}N$ values of 8.7 ± 2.8‰ (n = 12), while those inhabiting mesic environments had mean values of 6.3 ± 2.2‰ (n = 23) (Kelly 2000). This result may be affected by small sample sizes, but this relationship is recorded in other studies as well (Ambrose & DeNiro 1986a; Heaton *et al.* 1986a; Sealy *et al.* 1987; Schoeninger 1989; Cormie & Schwarcz 1996; Schwarcz *et al.* 1999; Kelly 2000; Dewar 2007; Pate & Anson 2008; Makarewicz & Sealy 2015; Hopper *et al.* 2018). Mean $\delta^{15}N$ values of herbivores from East Turkana, Kenya, where MAP is less than 250 mm per annum is 10.8 ± 1.0‰ (Schoeninger 1989) while in highland Kenya, where MAP exceeds 600 mm per annum, the mean is 7.1 ± 1.7‰ (Ambrose & DeNiro 1986a). The mean $\delta^{15}N$ values of

archaeological herbivores from Namaqualand, where MAP is between 20–50 mm per annum is 15.3 ± 0.9‰ (Dewar 2007: 270). Furthermore, the $\delta^{15}N$ values of juvenile archaeological springbok that died during a drought in Namaqualand range from 15.7‰ to 17.2‰ (Hopper *et al.* 2018) and the mean $\delta^{15}N$ values of herbivore collagen from the hyper-arid Dakhleh Oasis, range from 12.0‰ to 13.4‰ (Schwarcz *et al.* 1999: 631). Interestingly, the $\delta^{15}N$ values of animals from western Asia and northern Europe were markedly decreased following the LGM. This is likely associated with increases in moisture availability and precipitation that impacted the nitrogen cycle in soil (Hedges *et al.* 2004).

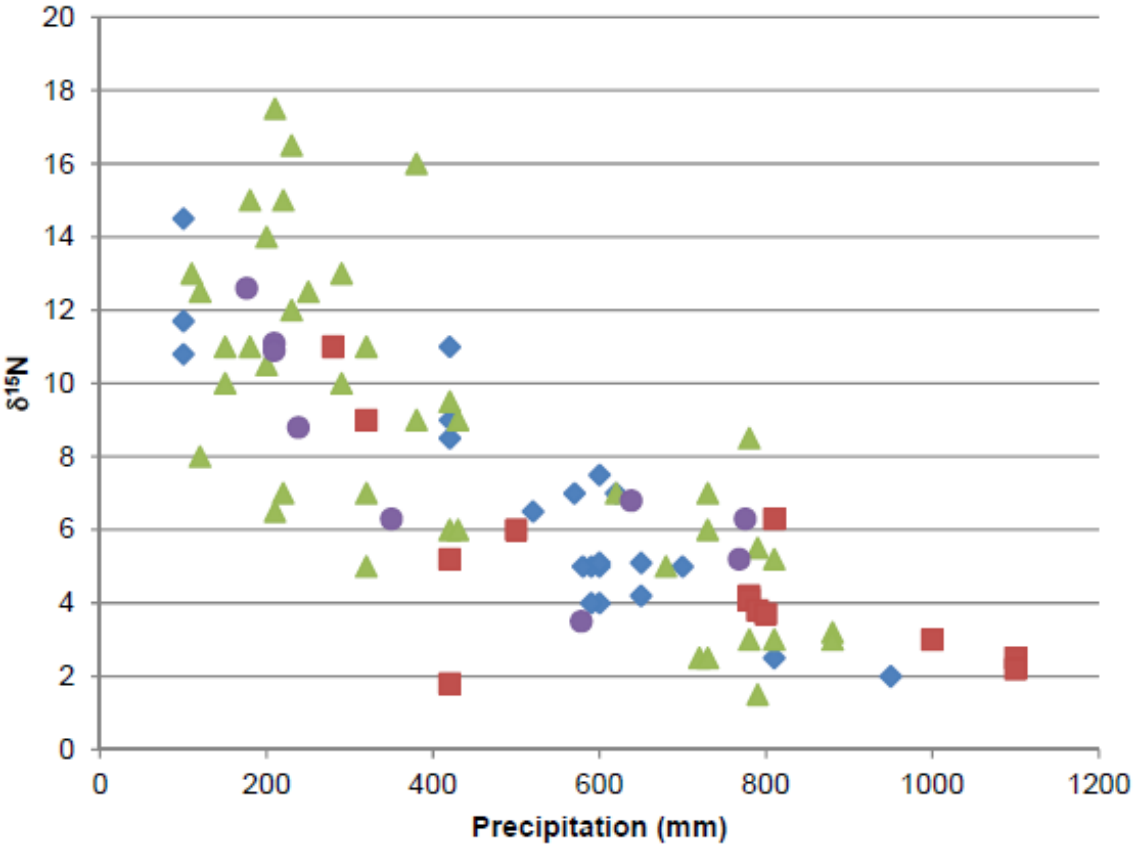


Figure 2.12: The relationship between precipitation and $\delta^{15}N_{collagen}$ faunal values from several studies. The data was compiled and extracted from southern Africa (Heaton et al. 1986a [blue diamond]; Sealy et al. 1987 [green triangle]), North America (Cormie & Schwarcz 1996 [red square]), and Australia (Pate & Anson 2008 [purple circle]) (In Luyt 2017: 43).

Four hypotheses are proposed to explain the relationship between aridity and $\delta^{15}N$ consumer values, including one dietary and three physiological hypotheses (Hartman 2011). The dietary hypothesis suggests that the $\delta^{15}N$ values of herbivore tissue reflect the $\delta^{15}N$ values of plants (Murphy & Bowman 2006). Murphy and Bowman (2006) found similar variations in both plants and kangaroos (*Macropus* spp.) along environmental gradients with increased values in arid environments. The offset between these values was relatively consistent, and thus

Murphy and Bowman (2006) suggest that $\delta^{15}N$ values of kangaroos are dependent on the $\delta^{15}N$ values of plants.

Other studies have rejected the dietary hypothesis and have suggested that variations in $\delta^{15}N$ plant values only account for one-third (-1.1‰ to -1.3‰/100 mm rain per year) of the covariance documented in herbivore bone collagen with rainfall (Heaton *et al.* 1986a; Heaton 1987; Sealy *et al.* 1987; Ambrose 1991). Therefore, $\delta^{15}N$ herbivore values are three times more sensitive to water stress than plants (Ambrose 1991). Physiological hypotheses were proposed to explain this relationship. The first physiological hypothesis was proposed by Ambrose and DeNiro (1986a), who found that ^{15}N is enriched in drought-tolerant animal tissue as proteins are catabolised to enhance water conservation. The second hypothesis suggests that animals living in arid environments have elevated $\delta^{15}N$ values resulting from nitrogen conservation through increased urea recycling and dependence on symbiotic gastrointestinal bacteria to accommodate for ^{15}N depletion in arid plants (Sealy *et al.* 1987). Finally, the third hypothesis explains that increased $\delta^{15}N$ values in water-stressed animals is likely the result of reduced nitrogen uptake and enhanced water recycling (Balter *et al.* 2006). This is accomplished by assimilating hydrolysed urea, enriched in ^{15}N, into amino acids which are then synthesised into body tissue (Balter *et al.* 2006).

Drought-tolerant or WI species likely have higher $\delta^{15}N$ values than obligate or WD species (Ambrose & DeNiro 1986a; Ambrose 1991; Luyt 2017). Sealy *et al.* (1987) not only documented lower $\delta^{15}N$ values in obligate drinkers but also found lower $\delta^{15}N$ values in grazers compared to browsers, especially those living in arid environments (Ambrose 1991). This could be related to the nutritional quality and digestibility of these diets, in particular, grass diets are more easily digestible but are of lower nutritional quality compared to trees and shrubs (Codron *et al.* 2007a; Robbins *et al.* 2010). Furthermore, the shallow roots of grasses may result in low $\delta^{15}N$ values (Evans & Ehleringer 1993). Alternatively, $\delta^{15}N$ values may be influenced by an animals' digestive physiology, such as the location of symbiotic cellulose-digesting bacteria in a herbivores gut (Luyt 2017). In herbivores with simple stomach structures, like equids, bacterially assisted fermentation occurs in the hindgut while in ruminants it occurs in the foregut (Langer 1984, 2002; Luyt 2017). Ruminants include browsers, such as duiker, eland (*Taurotragus oryx*), kudu (*Tragelaphus strepsiceros*), and grysbok (*Raphicerus* sp.), and grazers, such as blue wildebeest (*Connochaetes taurinus*), gemsbok (*Oryx gazella*), and red hartebeest (*A. buselaphus caama*) (Luyt 2017). The digestion and absorption of microbial bacteria by ruminants may lead to trophic level

enrichment (Sealy *et al.* 1987; Ambrose 1991). Conversely, hindgut fermenters do not digest and absorb these bacteria which are excreted in faeces (Codron & Codron 2009). Codron and Codron (2009) report a mean $\delta^{15}N$ value of 5.17 ± 1.5‰ (n = 1486) in ruminant faeces and a mean of 4.45 ± 1.3‰ (n = 267) in non-ruminant faeces. Notably, all the non-ruminants in this study were grazers so Codron and Codron (2009) compared these with the ruminant grazers and found that these differences persisted. However, the difference was small (<1‰) suggesting that eco-physiological adaptations only account for a small portion of this difference with dietary protein sources playing a primary role in $\delta^{15}N$ faecal values (Codron & Codron 2009).

Elevated CO_2 concentrations are linked to declines in the nitrogen content of plants (Cotrufo *et al.* 1998; Hungate *et al.* 2004; Luo *et al.* 2004; Bigras & Bertrand 2006). Plant nitrogen content also decreases with increased MAT (Yin 1993) and decreased MAP (Olff *et al.* 2002; Swap *et al.* 2004). The relative importance of each variable in driving a decline in plant nitrogen content is presently unclear (Faith 2011b). However, given the abrupt climate reversals associated with the YD, atmospheric CO_2 is likely the only variable to have uniformly increased since the LGM (Monnin *et al.* 2001). This would affect nitrogen flow through the food chain (Fig. 2.13) and may have resulted in reduced carrying capacity or extinctions (Pastor *et al.* 2006; Faith 2011b). The detrimental effects of reduced nutrient availability resulting from environmental change have been demonstrated by Hjeljord and Histol (1999), who found that calves and yearling moose (*Alces alces*) from Norway had reduced body mass during warmer summers, likely due to reduced forage quality.

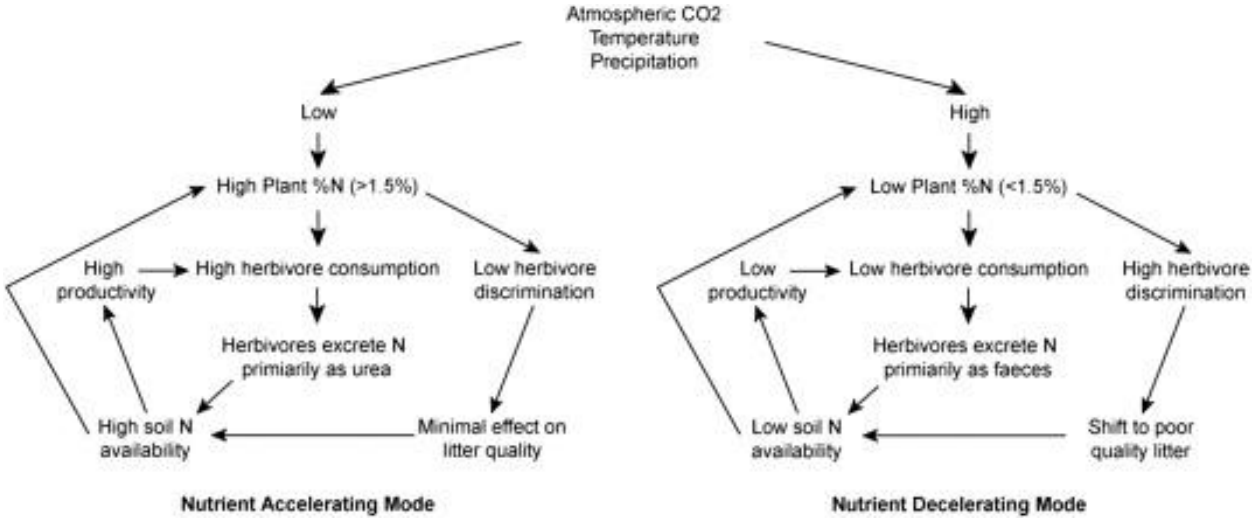


Figure 2.13: Plant-herbivore dynamics with reference to environmental parameters (In Faith 2011b: 1678).

Nutritional stress increases nitrogen isotope fractionation during tissue synthesis (Hobson *et al.* 1993; Adams & Sterner 2000; Kelly 2000; Oelbermann & Scheu 2002; Robbins *et al.* 2005; Fuller *et al.* 2005; Reitsema 2013; Kuitems *et al.* 2015). Under nutritional stress, the body may catabolise its tissues to maintain adequate nitrogen balance resulting in ^{15}N enrichment (Hobson & Clark 1992; Hobson *et al.* 1993; Robbins *et al.* 2005; Parker *et al.* 2005; Reitsema 2013). These effects were initially observed in birds by Hobson and Clark (1992) and Hobson *et al.* (1993). Hobson *et al.* (1993) reported elevated $\delta^{15}N$ values in incubating birds that fasted for 19–25 days. Studies by Mekota *et al.* (2006) and Hatch *et al.* (2006) reported elevated $\delta^{15}N$ values in humans being treated for eating disorders. Hair was sampled longitudinally (root to end) and was enriched by approximately 0.5‰ to 2.0‰ during periods of nutritional stress relative to the treatment period. Both studies found an inverse relationship between Body Mass Index and $\delta^{15}N$ (Hatch *et al.* 2006; Mekota *et al.* 2006). The effects of nutritional stress on $\delta^{15}N$ have been widely reported (see Polischuk *et al.* 2001; Cherel *et al.* 2005; Barboza & Parker 2006; Boag *et al.* 2006; Barboza & Parker 2008; Gustine *et al.* 2011), but there are exceptions (Ambrose 2000; Kempster *et al.* 2007). Nutritional stress may also lead to ^{13}C enrichment of tissues as ^{13}C-depleted lipid reserves are metabolised (DeNiro & Epstein 1977; Tieszen *et al.* 1983), however, no significant change is reported in some studies (Varela *et al.* 2015). These exceptions are reviewed in Hatch (2012), and it is suggested that $\delta^{15}N$ and $\delta^{13}C$ are not affected by mild nutritional stress.

2.3.4 ZOOMS AND STABLE CARBON AND NITROGEN ISOTOPES

Zooarchaeological studies could benefit from the combined use of ZooMS and stable isotopes. To date, one southern African study combines both techniques (Coutu *et al.* 2016). This study provided the earliest evidence of large-scale ivory processing in southern Africa, the pioneer of a larger more extensive trade-network that developed later (Coutu *et al.* 2016: 431). Furthermore, species-level identifications were achieved by ZooMS and the isotope results showed that the ivory was sourced from a widespread area.

The combination of ZooMS and stable isotopes has the potential to validate and verify one another, reduce bias, strengthen interpretations, provide additional insight into behavioural, dietary, and physiological adaptations to environmental change, and increase taxonomic resolution (van der Sluis *et al.* 2014; Coutu *et al.* 2016; Buckley 2018; Thomas & Miller 2018, Janzen *et al.* 2021).

2.4 PALAEOENVIRONMENT

Palaeoenvironmental reconstructions provide valuable insight into the archaeological record as the environment provides the context in which organisms live, interact, and adapt (Lyman 2017). The environment is complex and multifaceted, varying along spatial and temporal scales (Lyman 2017). A wide range of proxy data are used to reconstruct past environments, producing both complementary and contradictory data as individual proxies respond to climate change at different rates, experience some degree of temporal lag, and/or have variable resolutions (Jones & Mann 2004; Scott & Lee-Thorp 2004; Lewis 2011; Meadows 2014; Stone 2014; Stewart & Mitchell 2018; Lukich *et al.* 2020; Stratford *et al.* 2021). To overcome these issues multiple proxies should be employed and the limitations of each proxy, its archive, and the proxy's provenance should be fully understood (Jones & Mann 2004; Meadows 2014; Stone 2014; Zhao *et al.* 2016a).

Palaeoenvironmental reconstructions were initiated relatively late in southern Africa and were constrained by uncertain chronologies and inadequate comparative collections (van Zinderen Bakker 1962; Coetzee 1967; Martin 1968; Scott 1976, 1982a, b, 1989; van Zinderen Bakker & Coetzee 1988). Some of these issues have been addressed by advances in and access to high precision dating facilities, large comparative collections, and the expansion of proxy records including biomarkers (Kristen *et al.* 2010; Norström *et al.* 2014; Carr *et al.* 2015), dinoflagellate cysts (Dupont *et al.* 2004), faunal remains (Klein 1972, 1978, 1980; Avery 1982), foraminifera (Strachan *et al.* 2014, 2015, 2016), isotopes (Heaton *et al.* 1986b; Talma & Vogel 1992; Holmgren *et al.* 1995, 1999, 2003; Abell & Plug 2000; Smith *et al.* 2002; Bar-Matthews *et al.* 2010; Kristen *et al.* 2010; Chase *et al.* 2012; Weldeab *et al.* 2013; Sealy *et al.* 2016, 2020; Ecker *et al.* 2018), molluscs (Voigt 1982), phytoliths (Rossouw *et al.* 2009; Burrough *et al.* 2012; Backwell *et al.* 2014; Cordova & Avery 2017), and pollen (van Zinderen Bakker 1962; Scott *et al.* 2012; Truc *et al.* 2013). Figure 2.14 shows the published proxy data from southern Africa.

Nevertheless, the southern African record is impeded by significant spatial and temporal gaps leading to broad reconstructions that overlook regional differences (Meadows & Baxter 1999; Stone 2014; Stratford *et al.* 2021); resulting from poor preservation (Meadows *et al.* 2010), intermittent records (Talma & Vogel 1992; Holmgren *et al.* 2003), unreliable chronologies, and/or the absence of suitable proxies (Chase & Meadows 2007; Kristen *et al.* 2007; Neumann *et al.* 2008; Stone 2014; Fitchett *et al.* 2017a). Thus, the use of feasible proxies

from well-dated and biogeoclimatically diverse sites is critical to reconstructing palaeoenvironmental conditions across southern Africa through time.

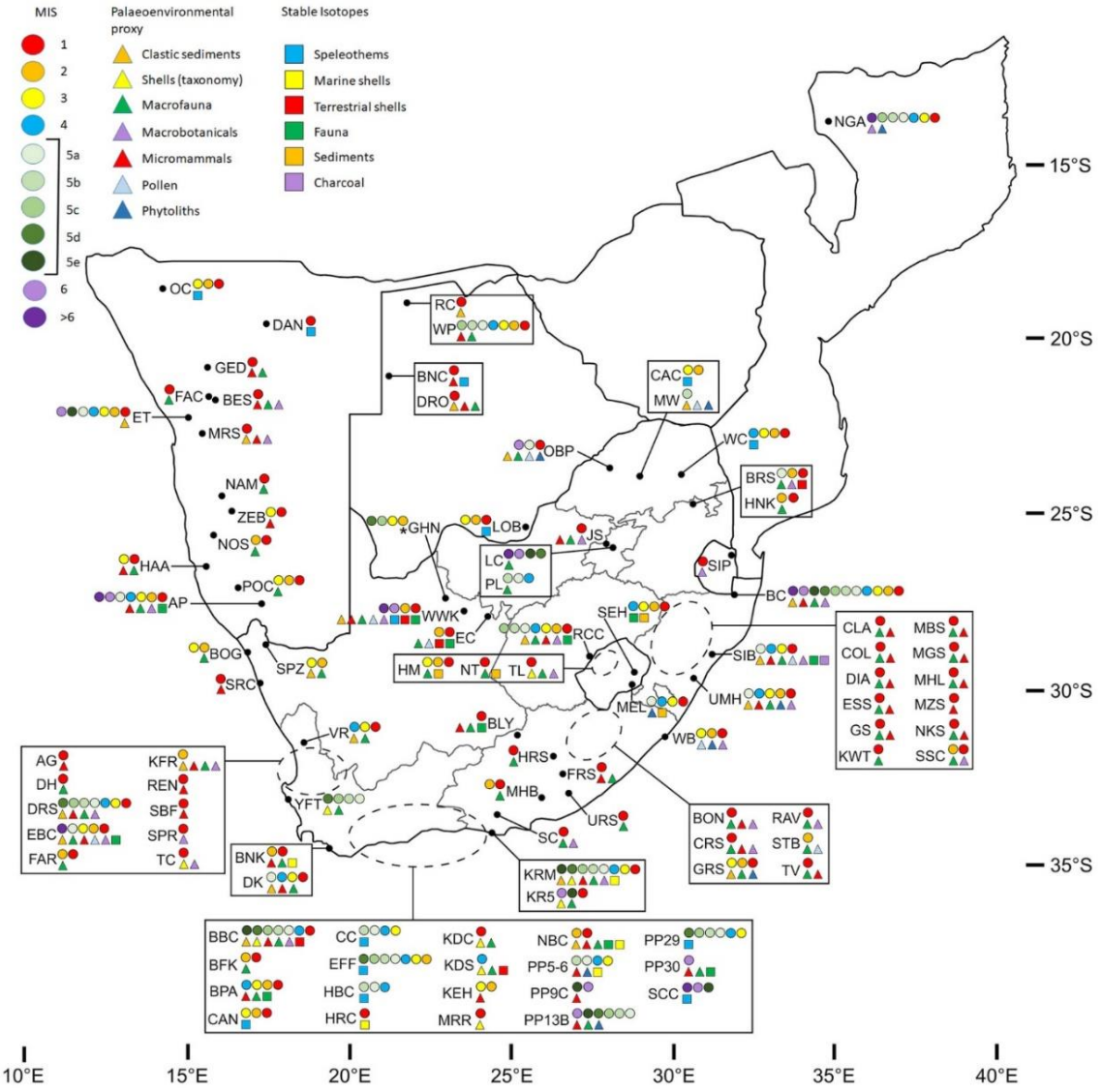


Figure 2.14: Map of southern Africa with locations of caves and rock shelter sites with published dates and palaeoenvironmental data from Marine Isotope Stage 6 to 1. Sites and abbreviations are listed in Table 1 in Stratford et al. (2021: 882-889) (In Stratford et al. 2021: 881).

2.4.1 THE PALAEOENVIRONMENT OF SOUTHERN AFRICA

Southern Africa's environment is influenced by several oceanic and atmospheric circulation systems (Fig. 2.15). It encompasses the sub-tropics to mid-latitudes, comprises several different climates and biomes, and is surrounded by the Atlantic, Indian, and Southern Ocean (Mucina & Rutherford 2006; Chase & Meadows 2007; Mills *et al.* 2012; Green *et al.* 2015; Sealy *et al.* 2016; Fitchett *et al.* 2017a). Climatic changes in southern Africa are primarily driven by circulation systems which are influenced by polar ice cap encroachment and retreat

and orbital forcing mechanisms at global, hemispheric, and regional levels (Tyson 1986; Tyson & Preston-Whyte 2000; Lutjeharms *et al.* 2001; Stuut *et al.* 2004; Stone 2014; Chase *et al.* 2015a, b, 2017; Chevalier & Chase 2015, 2016; Chase 2021).

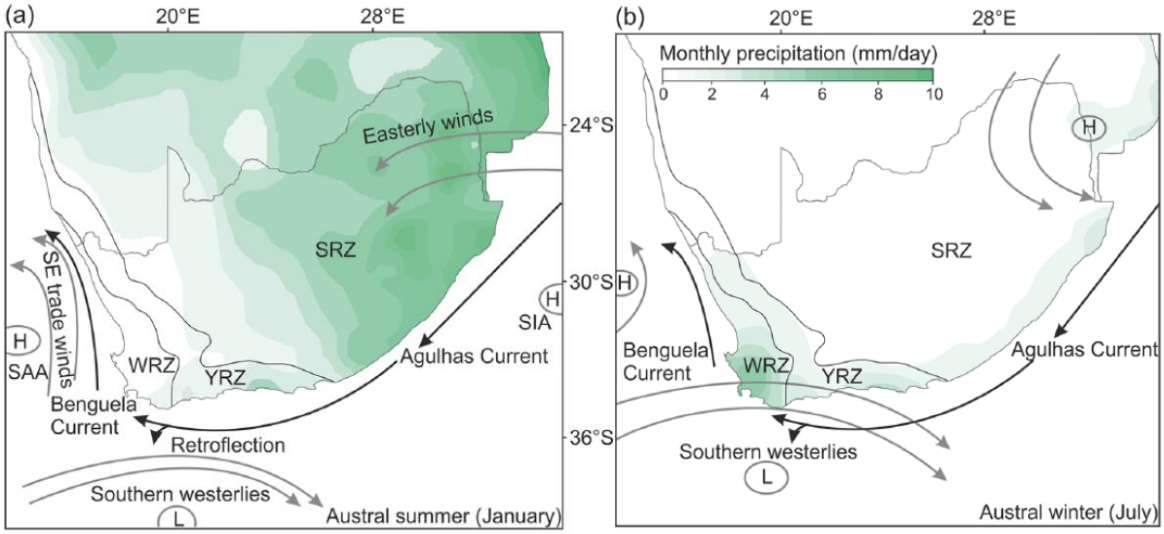


Figure 2.15: Modern oceanic and atmospheric circulation systems. Mean monthly precipitation is included from 1981-2010 across southern Africa during (a) austral summer and (b) austral winter. The three rainfall zones (i.e., SRZ, YRZ, and WRZ) are shown as well as the South Atlantic Anticyclone, South Indian Anticyclone, Benguela Current, and Agulhas Current (Tyson & Preston-Whyte 2000) (In Zhao et al. 2016b: 844).

Southern Africa is subdivided into three climate zones (Fig. 2.15), namely, the Summer Rainfall Zone (SRZ), Year-round Rainfall Zone (YRZ), and WRZ (Chase & Meadows 2007; Engelbrecht *et al.* 2015). The SRZ and WRZ primarily interact through tropical-temperate troughs, which result in significant precipitation events and likely plays a dominant role in precipitation trends in the arid interior (Nicholson 1986; Tyson 1986; Chevalier & Chase 2015). This interaction also influences biome distribution and the proportion of C_3 to C_4 grasses (Vogel *et al.* 1978; Zhao *et al.* 2016b). For example, dry conditions and lower atmospheric CO_2 associated with glacial periods may have led to the replacement of C_3 vegetation with C_4 grasslands (Ehleringer *et al.* 1997; Schefuβ *et al.* 2003).

The position of the Intertropical Convergence Zone (ITCZ), sub-tropical high-pressure cells, sea surface temperature (SST) of the Indian Ocean, and the Agulhas current likely affect the SRZ (Fig. 2.15) (Tyson & Preston-Whyte 2000; Holmgren *et al.* 2003; Chase & Meadows 2007; Dupont *et al.* 2011; Stone 2014; Zhao *et al.* 2016b). The SRZ and WRZ are separated by the YRZ which receives aseasonal rainfall (Chase & Meadows 2007). Austral winter rainfall is received in the WRZ as frontal systems embedded in westerlies shift northwards

(Tyson & Preston-Whyte 2000; Chase & Meadows 2007; Mills *et al.* 2012; Stager *et al.* 2012; Zhao *et al.* 2016b).

The WRZ likely expanded beyond its current limits during glacial periods (Fig. 2.16). Three hypotheses are proposed for this expansion, but the geographic limits of these expansions are uncertain (Carr *et al.* 2006; Chase & Meadows 2007; Stager *et al.* 2012; Thackeray & Fitchett 2016; Fitchett & Bamford 2017). The first predicts a northward expansion extending into Namibia, the second predicts an eastward expansion encroaching on the present-day YRZ, and the third predicts an expansion into the interior region of southern Africa (van Zinderen Bakker 1967, 1976; Heine 1982; Cockcroft *et al.* 1987; Barrable *et al.* 1998; Carr *et al.* 2006; Chase & Meadows 2007; Stager *et al.* 2012; Fitchett & Bamford 2017; Engelbrecht *et al.* 2019).

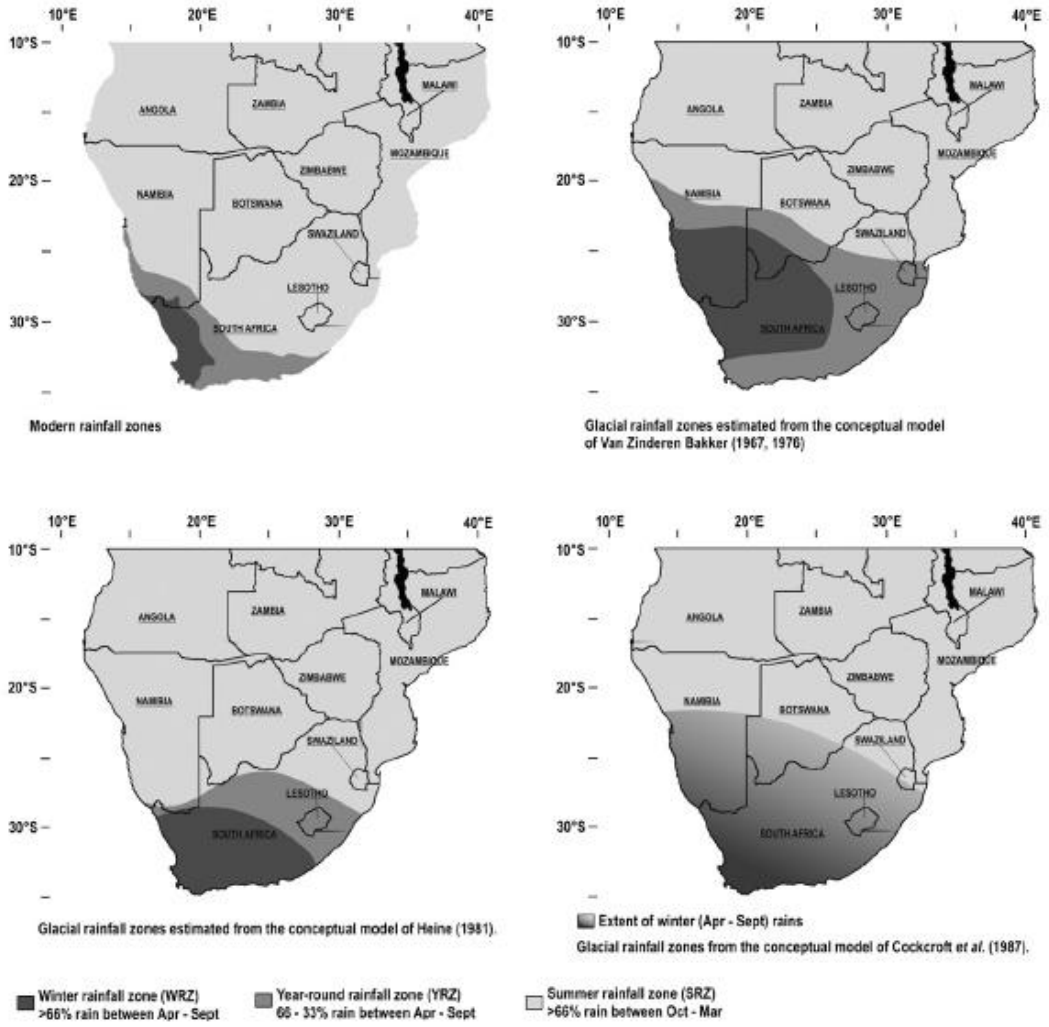


Figure 2.16: An evaluation of modern southern African rainfall zones. Conceptual models have been proposed (see Engelbrecht et al. 2019) to elucidate the rainfall seasonality and distribution during glacial periods (In Chase & Meadows 2007: 109).

2.4.2 MARINE ISOTOPE STAGE 3 (57–29 KA)

Palaeoenvironmental conditions in southern Africa were relatively mild with varying degrees of aridity during MIS 3 (Barham & Mitchell 2008). Humid conditions are recorded at Gladysvale, Lobatse, and Wolkberg Caves between ca. 56–42 ka (Holzkämper *et al.* 2009), increased precipitation is documented between ca. 55–48 ka at Tswaing Crater (Kristen *et al.* 2007), arid events are widespread in northern Botswana between 43–40 ka and 28–25 ka (Stokes *et al.* 1997), cold and dry conditions occur between ca. 44–42 ka at Thabana Ntlenyana, in Lesotho (Grabs & Mills 2011), cool and moist conditions are documented between ca. 35–33 cal. kBP at Wonderwerk Cave with a brief dry period at ca. 34 cal. kBP (Brook *et al.* 2010), and moist conditions are suggested in South Africa's WRZ (Cowling *et al.* 1999; Carr *et al.* 2006). Widespread human occupation is recorded across a range of biogeoclimatic zones in the interior of southern Africa (Opperman & Heydenrych 1990; Mitchell & Steinberg 1992; Mitchell 1994; Opperman 1996; Wadley 1997, 2004; Jacobs *et al.* 2008; Stewart *et al.* 2012; Mitchell & Arthur 2014; Collins *et al.* 2017; Pargeter *et al.* 2017; Ames *et al.* 2020).

Human occupation is recorded at GRS between 43–28 ka. The palaeoenvironmental conditions were reconstructed using sedimentological and microbotanical remains and suggest that the local vegetation was dominated by C_3 grasslands, drought-resistant C_4 morphotypes, and a few woody plants, indicating relatively dry and cool conditions. Although dry, the presence of both cool (C_3) and warm (C_4) growing season grasses suggests that some year-round precipitation was received (Ames *et al.* 2020). At Melikane, changes in vegetation and environmental conditions are recorded between ca. 46–38 ka, especially after 42 ka (Stewart & Mitchell 2018: 6). Relatively dry conditions are inferred from reduced woodland vegetation, a minor increase in the $\delta^{13}C$ sediment values (-23.9‰ to -22.8‰), and a slight increase in C_4 grass phytoliths; however, the effects of reduced pCO_2 and warmer conditions cannot be discounted (Stewart *et al.* 2016; Stewart & Mitchell 2018). Alternating periods of intense roof fall and recurrent influxes of colluvial gravel suggest that the climatic conditions were likely unstable during this time (Carter 1976; Stewart *et al.* 2012), but the Senqu River likely provided occupants with a constant source of water (Stewart *et al.* 2016). Cool conditions are indicated in the Sehonghong area between 35–29 ka by high proportions of C_3 vegetation (Loftus *et al.* 2015). Interestingly, the $\delta^{13}C$ enamel values from herbivores suggest that they consumed a substantial proportion of C_4 vegetation suggesting that alcelaphines and zebras (*Equus* sp.) seasonally migrated to lower altitudes (Loftus *et al.*

2015; Stewart & Mitchell 2018). Similar conditions are recorded at Ha Makotoko and Ntloana Tšoana ca. 30 ka (Roberts *et al.* 2013), and cool and dry conditions are recorded at Thabana Ntlenyana between ca. 27.4–23.1 ka (Grab & Mills 2011).

At Boomplaas Cave, C_4 grass increased significantly accompanied by some shrubby vegetation between 39.7 and 36.0 cal. kBP (Deacon *et al.* 1984; Sealy *et al.* 2016). However, the presence of shrubby vegetation may not be the result of the climate conditions but rather reduced pCO_2 associated with glacial periods (Ehleringer *et al.* 1997; Chase & Meadows 2007). Microfaunal remains (Avery 1982, 2004; Deacon *et al.* 1984) and the relatively high macrofaunal diversity (Faith 2013a), suggest that conditions were moister during this period with increased summer rainfall (Sealy *et al.* 2016). This corresponds with enriched $\delta^{13}C$ values from the Cango Cave Stalagmite (Talma & Vogel 1992).

2.4.3 MARINE ISOTOPE STAGE 2 (29–14 KA)

Regional records suggest that the environment was cold and dry during MIS 2, culminating during the LGM (ca. 24–18 cal. kBP) when Antarctic sea ice reached its maximum extent (Opperman 1996; Holmgren *et al.* 2003; Chase & Meadows 2007; Barham & Mitchell 2008; Lewis 2008, 2011; Sealy *et al.* 2016; Loftus *et al.* 2019). Engelbrecht *et al.* (2019: 24) suggest that annual average temperatures during the LGM were 4–6 °C lower than present, with mid-winter temperatures dropping as much as 8–10 °C over the eastern interior and escarpment regions. Pollen records from the interior SRZ (Scott 1982a, b; Thackeray & Scott 2006; Scott *et al.* 2012; Truc *et al.* 2013) and isotope records from Cold Air Cave parallel Engelbrecht's *et al.* (2019) predictions and suggest that cool and dry conditions prevailed between 24–17.5 ka, interrupted by a brief period of relatively warmer and moister conditions between 20–19 ka (Holmgren *et al.* 2003; Scott *et al.* 2012). A statistical reanalysis of 27 pollen records across southern Africa suggest that two cold periods may have occurred during the LGM at ca. 24 and 17 cal. kBP (Scott *et al.* 2012), roughly corresponding to the North Atlantic Heinrich events (Hemming 2004; Fitchett *et al.* 2017a: 285). Similar temperature depressions are predicted in the YRZ (Heaton *et al.* 1986b; Thackeray 1990; Talma & Vogel 1992); although there is marked variability in the Cango Cave Stalagmite record between 18 and 16 kBP (Talma & Vogel 1992). Larger temperature depressions are reported at high altitude sites such as those in the Western Cape mountains (Boelhouwers & Meiklejohn 2002) and the Eastern Cape Drakensberg (Lewis & Illgner 2001).

The LGM and earlier Pleistocene glacial events have been linked to reduced solar radiation (e.g., Imbrie *et al.* 1992) and increased ice volumes which may have resulted in increased

pressure and pole-equator temperature gradients causing atmospheric and oceanic circulation systems to shift northwards (Stuut *et al.* 2004; Chase & Meadows 2007; Sealy *et al.* 2016). This may have resulted in the expansion of the WRZ and encouraged the growth of C_3 instead of C_4 vegetation in parts of southern Africa as seen at Boomplaas Cave and the Cango Cave speleothem (Sealy *et al.* 2016). Interestingly, low pCO_2 levels like those experienced during the LGM (ca. 190 ppm compared to 270 ppm in the Holocene) would have favoured the growth of C_4 plants (Ehleringer *et al.* 1997; Sealy *et al.* 2020). This is documented in marine cores from tropical and sub-tropical Africa (Collins *et al.* 2011; Badewien *et al.* 2015) but is not documented in the WRZ or YRZ in southern Africa (Sealy *et al.* 2020).

Climate projections compiled by Engelbrecht *et al.* (2019: 24) suggest that southern Africa was wetter during the LGM as the WRZ was displaced northward, leading to increases in winter rainfall as far as Botswana, central Namibia, and the present-day SRZ. This concurs with proxy records from the interior of South Africa. However, cooler conditions may have resulted in decreased rates of evaporation indicating increased moisture availability, although this could be confused with increased rainfall (Chase *et al.* 2017; Engelbrecht *et al.* 2019). The current WRZ, including the western escarpment and Cape Fold mountains, most likely received the largest increase in precipitation which combined with cold temperatures resulted in the formation of periglacial features (Engelbrecht *et al.* 2019: 24). In contrast, the southern Cape coast probably experienced less rainfall, relatively warm temperatures, and frequent berg winds (Engelbrecht *et al.* 2019: 24); however, other studies suggest that conditions were cool and dry (Thackeray & Fitchett 2016). Sea levels were lower during the LGM, extending coastal plains which possibly led to changes in local atmospheric systems such as enhanced or expanded continental anticyclones that blocked winter rainfall systems in the southern Cape (Cowling *et al.* 1999; Carr *et al.* 2006). Furthermore, Engelbrecht *et al.* (2019: 24) suggests that the YRZ may have extended as far as the Gauteng and Free State provinces. These projections must be taken with some caution, and biases need to be corrected and accounted for (Engelbrecht *et al.* 2019: 24).

During MIS 2, only a few interior sites are occupied in the southern African (Opperman & Heydenrych 1990; Opperman 1992, 1996; Deacon 1995; Mitchell 1996a, 2013; Wadley 1997; Mitchell & Arthur 2014; Stewart *et al.* 2016; Pargeter *et al.* 2017, 2018; Loftus *et al.* 2019). No occupation is recorded at GRS between 28 and 13.5 ka, roughly coinciding with Marine Isotope Stage (MIS) 2 (29–14 ka) (Ames *et al.* 2020). Charcoal, isotope, and pollen records from Strathalan suggest that C_3 vegetation was present and that conditions were cool

and moist, likely accompanied by a strong winter rainfall regime between ca. 26–24 kBP (Vogel *et al.* 1978; Opperman & Heydenrych 1990; Lewis 2008). Lower temperatures are indicated by the presence of high-altitude vegetation at Strathalan (after ca. 24 kBP), Wonderkrater, and Mahwaqa peatland (Scott 1982a, b; Opperman & Heydenrych 1990; Low & Rebelo 1996; Neumann *et al.* 2014). Pdf-based pollen analysis of sites across the SRZ (Truc *et al.* 2013; Chevalier & Chase 2015) indicate sustained temperature depressions following the LGM in southeastern Africa, however, there is contention over the nature of rainfall in South Africa's SRZ with arguments focusing on moisture availability and the impact of northern and southern weather systems (Stewart & Mitchell 2018: 8; Engelbrecht *et al.* 2019: 4). Dry conditions have been attributed to cooler Indian Ocean SSTs causing reductions in available moisture (Truc *et al.* 2013; Chevalier & Chase 2016). Opposing arguments suggest that constant moisture availability was ensured by lower evapotranspiration during and shortly after the LGM (Scott & Thackeray 1987; Scott *et al.* 2003, 2004, 2008, 2012; Scott 2016; Chevalier & Chase 2016).

Dry conditions are recorded at Rietvlei wetland from ca. 30 to 16 cal. kBP (Carr *et al.* 2010; Quick *et al.* 2015), Florisbad (Toffolo *et al.* 2017), and Mfabeni peatlands after ca. 23 ka accompanied by increases in grassy vegetation (Finch & Hill 2008; Baker *et al.* 2017). However, these conditions are contradicted by CD 15410-06P, a marine core located off the Eastern Cape coast (Simon *et al.* 2015) and the Voordrag Kwa-Zulu Natal Midlands pollen record (Botha *et al.* 1992). Moist and cool conditions are indicated from the Wonderwerk Cave speleothem between ca. 22 and 14 cal. kBP with brief dry periods at 22 and 15 cal. kBP (Brook *et al.* 2010). This is paralleled by pollen records dating between 32 and 12.5 cal. kBP, with some fluctuations in moisture and temperature (Scott 1982a, b; Scott & Thackeray 2015). Moist conditions are indicated by the isotope record from the Lobatse Cave stalagmite (Holmgren *et al.* 1995; Brook *et al.* 1997, 1998), while decreases in precipitation are recorded at Wonderkrater (Truc *et al.* 2013; Chevalier & Chase 2015). Contrasting conditions are inferred by the proxy records from Boomplaas Cave (Engelbrecht *et al.* 2019: 5), with charcoal, micromammal, and pollen records suggesting that conditions were dry to moderately wet with a lack of trees (Klein 1980; Scholtz 1986; Thackeray 1987; Deacon & Lancaster 1988; Thackeray & Fitchett 2016), whereas increases in ungulate diversity and isotopic records indicate an increase in winter rainfall, the presence of C_3 grasses, and a high level of effective moisture (Sealy *et al.* 2016; Pargeter *et al.* 2018; Faith *et al.* 2019). Modern datasets from eastern and southern Africa show a relationship between MAP and species

diversity (Thackeray 1980; Faith 2013a), therefore high levels of ungulate diversity at Boomplaas Cave could indicate higher productivity during the LGM (Sealy *et al.* 2016: 923). Interestingly, the $\delta^{13}C$ values from Boomplaas fauna and the Cango Cave speleothem differ, with the $\delta^{13}C$ faunal values indicating a larger proportion of C_4 grass during the LGM (Sealy *et al.* 2016: 923). This trend is documented elsewhere (e.g., Lister 2013) and emphasises the role of dietary preference on isotopic results (Sealy *et al.* 2016: 923).

The Maloti-Drakensberg region became significantly cooler ca. 24 ka (Lewis 2008; Mills *et al.* 2009a, b; Scott *et al.* 2012; Stewart & Mitchell 2018). Periglacial features are found along the escarpment and include glacial moraines at approximately 3000 masl on the Sekhokong and Tsatsa-La-Mangaung mountain ranges in Lesotho between ca. 20.8–19.6 ka (Mills *et al.* 2009a, b). An increase in precipitation, specifically snow, was required to maintain these glaciers (Mills *et al.* 2012). Similar, periglacial features are recorded at lower altitudes, ca. 1700 masl, in the Eastern Cape Drakensberg (Mills *et al.* 2017), and may have developed alongside mean temperature depressions of 6 °C (Stewart & Mitchell 2018). High-altitude sites like Sehonghong, Ha Makotoko, and Rose Cottage Cave were occupied during MIS 2 (Mitchell 1995, 1996a; Wadley 1995, 1996, 1997; Mitchell & Arthur 2014; Pargeter *et al.* 2017). However, occupations in the southern Drakensberg foothills are extremely rare (Opperman & Heydenrych 1990; Opperman 1992, 1996; Ames *et al.* 2020). Some researchers suggest that cold and dry conditions lead to population contraction and the occupation of high-altitude sites with more reliable freshwater sources in the Maloti-Drakensberg (Scott *et al.* 2012; Pargeter *et al.* 2017; Stewart & Mitchell 2018; Ames *et al.* 2020: 14).

After 17.5 ka, rapid warming is recorded in both the pollen-derived temperature index from Wonderkrater and the Makapansgat $\delta^{18}O$ record (Holmgren *et al.* 2003). Similar conditions are recorded in the Southern Hemisphere tropical, polar ice-core, and terrestrial lake sediment records (Thompson *et al.* 1995; Blunier *et al.* 1998; Gasse & van Campo 1998; Steig *et al.* 2000; Johnson *et al.* 2002). Following the LGM, warmer conditions are documented at Boomplaas Cave and are accompanied by an increase in C_4 grass and the return of trees in the valley (Deacon 1995; Sealy *et al.* 2016). Cool and dry conditions with a mix of C_3 and C_4 vegetation is documented at Equus Cave at 17 ka (Johnson *et al.* 1997: 135). Similar conditions, with increased windiness, are recorded at the Golden Gate Highlands National Park between ca. 17–16 ka (Stewart & Mitchell 2018: 8), while cool and moist conditions with increased grassland vegetation are recorded at Aliwal North between ca. 16–14 kBP

(Coetzee 1967; Lewis 2008; Scott *et al.* 2012). Isotope and charcoal records from Rose Cottage Cave suggest that conditions were cooler with increased moister availability at ca. 16 ka, followed by dry and warm conditions (Smith *et al.* 2002; Stewart & Mitchell 2018). Parallel conditions are recorded at Braamhoek and Mahwaqa ca. 16 ka, with possible increases in winter rainfall (Finné *et al.* 2010; Neumann *et al.* 2014; Norström *et al.* 2014). In contrast, pollen records from Mfabeni peatland indicate that the region received a larger component of summer rainfall between ca. 17–15 ka (Chevalier & Chase 2015). More diverse fauna are found at Sehonghong with small, browsing, and canopy-loving antelope re-appearing in the record (Plug & Mitchell 2008). By ca. 15.7–15.2 ka, warmer conditions are indicated by elevated $\delta^{13}C$ sediment values (Loftus *et al.* 2015; Pargeter *et al.* 2017). These are subsequently replaced by cooler conditions ca. 14.6–13 ka following the onset of the Antarctic Cold Reversal (ACR) (Pedro *et al.* 2016; Stewart & Mitchell 2018). In general, the early Last Glacial Interglacial Transition was characterised by relatively humid conditions that terminated abruptly at ca. 14.2 cal. kBP (Chase *et al.* 2017). This aligns relatively well with the strengthening of the Atlantic Meridional Overturning Circulation associated with the post-Henrich Stadial 1 (ca. 18–14.6 ka) (McManus *et al.* 2004) and the onset of the ACR (Pedro *et al.* 2016).

The ACR is not widely documented in southern Africa with weak ACR signals along the west coast (Farmer *et al.* 2005), in pollen records from the marine core (GeoB1023-5), off the Namibian coast (Dupont *et al.* 2004), in the southern and central regions of the SRZ (Holmgren *et al.* 2003; Norström *et al.* 2009; Chase *et al.* 2017), and unclear signals along the east coast (Bard *et al.* 1997). The ACR has been associated with Antarctic ice expansion, a northward shift in the westerly storm belt, cooler Southern Ocean SSTs, and an equatorward shift of the Subtropical Front, resulting in reduced precipitation in the SRZ (Fischer *et al.* 2007; Barker *et al.* 2009; Chase *et al.* 2017; Kylander *et al.* 2021), and increased winter rainfall in the southern Cape (Pedro *et al.* 2016). However, these changes may be associated with another global climate event, namely the YD. The YD event is well recognised in the Northern Hemisphere and is associated with a cooling period between ca. 13.5 and 11.5 cal. kBP (Alley *et al.* 1993; Andres *et al.* 2003; Thackeray & Scott 2006; Thackeray *et al.* 2019). There is increasing support for its occurrence in southern African records (Scott & Thackeray 1987; Tusenius 1989; Cohen *et al.* 1992; Scott *et al.* 1995, 2003; Abell & Plug 2000; Dupont *et al.* 2004; Thackeray & Scott 2006; McCarthy *et al.* 2010; Quick *et al.* 2011; Backwell *et al.* 2014; Chase *et al.* 2015a; Loftus *et al.* 2015; Collins *et al.*

2017; Thackeray 2018; Ames *et al.* 2020), although the associated climate conditions remain unclear and vary regionally (Chase *et al.* 2011; Fitchett *et al.* 2017a). Furthermore, there is a lack of evidence for this event along the warm, moist east coast. This may be due to a lack of samples but could more interestingly reflect a microclimatic effect whereby persistent local warming driven by the warm Agulhas current conceals global scale cooling (Fitchett *et al.* 2017a: 283).

2.4.4 MARINE ISOTOPE STAGE 1 (14–5 KA)

The transition from MIS 2 to 1 was characterised by relatively wet conditions, with the western and southern regions becoming more humid and the northeast region becoming drier (Scott *et al.* 2012: 16). Temperatures appear to have ameliorated by ca. 14 cal. kBP at Braamhoek and Craigrossie (Scott 1989, Norström *et al.* 2009; Scott *et al.* 2012). Evidence of warming is evident in the interior highland of southern Africa by ca. 13.5 ka (Loftus *et al.* 2015), thereafter rapid temperature changes occur (Truc *et al.* 2013; Pedro *et al.* 2016; Stewart & Mitchell 2018). Cool and dry conditions are recorded across the Maloti-Drakensberg (Smith *et al.* 2002; Loftus *et al.* 2015; Pargeter *et al.* 2017; Stewart & Mitchell 2018) and at Sekhokong, Lesotho from 14.3 cal. kBP (Kylander *et al.* 2021). Pollen records from Wonderkrater indicate a significant cold reversal during the YD period with temperature depressions of 6 ± 2 °C and reduced summer rainfall (Truc *et al.* 2013: 575; Stewart & Mitchell 2018: 9). This is supported by pollen records from sites located in the southern Savanna biome (Scott *et al.* 2012), and by the depositional hiatus in the Cold Air Cave speleothem (Holmgren *et al.* 2003).

A TP occupation is recorded at GRS, making GRS one of the few sites in the southern African interior to preserve a YD occupation (Collins *et al.* 2017; Ames *et al.* 2020). The microbotanical data suggests that relatively cool and moist grassland conditions prevail with woody vegetation likely growing along stream margins (Ames *et al.* 2020). The proportion of C_3 to C_4 grass is comparable and suggest that growing conditions were somewhat cooler than present. The prevalence of Panicoideae implies that conditions were moister with a likely increase in summer rainfall compared to the LP (Ames *et al.* 2020: 12). The region received at least some year-round rainfall (Ames *et al.* 2020). Regional wetness was experienced at Braamhoek wetland from 14 ka to ca. 13.6 or 13.2 ka (dependent on proxy record), followed by persistent cold between ca. 12.6 and 11.3 ka as indicated by the presence of fynbos pollen (Finné *et al.* 2010; Norström *et al.* 2014). Proxy records from Braamhoek and palaeogeomorphogical evidence from eastern Lesotho suggest that mid-latitude cyclones

were more intense and that the westerly storm belt migrated northwards during the TP (Norström *et al.* 2009, 2014; Finné *et al.* 2010; Mills *et al.* 2012). Variable conditions are recorded at several sites during this period, for example, more humid conditions are documented at Lake Tswaing between ca. 14–10 kBP (Kristen *et al.* 2010), wet conditions at Sudwala Cave (Green *et al.* 2015) and Tsoaing River Basin before ca. 12.2 kBP (Grab *et al.* 2005), cold and moist conditions at Bushmans Rockshelter between 12.2 and 11.65 ka (Abell & Plug 2000), cool conditions with increased moisture availability are indicated at Wonderwerk Cave (Lee-Thorp & Ecker 2015), dry and warm conditions are recorded at Rietvlei between 14.8 and 11.0 cal. kBP (Quick *et al.* 2015), and warmer temperatures are recorded across the Caledon River Valley at ca. 12.9 cal. kBP (Esterhuysen & Smith 2003). Moister conditions are indicated across the Caledon River Valley from ca.12 to 10 kBP (Scott 1986; Wadley *et al.* 1992). These are subsequently replaced by drier conditions in the Aliwal North district by ca. 11 kBP (Coetzee 1967; Scott 1989), at Ravenscraig between ca. 11.8–11.2 ka (Tusenius 1989), and the upper Caledon River Valley by 9 kBP (Wadley *et al.* 1992). Moist conditions with a strong winter rainfall regime are indicated at Elands Bay Cave (Klein & Cruz-Uribe 1987; Cartwright & Parkington 1997; Parkington *et al.* 2000; Stowe & Sealy 2016). This trend extends across the region and is documented at Pakhuis Pass, De Rif (Scott & Woodborne 2007a, b; Chase *et al.* 2011; Quick *et al.* 2011), and in Namibia (Chase *et al.* 2009).

The period between the TP and the Holocene is marked by the mass extinction of several large grazers and may account for the transition from large to small bovids seen in archaeological assemblages throughout southern Africa (Klein 1972, 1978, 1983; Plug & Engela 1992; Mitchell 1993; Faith 2011a, 2012; 2013b, 2014; Sealy *et al.* 2016, 2020; Ecker *et al.* 2018). Several mechanisms have been proposed for this change including increased aridity and reduced productivity or availability of grassland habitats (Klein 1980, 1984; Brink 1987, 1999, 2016; Brink & Lee-Thorp 1992), structural changes in grassland habitats (Faith 2014), intensified competition among grazers (Thackeray 1984, 2015), increased seasonality (Faith 2011a), altered rainfall regimes (Faith 2014), elevated atmospheric CO_2 concentrations (Faith 2014), and/or increased niche specialisation (Codron *et al.* 2008). Environmental and climate change affected faunal communities, but the primary forces behind these changes are unclear (Ecker *et al.* 2018: 133).

Relatively warm and arid conditions are reported in the central, eastern, and northern regions of southern Africa's SRZ, while relatively mesic conditions are reported in the southwestern

WRZ during the Early Holocene (Scott & Lee-Thorp 2004; Lewis 2008). These conditions are reversed in the MH (Scott & Lee-Thorp 2004: 81). Several forcing mechanisms are proposed for this trend. Chase *et al.* (2009, 2010) suggest that Northern Hemisphere forcing is responsible for these conditions, aligning with the African Humid Period from ca. 14.8 to 5.5 cal. kBP (Kutzbach 1981; Kutzbach & Street-Perrott 1985; Street-Perrott & Perrott 1993; deMenocal *et al.* 2000; Metwally *et al.* 2014). However, others suggest that this trend resulted from Southern Hemisphere precessional forcing (Scott 1993; Street-Perrott & Perrott 1993; Partridge *et al.* 1997; Scott 1999a, b; Scott *et al.* 2008; Brook *et al.* 2010; Metwally *et al.* 2014). Scott *et al.* (2012: 16) argue that increased precessional forcing and Indian Ocean SST led to increased rainfall in the northeastern SRZ with some delay in the central interior as the ITCZ migrated south. Alternatively, Truc *et al.* (2013) argue that this relationship, especially in the Savanna biome, may have superseded the influence of latitudinal shifts in the ITCZ. Overall, local, regional, and global forcing mechanisms are responsible for changes in rainfall, seasonality, and temperature between spatially separated biomes highlighting the complexity of climate change across southern Africa (Scott & Lee-Thorp 2004; Burrough & Thomas 2013; Metwally *et al.* 2014).

Warm and dry conditions are recorded in the SRZ during the early Holocene (Scott 1987, 1993, 1999a, b, 2016; Holmgren *et al.* 2003; Scott & Lee-Thorp 2004; Kristen *et al.* 2007, 2010; Scott *et al.* 2008, 2012; Truc *et al.* 2013; Metwally *et al.* 2014). Importantly, isotope results do not always represent precipitation-evaporation as clearly as previously thought (Stager *et al.* 2013; Sundqvist *et al.* 2013). Dry to arid conditions prevail at Wonderwerk Cave between 12 and 6 cal. kBP, although sub-humid conditions may have been reached during this period (Brook *et al.* 2010; Horwitz & Chazan 2015; Lee-Thorp & Ecker 2015; Scott & Thackeray 2015), at Elands Bay Cave after 9.6 ka (Klein & Cruz-Uribe 2016), at Boomplaas Cave between ca. 12.1 and 10.1 cal. kBP (Scholtz 1986; Deacon & Lancaster 1988; Sealy *et al.* 2016), in the southern Drakensberg (Tusenius 1989), and at Blydefontein (Bousman 1991; Scott *et al.* 2005). Warm and moist conditions are documented at Braamhoek wetland between 10.2 and 8.5 cal. kBP, with a strong summer rainfall component between ca. 10.2–9.2 ka, followed by more arid conditions (Norström *et al.* 2009, 2014). Moist conditions are documented along the east coast at Mahwaqa, Lake Eteza, and Mfabeni peatlands between 10 and 8 cal. kBP (Neumann *et al.* 2010, 2014; Baker *et al.* 2014). Moist or mesic conditions characterise the WRZ between ca. 10 and 8 cal. kBP (Klein 1991; Chase & Thomas 2006; Meadows *et al.* 2010; Quick *et al.* 2011; Weldeab *et al.* 2013).

Warm conditions are recorded across the Maloti-Drakensberg between ca. 11.5–8.5 ka and coincides with the replacement of open grassland with more closed woody vegetation (Stewart & Mitchell 2018: 9). The $\delta^{13}C$ values from tooth enamel and sediment indicate warm conditions at Ha Makotoko ca. 11.4 cal. kBP, followed by cooler conditions ca. 10.5 ka before returning to warmer conditions with a more stable C_4 vegetation component, paralleling global records (Smith *et al.* 2002; Roberts *et al.* 2013). Similar trends are recorded at Ntloana Tšoana, Sehonghong, and Rose Cottage Cave, although slightly higher temperatures are recorded at Rose Cottage Cave (Plug & Mitchell 2008; Stewart & Mitchell 2018). Increased humidity is documented at Tloutle ca. 9.9–9.5 ka and conditions were mesic enough to support patches of forest (Plug 1993; Esterhuysen & Mitchell 1997; Stewart & Mitchell 2018). At Rose Cottage Cave, cool conditions are inferred from $\delta^{13}C$ enamel values (Smith *et al.* 2002) and the charcoal record (Esterhuysen *et al.* 1999; Esterhuysen & Smith 2003) at ca. 9.5–9.3 ka. Furthermore, the presence of kudu and wildebeest suggest that sweet C_4 grasslands and canopy cover increased between ca. 9.5–8.8 ka (Wadley 2000a) and the charcoal record suggests that conditions were drier (Esterhuysen 1996). Wet conditions are suggested at Ha Makotoko ca. 8.7 kBP by the presence of *Podocarpus* (Esterhuysen & Mitchell 1997) and is associated with cooling between 9 and 8 kBP. Similar conditions are reported at Tloutle (Mitchell 1993; Esterhuysen & Mitchell 1997; Esterhuysen *et al.* 1999; Smith *et al.* 2002). These records coincide with fluctuating temperature and moisture conditions captured in the phytolith and sedimentary records from Tsoaing River Basin between ca. 8.6–8.45 kBP, although, moisture retention after ca. 8.45 kBP may reflect changes in rainfall seasonality or intensity (Grab *et al.* 2005: 59). Finally, the highest number of LSA occupations are recorded in eastern Lesotho between ca. 9–8.6 kBP (Mitchell 1994).

A short-lived cold event occurs at 8.2 ka and was driven by a large meltwater pulse in the north Atlantic Ocean (Alley *et al.* 1997; Mayewski *et al.* 2004; Alley & Ágústsdóttir 2005; Wanner *et al.* 2015). From ca. 8.4–7.8 cal. kBP, changes in cosmic ray flux or solar radiation are documented (Stager & Mayewski 1997). This event has been commonly associated with climate changes in the Northern Hemisphere, but evidence for this event has been documented in Africa (Partridge *et al.* 1990; Lario *et al.* 1997; Stager & Mayewski 1997; Gasse 2000; Cremaschi 2002; Smith *et al.* 2002; Thompson *et al.* 2002; Esterhuysen & Smith 2003; Holmgren *et al.* 2003; Stager *et al.* 2003; Finné *et al.* 2010; Scott *et al.* 2012; Neumann *et al.* 2014; Norström *et al.* 2014; Chase *et al.* 2015a; Fitchett *et al.* 2017b). The widespread occurrence of this event suggests that there was a relationship between the Northern and

Southern Hemisphere, thus providing important insight into climate teleconnections and ocean heat transport during the Holocene (Fitchett 2019: 49).

Southern African records aligning with this event include those from the Caledon River Valley in western Lesotho (Smith *et al.* 2002), the Mafadi core (ca. 8.1–7.6 ka) on the border of eastern Lesotho, the South African Drakensberg (Fitchett *et al.* 2017a, b), Makapansgat speleothem (Holmgren *et al.* 2003), Braamhoek wetland ca. 8 cal. kBP (Finné *et al.* 2010; Norström *et al.* 2014), and in the south-western Cape (Chase *et al.* 2015a). Moisture availability decreases at Mahwaqa from ca. 8.5 to 6.8 cal. kBP, and is paralleled by drying events at Braamhoek, Florisbad, Tloutle, and Rietvlei (Esterhuysen & Mitchell 1997; Neumann *et al.* 2014; Quick *et al.* 2015). A shift to C_3 grasslands and temperature depressions of approximately 3 °C and 4 °C are recorded between ca. 8.4–8.0 cal. kBP at Rose Cottage Cave and Tloutle, respectively. This roughly aligns with the 8.2 ka cold event (Wadley *et al.* 1992; Smith *et al.* 2002; Stewart & Mitchell 2018). At Sehonghong, several large grazers became extinct and were replaced by WD species (i.e., common reedbuck) between ca. 8.0–6.5 ka (Stewart & Mitchell 2018: 11). Similar trends are documented above the escarpment in the Eastern Cape Drakensberg (Opperman 1987).

In contrast, there is extensive proxy evidence for the occurrence of a MH Altithermal in southern Africa, between 7 and 5 cal. kBP (Lee-Thorp & Talma 2000; Scott & Lee-Thorp 2004; Grab *et al.* 2005; Scott *et al.* 2012; Chase *et al.* 2013; Truc *et al.* 2013). It is characterised by improved moisture availability, at least in the SRZ, and warmer temperatures (Chevalier & Chase 2015). However, the duration and timing of this event varies between records, possibly signalling spatial variability (Scott 1993) or uncertainty in the individual chronological records (Haberzettl *et al.* 2014). A brief and intense period of occupation is recorded at GRS between 7.3–6.8 ka during which warmer temperatures and summer rainfall are recorded (Ames *et al.* 2020). Similar conditions are inferred from the Mafadi core after 7 ka with further warming documented between ca. 6.6–5.7 ka (Fitchett *et al.* 2017b; Fitchett & Bamford 2017; Stewart & Mitchell 2018) and is paralleled at Braamhoek and Rietvlei (Neumann *et al.* 2014; Norström *et al.* 2014; Quick *et al.* 2015). Warm, wet conditions with increased C_3 vegetation are suggested from the Cold Air Cave stalagmite between 6.4–5.1 ka, with two reversals recorded between 5.7–5.1 ka (Lee-Thorp *et al.* 2001). Similar results are reported by Holmgren *et al.* (2003) in another stalagmite from Cold Air Cave. Warm SSTs are documented from 7 to 5 cal. kBP in the Mozambique Channel (Bard *et al.* 1997). Increased moisture availability or wetter conditions are recorded

in southern Africa at Lake Tswaing after ca. 7.5 kBP, reaching a maximum at ca. 5.5 kBP (Kristen *et al.* 2010), Tsoaing River Basin between ca. 7.9–7.7 ka (Grab *et al.* 2005), Wonderwerk Cave from ca. 7.5–5 ka (Avery 1981; Thackeray 1984, 2015; Lee-Thorp & Ecker 2015), western Free State between ca. 7.7 and 6.3 kBP (Butzer 1984a, b), western Lesotho between ca. 6.9 and 5 kBP (Esterhuysen & Mitchell 1997), and Mahwaqa at ca. 6.2 cal. kBP (Neumann *et al.* 2014). Dry conditions are documented during the later Holocene at Tsoaing River Basin ca. 6.7–6.1 ka (Grab *et al.* 2005), western Free State ca. 6.3 and 4.5 kBP (Butzer 1984a, b), at Braamhoek, Mahwaqa, and Rietvlei from ca. 5.6 cal. kBP (Scott *et al.* 2012; Neumann *et al.* 2014), Wonderwerk Cave (Horwitz & Chazan 2015; Scott & Thackeray 2015), and in the central Free State ca. 5 kBP (Scott & Nyakale 2002).

Notably, many of these reconstructions are based on pollen records (Ecker *et al.* 2018). Recent statistical models on pollen records from the SRZ have produced contrasting reconstructions (Ecker *et al.* 2018: 133). For example, increases in moisture availability are documented at some sites (e.g., Tswaing Crater and Wonderkrater) while dry conditions are documented at other sites (e.g., Lake Eteza, Equus Cave, Braamhoek, and Blydefontein) (Chevalier & Chase 2015; Scott 2016; Ecker *et al.* 2018). The use of Principal Components Analysis on pollen records show that moisture decreased at several sites from 8–7 ka with slightly cooler temperatures after 6 ka (Scott *et al.* 2012; Scott 2016). Unfortunately, this method cannot distinguish between aridity and temperature signals and is further challenged by poor chronological records (Ecker *et al.* 2018: 133).

Several studies suggest that conditions became gradually drier in the WRZ between ca. 8 and 3 cal. kBP (Martin 1968; Meadows & Baxter 2001; Chase & Thomas 2006; Scott & Woodborne 2007a, b; Meadows *et al.* 2010; Weldeab *et al.* 2013), although relatively moist conditions are suggested at Katbakkies Pass and Seweweekspoort between 8 and 1.7 cal. kBP with brief interruptions between 8.0–7.3, 6.6–6.2, 5.7–5.2, and 3.2–2.7 cal. kBP (Zhao *et al.* 2016b). Notably, moister conditions occur at De Rif 2010 between 7.1 and 6.7 cal. kBP (Valsecchi *et al.* 2013). Dry conditions are recorded in the YRZ and WRZ during the Holocene Altithermal as seen at Boomplaas Cave (Scholtz 1986), Cecilia Cave (Baxter 1989), Elands Bay Cave (Klein & Cruz-Uribe 1987; Klein 1991; Parkington *et al.* 2000), Groenvlei (Martin 1968), Klaarfontein (Meadows & Baxter 2001), Pakhuis Pass (Scott & Woodborne 2007a, b), Seweweekspoort (Chase *et al.* 2012, 2013), Truitjies Kraal (Meadows *et al.* 2010), and Vankervelsvlei (Irving 1998). This period of relative aridity has been associated with reductions in the extent of Antarctic sea-ice (Fischer *et al.* 2007) and

poleward displacement of the westerlies (Zhao *et al.* 2016b). However, at Byneskranskop (Avery 1993) and Katbakkies Pass (Meadows *et al.* 2010; Chase *et al.* 2015b), more mesic conditions with increased summer rainfall are recorded. Warmer SSTs are indicated at Nelson Bay Cave by ca. 6.8 ka and are likely the result of more intense westerlies and their associated frontal disturbances (Cohen & Tyson 1995), although this may also be the result of slightly higher Agulhas currents or temperatures (Scott & Lee-Thorp 2004).

CHAPTER 3: MATERIALS AND METHODS

3.1 SAMPLE COLLECTION

The faunal assemblage was recovered from three 1×1 m squares (B4, C4, and C5) excavated at Grassridge Rockshelter (GRS) from 2014 to 2019. Samples from the late Pleistocene (LP) and terminal Pleistocene (TP) come exclusively from unit B4, as these occupations have currently only been recovered from this square. A single-context recording system was utilised, each stratigraphic unit was excavated and recorded individually with thick contexts sub-divided into 30 mm spits (Collins *et al.* 2017: 163). Artefacts measuring more than 20 mm and some small finds were piece-plotted in three dimensions using a total station. The excavated sediment was sieved through a 1.5 mm mesh and the finds were sorted at the site (Collins *et al.* 2017: 163). The faunal remains were sent to the University of the Witwatersrand for analysis and curation.

3.2 SAMPLE SELECTION

One hundred long bone fragments were selected for this study, comprising ten bone fragments from the LP (43–28 ka), 20 from the TP (13.5–11.6 ka), and 70 from the mid-Holocene (MH; 7.3–6.8 ka). The sample size in each layer reflects the overall size of the faunal assemblage from each occupational layer and the position of the plotted bones is shown in Figure 3.1. The selected samples were cortical long bone fragments larger than 20 mm in length. An attempt was made to select well-preserved bone fragments by avoiding those that appeared crumbly, chalky, or patently burnt (Sealy *et al.* 2014).

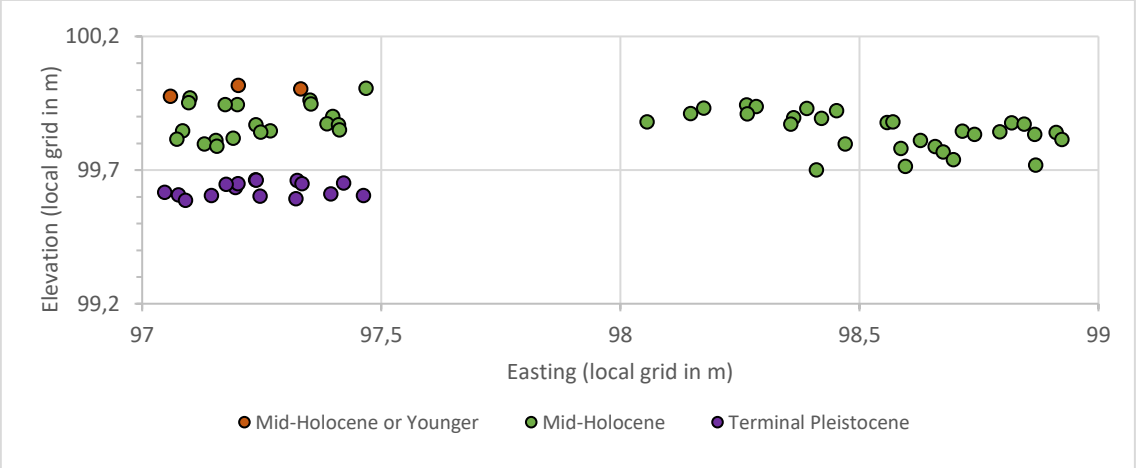


Figure 3.1: Scatter plot showing the elevation and easting position of the GRS plotted finds which are categorised by time period.

The surface of each bone fragment was cleaned with a soft-bristled toothbrush and water and air-dried for approximately 24 hours before being analysed for surface modifications under an OLYMPUS SZ51 microscope (Appendix 1). The anterior and posterior side of each bone fragment was photographed. The TP and MH bone fragments were cut in half in the fumehood using a Dremel tool fitted with a diamond cutting wheel. One half was placed into a labelled plastic bag and sent for Zooarchaeology by Mass Spectrometry (ZooMS) analysis at the University of Manchester, while the other half was used for stable carbon and nitrogen isotope analysis at iThemba Labs. Only the TP and MH bone fragments underwent both ZooMS and stable isotope analysis as the LP bones were relatively small (<20 mm), and collagen preservation was expected to be poor (see Lee-Thorp *et al.* 1989).

3.3 ZOOMS ANALYSIS

3.3.1 BONE PREPARATION

Due to travel restrictions relating to the COVID-19 pandemic, ZooMS was undertaken by Finlay Thomas at the University of Manchester, following the acid-soluble approach set out in van der Sluis *et al.* (2014). Approximately 50 mg of each bone fragment was powdered onto a piece of foil in a fumehood, using a diamond-tipped dental drill-bit. The remainder was retained in the collection. The bone powder was then transferred into a 1.5 mL tube and the foil was discarded. The surface and drill-bit were wiped down with methanol before and after each bone fragment was powdered.

3.3.2 COLLAGEN PEPTIDE ISOLATION

Each sample was covered with 1 mL 0.6 M hydrochloric acid (HCl) and refrigerated for approximately 18 hours. The tubes were then spun at 12 400 rpm for three minutes to precipitate the powder. Thereafter, 500 µL acid solution was removed from each sample into Vivaspin® 500 centrifugal concentrators (10 kDa membrane) and then spun at 12 400 rpm for 30 minutes. The filtrate was discarded, and the membranes were rinsed twice with 500 µL 50 mM ammonium bicarbonate (ABC). The retentate was resuspended in 100 µL 50 mM ABC and then transferred into 0.5 mL tubes.

Trypsin (Promega, porcine sequencing grade) was prepared at a concentration of 10 µg per 100 µL resuspension buffer. Collagen was digested by adding 2 µL trypsin to each sample, followed by an incubation period of roughly 18 hours at 37 °C. A combination of α-cyano-4-hydroxycinnamic acid and 50% acetonitrile 0.1% trifluoroacetic acid (TFA) solution was used to prepare the matrix-assisted laser desorption/ionisation (MALDI) matrix solution at a concentration of 1 mg per 100 µL, respectively. Subsequently, 1 µL of the

digested collagen sample was diluted in 1/20 0.1% TFA and spotted onto a MALDI plate with an equal volume of the matrix solution. This was allowed to air dry at room temperature before being analysed by the mass spectrometer.

3.3.3 MALDI-MS ANALYSIS

A Bruker Rapiflex Tissuetyper instrument was used for matrix-assisted laser desorption/ionisation -Time of Flight (MALDI-ToF) mass spectrometry over the *m/z* range of 700–3700. Spectra were identified manually by comparing their biomarkers with those in the reference database (Buckley & Collins 2011; Bradfield *et al.* 2019, 2021; Janzen *et al.* 2021).

3.4 ISOTOPIC ANALYSIS

3.4.1 BONE PREPARATION

The TP and MH bone fragments were further sub-sampled into bone chunks (± 5 mm) in the fumehood using a Dremel tool fitted with a diamond cutting wheel and the remaining fragment was retained in the collection.

3.4.2 PRETREATMENT

Bone collagen was isolated following the standard procedures employed by Sealy *et al.* (2014), however, the sodium hydroxide step was excluded as collagen preservation was expected to be poor (Rudakova & Zaikov 1987; https://www.radiocarbon.com/carbon-dating-pretreatment.htm consulted March 2021; Guiry & Szpak 2021: 12). Each bone chunk was placed into a beaker and covered with 20–30 mL of 0.2 M HCl at room temperature. The HCl solution was added at the beginning of each day and subsequently decanted and replaced with 50 mL of de-ionised water at the end of each day so that the progress of demineralisation could be monitored closely. In addition, HCl solution was poured off and replaced if it became yellow or contained debris. This continued until a collagen pseudomorph remained, in some cases, these were fragmented or discoloured possibly indicating poor preservation (Zhu 2016: 51). A Stemi DV4 microscope was used to monitor demineralisation and bones were considered demineralised when they were transparent, soft, flexible, and no longer effervescing. This process took anywhere between 7–54 hours (excluding time in distilled water). The bone collagen pseudomorph and beaker were rinsed with distilled water three times before being placed in an EcoTherm oven overnight at 70 °C to dry. Once dried the samples were transferred into a labelled plastic bag.

3.4.3 DETERMINATION OF STABLE CARBON AND NITROGEN ISOTOPE RATIOS

Approximately 0.5 mg of each sample was transferred into a tin cup before being combusted in a Flash 2000 organic elemental analyser set to 1020 °C. The resultant carbon dioxide

(CO_2) and dinitrogen (N_2) gases were purified and carried by a helium carrier gas into a Delta V Advantage isotope mass spectrometer (Thermo Scientific, Germany) through a ConfloIV interface. The raw data were calibrated using Urea ($\delta^{13}C$ = -39.73‰, $\delta^{15}N$ = -0.73‰) and Merck Gel ($\delta^{13}C$ = -20.57‰, $\delta^{15}N$ = 6.80‰). The standard deviation of repeated measurements (n = 14) of homogenous materials analysed in the same run was better than 0.22‰ and 0.06‰ for $\delta^{13}C$ and $\delta^{15}N$, respectively. Carbon results were reported relative to Vienna Pee Dee Belemnite (V-PDB) while atmospheric nitrogen (AIR) was used for nitrogen.

3.4.4 QUALITY INDICATORS

All but one sample yielded a collagen pseudomorph. The C: N ratios, weight C%, and weight N% of each sample was recorded to determine the collagen quality of each sample (Appendix 2).

3.5 STATISTICAL ANALYSIS

All statistical analyses were conducted using the free PAST statistical software (4.03 version). Both descriptive (i.e., measures of central tendency) and inferential (i.e., Chi-square, Mann-Whitney U-test [MW], Shapiro-Wilk test) statistics were selected to analyse the data (Appendix 3).

Faunal samples were identified using ZooMS and placed into categories, namely, unsuccessful, sub-family, tribe, genus, species, and unknown. These were further categorised into two categories, namely, successful identifications (i.e., those identified to at least tribe including the unknowns for which reference data was not available despite high-resolution collagen barcodes being produced) and unsuccessful identifications (i.e., those with low resolutions or no collagen peptide markers). Success data in a contingency table was analysed using a chi-square test to determine whether success differed in the LP, TP, and MH occupations. Additionally, the success of ZooMS and the effects of heating and the bones surface condition were analysed, again using a chi-square test.

For the faunal data, the samples were classified into three groups, namely, browser, intermediate feeder, or grazer according to Skinner and Chimimba (2005) or stable carbon isotope ratios (Appendix 2). Where necessary, low-resolution samples were excluded. The number of browsers and grazers in each occupational layer was compiled into a contingency table and a chi-square test was used to determine whether there were differences in the type of taxa inhabiting GRS throughout the sequence. These were then divided into LP-TP and TP-MH to see if this result was driven by major faunal turnover throughout the sequence or

between two periods. Faunal change is expected to correlate with vegetation change resulting from palaeoenvironmental change. Furthermore, the number of water-dependent (WD) and water-independent (WI) taxa in each occupational layer was compiled into a contingency table and a chi-square test was used to determine whether there were changes in water availability through the sequence. To increase the sample size, these samples were combined with Opperman's, and the same tests were applied (Appendix 4).

In many cases, Shapiro-Wilk tests indicate non-normal distributions in the stable isotope data (Appendix 3) and so non-parametric tests were employed. Violin plots with box plots were plotted to examine the distribution of $\delta^{13}C$ values in TP and MH browsers and grazers. Mann-Whitney U-tests were used to examine differences between the stable isotope ratios of browsers and grazers, changes in the stable isotope ratios between the TP and MH, the dietary grouping of the unknown and other taxa (i.e., springbok [*Antidorcas marsupialis*], eland, Reduncini), and differences in stable isotope ratios of WD and WI taxa. Additionally, the effect of a large number of MH grey rhebok (n = 33) on the distribution of $\delta^{13}C$ values and MH browser trend was examined using violin plots with box plots and MW U-tests. Unfortunately, too few individual taxa were identified in each occupational layer for meaningful statistical analyses.

CHAPTER 4: RESULTS

The results of this study are presented in this chapter. Faunal and isotopic results are presented in Table 4.1, and the collagen quality indicators and collagen fingerprints are in Appendix 2 and 5, respectively. The C: N ratios of the extracted collagen ranged between 3.2 and 3.6 and the $_{wt}$C% and $_{wt}$N% ranged between 24.6–47.6% and 8.7–17.5%, respectively. These values fall within the acceptable range for well-preserved collagen (Ambrose 1990). Only one sample (069) did not meet these requirements and had to be excluded from this study. Notably, low-resolution samples are excluded when necessary. Three sections are included, the first examines the success of faunal identification using Zooarchaeology by Mass Spectrometry (ZooMS), the second examines faunal change between the late Pleistocene (LP), terminal Pleistocene (TP), and mid-Holocene (MH) occupations at Grassridge Rockshelter (GRS), and the third examines shifts in the stable carbon and nitrogen isotope ratios between the TP and MH. Statistical tests are used to distinguish significant differences and similarities in this dataset and the significance level is at $\alpha \leq 0.05$ for all statistical analyses (see Appendix 3).

*Table 4.1: Table of fauna identified using ZooMS and their stable carbon and nitrogen isotopes. Diet based on life history (Skinner & Chimimba 2005) unless the faunal resolution is low then stable carbon isotope ratios (italics) are used to infer diet. C_3 browser (B) between -29.5‰ and -17.5‰, C_4 grazer (G) between -10.5‰ and -2.5‰, intermediate (M) falls between -17.5‰ and -10.5‰ (Adapted from Lee-Thorp 2008). Water-dependent (WD) and water-independent (WI). *Springbok $\delta^{13}C$ values not significantly different from browsers. **Reduncini (browser) most likely grey rhebok, inferred from C_3 signature. Heated: ✓ = bone was heated, ✗ = bone was not heated. Surface preservation: 1 = < ¼ of total cortical surface is well preserved, 2 = ¼ - ½, 3 = ½ - ¾, 4 = ≥ ¾ (Fernandez-Jalvo & Andrews 2016). Diet of suni and carbon signature differ, likely misidentification of suni.*

Taxon	No.	$\delta^{13}C$ (‰)	$\delta^{15}N$ (‰)	C/N ratios	Diet	Water	Layer	Heated	Surface Condition
Aepycerotini/Antilopini/Neotragini	032	-10.9	3.7	3.2	*M*	-	MH	✓	3
	036	-11.1	4.3	3.2	*M*	-	MH	✗	3
	049	-17.5	12.0	3.2	*B*	-	TP	✗	2
	100	-19.6	8.5	3.3	*B*	-	MH	✗	3
Alcelaphini	009	-13.8	6.2	3.2	G	WD	MH	✓	3
	023	-6.4	12.0	3.2	G	WD	TP	✗	3
	024	-7.5	12.7	3.2	G	WD	TP	✗	3
	026	-7.0	12.8	3.2	G	WD	TP	✓	3
	048	-6.8	6.1	3.2	G	WD	TP	✓	2
	052	-6.2	10.2	3.2	G	WD	TP	✗	3
	054	-6.2	13.1	3.2	G	WD	TP	✗	2

	056	-6.5	10.7	3.2	G	WD	TP	×	2
	060	-6.7	6.0	3.2	G	WD	MH	✓	3
	080	-13.4	5.3	3.2	G	WD	MH	✓	3
	087	-6.7	8.7	3.2	G	WD	MH	×	2
	092	-	-	-	G	WD	LP	×	1
	093	-	-	-	G	WD	LP	×	3
	095	-	-	-	G	WD	LP	×	3
	098	-	-	-	G	WD	LP	✓	2
	099	-	-	-	G	WD	LP	✓	2
Antelopini *Springbok (*A. marsupialis*)	005	-16.4	7.0	3.2	M/*B*	WI	MH	×	3
	008	-18.8	9.4	3.2	M/*B*	WI	MH	×	3
	031	-20.0	5.8	3.2	M/*B*	WI	MH	×	3
	051	-17.6	12.0	3.2	M/*B*	WI	TP	×	2
Antilopinae Low resolution	021	-7.9	6.0	3.2	*G*	-	TP	✓	2
	022	-13.3	8.2	3.2	*M*	-	TP	×	3
	046	-7.4	11.7	3.3	*G*	-	MH	✓	2
	069	-	-	-	-	-	MH	✓	2
	072	-12.2	4.3	3.2	*M*	-	MH	×	3
	090	-	-	-	-	-	LP	✓	2
	091	-	-	-	-	-	LP	✓	2
	097	-	-	-	-	-	LP	✓	2
Unknown Antilopinae 1	002	-5.6	3.2	3.2	*G*	-	MH	×	3
	019	-6.1	5.8	3.2	*G*	-	TP	✓	3
	028	-7.8	4.0	3.2	*G*	-	MH	×	3
	039	-5.3	2.8	3.2	*G*	-	MH	×	3
	044	-6.1	3.1	3.2	*G*	-	MH	×	3
	076	-6.9	2.3	3.2	*G*	-	MH	✓	3
	077	-10.5	3.7	3.2	*G*	-	MH	✓	3
Unknown Antilopinae 2	050	-17.5	5.4	3.2	*B*	-	TP	×	3
	078	-20.0	6.2	3.2	*B*	-	MH	×	3
	084	-19.3	4.3	3.2	*B*	-	MH	×	3
	096	-	-	-	*B*	-	LP	×	2
Cephalophini Blue Duiker (*P. monticola*)	035	-17.5	6.1	3.2	B	WI	MH	×	2
Equid	020	-9.6	6.3	3.2	G	WD	TP	×	2
	094	-	-	-	G	WD	LP	×	3
Hippotragini	068	-9.5	3.2	3.3	G	WD	MH	×	1
Neotragini Suni (*N. moschatus*)	025	-9.8	6.3	3.2	B	WI	TP	✓	3
Reduncini Browser **Grey rhebok (*P. capreolus*)	003	-19.8	4.6	3.2	*B*	WI	MH	×	3
	004	-18.9	3.8	3.2	*B*	WI	MH		3
	006	-19.1	4.9	3.2	*B*	WI	MH	×	3
	007	-20.0	5.5	3.2	*B*	WI	MH	×	3
	010	-19.8	5.8	3.2	*B*	WI	MH	×	3
	011	-19.9	6.0	3.3	*B*	WI	MH	×	3
	012	-19.0	4.2	3.2	*B*	WI	MH	✓	3

Reduncini Browser **Grey Rhebok (*P. capreolus*)	013	-19.6	5.6	3.3	*B*	WI	MH	×	3
	027	-19.5	4.4	3.2	*B*	WI	MH	✓	3
	029	-18.0	3.1	3.2	*B*	WI	MH	×	3
	030	-19.2	4.8	3.2	*B*	WI	MH	×	3
	033	-19.7	4.7	3.2	*B*	WI	MH	✓	2
	034	-19.9	4.0	3.2	*B*	WI	MH	×	3
	037	-19.9	3.8	3.2	*B*	WI	MH	×	3
	038	-20.3	4.7	3.2	*B*	WI	MH	×	3
	041	-19.2	5.4	3.3	*B*	WI	MH	×	3
	042	-19.2	4.7	3.3	*B*	WI	MH	✓	3
	043	-19.4	4.9	3.2	*B*	WI	MH	✓	2
	047	-18.9	6.2	3.2	*B*	WI	TP	×	3
	055	-18.9	8.2	3.2	*B*	WI	TP	×	3
	057	-19.4	3.7	3.6	*B*	WI	MH	×	3
	058	-19.3	4.8	3.2	*B*	WI	MH	×	2
	059	-19.3	4.9	3.2	*B*	WI	MH	✓	3
	061	-19.5	5.0	3.2	*B*	WI	MH	×	2
	062	-19.5	5.3	3.2	*B*	WI	MH	✓	1
	064	-19.6	5.3	3.2	*B*	WI	MH	×	1
	065	-20.7	4.2	3.2	*B*	WI	MH	×	2
	073	-19.8	4.6	3.2	*B*	WI	MH	×	3
	074	-20.8	5.3	3.3	*B*	WI	MH	×	3
	079	-19.6	4.2	3.2	*B*	WI	MH	×	2
	081	-19.8	5.1	3.2	*B*	WI	MH	✓	3
	082	-19.4	4.6	3.2	*B*	WI	MH	✓	3
	083	-20.2	4.0	3.2	*B*	WI	MH	✓	3
	088	-18.7	4.0	3.2	*B*	WI	MH	×	3
	089	-20.0	4.6	3.2	*B*	WI	MH	✓	3
Reduncini Grazer	014	-13.2	7.6	3.2	*G*	WD	MH	×	3
	016	-13.2	6.9	3.2	*G*	WD	MH	×	3
	017	-5.5	5.8	3.2	*G*	WD	TP	✓	3
	045	-11.8	7.5	3.2	*G*	WD	MH	×	2
	086	-6.0	3.6	3.2	*G*	WD	MH	×	3
Struthionidae Ostrich (*S. camelus*)	066	-20.3	5.2	3.3	B	WI	MH	×	3
Tragelaphini Common eland (*T. oryx*)	018	-18.4	11.2	3.2	B	WI	TP	×	2
	040	-18.7	5.7	3.2	B	WI	MH	×	3
	053	-19.9	8.5	3.2	B	WI	TP	✓	2
	063	-17.9	4.7	3.2	B	WI	MH	×	3
	070	-18.3	7.0	3.2	B	WI	MH	✓	2
	071	-19.6	7.5	3.3	B	WI	MH	×	2
Phacochoerini Warthog (*Phacochoerus africanus*)	015	-	-	-	G	-	MH	×	3
	075	-9.0	7.0	3.2	G	-	MH	×	2

4.1 THE SUCCESS OF ZOOMS AT GRS

Overall, ZooMS identified 57% (n = 57) of the sample to tribe, 15% (n = 15) to species, 12% (n = 12) to sub-family, 11% (n = 11) were unknown (collagen fingerprint not in the reference database), 3% (n = 3) were unsuccessful, and 2% (n = 2) were identified to genus (Fig. 4.1). Samples identified to at least tribe (including the unknowns) are considered successful while those with a low resolution (> tribe level) or no collagen markers are considered unsuccessful. No significant difference (χ^2 (2) = 2.01, p = 0.36) was found between the number of successful and unsuccessful samples in each occupational layer. Additionally, no significant difference was found between heated bone (χ^2 (1) = 0.01, p = 0.90) or the surface condition of bone (χ^2 (1) = 2.94, p = 0.09) and the success of ZooMS.

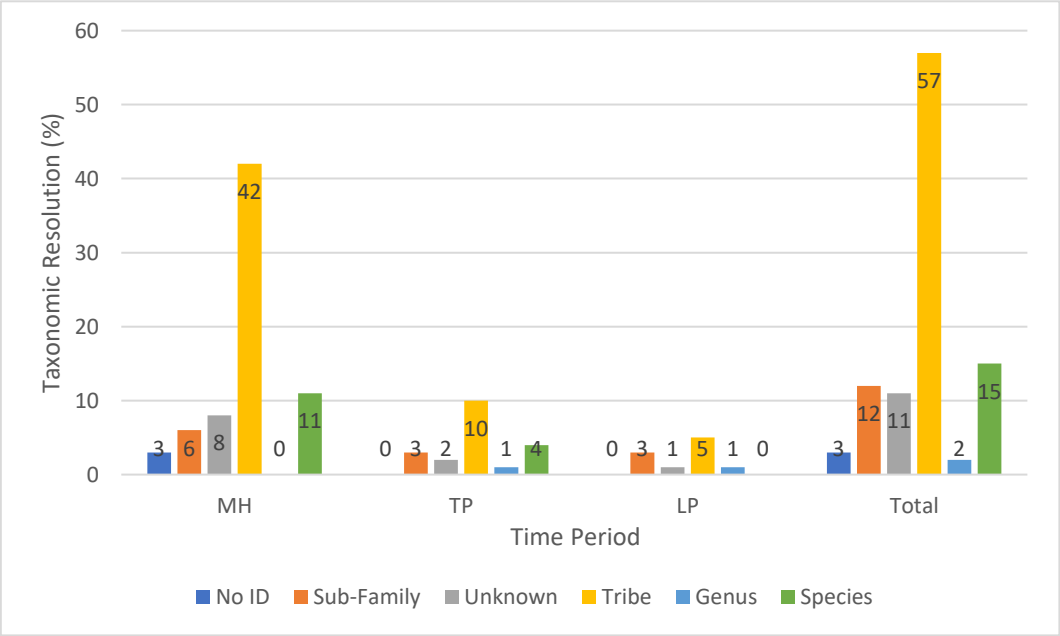


Figure 4.1: Cluster diagram showing the taxonomic resolution for each period and the overall sample. Number of samples for each category is given on the graph.

4.2 FAUNAL REMAINS

Fauna are split into three groups, namely browsers, intermediate feeders, and grazers (Table 4.1). Where possible, diet was assigned following Skinner and Chimimba (2005), however, $\delta^{13}C$ values have been used to infer diet in samples with low resolutions and in tribes containing taxa with specified diets (i.e., Reduncini) or dietary preferences (i.e., springbok). Changes in the number of browsers and grazers should correspond to changes in vegetation which is influenced by the environment.

Figure 4.2 shows a decline in grazers and increase in browsers from the LP to MH at GRS. Chi-squared analysis shows a significant difference (χ^2 (2) = 12.43, p = 0.002) between the

number of browsing and grazing taxa through time. Moreover, a significant difference (χ^2 (1) = 5.63, p = 0.02) was found between the number of browsers and grazers in the TP and MH, but not in the LP and TP. This suggests that the trend is driven by major faunal turnover in the TP and MH. A similar trend was observed in Opperman's ungulate faunal assemblage (Appendix 6). In both cases, more than 30% of the expected values were smaller than five. To combat this issue the ungulate assemblages were combined (Appendix 4). A significant difference (χ^2 (2) = 31.69, p < 0.001) was found between browsers and grazers in all layers, the LP and TP (χ^2 (1) = 10.89, p < 0.001), and the TP and MH (χ^2 (1) = 6.10, p = 0.01).

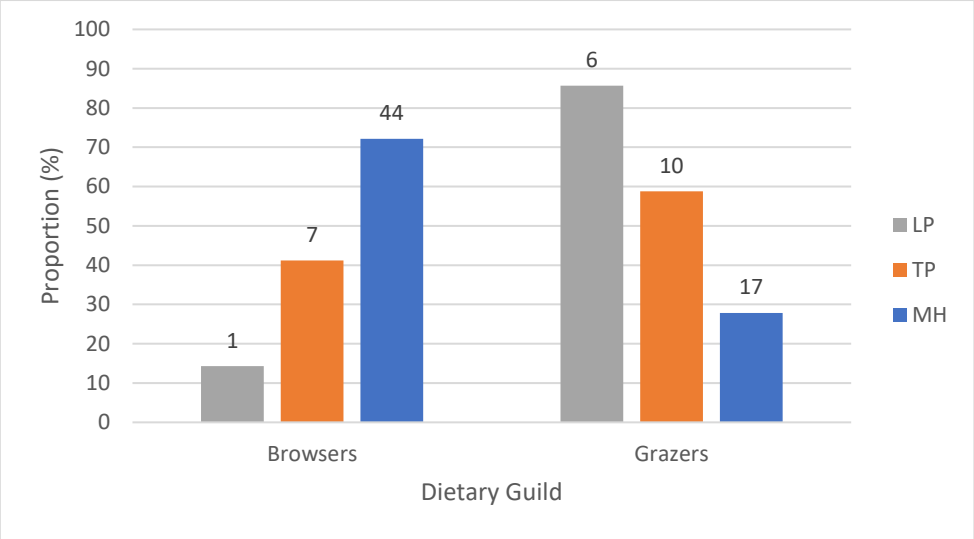


Figure 4.2: Cluster diagram showing the proportion (%) of bovid browsers and grazers for each occupational period at GRS with n-values included.

4.3 STABLE CARBON AND NITROGEN ISOTOPES

All $\delta^{13}C$ and $\delta^{15}N$ values are reported in Table 4.1. $\delta^{13}C$ bone collagen values between -29.5‰ and -17.5‰ indicate a majority C_3 diet and those between -10.5‰ and -2.5‰ indicate a majority C_4 diet (Adapted from Lee-Thorp 2008).

Springbok are often classified as intermediate feeders consuming a mix of C_3, C_4, and CAM plants (Gagnon & Chew 2000; Skinner & Chimimba 2005). However, studies have shown that springbok preferentially select C_3 browse over C_3/C_4 graze in most environments (Codron *et al.* 2008; Lehmann *et al.* 2013; Venter & Kalule-Sabiti 2016). The $\delta^{13}C$ values of GRS springbok are not significantly different (MW z = -0.91, p = 0.36) from GRS browsers. Therefore, springbok have been included in the browser category.

The combined use of ZooMS and stable carbon isotopes allowed higher resolution taxonomic identifications in the Reduncini tribe. Presently, the southern African Reduncini tribe

includes lechwe (*Kobus leche*), waterbuck (*K. ellipsiprymnus*), southern reedbuck, mountain reedbuck, and grey rhebok: the last three were recorded at GRS by Opperman (1984, 1987, 1988). Most Reduncini are medium to large grazers associated with water, but grey rhebok is the only water-independent (WI) browser (Skinner & Chimimba 2005; Castelló 2016). Reduncini make up 40% (n = 40) of the GRS sample. $\delta^{13}C$ values of ≤ -18.0‰ are documented in 87.5% (n = 35) of GRS Reduncini's indicating a C_3 browsing diet (Table 4.1). Since grey rhebok are the only browsing Reduncini (Skinner & Chimimba 2005; Castelló 2016) we can assume that these samples are grey rhebok.

Herbivore niche separation is indicated by non-normal bimodal distributions of $\delta^{13}C$ values in the TP and MH (Fig. 4.3). $\delta^{13}C$ values range from majority C_3 diets (min: -20.8‰) to majority C_4 diets (max: -5.3‰) (Fig. 4.4, 4.5, 4.6; Table 4.1).

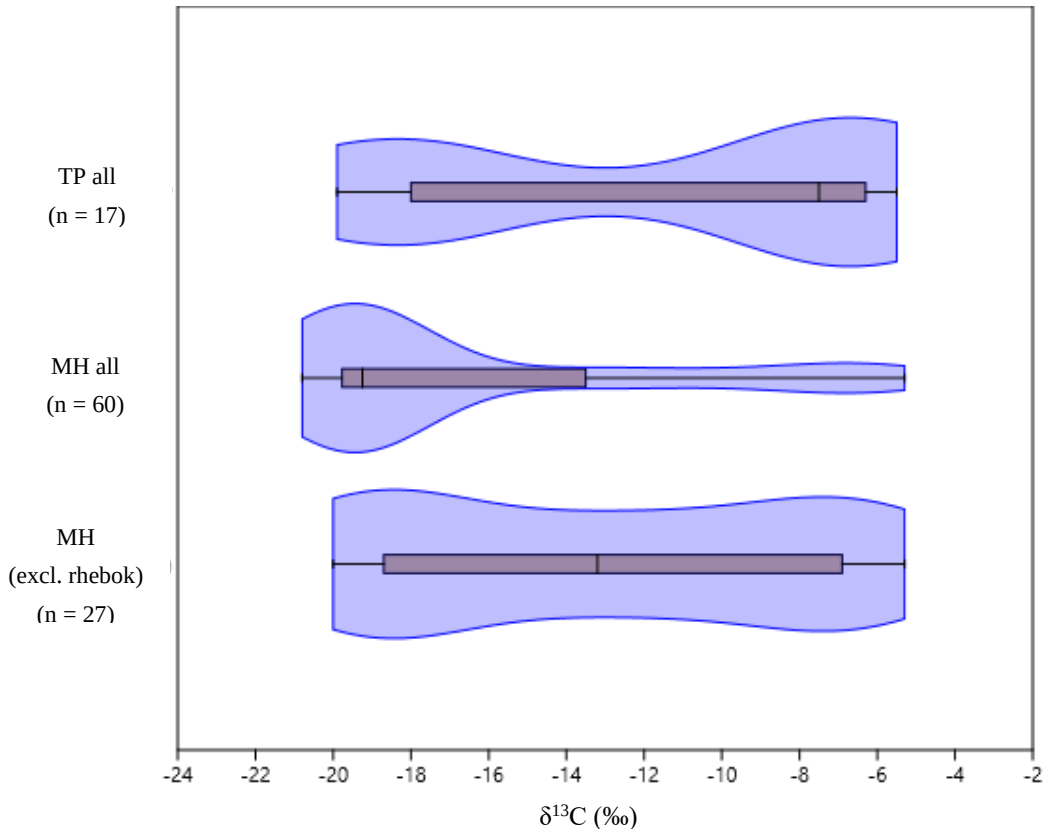


Figure 4.3: Violin plot with box plot included for the $\delta^{13}C$ values of TP and MH taxa. Taxa include browsers and grazers. A third violin plot with a box plot excluding MH grey rhebok is presented to investigate the effect of their large sample size (n =33) on the MH distribution.

This trend is subtle in the MH and is likely driven by the large number of MH grey rhebok (n = 33). Once removed, this trend becomes more apparent with browsers and grazers clustering around the C_3 and C_4 mean with no overlap between these taxa (Fig 4.6). Larger variation in

the $\delta^{13}C$ values of MH grazers compared to TP grazers may explain the less distinct peaks observed in the MH (Fig. 4.3, 4.6). The $\delta^{15}N$ values range from 5.4‰ to 13.1‰ (TP) and 2.3‰ to 9.4‰ (MH) (Fig. 4.4, 4.5, 4.6; Table 4.1). No significant difference was found between the $\delta^{15}N$ values TP or MH browsers and grazers.

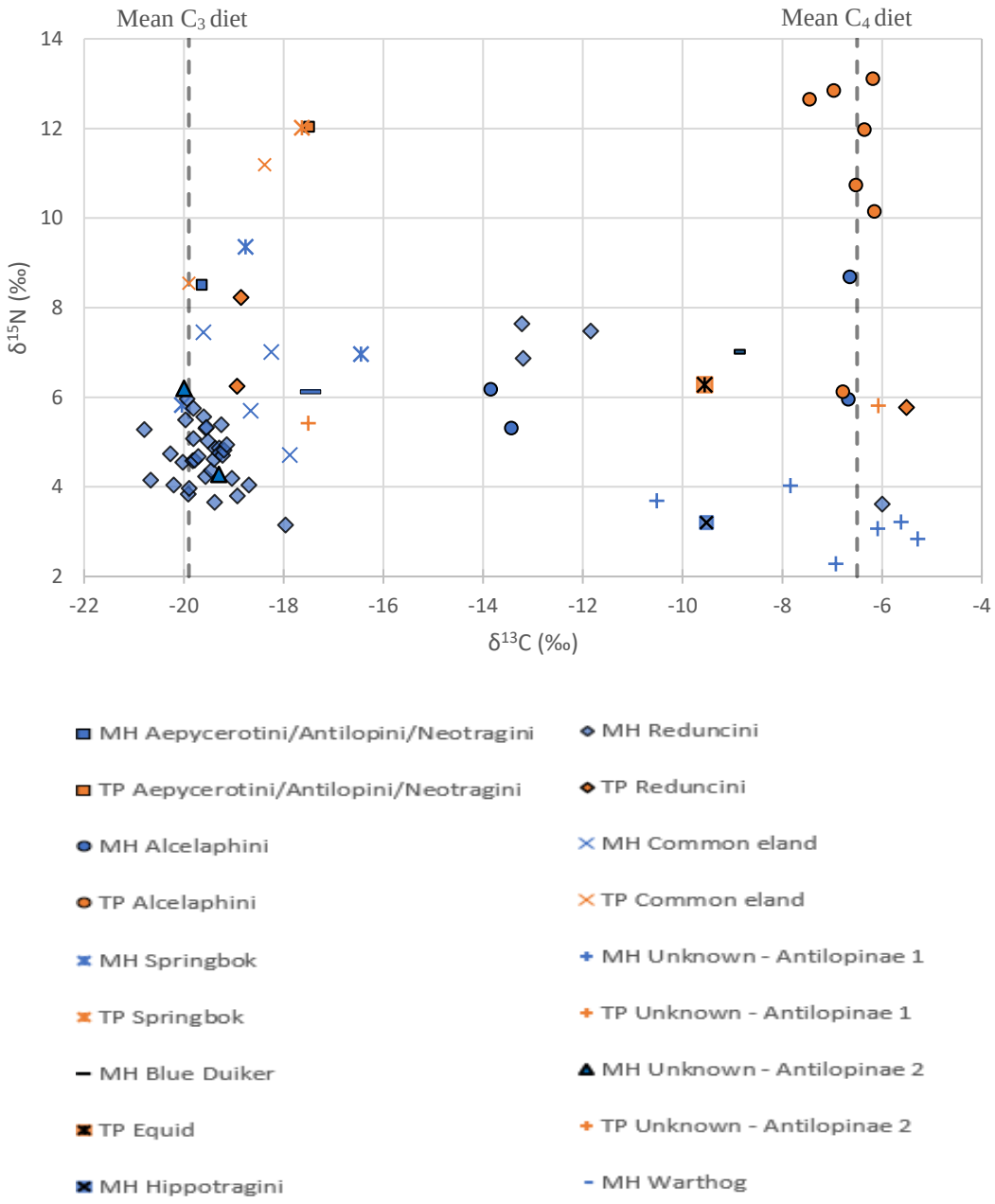


Figure 4.4: Scatter plot containing the $\delta^{13}C$ and $\delta^{15}N$ values of TP (orange) and MH (blue) taxa. The dotted grey lines represent the mean $\delta^{13}C$ values for C_3 and C_4 consumers which were adjusted by 1.5‰ from modern means.

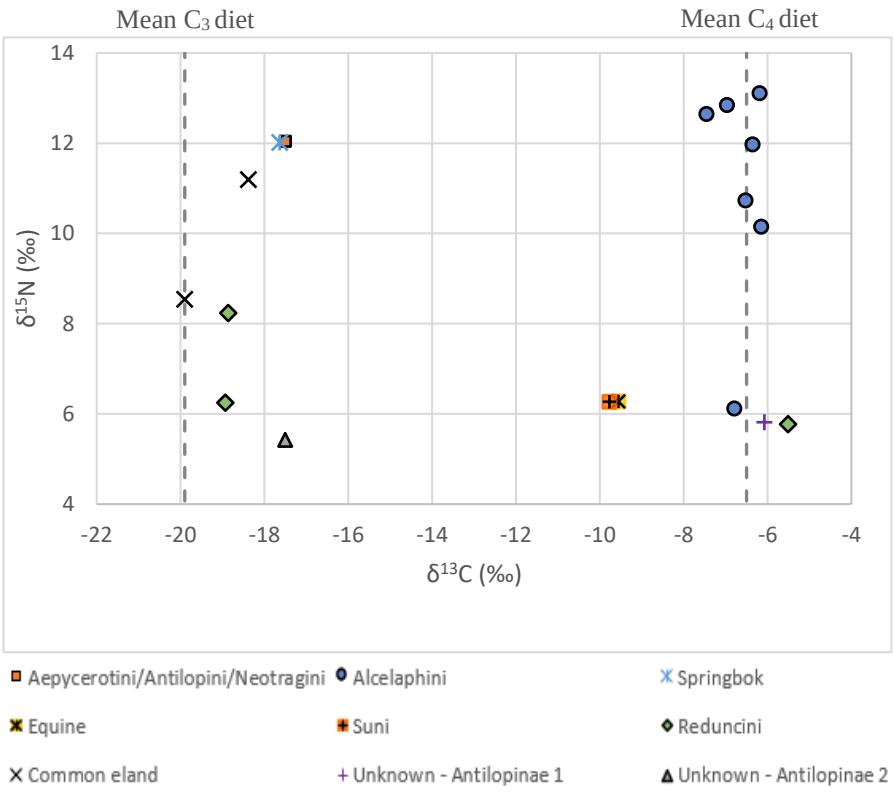


Figure 4.5: $\delta^{13}C$ vs $\delta^{15}N$ values for individual taxa from the TP. The dotted grey lines represent the mean $\delta^{13}C$ values for C_3 and C_4 consumers which were adjusted by 1.5‰ from modern means.

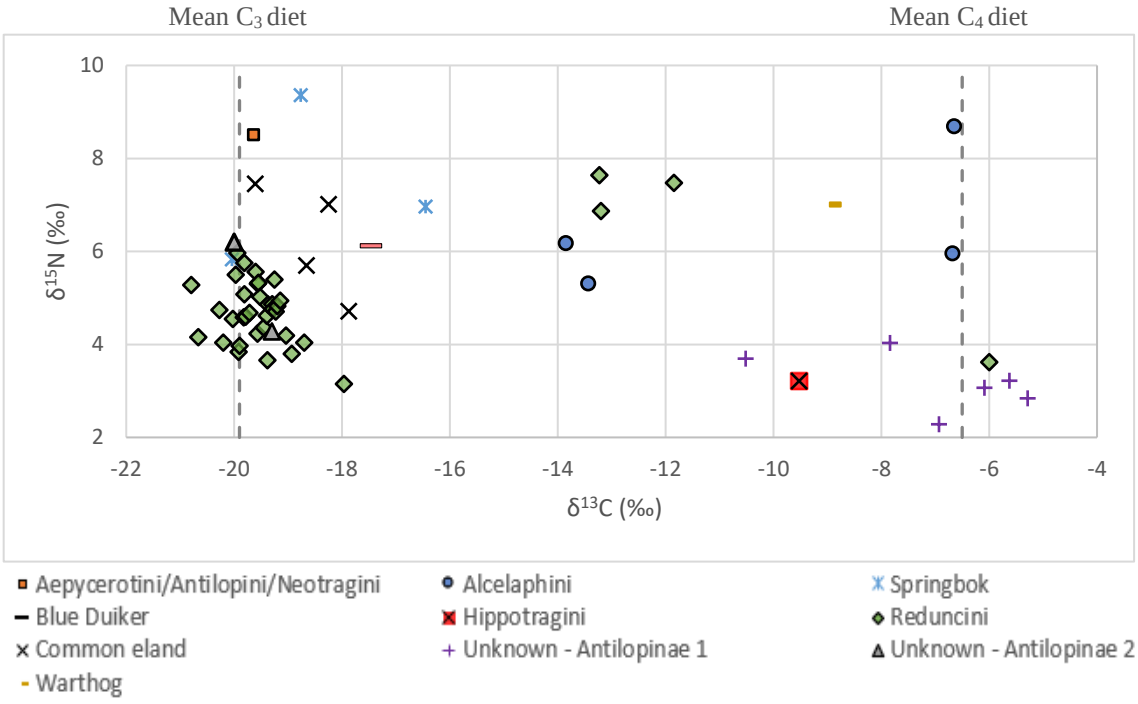


Figure 4.6: $\delta^{13}C$ vs $\delta^{15}N$ values for individual taxa from the MH. The dotted grey lines represent the mean $\delta^{13}C$ values for C_3 and C_4 consumers which were adjusted by 1.5‰ from modern means.

Figure 4.7 shows the spread of $\delta^{13}C$ and $\delta^{15}N$ values of TP and MH browsers and grazers.

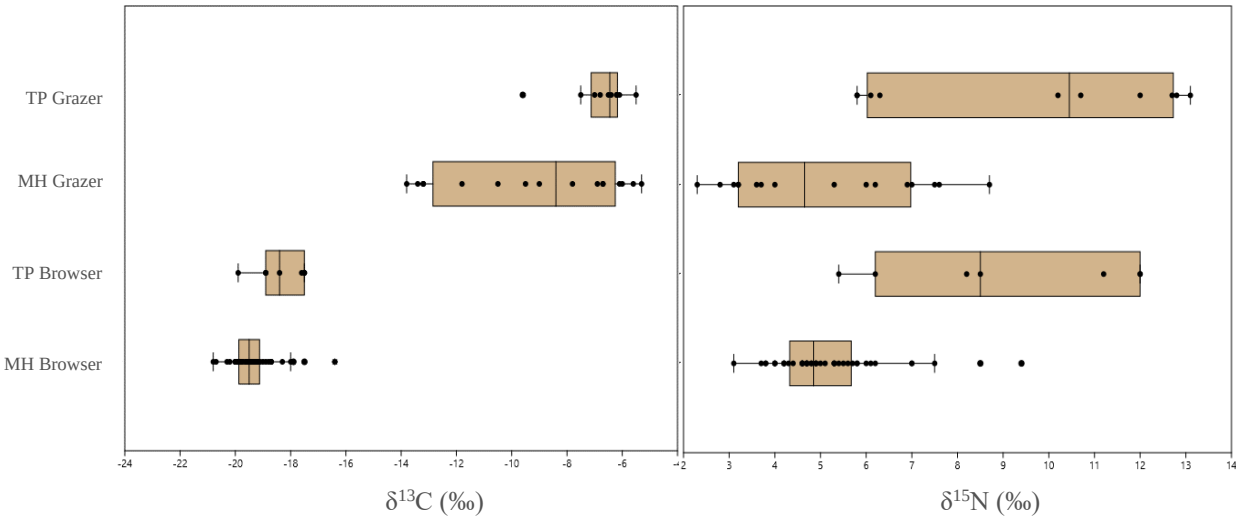


Figure 4.7: Box and jitter plots showing the $\delta^{13}C$ and $\delta^{15}N$ values of TP and MH browsers and grazers.

Browsing ungulates have mean $\delta^{13}C$ values of -18.4 ± 0.9‰ (TP, n = 7) and -19.4 ± 0.8‰ (MH, n = 44), ranging from -19.9‰ to -17.5‰ and -20.8‰ to -16.4‰, respectively. There is a significant difference between the $\delta^{13}C$ values (MW z = 2.52, p = 0.01) of TP and MH browsers. The MH browsing assemblage is dominated by grey rhebok. Grey rhebok have mean $\delta^{13}C$ values of -18.9‰ (TP, n = 2) and -19.6 ± 0.5‰ (MH, n = 33), ranging from -20.8‰ to -18.0‰ in the MH. Grey rhebok were subsequently removed from the MH (and TP) browsing sample, to assess their impact on the distribution of MH $\delta^{13}C$ browser values (Fig. 4.8). The remaining browsers had mean $\delta^{13}C$ values of -18.2 ± 1.0‰ (TP, n = 5) and -18.7 ± 1.1‰ (MH, n = 11), ranging from -19.9‰ to -17.5‰ and -20.0‰ to -16.4‰, respectively. No significant difference (MW z = 1.02, p = 0.31) was found between the remaining TP and MH browsers and the mean $\delta^{13}C$ value of TP grey rhebok fell within two standard deviations of the MH grey rhebok. However, a significant difference (MW z = 2.08, p = 0.04) was found between MH grey rhebok and the remaining MH browsers. The mean $\delta^{15}N$ browser values are 9.1 ± 2.7‰ (TP, n = 7) and 5.2 ± 1.2‰ (MH, n = 44), ranging from 5.4‰ to 12.0‰ and 3.1‰ to 9.4‰, respectively. There is a significant difference (MW z = 3.37; p < 0.001) between the $\delta^{15}N$ values of TP and MH browsers.

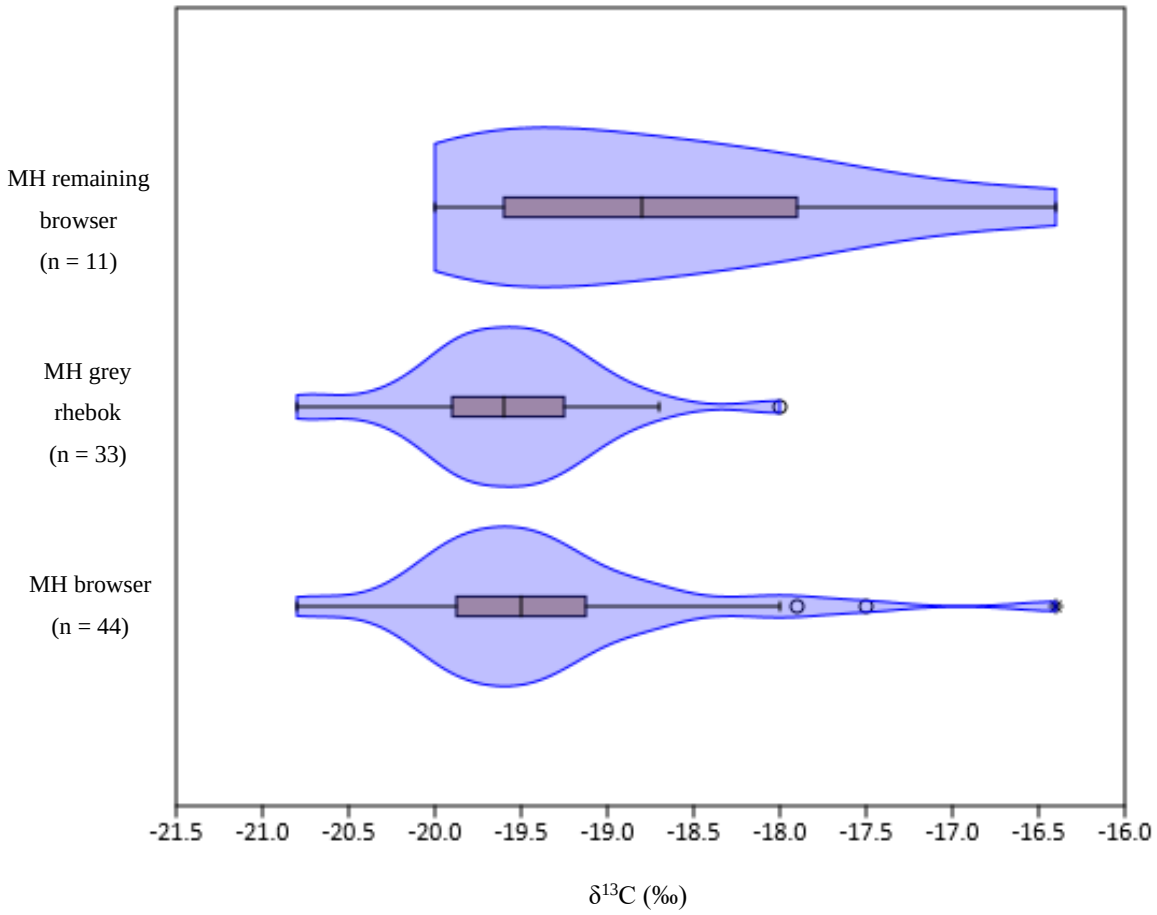


Figure 4.8: Violin plots with box plots for the $\delta^{13}C$ values of the remaining MH browsers, MH grey rhebok, and MH browsers.

Grazing ungulates have mean $\delta^{13}C$ values of -6.8 ± 1.1‰ (TP, n = 10) and -9.1 ± 3.1‰ (MH, n = 16), ranging from -9.6‰ to -5.5‰ and -13.8‰ to -5.3‰, respectively. No significant difference (MW z = -1.53, p = 0.13) was found between the $\delta^{13}C$ values of TP and MH grazers. Mean $\delta^{15}N$ values are 9.6 ± 3.2‰ (TP, n = 10) and 5.1 ± 2.1‰ (MH, n = 16), ranging from 5.8‰ to 13.1‰ and 2.3‰ to 8.7‰, respectively. There is a significant difference (MW z = -2.87, p = 0.004) between the $\delta^{15}N$ values of TP and MH grazers. Some grazing ungulates have a propensity to migrate in some environments. At GRS, migratory grazers include Alcelaphini and Equid while non-migratory grazers include Reduncini and Hippotragini (Skinner & Chimimba 2005; Hodgkins *et al.* 2020). The mean $\delta^{13}C$ values of TP migratory grazers were -7.0 ± 1.1‰ (n = 8) and non-migratory grazers was -5.5‰ (n = 1). The mean $\delta^{13}C$ values of MH migratory grazers were -10.15 ± 4.0‰ (n = 4) and non-migratory grazers was -10.74 ± 3.1‰ (MH, n = 5). No significant difference was found between the $\delta^{13}C$ values of TP and MH migratory grazers (MW z = 1.28, p = 0.2) or MH

migratory and non-migratory grazers (MW z = 0.37, p = 0.7), however, sample sizes may be too small for meaningful assessment.

4.3.1 WATER DEPENDENCY

Changes in the number of water-dependent (WD) and WI taxa and $\delta^{13}C$ and $\delta^{15}N$ may indicate changes in water availability over time (Fig. 4.9). Water-dependent taxa include Alcelaphini, Equid, and grazing Reduncini, while WI taxa include grey rhebok, common eland, blue duiker, and springbok (Skinner & Chimimba 2005). There is a significant difference ($\chi^2(2) = 24.41$, $p < 0.001$) between the number of WD and WI taxa in the LP, TP, and MH. Furthermore, a significant difference ($\chi^2(1) = 12.71$, $p = 0.002$) was found between the number of WD and WI taxa in the TP and MH but not in the LP and TP. This may be the result of small sample size and low expected values (Appendix 3).

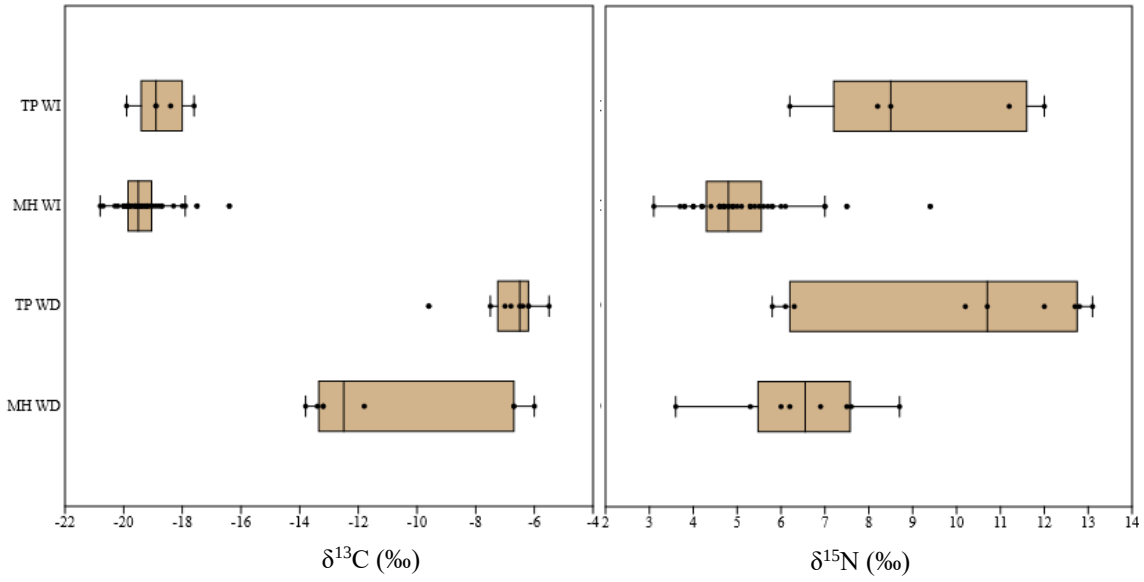


Figure 4.9: Box and jitter plots showing the $\delta^{13}C$ and $\delta^{15}N$ values of TP and MH WD and WI taxa.

The mean $\delta^{13}C$ values of WD taxa are -6.9 ± 1.2‰ (TP, n = 9) and -10.6 ± 3.5‰ (MH, n = 8), ranging from -9.6‰ to -5.5‰ and -13.8‰ to -6.0‰, respectively. Mean $\delta^{15}N$ values are 10.0 ± 3.1‰ (TP, n = 9) and 6.5 ± 1.6‰ (MH, n = 8), ranging from 5.8‰ to 13.1‰ and 3.6‰ to 8.7‰, respectively. Water-independent taxa have mean $\delta^{13}C$ values of -18.7 ± 0.8‰ (TP, n = 5) and -19.3 ± 0.8‰ (MH, n = 41), ranging from -19.9‰ to -17.6‰ and -20.8‰ to -16.4‰, respectively. Mean $\delta^{15}N$ values are 9.2 ± 2.4‰ (TP, n = 5) and 5.1 ± 1.2‰ (MH, n = 41) ranging from 6.2‰ to 12.0‰ and 3.1‰ to 9.4‰, respectively. No significant difference was found between the $\delta^{13}C$ values of TP and MH WD or WI taxa. There is,

however, a significant difference between the $\delta^{15}N$ values of TP and MH WD (MW z = -1.97 p = 0.05) and WI (MW z = -3.39, p = 0.001) taxa. A significant difference (MW z = -2.52, p = 0.01) was found between the $\delta^{15}N$ values of MH WD and WI taxa but no significant difference was found between TP WD and WI taxa.

4.3.2 INDIVIDUAL TAXA

Alcelaphini

Alcelaphini have mean $\delta^{13}C$ values of -6.7 ± 0.5‰ (TP, n = 7) and -10.2 ± 4.0‰ (MH, n = 4), ranging from -7.5‰ to -6.2‰ and -13.8‰ to -6.7‰, respectively. Mean $\delta^{15}N$ values are 11.1 ± 2.5‰ (TP, n = 7) and 6.6 ± 1.5‰ (MH, n = 4), with a range of 6.1‰ to 13.1‰ and 5.3‰ to 8.7‰, respectively. No significant difference was found between the $\delta^{13}C$ values of TP and MH Alcelaphini, however, a significant difference (MW z = -2.17, p = 0.03) was found in the $\delta^{15}N$ values.

Reduncini

Reduncini have been split into browsers (most likely grey rhebok) and grazers (Fig. 4.5, 4.6; Table 4.1). A significant difference (MW z = -3.56, p < 0.001) was found between the $\delta^{13}C$ values of browsing and grazing Reduncini. Browsers have mean $\delta^{13}C$ values of -18.9‰ (TP, n = 2) and -19.6 ± 0.5‰ (MH, n = 33), ranging from -20.8‰ to -18.0‰ in the MH. Mean $\delta^{15}N$ values are 7.2 ± 1.4‰ (TP, n = 2) and 4.7 ± 0.7‰ (MH, n = 33), ranging from 6.2‰ to 8.2‰ and 3.1‰ to 6.0‰, respectively.

Grazers have mean $\delta^{13}C$ values of -5.5‰ (TP, n = 1) and -11.1 ± 3.4‰ (MH, n = 4), ranging from -13.2‰ to -6.0‰ in the MH. There is no significant difference between MH grazers and MH Reduncini grazers (MW z = 0.91; p = 0.36). Mean $\delta^{15}N$ values are 5.8‰ (TP, n = 1) and 6.4 ± 1.9‰ (MH, n = 4), ranging from 3.6‰ to 7.6‰ in the MH.

Tragelaphini

Tragelaphini, comprising common eland, have mean $\delta^{13}C$ values of -19.2 ± 1.1‰ (TP, n = 2) and -18.6 ± 0.7‰ (MH, n = 4), ranging from -19.9‰ to -18.4‰ and -19.6‰ to -17.9‰, respectively. No significant difference was found between the $\delta^{13}C$ values of the Tragelaphini and browsers. Mean $\delta^{15}N$ values are 9.9 ± 1.9‰ (TP, n = 2) and 6.2 ± 1.3‰ (MH, n = 4), ranging from 8.5‰ to 11.2‰ and 4.7‰ to 7.5‰, respectively.

Antelopini

Antelopini, comprising springbok, have mean $\delta^{13}C$ values of -17.6‰ (TP, n = 1) and -18.4 ± 1.8‰ (MH, n = 3), with a range of -20.0‰ to -16.4‰ in the MH. Mean $\delta^{15}N$ values are 12.0‰ (TP, n = 1) and 7.4 ± 1.8‰ (MH, n = 3), with a range of 5.8‰ to 9.4‰ in the MH.

Other

The $\delta^{13}C$ and $\delta^{15}N$ values of taxa represented by one sample or with low taxonomic resolutions, including blue duiker, Hippotragini, suni, equid, ostrich, warthog, and Aepycerotini/Antilopini/Neotragini, are found in Table 4.1. The suni specimen is highlighted here as it has a $\delta^{13}C$ value of -9.8‰, suggesting that this specimen consumed a C_4 diet calling into question the identification of this sample.

Two unknown Antilopinae (n = 9) were identified. These samples produced good collagen fingerprints but could not be identified as no comparative collagen fingerprint was found in the reference database. Unknown Antilopinae 1 had mean $\delta^{13}C$ values of -6.1‰ (TP, n = 1) and -7.0 ± 1.9‰ (MH, n = 6), ranging from -10.5‰ to -5.3‰ in the MH. The $\delta^{13}C$ values of this specimen were not significantly different from grazers. Mean $\delta^{15}N$ values are 5.8‰ (TP, n = 1) and 3.2 ± 0.6‰ (MH, n = 6), ranging from 2.3‰ to 4.0‰ in the MH. Unknown Antilopinae 2 had mean $\delta^{13}C$ values of -17.5‰ (TP, n = 1) and -19.7 ± 0.5‰ (MH, n = 2), ranging from -20.0‰ to -19.3‰ in the MH. The $\delta^{13}C$ values of this specimen were not significantly different from browsers. Mean $\delta^{15}N$ values are 5.4‰ (TP, n = 1) and 5.3 ± 1.3‰ (MH, n = 2), ranging from 4.3‰ to 6.2‰ in the MH. It is also found in the LP assemblage.

CHAPTER 5: DISCUSSION

This chapter discusses the results of this study and addresses the research questions posed in the introduction. The following is discussed: the success of Zooarchaeology by Mass Spectrometry (ZooMS) at Grassridge Rockshelter (GRS), shifts in fauna and stable isotope ratios through time, and the palaeoenvironmental conditions at GRS during the late Pleistocene (LP, ca. 43–28 ka), terminal Pleistocene (TP, ca. 13.5–11.6 ka), and mid-Holocene (MH, ca. 7.3–6.8 ka) occupations.

5.1 ZOOMS

Readable collagen signatures were produced for 85% (n = 85) of the sample with most samples identified to tribe. The success of ZooMS increased through time (Fig. 5.1). However, no significant difference was found between the LP, TP, and MH, suggesting that bone preservation was relatively good throughout the sequence. Additionally, Opperman (1987, 1988) describes the preservation of Middle Stone Age (MSA) and Later Stone Age (LSA) bone fragments as good; based on visual impressions and morphological identifications. Collagen preservation is indicated in the TP and MH bones by collagen quality indicators (Appendix 2).

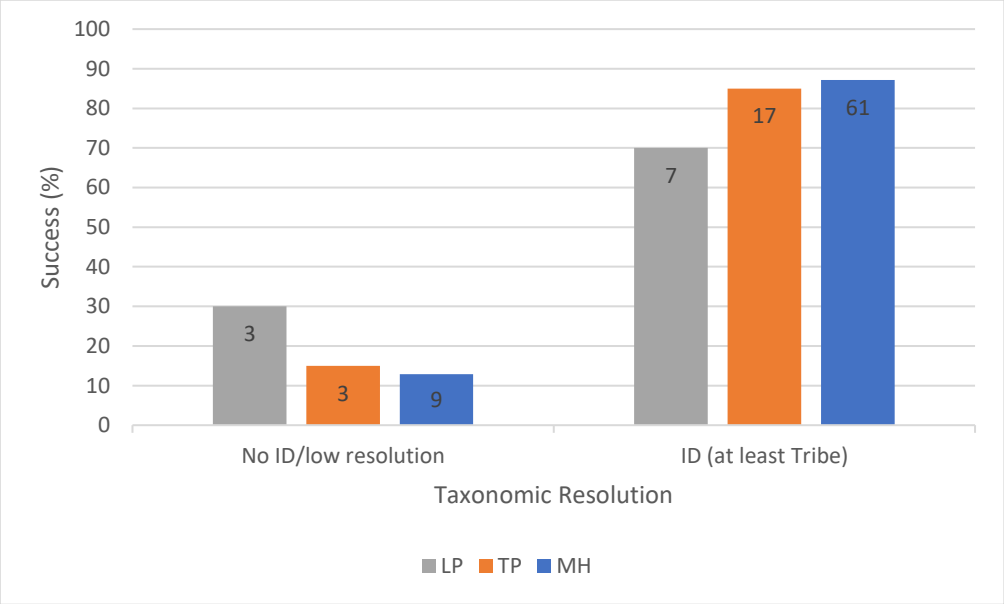


Figure 5.1: Clustered column showing an increase in successful ZooMS identifications (to at least tribe) and decrease in unsuccessful ZooMS identifications through time. The n-values are included.

Faunal identifications using ZooMS were not expected in the LP assemblage as collagen preservation was anticipated to be poor due to post-depositional water movement recorded in

this profile (Collins *et al.* 2017; Ames *et al.* 2020), and the age of the samples (Lee-Thorp 1989). Collagen rarely survives in usable quantities after 10 000 years, especially in warm or tropical environments (Lee-Thorp 1989; Ambrose 1990; Holmes *et al.* 2005; Lee-Thorp & Sponheimer 2006). Several factors may have contributed to the better-than-expected collagen preservation at GRS, including neutral pH values (7.9–8.8) of the surrounding matrix (Gordon & Buikstra 1981; Ames *et al.* 2020) and cooler conditions and protection from environmental factors such as solar irradiation provided by the rockshelter (Ambrose 1990; Nielsen-Marsh *et al.* 2000; Turner-Walker 2008).

Taphonomic conditions may also be linked to better bone preservation. Burnt bones or bones with poor surface preservation were avoided when selecting the sample. Despite these efforts, some of the samples experienced some degree of heating and have varying levels of surface preservation. These variables did not, however, significantly impact the success of ZooMS or stable isotope analysis (Appendix 3). Similarly, no correlation was found between surface preservation or heating and the success of ZooMS by Bradfield *et al.* (2019). DeNiro *et al.* (1985) found little to no change in the C: N ratios of boiled or roasted bones, although a large change was recorded in burnt or cremated bones. Janzen *et al.* (2021), however, suggests that boiling resulted in the low success rate of ZooMS in Zambia. Alternatively, other factors, like sandy soil matrices (Pate 1997), high or fluctuating temperatures, or dynamic hydrological conditions (Klinken 1991; Trueman *et al.* 2004) may have affected collagen preservation in this region. Additional consideration and screening techniques for collagen preservation should be considered before undertaking ZooMS analysis (see Bouchard *et al.* 2020; Le Meillour *et al.* 2020; Chowdhury *et al.* 2021).

The success of ZooMS at various sites and times periods including those from southern Africa are documented in Table 5.1. Overall, the success of ZooMS at GRS is better than or on par with global and southern African studies and may suggest that ZooMS can be used to identify faunal remains from warmer climates or older assemblages (Asara *et al.* 2007; Buckley *et al.* 2008b, 2011; Buckley & Kansa 2011; Cappellini *et al.* 2012; Harvey *et al.* 2016; Desmond *et al.* 2018; Prendergast *et al.* 2019; Janzen *et al.* 2021). Its use may transform zooarchaeological studies and renew interest in and add value to previously inaccessible avenues of research. Additional information about the palaeoenvironmental conditions, subsistence strategies, animal symbolism, and the spread of herding economies and foodways may be gained by using this novel method.

Table 5.1: Success of ZooMS on faunal remains from several sites with varying ages. Results are ordered from most successful to least successful. Success is determined by the level of taxonomic resolution, with successful samples identified to at least tribe.

Global				
Location	**n**	**Approximate age (BP)**	**Success (%)**	**Reference**
Taforalt, Morocco	13	13500–15000	100	Desmond *et al.* 2018
Domuztepe, Turkey	111	7400–7750	100	Buckley & Kansa 2011
Luxmanda, Tanzania	79	3000	68.4	Prendergast *et al.* 2019
Quebec, Canada	15	350–600	66.7	McGrath *et al.* 2019
Les Cottés, France	145	23000–37000	57.9	Welker *et al.* 2015
Odense, Denmark	20	< 2000	45.0	Brandt *et al.* 2018
Barrow Island, Australia	134	60–70	36.6	Peters *et al.* 2021
Zambia	192	500–4000	25.5	Janzen *et al.* 2021
Southern Africa				
Location	**n**	**Approximate age (BP)**	**Success (%)**	**Reference**
Leopard Cave, Namibia	28	800–2500	100	Le Meillour *et al.* 2020
Kwa-Zulu Natal, South Africa	26	< 2000	100	Coutu *et al.* 2016
Western Coast, South Africa	9	1300–2000	88.9	Coutu *et al.* 2021
Grassridge Rockshelter, South Africa	100	6000–40000	85	This study
Panga ya Saidi, Kenya	105	320–1180	63	Culley *et al.* 2021a
Kwa-Zulu Natal, South Africa	83	150–8500	50.6	Bradfield *et al.* 2021
North interior region, South Africa	77	< 2000	15.6	Bradfield *et al.* 2019

5.1.1 UNEXPECTED TAXA

Two unexpected taxa, namely ostrich and blue duiker were identified at GRS using ZooMS. Ostriches inhabit open, short-grassland and semi-desert biomes in southern Africa (Cooper *et al.* 2009, 2010) and are currently found in the Grassridge region (Fig. 5.2; see Stewart *et al.* 2020: 6459).

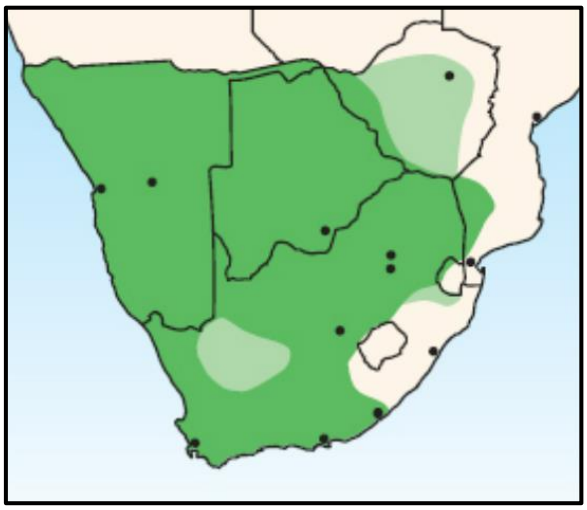


Figure 5.2: The current distribution of ostrich in southern Africa (In Sinclair et al. 2020: 158).

However, ostrich bone is rarely found in the archaeological record. It is only found at a few southern African sites, including Ysterfontein 1 (Avery *et al.* 2008), Varsche Rivier 003 (Steele *et al.* 2016), and Duinefontein 2 (Cruz-Uribe *et al.* 2003), at some North African sites (Merzoug 2011), and has not been identified in Asian assemblages (Janz *et al.* 2009). The mass spectra produced for this sample was poor (Appendix 5), however, the identification of this sample was enabled by the preservation of a unique collagen marker (M. Buckley, personal communication, 2021). Figure 5.3 is a photograph of the bone fragment.



Figure 5.3: Photograph of specimen 066 which has been identified as ostrich using ZooMS.

The lack of ostrich bone is surprising as ostrich provide large quantities of nutrient-rich meat and other tissues (Horbańczuk *et al.* 2003, 2004; Belichovska *et al.* 2015). Ostriches are regularly recorded in Khoe-San rock art (Hollmann 2001, 2003), and hunters are depicted using ostrich skin and feathers to disguise themselves as they approach ungulates at waterholes (Fig. 5.4). Their significance and use are further emphasised in folktales and historical ethnographies (Low 2009, 2011). Several explanations are given for the apparent absence of ostrich bone in the archaeological record including issues of differential bone preservation, taphonomic bias, morphological identification bias, and even taboo on ostrich meat (Merzoug 2011, Kuper 2015).

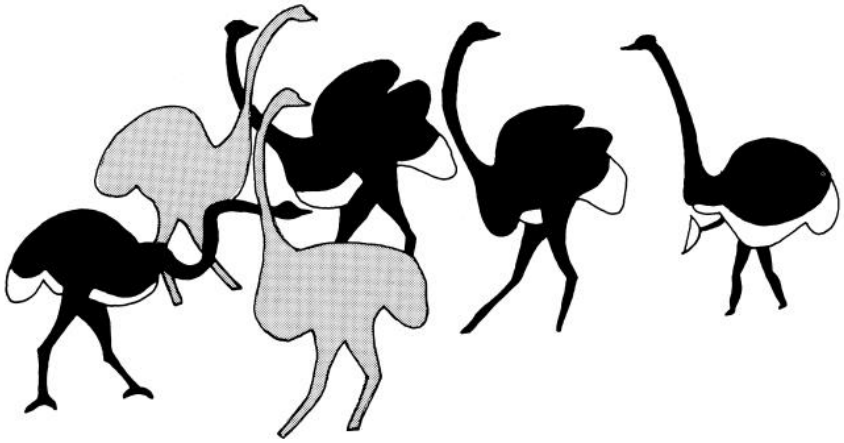


Figure 5.4: A painting with five ostriches showing curiosity behaviour when approached by a bushman disguised as an ostrich. Found in the Hershel District (In Thackeray 1983: 39).

Blue duikers are not currently found in the Grassridge region (Fig. 5.5). The unusual presence of blue duiker is similarly reported at Abbots Cave and Lame Sleep Shelter located in the semi-desert Karoo, South Africa (Plug 1993) and at Ha Makotoko, Muela, and Mhlwazini in the highlands (Plug 1997). Their presence at GRS and the above-mentioned sites is ecologically unlikely (Plug 1993, 1997; Horsburgh *et al.* 2016). They are typically found along the eastern and south-eastern coastal regions (Fig 5.5) in forests, thickets, or dense coastal bush (Klein 1984; Plug 1997; Skinner & Chimimba 2005; Avery 2019).

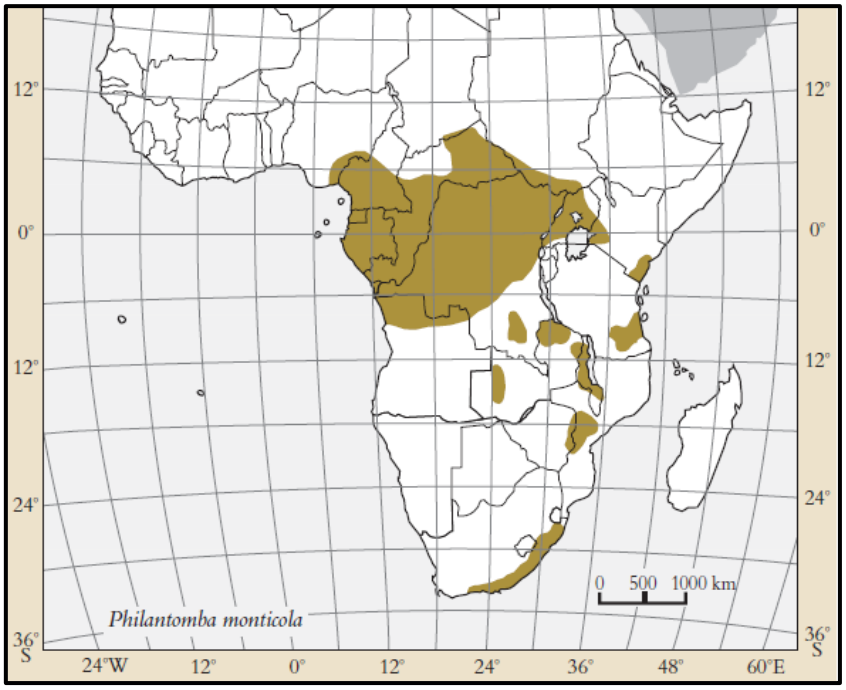


Figure 5.5: Current distribution of blue duiker in Africa (In Skinner & Chimimba 2005: 670).

Blue duiker may have had a larger distribution in the past; however, we would expect the associated fauna to be vastly different if blue duiker naturally occurred at GRS and the other sites (see Clark 2017). Alternatively, blue duiker remains may have reached GRS through social or mobile networks between the coastal, thicket, and montane grassland regions. Broad social networks across a range of biomes during the TP and MH are implied by the presence of marine shells and beads at GRS (Collins *et al.* 2017; Ames *et al.* 2020), and isotopic data (Stewart *et al.* 2020). These sites are, however, located more than 100 km away from GRS (Deacon 1976; Robertshaw 1984; Hayward *et al.* 2005; Skinner & Chimimba 2005; Avery 2019). Some ritual or social importance was possibly associated with blue duikers, but no written records or ethnographic evidence exists to support this (Plug 1993, 1997; Horsburgh *et al.* 2016). In rare instances, symbolic value has been associated with the collection of some faunal remains, such as the lion teeth cited by Fagan (1967) and Orton *et al.* (2011), while other faunal remains may have had mechanical value and were transported as they provided certain functions, like the modified *Raphicerus* metapodial reported by Smith (2006).

It is possible that this specimen was misidentified, and that blue duiker shares a similar collagen signature with another closely related bovid (Fig. 5.6). Table 5.2 shows a list of the identified peptide markers for some of the small antelope previously identified at GRS (Opperman 1984, 1987, 1988) and compares these with blue duiker. The collagen signatures of these species differ from blue duiker increasing confidence in the identification; however, the reference database is incomplete (Janzen *et al.* 2021) and does not include extinct bovids.

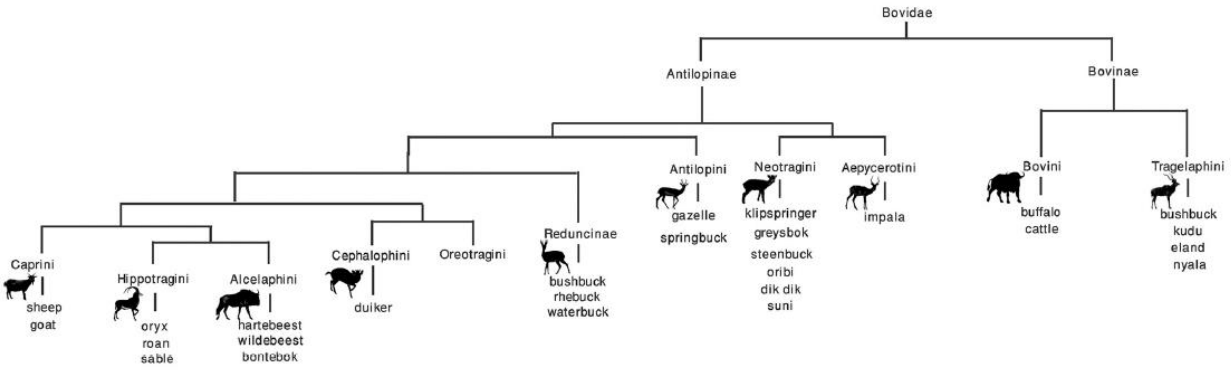


Figure 5.6: Phylogenetic tree showing southern African representatives from various tribes and sub-families of the Bovidae family (In Bradfield et al. 2021: 14).

Table 5.2: List of identified peptide markers found in Bradfield et al. (2021) and Janzen et al. (2021). Collagen peptide markers of blue duiker and other small antelope that have previously been identified at GRS (Opperman 1984, 1987, 1988). Differences are highlighted in green. No peptide markers have been reported for grysbok.

	A	B	X1	C	X2	D	X3	F	G	X4
Blue duiker	1208	1427	1514	1580	-	2131	-	2883	3059	-
Common duiker	1208	1427	1532	1580	-	2131	-	2853	3059	-
Klipspringer	1208	1427	-	1580	-	2131	-	2883	3033	-
Steenbok	1196	1427	-	1550	-	2131	2581	2883	3033	3027
Oribi	1196	1427	-	1550	-	2131		2883	3033	-
Grysbok	-	-	-	-	-	-	-	-	-	-

5.2 VARIABILITY IN FAUNAL ABUNDANCE AND STABLE ISOTOPE RATIOS

Shifts in faunal species composition and stable carbon and nitrogen isotope ratios are documented at GRS. These shifts are intrinsically linked with vegetation change and likely result from changing palaeoenvironmental conditions (Boone 2019; Ames *et al.* 2020).

5.2.1 FAUNAL CHANGE

Ethnographic data suggest that recent southern African hunter-gatherers typically foraged within 8–12 km of their residence (Lee 1972; Bartram *et al.* 1991), thus we assume that the ungulate assemblage represents the taxa inhabiting the Grassridge region except for the blue duiker (Table 5.3).

Table 5.3: Ungulate faunal assemblage in the LP, TP, and MH from this study and Opperman's (1984, 1987, 1988).

This Study ZooMS Identification					**Opperman Morphological Identification**				
Taxa		**LP**	**TP**	**MH**	**Taxa**		**LP**	**TP**	**MH**
Browser		1	6	43	**Browser**		-	8	82
Cephalophini	Blue duiker	-	-	1	Cephalophini	Common duiker	-	-	1
Tragelaphini	Common eland	-	2	4	Tragelaphini	Common eland	-	-	3
Reduncini	Grey rhebok	-	2	33	Reduncini	Grey rhebok	-	5	37
Antilopinae	Unknown Antilopinae 2	1	1	2	Neotragini	Grysbok/steenbok	-	-	4
Antilopini	Springbok	-	1	3	Oreotragini	Klipspringer	-	3	26
					Antilopini	Springbok	-	-	11

This Study ZooMS Identification					Opperman Morphological Identification				
Taxa		**LP**	**TP**	**MH**	**Taxa**		**LP**	**TP**	**MH**
Grazer		6	10	17	**Grazer**		7	7	34
Alcelaphini		5	7	4	Alcelaphini	All	6	6	4
						Blesbok	-	2	-
						Hartebeest/Wildebeest	6	4	4
Reduncini		-	1	4	Reduncini	All	1	1	24
						Mountain reedbuck	-	1	24
						Southern reedbuck	1	-	-
Phacochoerini	Warthog	-	-	2	Phacochoerini	Warthog	-	-	3
Equus	Zebra	1	1	-	Equus	Zebra	-	2	-
Hippotragini		-	-	1	Antilopini	Oribi	-	-	3
Antilopinae	Unknown Antilopinae 1	-	1	6					

The ungulates from this study and Opperman's (1984, 1987, 1988) were combined to increase sample size and reduce the number of expected values smaller than five (Appendix 4). Major faunal turnover is documented at GRS with grazing ungulates declining after Marine Isotope Stage (MIS) 3. This trend is well documented in southern Africa and has been associated with changing vegetation and environmental conditions (Klein 1972, 1974, 1980, 1984; Vrba 1985, 1995; Brink 1987, 1999; Brink & Lee-Thorp 1992; Faith 2011a, 2012, 2013a, b, 2014; Faith & Behrensmeyer 2013).

Conversely, Beard's (2018: 20) morphological study found no significant difference between the number of browsers, grazers, and intermediate feeders during the TP and MH. The number of browsers, grazers, and intermediate feeders in this study, Opperman's (1984, 1987, 1988), and Beard's (2018) were plotted and compared (Fig. 5.7). The intermediate feeders were excluded from Beard's assemblage and no significant difference (χ^2 (1) = 0.60, p = 0.44) was found between TP and MH browsers and grazers (Appendix 7). Furthermore, Beard's data shows a decline in browsers and an increase in grazers through time (Fig. 5.7). This trend is likely obscured by uneven and small sample sizes (Beard 2018). It may also be affected by morphological identification biases (Buckley & Kansa 2011; Horsburgh *et al.* 2016).

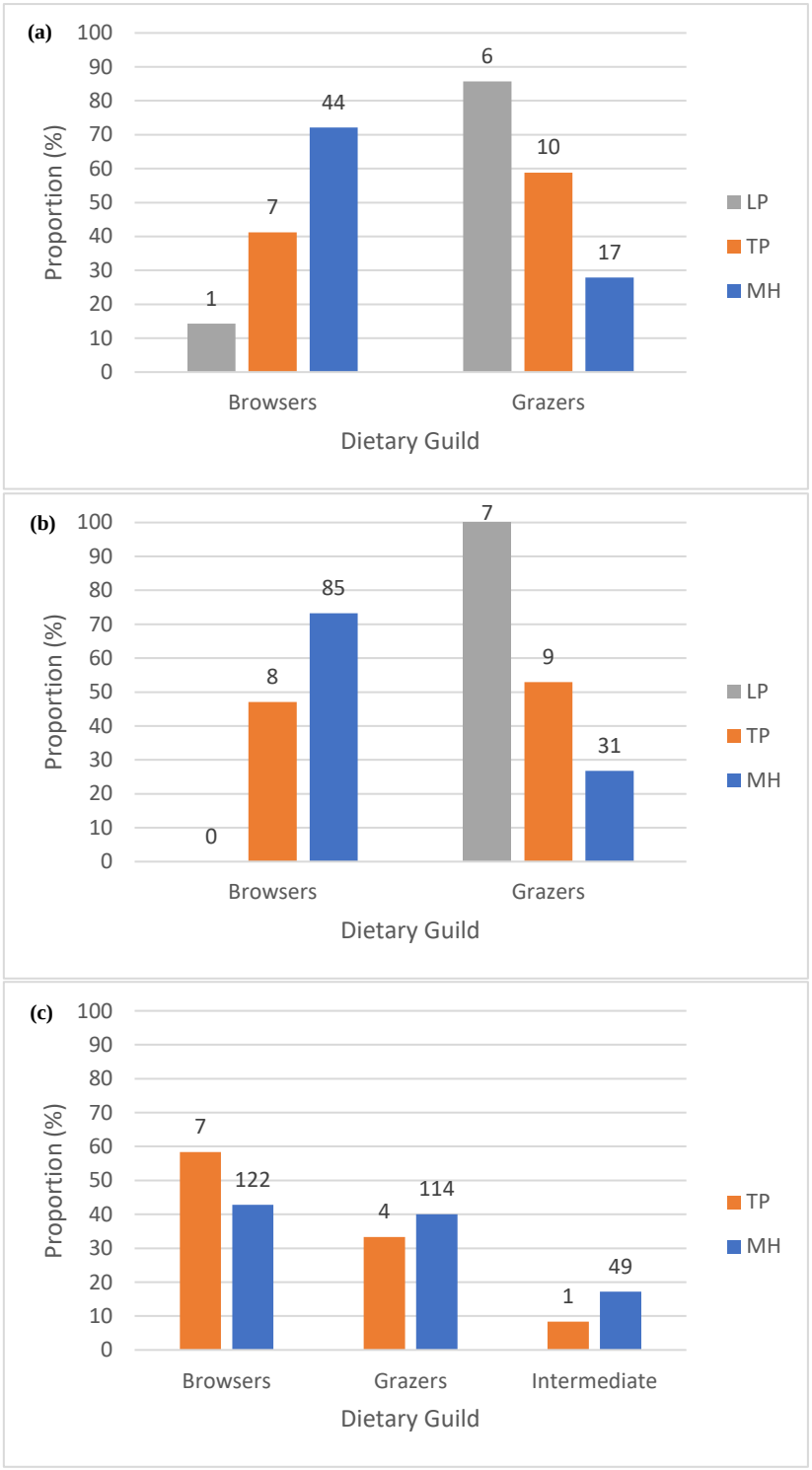


Figure 5.7: Proportion (%) of bovid browsers (incl. springbok), grazers, and intermediate feeders for each occupational period at GRS with n-values included. (a) This study, (b) Opperman (1984, 1987, 1988), and (c) Beard (2018). A decline in grazers and increase in browsers from the LP to MH layers are documented in this study and Opperman's. While Beard's (2018) shows a slight increase in grazers and decline in browsers from the TP to MH. No significant difference ($\chi 2$ (1) = 0.60, p = 0.44) was found between Beard's TP and MH browsers and grazers.

Shifts in bovid size class (Fig. 5.8) were documented by Opperman (1984, 1987, 1988) and Beard (2018), indicating a shift in subsistence activity with GRS inhabitants focusing on large bovids during the TP and browsers and small territorial bovids inhabiting the surrounding hilly region during the MH. A similar trend is documented here with browsers (mostly grey rhebok) increasing during the MH. Similarly, Geoghegan (2019) documented a shift in subsistence behaviour at GRS from the TP to MH. She suggests that this shift was most likely related to changing environmental conditions as opposed to overexploitation or resource stress (Geoghegan 2019: 42).

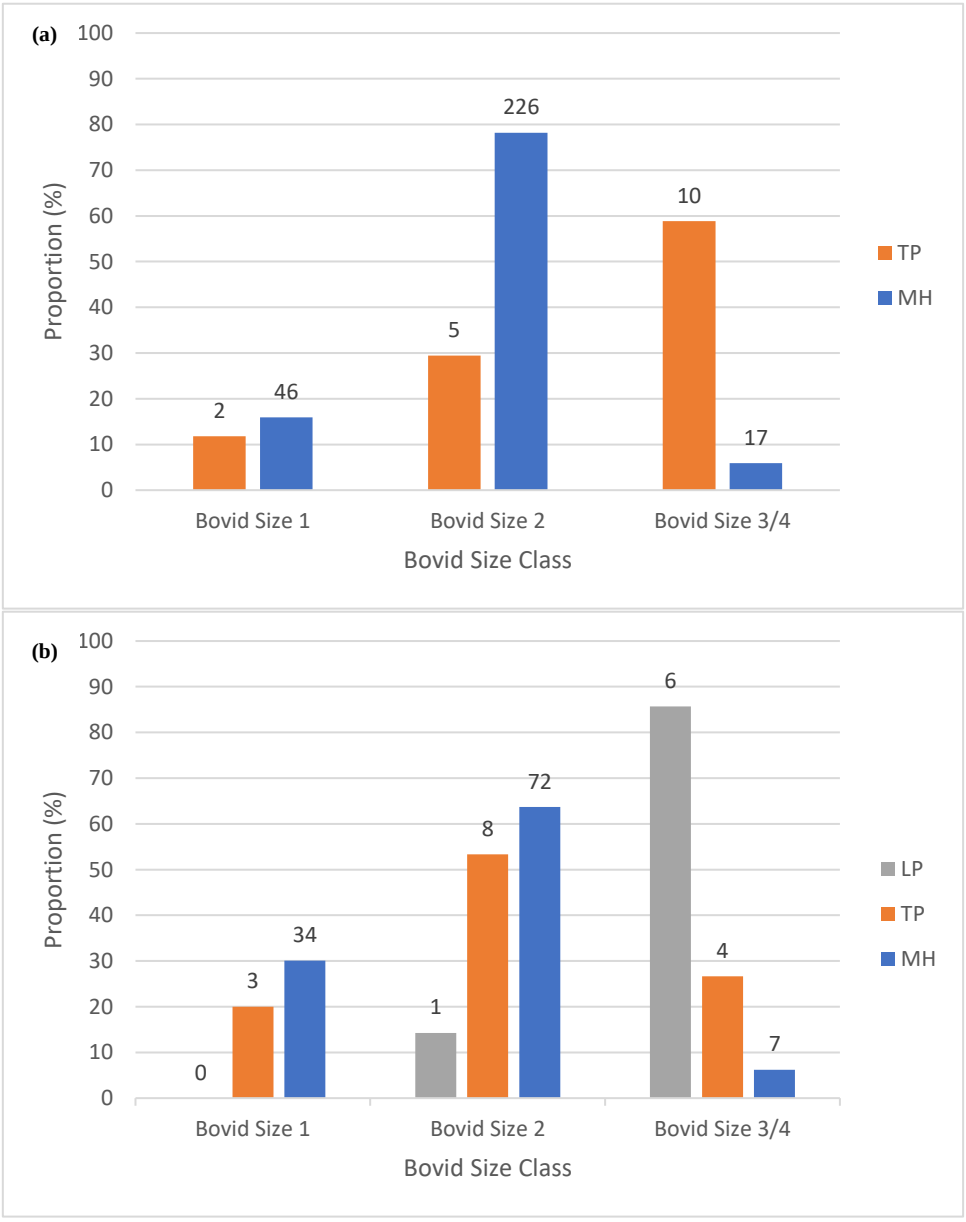


Figure 5.8: (a) Beard (2018) bovid size classes in the TP and MH, bovid size class 3 and 4 were combined by Beard to increase the sample size of the category. (b) Opperman (1984, 1987, 1988) bovid size classes in the LP, TP, and MH, bovid size class 3 and 4 were combined to allow for comparison with Beard (2018).

A similar trend of hunting smaller game is recorded roughly 100 km away at Colwinton, located above the escarpment (Opperman 1982, 1987), while a contrasting trend of hunting larger game (i.e., Equids and Alcelaphini) is recorded at Te Vrede and Bonawe, located below the escarpment (Opperman 1984, 1987). Shifts from large bovids in the Pleistocene to browsers and small territorial bovids in the Holocene is recorded at several southern African sites located across a range of biomes (Klein 1972, 1978, 1983; Plug & Engela 1992; Bousman 2005; Barham & Mitchell 2008; Faith 2013a, b; Sealy *et al.* 2016, 2020; Stewart & Mitchell 2018) and likely relates to faunal turnover resulting from palaeoenvironmental change associated with the transition from the glacial to interglacial period (Faith 2014). These shifts are less noticeable at coastal sites (e.g., Nelson Bay Cave) where shellfish were widely available (Klein 1972, 1974).

5.2.2 STABLE ISOTOPE CHANGE

Stable isotope analysis was not performed on the LP faunal remains as preservation was expected to be poor. Shifts in the $\delta^{13}C$ and $\delta^{15}N$ bovid values from the TP to MH are explored here.

Carbon

Herbivore niche separation is indicated by non-normal bimodal distributions of the $\delta^{13}C$ values in the TP and MH (Fig. 4.3, 4.5, 4.6). This trend appears to be subtle in the MH, a period dominated by browsers (n = 44), specifically grey rhebok (n = 33), and more generalised grazers (n = 16). Grey rhebok (n = 33) were removed from the MH browser assemblage to see if their abundance affected the $\delta^{13}C$ distribution. The $\delta^{13}C$ values from the remaining MH browsers (n = 11) and MH grazers (n = 16) were plotted (Fig. 4.3). Following the removal of MH grey rhebok, two peaks are formed with browsers and grazers clustering on either end of the C_3 and C_4 spectrum (Fig 4.3, 4.6), suggesting that the abundance of grey rhebok drove the $\delta^{13}C$ MH trend. Notably, the TP peaks are more distinctive than the MH peaks and are likely related to more variable $\delta^{13}C$ values in MH grazers. Similar non-normal bimodal distributions are observed in modern African ungulates inhabiting the Summer Rainfall Zone (SRZ) (Lee-Thorp & van der Merwe 1987; Hofmann 1989; Cerling & Harris 1999; Cerling *et al.* 2003; Sponheimer *et al.* 2003a; Codron *et al.* 2008).

The mean $\delta^{13}C$ values of C_3 and C_4 plants differ by approximately 14‰ (Fig 5.9). This difference is subsequently passed onto C_3 and C_4 consumers through diet with some further fractionation (Fig. 5.9) (Bender 1968; Smith & Epstein 1971; Ehleringer & Cerling 2002; Sponheimer *et al.* 2009). At GRS, the mean $\delta^{13}C$ values of browsers (C_3) and grazers (C_4)

differ by 11.7‰ in the TP and 10.3‰ in the MH. These differences deviate from 14‰ (Fig. 5.9) by 2.3‰ (TP) and 3.7‰ (MH) and may result from changes in diet, vegetation, or palaeoenvironmental conditions (Vogel 1983; Sponheimer *et al.* 2009).

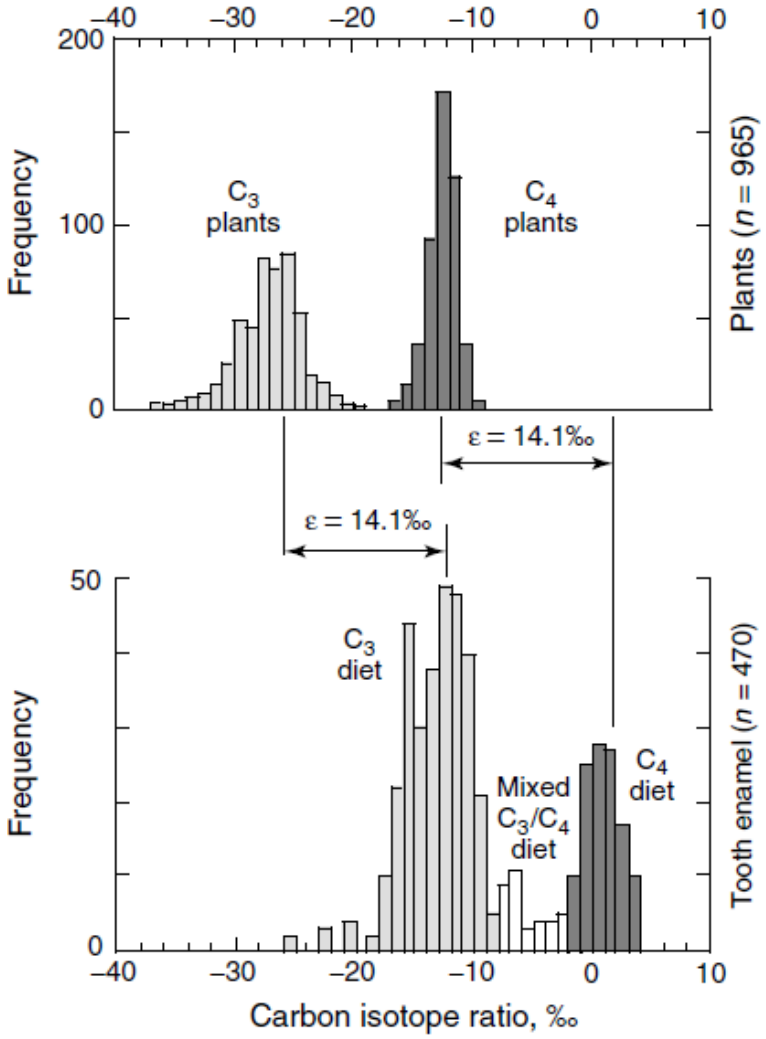


Figure 5.9: Histograms of the carbon isotope ratios of modern plants and modern tooth enamel (In Ehleringer & Cerling 2002: 188).

Modern C_3 browsers and grazers inhabiting C_4-dominated grasslands have mean $\delta^{13}C_{collagen}$ values of -21.4 ± 1.1‰ and -8.0 ± 1.1‰, respectively, with intermediate feeders falling within this range (Vogel 1978; Lee-Thorp 1989). These values were adjusted to -19.9 ± 1.1‰ and -6.5 ± 1.1‰, to account for the "Suess effect" as the $\delta^{13}C$ value of atmospheric CO_2 today is approximately 1.5‰ more negative than the pre-industrial value. This resulted from the emission of ^{13}C-depleted CO_2 from fossil fuels to the atmosphere (Marino & McElroy 1991; Keeling *et al.* 2017). Table 5.4 shows the mean $\delta^{13}C$ values of TP and MH browsers

and grazers from GRS. A shift to more negative $\delta^{13}C$ is recorded from the TP to MH in both browsing and grazing taxa and may indicate changes in diet, vegetation, water availability, and/or temperature, creating minor isotope variation and collectively producing the overall trend (Tieszen 1991, van der Merwe & Medina 1991; Peisker & Henderson 1992; Ehleringer *et al.* 1997; Heaton 1999; Ghannoum *et al.* 2002; Swap *et al.* 2004; Weiguo *et al.* 2005; Murphy & Bowman 2009; Diefendorf *et al.* 2010; Kohn 2010; Cernusak *et al.* 2013; Sponheimer & Cerling 2014; Lightfoot *et al.* 2020). It would be difficult to quantify the influence of each of these factors (Hedges *et al.* 2004).

Table 5.4: Mean $\delta^{13}C$ values for TP and MH browsers and grazers showing a trend to more negative values from the TP to MH. Significance between TP and MH is shown.

	TP	**MH**	**Trend TP→MH**	**Significance**
$\delta^{13}C$ browser	-18.4 ± 0.9‰ (n = 7)	-19.4 ± 0.8‰ (n = 44)	More negative	p = 0.01
$\delta^{13}C$ grazer	-6.8 ± 1.1‰ (n = 10)	-9.1 ± 3.1‰ (n = 16)	More negative	p = 0.13

More variation is documented in MH grazers (Fig. 4.6, 5.10; Table 5.4), suggesting that the diet of MH grazers was more variable or contained more C_3 grasses than TP grazers. The $\delta^{13}C$ values of TP grazers are similar to modern grazers inhabiting C_4-dominated grasslands. Unsurprisingly, Grassridge browsers consumed a majority C_3 diet during the TP and MH.

Variation in the $\delta^{13}C$ values of TP and MH browsers from Grassridge is small (Fig. 5.10). Larger variations are observed in arid regions which contain CAM plants and in assemblages that contain fauna from various bioregions, such as those from East Africa (Ambrose & DeNiro 1986a). Variation in the $\delta^{13}C$ values of modern grazers are more similar to GRS MH grazers with smaller variations in TP and early Holocene grazers (Fig 5.10). This likely correlates with the transition from highly specialised to more generalised grazers resulting from major faunal turnover that occurred throughout southern Africa during the Pleistocene-Holocene transition (13–8.2 ka) (Codron *et al.* 2008; Faith 2012, 2014; Faith & Behrensmeyer 2013; Ecker *et al.* 2018; Faith *et al.* 2019).

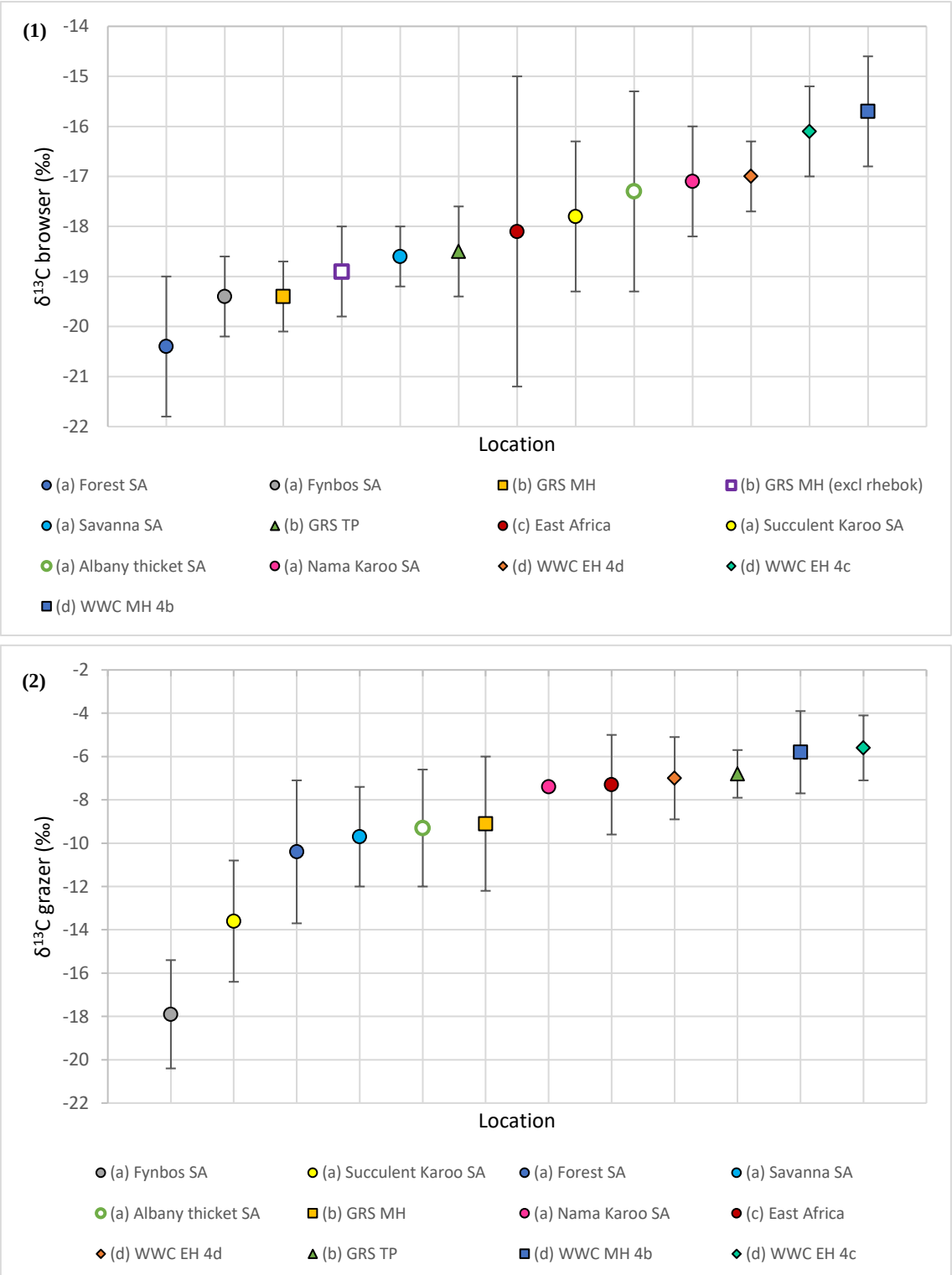


Figure 5.10: The mean $\delta^{13}C$ values with one standard deviation for (1) browsers and (2) grazers across a range of biomes and time periods. Any $\delta^{13}C$ enamel values have been adjusted -9‰ so that they can be compared with $\delta^{13}C$ collagen values. Modern values have been adjusted by 1.5‰ to account for the 'fossil fuel' effect and are represented by a circle. Mid-Holocene samples are represented by a square, early Holocene by a diamond, and TP by a triangle. These values come from (a) Luyt 2017, (b) This study, (c) Ambrose & DeNiro 1986a, and (d) Ecker et al. 2018 (Wonderwerk Cave, WWC).

Nitrogen

Higher $\delta^{15}N$ values are expected in water-independent (WI) taxa (mostly browsers) compared to water-dependent (WD) taxa (mostly grazers) (Schoeninger & DeNiro 1984; Ambrose & DeNiro 1986a, 1987; Sealy *et al.* 1987; Kelly 2000). At GRS, no significant difference was found between the $\delta^{15}N$ values of browsers and grazers in the TP or MH (Appendix 3). Similarly, Luyt (2017) found no significant difference between the median $\delta^{15}N$ values of browsers and grazers from the Succulent Karoo, Nama-Karoo, Savanna, or Albany Thicket biome, however, grazers from the Fynbos and Forest biome were enriched in ^{15}N compared to browsers (Fig. 5.11; Table 5.5).

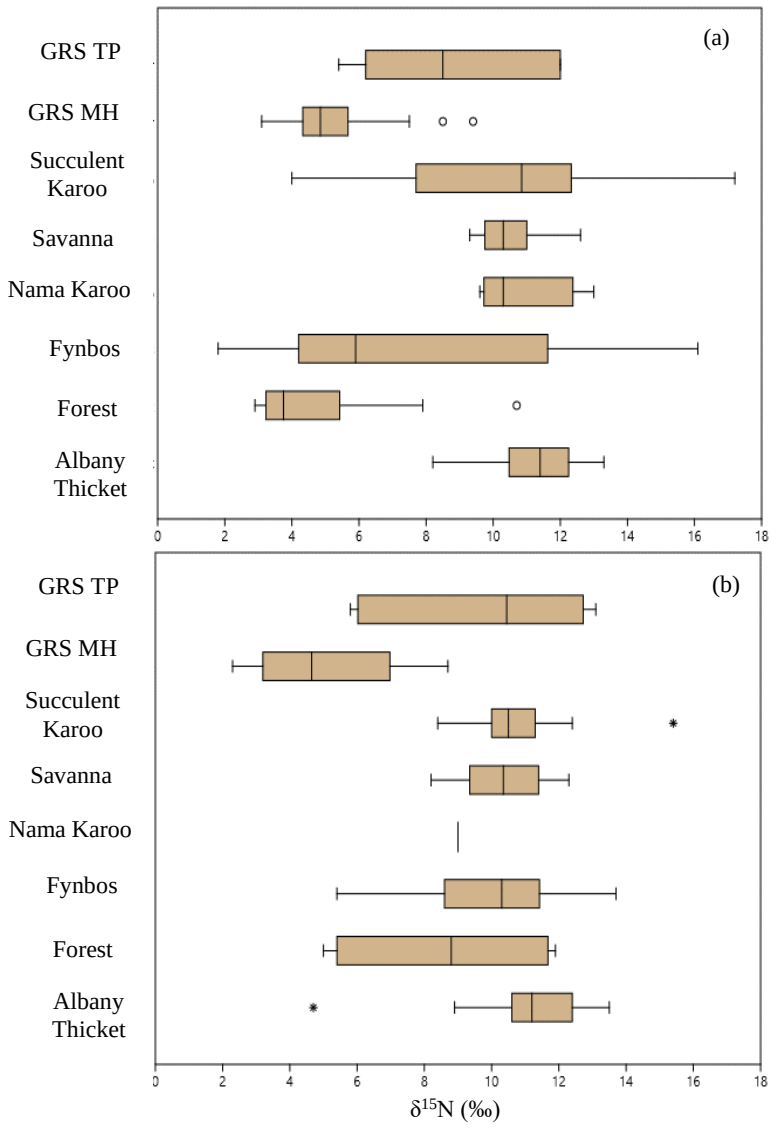
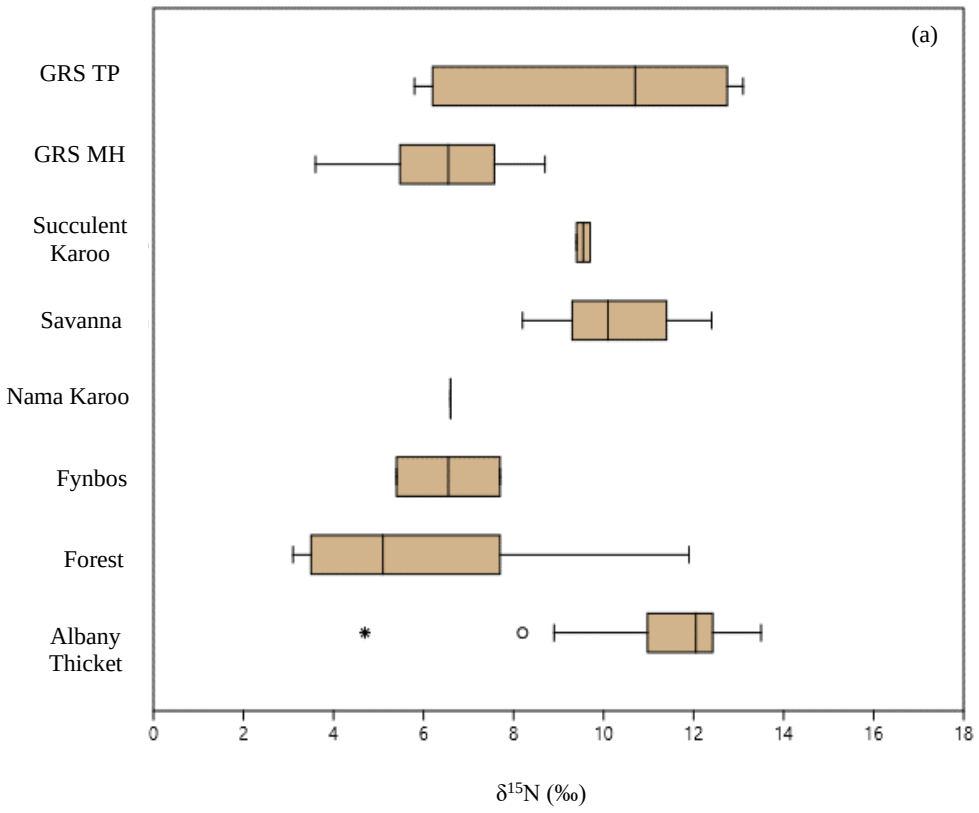


Figure 5.11: Comparison of $\delta^{15}N$ values of modern (a) browsers and (b) grazers from different biomes (Luyt 2017: 258–265) and TP and MH GRS browsers and grazers (Adapted from Luyt 2017: 119).

Table 5.5: Comparison of modern browser and grazer $\delta^{15}N$ medians across biomes (Luyt 2017: 258–265) and $\delta^{15}N$ medians from GRS TP and MH taxa with significance (Adapted from Luyt 2017: 171).

Biome/Site	Browser $\delta^{15}N$ median	Grazer $\delta^{15}N$ median	Significance
Albany thicket	11.4 (n = 18)	11.2 (n = 47)	p = 0.021
Forest	3.8 (n = 14)	8.8 (n = 4)	p = 0.026
Fynbos	10.1 (n = 14)	10.3 (n = 14)	p = 1.000
Nama Karoo	10.3 (n = 5)	9.0 (n = 1)	p = 0.226
Savanna	10.3 (n = 17)	10.4 (n = 24)	p = 1.000
Succulent Karoo	10.9 (n = 32)	10.5 (n = 27)	p = 1.000
GRS MH	4.9 (n = 44)	4.7 (n = 16)	p = 0.592
GRS TP	8.5 (n = 7)	10.5 (n = 10)	p = 0.660

Grassridge taxa were separated into two categories (Table 4.1), namely WD taxa which include Alcelaphini, equid, and grazing Reduncini and WI taxa which include grey rhebok, common eland, blue duiker, and springbok (Skinner & Chimimba 2005; Hempson *et al.* 2015). No significant difference was found between WD and WI taxa in the TP but significantly lower $\delta^{15}N$ values are recorded in WI taxa from the MH (Fig. 4.9, 5.12). Luyt (2017) found no significant difference between WD and WI taxa in most biomes, except in the Nama-Karoo biome where WI taxa were more positive and in the Forest biome where WD taxa had more positive values (Fig. 5.12).



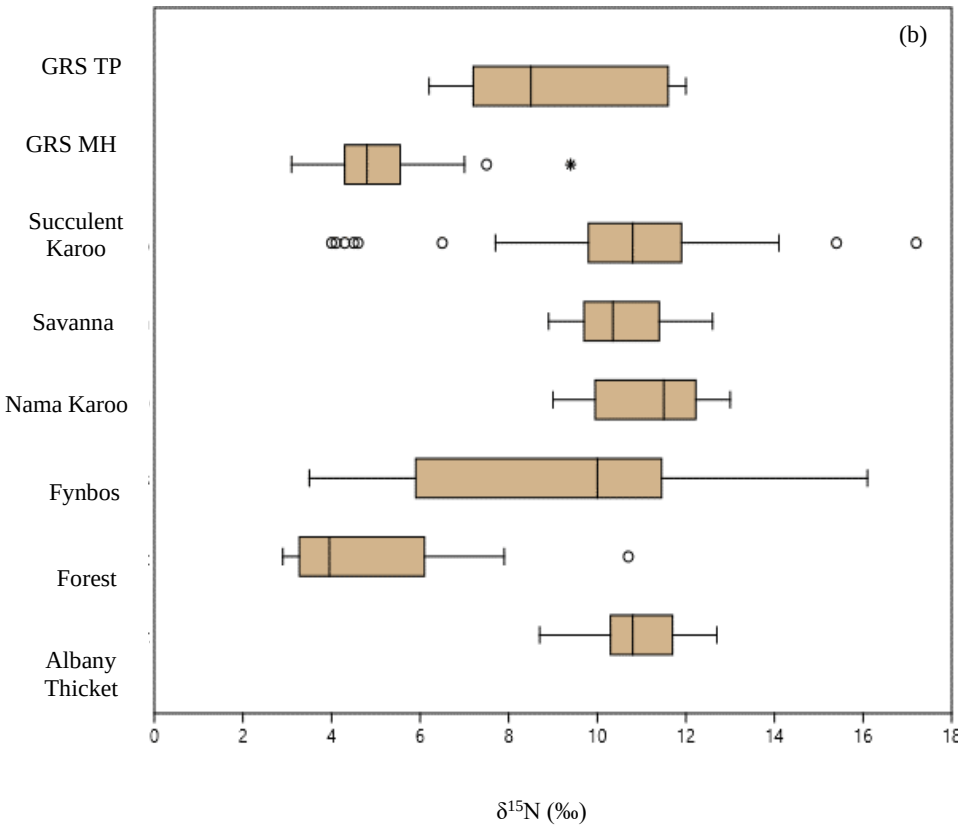


Figure 5.12: $\delta^{15}N$ (‰) values for modern (a) WD and (b) WI taxa from various biomes (Luyt 2017: 258–265) and TP and MH GRS taxa (Adapted from Luyt 2017: 136–137).

Grassridge TP taxa have a mean $\delta^{15}N$ value of 9.4 ± 2.9‰ while MH taxa have a mean of 5.1 ± 1.5‰ (Table 5.6). A significant difference was found between the $\delta^{15}N$ values of TP and MH taxa (Fig. 4.4; Table 5.6). Elevated $\delta^{15}N$ values are recorded in plants and animals from arid environments (Ambrose & DeNiro 1986a; Heaton *et al.* 1986a; Sealy *et al.* 1987; Schoeninger 1989; Cormie & Schwarcz 1996; Gröcke *et al.* 1997; Schulze *et al.* 1998; Schwarcz *et al.* 1999; Kelly 2000; Hedges *et al.* 2004; Swap *et al.* 2004; Murphy & Bowman 2006; Dewar 2007; Pate & Anson 2008; Makarewicz & Sealy 2015; Luyt 2017; Hopper *et al.* 2018). Therefore, a shift to more negative $\delta^{15}N$ values in the MH may indicate more mesic conditions during this occupation.

Table 5.6: Mean $\delta^{15}N$ values for TP and MH browsers and grazers showing a trend to more negative values from the TP to MH. Significance between TP and MH is shown for each.

	TP	**MH**	**Trend TP→MH**	**Significance**
$\delta^{15}N$ browser	9.1 ± 2.7‰ (n = 7)	5.2 ± 1.2‰ (n = 44)	More negative	$p < 0.001$
$\delta^{15}N$ grazer	9.6 ± 3.2‰ (n = 10)	5.1 ± 2.1‰ (n = 16)	More negative	$p = 0.004$
$\delta^{15}N$ taxa	9.4 ± 2.9‰ (n = 60)	5.1 ± 1.5‰ (n = 17)	More negative	$p < 0.001$

Interestingly, more positive browser $\delta^{13}C$ and higher $\delta^{15}N$ in browsers and grazers in the TP are likely due to lower moisture availability (Table 5.4, 5.6). A shift to more negative $\delta^{13}C$ and $\delta^{15}N$ in browsers and grazers from the TP to MH could indicate more mesic conditions in the MH (Peisker & Henderson 1992; Gröcke *et al.* 1997; Schulze *et al.* 1998; Kelly 2000; Ghannoum *et al.* 2002; Hedges *et al.* 2004; Swap *et al.* 2004; Weiguo *et al.* 2005; Murphy & Bowman 2006; 2009; Pate & Anson 2008; Cernusak *et al.* 2013; Makarewicz & Sealy 2015; Lightfoot *et al.* 2016, 2020; Luyt 2017; Hopper *et al.* 2018).

5.2.3 ZOOMS AND STABLE ISOTOPES

The combined use of ZooMS and stable carbon and nitrogen isotopes proved to be beneficial and emphasised the importance of using multiple proxies. Together, these methods provided information about diet, identified an issue with the identification of the suni antelope, and allowed for higher resolution identifications.

To begin, the $\delta^{13}C$ values of springbok and eland are consistent with those documented in southern Africa (Sponheimer *et al.* 2003a) confirming the expected dietary habits of these two species. Both springbok and eland were identified in Opperman's (1984, 1987, 1988) GRS faunal assemblage and were similarly found at nearby sites (Opperman 1982, 1987, 1992, 1996, Plug 1997). Springbok are the only extant Antilopini in South Africa (Skinner & Chimimba 2005). Currently, no collagen markers are recorded for extinct Antilopini but these taxa have not been identified at GRS or in the surrounding grassland region (Opperman 1982, 1987, 1992, 1996; Avery 2019). Eland belongs to the Tragelaphini tribe which contains kudu, nyala (*T. angasii*), and bushbuck (*T. sylvaticus*) in southern Africa (Skinner & Chimimba 2005). To date, the collagen markers of kudu, nyala, and bushbuck are not found in the reference database. However, these taxa have not been identified at GRS or the surrounding grassland region (Opperman 1982, 1987, 1992, 1996; Avery 2019), increasing our confidence in this identification. However, the reference database is incomplete which could result in misidentifications.

Two unknown ungulates were identified to family using ZooMS. In both cases, collagen was well preserved and good spectra were produced (Table 5.7). Stable carbon isotope ratios suggest that one of these ungulates was a browser and the other was a grazer. Unfortunately, narrower taxonomic identifications were not possible as no comparative peptide markers were found in the reference database.

Table 5.7: Collagen peptide markers for Unknown Antilopinae 1 and 2. Colours in sample indicate what occupation samples came from: yellow is LP, orange is TP, and green is MH.

Unknown Antilopinae 1								
Sample	A	B	C	D	X3	F	G	X4
2	1166,58	1427,68	1550,71	2103,10	2567,19	2883,35	3033,42	
28	1166,57	1427,70	1550,73	2103,10	2568,19	2883,40	3033,47	
39	1166,62	1427,73	1550,75	2103,10	2567,22	2883,42	3033,50	
44	1166,61	1427,71	1550,75	2103,10		2883,36	3033,45	
76	1166,63	1427,35	1550,77	2103,10	2567,25	2883,46	3033,53	
77	1166,63	1427,73	1550,76	2103,10	2568,22	2883,43	3033,50	
19	1166,61	1427,70	1550,73	2103,10			3033,42	
Unknown Antilopinae 2								
Sample	A	B	C	D	X3	F	G	X4
78	1208,67	1427,73	1550,76	2131,12	2581,23	2883,44	3033,51	3227,54
84	1208,68	1427,74	1550,76	2131,13	2581,24	2883,44	3033,52	3227,59
50	1208,65	1427,72	1550,74	2131,11	2581,20	2883,42	3033,53	3227,53
96	1208,67	1427,73	1551,38	2131,13		2884,43		

The combination of these methods called into question the identification of the suni antelope which had a C_4 signature (-9.8‰). Suni are small, highly selective browsers found in closed-canopy woodland, sand forests, bushland, and thickets (Lawson 1989; Skinner & Chimimba 2005). They have not been found in the Grassridge region (Fig. 5.13) (Skinner & Chimimba 2005; Avery 2019) but may have had a larger distribution in the past.

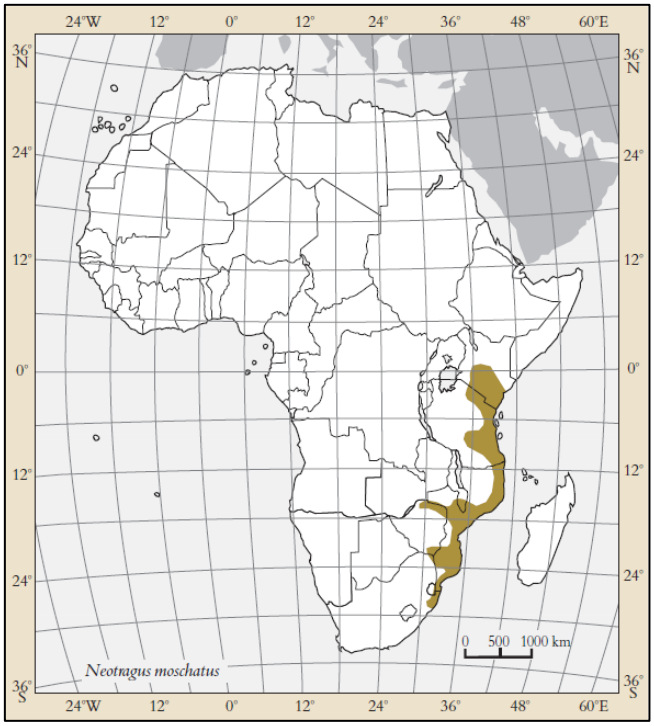


Figure 5.13: Current distribution of suni (In Skinner & Chimimba 2005: 712).

This is likely a misidentification resulting from the conservation of collagen markers in two or more bovids. Bradfield *et al.* (2021) had difficulty distinguishing between the collagen signatures of suni and barbary sheep (*Ammotragus lervia*). Barbary sheep are native to North Africa and do not occur in southern Africa (Castelló 2016). However, an unnamed extinct caprine antelope is documented in the mountainous regions of South Africa during the LP to MH (Brink 1999; Faith 2012, 2013a, 2014). The teeth of this extinct caprid are markedly hypsodont suggesting that it was a grazer, and its post-crania are similar to other caprines inhabiting rugged habitats (Brink 1999; Faith 2014). The $\delta^{13}C$ values of extinct caprines from Boomplaas Cave suggest that it consumed C_3 grass, but some individuals consumed a significant quantity of C_4 grass (Sealy *et al.* 2016). The $\delta^{13}C$ value of this sample (-9.8‰) suggests that this specimen consumed a significant quantity of C_4 grass, but it is depleted in ^{13}C compared to other GRS TP grazers (-6.8 ± 1.1‰, n = 10), suggesting that some C_3 grass was consumed. The collagen signature of this unnamed caprine may be similar to that of other caprine species, such as barbary sheep. To resolve this issue, bone samples from the unnamed extinct caprine antelope should be submitted for ZooMS analysis. These samples should then be compared with both suni antelope and barbary sheep to test this hypothesis.

Finally, the combination of ZooMS and stable carbon isotopes allowed higher resolution taxonomic identifications in the Reduncini tribe (Fig. 4.4; Table 4.1) Since grey rhebok are the only browsing Reduncini (Skinner & Chimimba 2005; Castelló 2016) we can assume that these samples are grey rhebok. This resolution would not have been possible without the combined use of stable carbon isotopes and ZooMS.

5.3 THE PALAEOENVIRONMENT

The palaeoenvironmental conditions at GRS during the LP, TP, and MH occupations are inferred using faunal remains identified by ZooMS and stable carbon and nitrogen isotopes (Table 4.1). The preferred and marginal habitats for each taxon found in this study and Opperman's are reported in Table 5.8. The results of this study are compared with Opperman's (1984, 1987, 1988) faunal and Ames *et al.* (2020) microbotanical data (Fig. 5.14).

The palaeoenvironmental information gathered from fauna are consistent with the microbotanical data, but some differences are observed between the isotope and microbotanical data. However, this is to be expected as individual proxies may have different responses to changing climates and stable carbon isotope ratios are affected by the selection and consumption of preferred diet (Jones & Mann 2004; Scott & Lee-Thorp 2004; Lewis

2011; Lister 2013; Meadows 2014; Stone 2014; Sealy *et al.* 2016; Stewart & Mitchell 2018; Lukich *et al.* 2020).

Table 5.8: Habitat selection matrix for each taxon based on their selection for preferred (green) and marginal (yellow) habitats using current literature (Gagnon & Chew 2000; Skinner & Chimimba 2005; Faith & Beherensmeyer 2013; Sinclair et al. 2020; Venter et al. 2020). Three habit categories exist, including open (O; grassland), intermediate (I; bushland, ecotone, shrubland, woodland), and closed (C; continuous tree cover) and species were assigned following Plummer & Bishop (1994). Diet is separated into three guilds, namely browser (B), intermediate feeder (M), and grazer (G).

Taxa	**Diet**	**Habitat**	**Grassland**		**Savanna**	**Floodplain**	**Thicket**	**Forest**	**Shrubland**	**Nama Karoo**	**Water**
			Short	Tall							
Blue duiker	B	C									WI
Common duiker	B	I									WI
Grey rhebok	B	I									WI
Reduncini grazer	G	I									WD
Mountain reedbuck	G	I									WD
Southern reedbuck	G	I									WD
Springbok	B/M	O									WI
Alcelaphini	G	O									WD
Hartebeest/ Wildebeest	G	O									WD
Blesbok	G	O									WD
Hippotragini	G	O/I									WD
Equid	G	O									WD
Common eland	B	I									WI
Klipspringer	B	I									WI
Oribi	G	I									WI
Steenbok/ Grysbok	B/M	I									WI
Ostrich	M	O									WI
Warthog	G	O									-

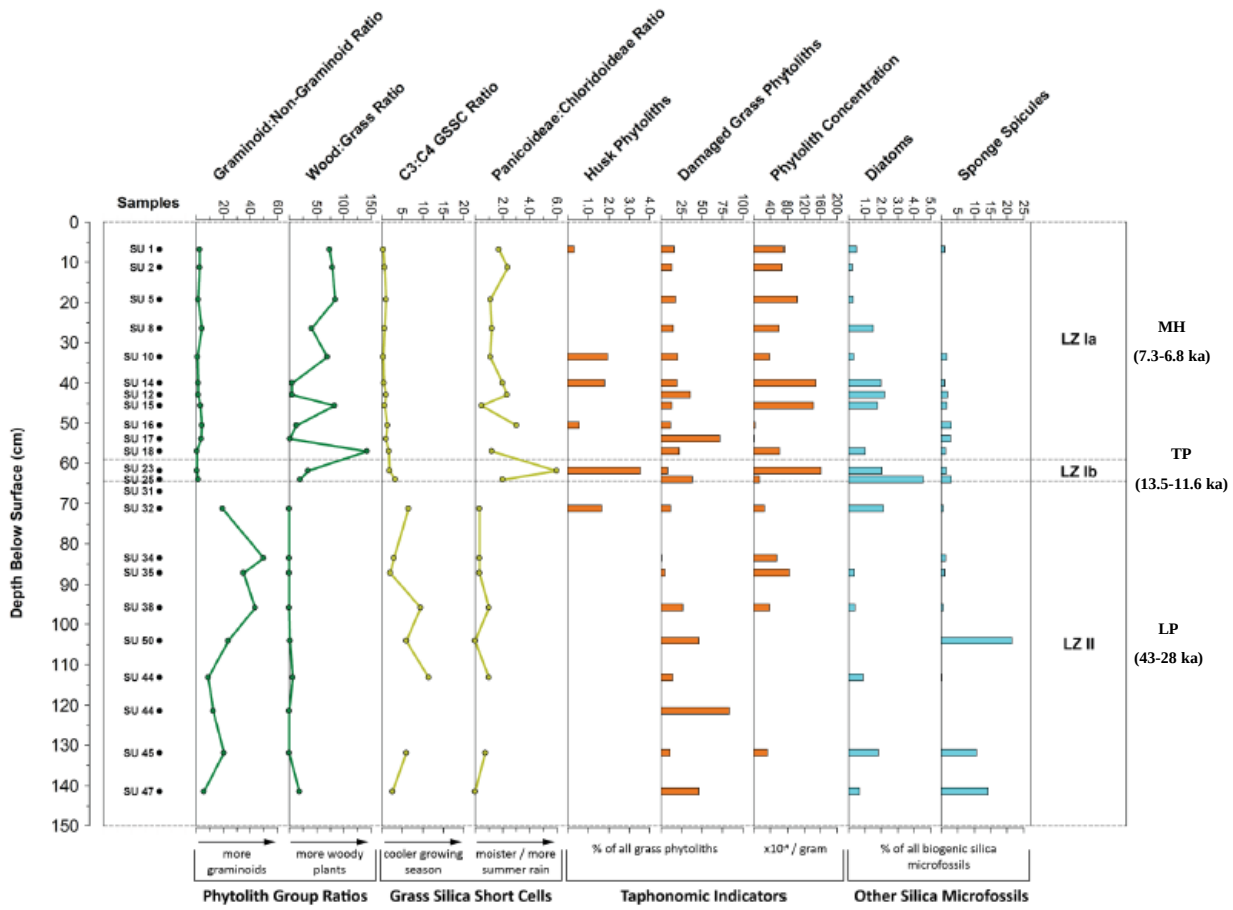


Figure 5.14: The taphonomic indicators, phytolith ratios, and proportion of recovered sponge spicules and diatoms in a stratigraphic presentation. Each Lithostratigraphic Zone is matched with the LP, TP, or MH occupation (Adapted from Ames et al. 2020: 11).

5.3.1 LATE PLEISTOCENE OCCUPATION (43–28 KA)

The LP occupation occurs in the latter part of MIS 3 (ca. 43–28 ka). The LP faunal assemblage is dominated by open grassland WD grazers (Fig. 5.7; Table 5.3). This faunal trend is similarly observed at other southern African sites (Clark & Kandel 2013; Wurz 2019). Together with the microbotanical data (Fig. 5.14) (Ames *et al.* 2020), this suggests that the Grassridge region was dominated by open C_3 grassland with some woody vegetation and C_4 grass. The predominance of open grassland grazing taxa, low tribal diversity, abundance of C_3 grass, and a slight abundance of drought-resistant C_4 grass suggests that palaeoenvironmental conditions were cool and dry, with some year-round rainfall. The presence of WD taxa, diatoms, and sponge spicules suggests that water was available nearby, at least seasonally.

No occupation is recorded at GRS between 28 and 13.5 ka, roughly coinciding with MIS 2 (29–14 ka) (Ames *et al.* 2020). Regional records suggest that palaeoenvironmental conditions

were cold and dry during MIS 2, culminating during the Last Glacial Maximum (LGM) (Carter 1976; Butzer *et al.* 1978; Vogel *et al.* 1978; Scott 1982a; Butzer 1984a; Opperman & Heydenrych 1990; Low & Rebelo 1996; Opperman 1996; Holmgren *et al.* 2003; Thackeray & Scott 2006; Chase & Meadows 2007; Barham & Mitchell 2008; Lewis 2008, 2011; Scott *et al.* 2012; Sealy *et al.* 2016; Mills *et al.* 2017; Stewart & Mitchell 2018; Loftus *et al.* 2019; Ames *et al.* 2020). This may explain the occupational gap at GRS as cold and dry conditions may have led to population contraction in the interior and the occupation of high-altitude sites with more reliable freshwater sources in the Maloti-Drakensberg (Scott *et al.* 2012; Pargeter *et al.* 2017; Stewart & Mitchell 2018; Ames *et al.* 2020). Alternatively, the depositional gap between Lithostratigraphic Zone (LZ) II (LP) and Ib (TP) may be explained by surface runoff and erosion of the accumulating sediments promoted by the hardened carbonate crust surface between these LZs (Ames *et al.* 2020).

5.3.2 TERMINAL PLEISTOCENE OCCUPATION (13.5–11.6 KA)

Grazers dominate the TP faunal assemblage at GRS but are less abundant than the LP (Fig. 5.7). Conversely, browsers increase in the TP, suggesting that the region was dominated by grassland with an increase in woody vegetation, and corresponds with the microbotanical data (Fig. 5.14) reported by Ames *et al.* (2020). Major faunal turnover is documented throughout southern Africa during the Pleistocene-Holocene transition (13–8.2 ka) and is characterised by the extinction of several open grassland ungulates and an increase in browsers and more generalised feeders (Codron *et al.* 2008; Faith 2012, 2014; Faith & Behrensmeyer 2013; Ecker *et al.* 2018; Faith *et al.* 2019). This change has been attributed to declines in the distribution, structure, or productivity of grassland habitats, likely resulting from increased seasonality, altered rainfall regimes, elevated pCO_2 concentrations, or a combination of these factors (Klein 1980; 1983; Brink 1987, 1999, 2005; Brink & Lee-Thorp 1992; Faith 2011a, 2012, 2013a, b, 2014).

A TP occupation was identified at GRS by the Grassridge Archaeological and Palaeoenvironmental Project (GAPP) following the relocation of Opperman's original excavation, reanalysis and re-dating of the stratigraphic sequence, and the initiation of new excavations (Collins *et al.* 2017; Ames *et al.* 2020). This occupation coincides with the Younger Dryas (YD) event; an event characterised by a significant cold reversal with temperature depressions of 6 ± 2 °C and severe aridity throughout southern Africa (Holmgren *et al.* 2003; Talbot *et al.* 2007; Scott *et al.* 2012; Truc *et al.* 2013: 575; Stewart & Mitchell 2018). Notably, the presence of WD taxa, diatoms, and sponge spicules at GRS indicate the

presence of water nearby, possibly encouraging TP inhabitants to occupy the Grassridge region during this period.

The $\delta^{13}C$ values of TP taxa are non-normally bimodally distributed (Fig. 4.3), with browsers and grazers clustering on either end of the C_3 and C_4 spectrum, suggesting that preferred dietary resources were available and supporting the presence of both open and intermediate habitats (Robinson & Wadley 2018). The mean $\delta^{13}C$ value of TP browsers are slightly more positive (1.4‰) than modern C_3 consumers while the mean $\delta^{13}C$ value of TP grazers (-6.5 ± 0.6‰ [n = 9]; after removal of an outlier) is similar to modern C_4 consumers. The consumption of CAM plants or C_4 grass by browsers could result in more positive $\delta^{13}C$ values. Although, this is unlikely as browsers rarely consume grass (Lee-Thorp 1989; Luyt 2017; Luyt *et al.* 2019; Sealy *et al.* 2020) and CAM plants are not widely distributed or abundant in the Grassridge region (Mucina & Rutherford 2006; Ames *et al.* 2020). More positive values may also result from fluctuating palaeoenvironmental conditions such as lower moisture availability (O'Leary 1995; Schleser 1995; Stewart *et al.* 1995; Hedges *et al.* 2004; Swap *et al.* 2004; Murphy & Bowman 2009).

Unlike the microbotanical data, the $\delta^{13}C$ values of grazers do not indicate an abundance of C_3 grass. Differences between the microbotanical data and stable carbon isotope ratios are expected as fauna may select and consume preferred dietary resources, emphasising the role of dietary preference on isotopic results (Lister 2013; Sealy *et al.* 2016). Nevertheless, C_4 grass became more prevalent in the TP (Ames *et al.* 2020). During the TP, temperatures were approximately 6 ± 2 °C lower than present (Holmgren *et al.* 2003; Talbot *et al.* 2007; Scott *et al.* 2012; Truc *et al.* 2013; Stewart & Mitchell 2018). Current Mean Annual Temperature (MAT) at Grassridge is approximately 13 °C with summer temperatures often exceeding 30 °C (Sampson 1970; Opperman 1987; Hoare & Bredenkamp 2001; Mucina & Rutherford 2006; Ames *et al.* 2020). Therefore, lower MAT of approximately 5 to 9 °C with summer temperatures of 22 to 26 °C was likely experienced at Grassridge during the TP. In southern Africa, C_4 grass distribution is strongly influenced by growing season temperature and rainfall seasonality. It is dominant (>50%) in areas where summer temperatures exceed 25 °C (Vogel 1978; Lee-Thorp & Beaumont 1995; Ehleringer *et al.* 1997; Sealy *et al.* 2020). Microbotanical data (Fig 5.14) from GRS shows a relatively even proportion of C_3 to C_4 grass which could indicate cooler growing conditions than present (Ames *et al.* 2020).

Grassridge currently receives 400 to 600 mm of Mean Annual Precipitation (MAP). Herbivores inhabiting regions with less than 400 mm MAP often have $\delta^{15}N$ values that

exceed 10‰, possibly reflecting elevated $\delta^{15}N$ plant values or ecophysiological adaptations to arid conditions (Ambrose & DeNiro 1986a; Heaton *et al.* 1986a; Heaton 1987; Sealy *et al.* 1987; Hedges *et al.* 2004; Balter *et al.* 2006; Murphy & Bowman 2006; Hartman 2011; Luyt 2017). Therefore, changes in MAP may be captured in the $\delta^{15}N$ values of Grassridge taxa. Grassridge taxa have a mean $\delta^{15}N$ value of 9.4 ± 2.9‰ (n = 17). These were compared with mean $\delta^{15}N$ values from other studies (Fig. 5.15). Elevated $\delta^{15}N$ values are recorded in taxa inhabiting arid regions while lower $\delta^{15}N$ values are recorded in taxa inhabiting mesic regions. Interestingly, the $\delta^{15}N$ values of Grassridge TP taxa are similar to those recorded in arid regions.

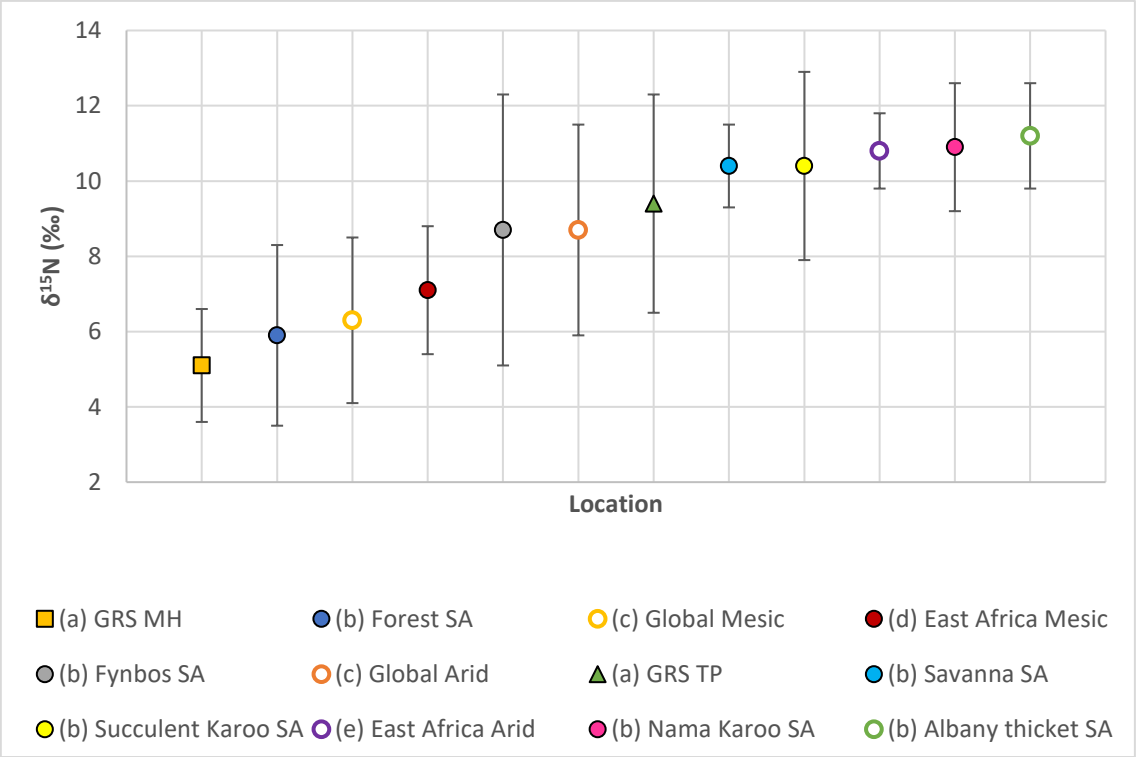


Figure 5.15: The mean $\delta^{15}N$ values with one standard deviation from fauna inhabiting mesic and arid regions. (a) This study, (b) Luyt 2017, (c) Kelly 2000, (d) Ambrose & DeNiro 1986a, and (e) Schoeninger 1989.

Notably, the predominance of Panicoideae (Fig. 5.14) indicates slightly moister conditions accompanied by increased summer rainfall, relative to the LP (Ames *et al.* 2020). The presence of WD taxa, increased tribal diversity, diatoms, and sponge spicules suggest that water was available nearby, at least seasonally.

Together, the proxy data suggest that the Grassridge region was dominated by grassland with an increase in woody vegetation. Both open and intermediate habitats occurred with woody vegetation likely growing along stream margins and in valleys nearby. Increases in tribal

diversity and the predominance of mesic C_4 grasses (Ames *et al.* 2020) suggest that conditions were somewhat moister, with a likely increase in summer rainfall relative to the LP. However, more positive $\delta^{13}C$ browser and $\delta^{15}N$ herbivore values suggest that conditions were drier than present (Table 5.4, 5.6). Despite dry conditions, WD taxa, diatoms, and spongy spicules are present, suggesting that water was available nearby.

5.3.3 MID-HOLOCENE OCCUPATION (7.3–6.8 KA)

The MH faunal assemblage is dominated by browsers and a relatively even proportion of open to intermediate habitat grazers (Table 5.3). Together, with the microbotanical data (Ames *et al.* 2020) this suggests that woody vegetation was abundant with an overall reduction in grassland. These changes may be associated with palaeoenvironmental change, rising pCO_2 (Bond & Midgley 2000; Buitenwerf *et al.* 2012), decreases in fire frequency and intensity (Trollope *et al.* 2002; Bond *et al.* 2003), or fewer frost events (Wakeling *et al.* 2012; O'Connor *et al.* 2014).

The $\delta^{13}C$ values of MH taxa are non-normally bimodally distributed (Fig. 4.3, 4.6). Following the removal of grey rhebok, the $\delta^{13}C$ values of MH browsers and grazers cluster around the C_3 and C_4 spectrum (Fig. 4.3, 4.6). The MH peaks are less distinctive than TP peaks, likely resulting from larger $\delta^{13}C$ variability in MH grazers and possibly implying greater dietary flexibility within a mosaic habitat or the consumption of more C_3 grass (Robinson & Wadley 2018; Hodgkins *et al.* 2020). However, greater variability in the MH compared with the TP may be partially due to larger MH sample sizes.

Grassridge browsers consumed a majority C_3 diet during the MH. The mean $\delta^{13}C$ values of MH browsers (n = 44) are slightly more negative (1‰) than TP browsers (n = 7) and similar to modern C_3 consumers (Table 5.4). A significant difference was found between the $\delta^{13}C$ values of TP and MH browsers (MW z = 2.52, p = 0.01). This may be associated with increases in moisture availability (Swap *et al.* 2004; Murphy & Bowman 2009; Lightfoot *et al.* 2020), the feeding behaviours (e.g., selective browsing) of grey rhebok that dominate the MH browser assemblage (Fig 4.8), or large sample size differences between the TP and MH (Table 5.4). More negative $\delta^{13}C$ and $\delta^{15}N$ values in MH browsers and the prevalence of mesic C_4 grasses (Fig. 5.14) may indicate an increase in moisture availability during the MH (Ambrose & DeNiro 1986a; Heaton 1986; Kelly 2000; Swap *et al.* 2004; Murphy & Bowman 2009; Ames *et al.* 2020). However, the feeding behaviours of grey rhebok may influence the $\delta^{13}C$ distribution of MH browsers (Fig 4.8). A significant difference (MW z = 2.08, p = 0.04) was found between MH grey rhebok and the remaining MH browsers. No significant

difference (MW z = 1.02, p = 0.31) was found between the remaining TP and MH browsers and the mean $\delta^{13}C$ value of TP grey rhebok fell within two standard deviations of the MH grey rhebok. This suggests that there was no significant change in the $\delta^{13}C$ values of TP and MH browsers but rather reflects the feeding behaviours of the dominant taxa in the MH. Finally, this result may not be environmentally significant given the large sample size differences between the periods and the fact that the absolute change is ca. 1‰ which is approximately the same as the standard deviation.

Grazers appear to be better adapted to palaeoenvironmental change, expanding or contracting their dietary niche in response to changes in the availability of graze (C_3 or C_4) or browse (de Graaff *et al.* 1973; Cerling *et al.* 2003; Sponheimer *et al.* 2003a; Lovegrove 2003; Codron *et al.* 2007b; Owen-Smith 2008; Lehmann *et al.* 2013, 2015; Owen-Smith *et al.* 2013; Strauss 2015; Venter & Kalule-Sabiti 2016; Vermeulen 2018; Venter *et al.* 2020). Larger variances in $\delta^{13}C$ grazer values may be explained by dietary niche expansion as woody vegetation became abundant with an overall reduction in grassland during the MH (Ames *et al.* 2020). Increased CAM or C_3 plant consumption may explain larger $\delta^{13}C$ variability in MH grazers (Thackeray & Lee-Thorp 1992; Thackeray *et al.* 1993; Robinson & Wadley 2018) and has been observed in modern grazers inhabiting biomes dominated by browse shrubs (i.e., Nama-Karoo biome). Given that grazers prefer grass, it is possible that C_3 grasses were common or more abundant than C_4 (Hodgkins *et al.* 2020). The microbotanical data (Fig. 5.14) suggests that C_3 grasses declined through the MH sequence with C_3 grasses being slightly more abundant in the bottom five layers and C_4 grasses being slightly more abundant in the top six layers (Ames *et al.* 2020: 12). Alternatively, more negative $\delta^{13}C$ grazer values may be associated with more mesic MH conditions (Peisker & Henderson 1992; Ghannoum *et al.* 2002; Weiguo *et al.* 2005; Cernusak *et al.* 2013). The microbotanical and stable isotope data suggest that both C_3 and C_4 grasses were available during the MH; however, the $\delta^{13}C$ values of grazers may be affected by the selection and consumption of preferred diet or seasonal migration between regions with varying proportions of C_3 and C_4 grasses.

Seasonal migrations between rainfall zones or high and low altitudes may have provided access to ^{13}C-depleted resources (Stewart & Mitchell 2018; Hodgkins *et al.* 2020). The Grassridge MH grazing bovids (tribal level) include Alcelaphini (n = 4), Reduncini (n = 4), and Hippotragini (n = 1). Only Alcelaphini has the propensity to migrate, so the $\delta^{13}C$ values of Reduncini and Hippotragini are expected to reflect the isotopic signature of the local environment (Hodgkins *et al.* 2020). Alcelaphini have a mean $\delta^{13}C$ value of -10.2 ± 4.0‰ (n

= 4) while grazing Reduncini and Hippotragini have a mean $\delta^{13}C$ value of -10.7 ± 3.1‰ (n = 5). No significant difference was found between MH migratory and non-migratory grazers, suggesting that grazers consumed a more generalised diet during the MH. This is likely related to vegetation change and may be the result of increased woody vegetation or C_3 grass relative to C_4 (Faith 2014; Ames *et al.* 2020; Hodgkins *et al.* 2020). This may indicate cooler growing conditions during the MH relative to present. However, sample sizes may be too small to make a meaningful assessment.

Lower $\delta^{15}N$ values are recorded from fauna inhabiting mesic regions (Ambrose & DeNiro 1986a; Heaton *et al.* 1986a; Sealy *et al.* 1987; Schoeninger 1989; Cormie & Schwarcz 1996; Schwarcz *et al.* 1999; Kelly 2000; Pate & Anson 2008; Makarewicz & Sealy 2015). The $\delta^{15}N$ values of MH taxa (n = 60) are significantly lower than those from the TP (n = 17) (Fig 5.15), suggesting that conditions were mesic during the MH. Furthermore, increased tribal diversity, more negative $\delta^{13}C$ browser and grazer values relative to the TP, and the predominance of C_4 Panicoideae indicate an increase in moisture availability (Hedges *et al.* 2004; Ames *et al.* 2020).

Together, the proxy data suggest a mosaic environment dominated by woody vegetation with an overall reduction in grassland relative to the TP. Increases in tribal diversity, lower $\delta^{13}C$ and $\delta^{15}N$ herbivore values, and the predominance of mesic C_4 grasses (Ames *et al.* 2020) suggest that conditions were moister with increased summer rainfall following the TP. The occurrence of WD taxa, diatoms, and spongy spicules suggest that water was available in the Grassridge region. Overall, conditions were mesic relative to earlier periods.

5.4 SUMMARY

A summary of the microbotanical (Ames *et al.* 2020), faunal (Opperman 1984, 1987, 1988; this study), and stable carbon and nitrogen isotope data (this study), as well as the associated palaeoenvironmental conditions are found in Table 5.9.

Table 5.9: Summary of palaeoenvironmental data from microbotanical, faunal, and stable isotope proxies (Data found in Opperman (1984, 1987, 1988), Ames et al. 2020, and this study).

Grassridge Rockshelter		Time Period		
		LP	**TP**	**MH**
Palaeoenvironmental Proxy	Microbotanical (Ames *et al.* 2020)	C_3 dominated grassland, C_4 grass present, drought-resistant slightly more abundant Limited woody vegetation Diatoms and spongy spicules present	Predominately grassland with more woody vegetation than LP C_3: C_4 grass is relatively even but mesic C_4 grass more prevalent than drought-resistant Diatoms and spongy spicules present	Woody vegetation is abundant C_3 grass being replaced by C_4 grass. Mesic C_4 grass more prevalent than drought-resistant Diatoms and spongy spicules present
	Fauna This study Opperman (1984, 1987, 1988)	Water-dependent open habitat grazers dominate, mostly Alcelaphini and equid, specialised grazer *R. arundinum*, and an unknown browser present	Water-dependent open habitat grazers still dominant, but browsers increase Increase tribal diversity	Browsers dominate, mix open and intermediate habitat grazers Water-dependent taxa present Highest tribal diversity Change in subsistence as indicated by increase in bovids preferring rocky outcrops
	Carbon Isotopes	No data available	Browsers are more positive than modern, possible low moisture availability Grazers similar to modern; more positive than MH Non-normal bimodal distribution, no overlap and cluster at C_3 and C_4 spectrum Expansion of C_4 grasses or specialised feeding strategies. More defined open and intermediate habitats	Browsers similar to modern Grazers more negative than modern and TP Browser and grazer $\delta^{13}C$ more negative than TP, more mesic conditions Non-normal bimodal distribution, less defined than TP with larger spread indicated in grazing taxa suggesting more dietary flexibility
	Nitrogen Isotopes	No data available	High $\delta^{15}N$ values in GRS taxa, more arid	Low $\delta^{15}N$ values in GRS taxa More negative than TP, more mesic
	Palaeoenvironmental Conditions	Dominated by open C_3 grasslands, some woody vegetation and C_4 grass Cool and dry, some year-round rainfall Water available nearby, at least seasonally	Grassland dominant, increase woody vegetation Intermediate and open habitats available Moister than LP, likely increase summer rainfall but drier than present Cooler growing conditions Water available nearby, at least seasonally	Mosaic environment, dominated by woody vegetation and reduced grassland Moister, increase summer rainfall Transition from cooler growing season to conditions more similar to current

CHAPTER 6: CONCLUSION

This study inferred the palaeoenvironmental conditions at Grassridge Rockshelter (GRS) during the late Pleistocene (LP), terminal Pleistocene (TP), and mid-Holocene (MH) occupations using fauna identified by Zooarchaeology by Mass Spectrometry (ZooMS) and stable carbon and nitrogen isotopes. Overall, this study uses ZooMS to successfully identify faunal remains from GRS, documents faunal and stable isotope shifts through time, increases the palaeoenvironmental resolution at GRS, and reveals some unexpected results. The limitations of this study are discussed, and future avenues of research are proposed.

Eighty-five percent (n = 85) of the GRS faunal sample was successfully identified to at least tribe, and was better than, or on par with, both local and global studies. The success of ZooMS increased through time but not significantly, suggesting that ZooMS can be used on older assemblages, up to ca. 40 ka, and in warmer environments where ancient DNA (aDNA) may be poor, if the taphonomic factors affecting collagen preservation have been considered.

Faunal turnover is indicated from the latter part of Marine Isotope Stage (MIS) 3 to the MH with grazers being replaced by browsers through time. Shifts in stable carbon and nitrogen isotope ratios are recorded from the TP to MH; although shifts in $\delta^{13}C$ browser values may be associated with fluctuating moisture availability, uneven sample sizes, or the dominance of grey rhebok in the MH. In particular, more positive $\delta^{13}C$ browser and elevated $\delta^{15}N$ herbivore values in the TP may be due to lower moisture availability. Furthermore, the abundance of grey rhebok in the MH may relate to subsistence change as GRS inhabitants shifted their focus from large bovids during the Pleistocene to browsers and small territorial bovids inhabiting the surrounding hilly region during the MH.

Faunal and stable isotope proxies complement the microbotanical data reported by Ames *et al.* (2020), although some differences are found between stable isotope and microbotanical data. Together, these data suggest that the latter part of MIS 3 (ca. 43–28 ka) was dominated by open C_3 grassland with very few trees and cool and dry conditions with some year-round rainfall. The TP environment was more similar to the present-day and was dominated by grassland with some woody vegetation. Relative to MIS 3, conditions were slightly moister with a likely increase in summer rainfall, but cooler and drier than the MH. The MH is characterised by a mosaic environment which was dominated by woody

vegetation and an overall reduction in grassland. Conditions were moister than the TP. Overall, the environmental conditions at GRS transition from dry and cool in the latter part of MIS 3 to mesic and warmer in the MH with summer rainfall increasing through time. Grassland is replaced by woody vegetation from MIS 3 to the MH, but C_4 grasses became more abundant. Water was likely available, at least seasonally, during the LP, TP, and MH occupations.

Grassridge faunal identifications have previously relied on the traditional osteomorphological approach. An approach that is widely practised throughout southern Africa (and globally) but often results in the neglect of morphologically unidentifiable bone fragments, typically constituting a large portion of faunal assemblages. Faunal identifications using ZooMS may allow morphologically ambiguous and unidentifiable bone fragments to be identified and reduce taphonomic and analytic bias, increase sample size, and address some of the key concerns of traditional and aDNA zooarchaeological analyses. However, ZooMS does not replace other zooarchaeological methods but rather complements, informs, and verifies them. As seen in this study, the combined use of ZooMS and stable carbon and nitrogen isotopes enhanced palaeoenvironmental reconstructions, improved and validated taxonomic identifications, and provided insight into the effects of environmental change on diet. Zooarchaeology by Mass Spectrometry also allowed for the identification of a blue duiker and ostrich, highlighting its potential to identify rare or unexpected taxa and clarify taxon-specific patterns of preservation.

6.1 LIMITATIONS

The current study was limited by the lack of a complete collagen peptide marker reference database, broad taxonomic resolutions, and uneven and small sample sizes.

Two unknown Antilopinae were identified in this study. In both cases, collagen was well preserved and good spectra were produced. Unfortunately, narrower taxonomic identifications were not possible as no comparative peptide markers were found in the reference database. In general, robust peptide marker reference databases are largely absent outside of Eurasia and are one of the limitations of ZooMS analysis in southern Africa (Janzen *et al.* 2021). Additionally, high levels of collagen conservation between bovid groups limits taxonomic resolution, typically producing tribal-level identifications as opposed to genus or species-level identifications (Bradfield *et al.* 2019, 2021; Janzen *et al.* 2021).

Collagen conservation and incomplete collagen peptide marker reference databases may lead to misidentifications as seen with the suni antelope from this study or reduced confidence in faunal identifications (i.e., blue duiker). Suni antelope and barbary sheep share a similar collagen signature making it difficult to distinguish between them. Barbary sheep are not found in southern Africa, suggesting that the suni shares a similar collagen signature with another C_4 bovid, such as the unnamed extinct caprid. Additional sampling and sequencing are required to resolve this issue. To date, eland are the only species from the Tragelaphini tribe to have published collagen markers. This may reduce confidence in our identifications as the collagen markers of several Tragelaphini are missing from the reference database, with identifications relying on historical and archaeological presence of eland at GRS and the surrounding grassland regions.

Finally, the results of this study are sensitive to small and uneven sample sizes and the feeding behaviours of particular species. Caution should be taken when working with small and uneven sample sizes as it makes any firm conclusions difficult.

Many of the limitations mentioned above can be addressed by expanding the collagen peptide reference database, including additional techniques (i.e., stable isotopes, bovid size classes), and increasing sample size.

6.2 FUTURE AVENUES OF RESEARCH

Future avenues of research should consider the factors affecting the success of ZooMS and stable carbon and nitrogen isotopes. They should focus on expanding the reference database, expanding the GRS sample, applying ZooMS to the GRS bone tool assemblage, and examining socio-cultural networks across the arid interior, interior montane grasslands, and the coast.

The following should be considered before employing ZooMS: the factors affecting collagen preservation (Richter 1986; Stiner *et al.* 1995; Taylor *et al.* 1995; Nielsen-Marsh *et al.* 2000; Collins *et al.* 2002; Lee-Thorp 2008; Gifford-Gonzalez 2018; Kendall *et al.* 2018), the types of taxa inhabiting the study region (Janzen *et al.* 2021; Peters *et al.* 2021), the potential taxonomic resolution (i.e., sub-family, tribe, genus, etc), and the completeness of the collagen peptide marker reference database (Bradfield *et al.* 2019, 2021; Janzen *et al.* 2021). This is particularly relevant in Africa where faunal remains are exposed to sub-optimal conditions that hinder collagen and aDNA preservation (Lee-Thorp 1989; Ambrose 1990; Klinken 1991; Holmes *et al.* 2005; Lee-Thorp & Sponheimer 2006; Pestle

& Colvard 2012; Buckley 2018). Importantly, the factors affecting collagen preservation should be well understood before implementing these techniques.

Notable contributions have been made to the African collagen peptide marker reference database; however, there are still notable gaps in the database that need to be addressed. To begin, all future studies should submit modern faunal samples with their archaeological samples to help expand the reference database. These samples should include taxa that may have occurred in the region in the past. Additional work is required in developing novel ZooMS markers for African bovids, thus allowing narrower taxonomic identifications. To date, no extinct African bovid collagen peptide markers have been published. The inclusion of extinct bovid taxa may enable identification of these taxa and shed light on their palaeobiogeography and biochronology.

Only 100 morphologically unidentifiable bone fragments were used in this study. Additional samples should be submitted for ZooMS and stable carbon and nitrogen isotope analysis to verify some of the trends identified in this study, such as the influence of feeding behaviours from dominant taxa, seasonal migration, and changes in faunal and stable carbon and nitrogen isotope ratios through time.

Bone tools were found at GRS by Opperman and the Grassridge Archaeological and Palaeoenvironmental Project (GAPP). The sample size is small (n = 11) but future research could include an examination of the excavated faunal remains for additional bone tools, followed by minimal or non-destructive ZooMS analysis. These results could be compared with those found here to see if there are any differences in the fauna selected for tool manufacture and subsistence. This may also provide insight into the symbolic associations attached to fauna.

Future research should examine the relationship between changing palaeoenvironmental conditions and socio-cultural networks and mobility across the arid interior, interior montane grasslands, and the eastern coastal region during the Late Quaternary. Current understanding of this relationship is insufficient with southern African palaeoenvironmental reconstructions being impeded by spatial and temporal gaps leading to broad reconstructions and faunal identifications being limited by morphological biases and high degrees of fragmentation. These issues may be alleviated by the combined use of ZooMS and stable isotopes. The inclusion of strontium and oxygen isotopes could prove useful, possibly providing additional palaeoenvironmental information, understanding of socio-cultural networks, and the effects of seasonal migration on isotopic signals.

REFERENCES

Aarnes, I., Svensen, H., Polteau, S. & Planke, S. 2011. Contact metamorphic devolatilization of shales in the Karoo Basin, South Africa, and the effects of multiple sill intrusions. *Chemical Geology* 281(3–4): 181–194.

Abell, P.I. & Plug, I. 2000. The Pleistocene/Holocene transition in South Africa: evidence for the Younger Dryas event. *Global and Planetary Change* 26(1–3): 173–179.

Adams, T.S. & Sterner, R.W. 2000. The effect of dietary nitrogen content on trophic level ^{15}N enrichment. *Limnology and Oceanography* 45(3): 601–607.

Alley, R.B, Bond, G., Chappellaz, J., Clapperton, C., Del Genio, A., Keigwin, L. & Peteet, D. 1993. Global Younger Dryas? *EOS Transactions American Geophysical Union* 74(50): 587–589.

Alley, R.B. & Ágústsdóttir, A.M. 2005. The 8k event: cause and consequences of a major Holocene abrupt climate change. *Quaternary Science Reviews* 24(10–11): 1123–1149.

Alley, R.B., Mayewski, P.A., Sowers, T., Stuiver, M., Taylor, K.C. & Clark, P.U. 1997. Holocene climatic instability: A prominent, widespread event 8200 yr ago. *Geology* 25(6): 483–486.

Ambrose S.H. 1993 Isotopic analysis of palaeodiets: methodological and interpretative considerations. In: Sandford M.K. (ed) *Investigations of Ancient Human Tissue: Chemical Analyses in Anthropology*: 59–130. New York: Gordan and Breach Scientific.

Ambrose, S.H. & DeNiro, M.J. 1986a. The isotopic ecology of East African mammals. *Oecologia* 69(3): 395–406.

Ambrose, S.H. & DeNiro, M.J. 1986b. Reconstruction of African human diet using bone collagen carbon and nitrogen isotope ratios. *Nature* 319(6051): 321–324.

Ambrose, S.H. & Norr, L. 1993. Experimental evidence for the relationship of the carbon isotope ratios of whole diet and dietary protein to those of bone collagen and carbonate. In: Lambert, J.B. & Grupe, G. (eds) *Prehistoric Human Bone*: 1–37. Berlin: Springer.

Ambrose, S.H. 1990. Preparation and characterization of bone and tooth collagen for isotopic analysis. *Journal of Archaeological Science* 17(4): 431–451.

Ambrose, S.H. 1991. Effects of diet, climate, and physiology on nitrogen isotope abundances in terrestrial foodwebs. *Journal of Archaeological Science* 18(3): 293–317.

Ambrose, S.H. 2000. Controlled diet and climate experiments on nitrogen isotope ratios of rats. In: Ambrose, S.H & Katzenberg, M.A. (eds) *Biogeochemical Approaches to Paleodietary Analysis*: 243–259. Boston: Kluwer Academic Publishers.

Ames, C.J., Gliganic, L., Cordova, C.E., Boyd, K., Jones, B.G., Maher, L. & Collins, B.R. 2020. Chronostratigraphy, site formation, and palaeoenvironmental context of Late Pleistocene and Holocene occupations at Grassridge Rock Shelter (Eastern Cape, South Africa). *Open Quaternary* 6(5): 1–19.

Amundson, R., Austin, A.T., Schuur, E.A., Yoo, K., Matzek, V., Kendall, C., Uebersax, A., Brenner, D. & Baisden, W.T. 2003. Global patterns of the isotopic composition of soil and plant nitrogen. *Global Biogeochemical Cycles* 17(1): 1–11.

An, C.B., Dong, W., Li, H., Zhang, P., Zhao, Y., Zhao, X. & Yu, S.Y. 2015. Variability of the stable carbon isotope ratio in modern and archaeological millets: evidence from northern China. *Journal of Archaeological Science* 53: 316–322.

Andres, M.S., Bernasconi, S.M., McKenzie, J.A. & Röhl, U. 2003. Southern Ocean deglacial record supports global Younger Dryas. *Earth and Planetary Science Letter* 216(4): 515–524.

Asara, J.M., Schweitzer, M.H., Freimark, L.M., Phillips, M. & Cantley, L.C. 2007. Protein sequences from mastodon and Tyrannosaurus rex revealed by mass spectrometry. *Science* 316(5822): 280–285.

Avery, D.M. 1981. Holocene micromammalian faunas from the northern Cape Province, South Africa. *South African Journal of Science* 77(6): 265–273.

Avery, D.M. 1982. Micromammals as palaeoenvironmental indicators and an interpretation of the late Quaternary in the southern Cape Province, South Africa. *Annals of the South African Museum* 85: 183–374.

Avery, D.M. 1993. Last Interglacial and Holocene altithermal environments in South Africa and Namibia: micromammalian evidence. *Palaeogeography, Palaeoclimatology, Palaeoecology* 101(3–4): 221–228.

Avery, D.M. 2004. Size variation in the common molerat *Cryptomys hottentotus* from southern Africa and its potential for palaeoenvironmental reconstruction. *Journal of Archaeological Science* 31(3): 273–282.

Avery, D.M. 2019. *A Fossil History of Southern African Land Mammals*. Cambridge: Cambridge University Press.

Avery, G., Halkett, D., Orton, J., Steele, T., Tusenius, M. & Klein, R.G. 2008. The Ysterfontein 1 Middle Stone Age rock shelter and the evolution of coastal foraging. *Goodwin Series* 10: 66–89.

Backwell, L.R., McCarthy, T.S., Wadley, L., Henderson, Z., Steininger, C.M., Deklerk, B., Barré, M., Lamothe, M., Chase, B.M., Woodborne, S. & Susino, G.J. 2014. Multiproxy record of late Quaternary climate change and Middle Stone Age human occupation at Wonderkrater, South Africa. *Quaternary Science Reviews* 99: 42–59.

Badenhorst, S. & Plug, I. 2011. Unidentified specimens in zooarchaeology. *Palaeontologica Africana* 46: 89–92.

Badewien, T., Vogts, A., Dupont, L. & Rullkötter, J. 2015. Influence of Late Pleistocene and Holocene climate on vegetation distributions in southwest Africa elucidated from sedimentary n-alkanes–Differences between 12°S and 20°S. *Quaternary Science Reviews* 125: 160–171.

Baker, A., Pedentchouk, N., Routh, J. & Roychoudhury, A.N. 2017. Climatic variability in Mfabeni peatlands (South Africa) since the late Pleistocene. *Quaternary Science Reviews* 160: 57–66.

Baker, A., Routh, J., Blaauw, M. & Roychoudhury, A.N. 2014. Geochemical records of palaeoenvironmental controls on peat forming processes in the Mfabeni peatland, KwaZulu Natal, South Africa since the Late Pleistocene. *Palaeogeography, Palaeoclimatology, Palaeoecology* 395: 95–106.

Balasse, M. 2003. Potential biases in sampling design and interpretation of intra-tooth isotope analysis. *International Journal of Osteoarchaeology* 13: 3–10.

Balter, V., Simon, L., Fouillet, H. & Lécuyer, C. 2006. Box-modelling of $^{15}N/^{14}N$ in mammals. *Oecologia* 147(2): 212–222.

Bard, E., Rostek, F. & Sonzogni, C. 1997. Interhemispheric synchrony of the last deglaciation inferred from alkenone palaeothermometry. *Nature* 385(6618): 707–710.

Barham, L.S. & Mitchell, P.J. 2008. *The First Africans: African Archaeology from the Earliest Tool Makers to Most Recent Foragers*. Cambridge: Cambridge University Press.

Barker, S., Diz, P., Vautravers, M.J., Pike, J., Knorr, G., Hall, I.R. & Broecker, W.S. 2009. Interhemispheric Atlantic seesaw response during the last deglaciation. *Nature* 457(7233): 1097–1102.

Bar-Matthews, M., Marean, C.W., Jacobs, Z., Karkanas, P., Fisher, E.C., Herries, A.I., Brown, K., Williams, H.M., Bernatchez, J., Ayalon, A. & Nilssen, P.J. 2010. A high resolution and continuous isotopic speleothem record of paleoclimate and paleoenvironment from 90 to 53 ka from Pinnacle Point on the south coast of South Africa. *Quaternary Science Reviews* 29(17–18): 2131–2145.

Barrable, A., Meadows, M.E. & Hewitson, B.C. 1998. Environmental reconstruction and climate modelling of the Late Quaternary in the winter rainfall region of the Western Cape, South Africa. *South African Journal of Science* 98: 611–616.

Bartram, L.E., Kroll, E.M. & Bunn, H.T. 1991. Variability in camp structure and bone food refuse patterning at Kua San hunter-gatherer camps. In: Kroll, E.M. & Price, T.D. (eds) *The Interpretation of Archaeological Spatial Patterning*: 77–148. Boston: Springer.

Baxter, A.J. 1989. Pollen analysis of Table Mountain cave deposit. Unpublished BSc Honour thesis. Cape Town: University of Cape Town.

Beard, T.R. 2018. A paleoenvironmental reconstruction using bovid remains from the Holocene at Grassridge Rockshelter, Eastern Cape, South Africa. Unpublished honours dissertation. Johannesburg: University of the Witwatersrand.

Belichovska, D., Hajrulai-Musliu, Z., Uzunov, R., Belichovska, K. & Arapcheska, M. 2015. Fatty acid composition of ostrich (Struthio camelus) abdominal adipose tissue. *Macedonian Veterinary Review* 38(1): 53–59.

Bender, M.M. 1968. Mass spectrometric studies of carbon 13 variations in corn and other grasses. *Radiocarbon* 10(2): 468–472.

Bern, M., Phinney, B.S. & Goldberg, D. 2009. Reanalysis of Tyrannosaurus rex mass spectra. *Journal of Proteome Research* 8(9): 4328–4332.

Bertrand, A. & Bigras, F.J. 2006. Atmospheric carbon dioxide enrichment reduces carbohydrate and nitrogen reserves in overwintering Picea mariana. *Scandinavian Journal of Forest Research* 21(1): 3–13.

Beta Analytic. 2021. AMS Carbon-14 Dating Lab Pretreatment Protocols (consulted May 2021): AMS Carbon-14 Dating Lab Pretreatment Protocols (radiocarbon.com)

Blow, M.J., Zhang, T., Woyke, T., Speller, C.F., Krivoshapkin, A., Yang, D.Y., Derevianko, A. & Rubin, E.M. 2008. Identification of ancient remains through genomic sequencing. *Genome Research* 18(8): 1347–1353.

Blunier, T., Chappellaz, J., Schwander, J., Dällenbach, A., Stauffer, B., Stocker, T.F., Raynaud, D., Jouzel, J., Clausen, H.L., Hammer, C.U. & Johnsen, S.J. 1998. Asynchrony of Antarctic and Greenland climate change during the last glacial period. *Nature* 394(6695): 739–743.

Bocherens, H. & Drucker, D. 2003. Trophic level isotopic enrichment of carbon and nitrogen in bone collagen: case studies from recent and ancient terrestrial ecosystems. *International Journal of Osteoarchaeology* 13(1-2): 46–53.

Boelhouwers, J.C. & Meiklejohn, K.I. 2002. Quaternary periglacial and glacial geomorphology of southern Africa: review and synthesis: Periglacial and Permafrost Research in the Southern Hemisphere. *South African Journal of Science* 98(1): 47–55.

Bogaard, A. & Outram, A.K. 2013. Palaeodiet and beyond: stable isotopes in bioarchaeology. *World Archaeology* 45(3): 333–337.

Bond, W.J. & Midgley, G.F. 2000. A proposed CO_2-controlled mechanism of woody plant invasion in grasslands and savannas. *Global Change Biology* 6(8): 865–869.

Bond, W.J., Midgley, G.F. & Woodward, F.I. 2003. What controls South African vegetation—climate or fire? *South African Journal of Botany* 69(1): 79–91.

Boone, R.B. 2019. Weather and climate impacts on browsing and grazing ungulates. In: Gordan, I.J. & Prins, H.H.T. (eds) *The Ecology of Browsing and Grazing II*: 197–213. Cham: Springer.

Bordy, E.M. & Catuneanu, O. 2002. Sedimentology of the Beaufort-Molteno Karoo fluvial strata in the Tuli Basin, South Africa. *South African Journal of Geology* 105(1): 51–66.

Bordy, E.M. & Eriksson, P. 2015. Lithostratigraphy of the Elliot Formation (Karoo Supergroup), South Africa. *South African Journal of Geology* 118(3): 311–316.

Botha, G.A., Scott, L., Vogel, J.C. & Von Brunn, V. 1992. Palaeosols and palaeoenvironments during the Late Pleistocene Hypothermal in northern Natal. *South African Journal of Science* 88: 508–508.

Bouchard, G.P., Riel-Salvatore, J., Negrino, F. & Buckley, M. 2020. Archaeozoological, taphonomic and ZooMS insights into The Protoaurignacian faunal record from Riparo Bombrini. *Quaternary International* 551: 243–263.

Bousman, C.B. & Brink, J.S. 2018. The emergence, spread, and termination of the Early Later Stone Age event in South Africa and southern Namibia. *Quaternary International* 495: 116–135.

Bousman, C.B. 1991. Holocene paleoecology and Later Stone Age hunter-gatherer adaptations in the South African interior plateau. Unpublished PhD thesis. Dallas: Southern Methodist University.

Bousman, C.B. 2005. Coping with risk: Later Stone Age technological strategies at Blydefontein Rock Shelter, South Africa. *Journal of Anthropological Archaeology* 24(3): 193–226.

Bradfield, J., Forssman, T., Spindler, L. & Antonites, A.R. 2019. Identifying the animal species used to manufacture bone arrowheads in South Africa. *Archaeological and Anthropological Sciences* 11(6): 2419–2434.

Bradfield, J., Kitchener, A.C. & Buckley, M. 2021. Selection preferences for animal species used in bone-tool-manufacturing strategies in KwaZulu-Natal, South Africa. *PloS ONE* 16(4): 1–24.

Brain, C.K. 1981. *The Hunters or the Hunted? An Introduction to African Cave Taphonomy.* Chicago: Chicago University Press.

Brandt, L.Ø., Haase, K. & Collins, M.J. 2018. Species identification using ZooMS, with reference to the exploitation of animal resources in the medieval town of Odense. *Danish Journal of Archaeology* 7(2): 139–153.

Brandt, L.Ø., Schmidt, A.L., Mannering, U., Sarret, M., Kelstrup, C.D., Olsen, J.V. & Cappellini, E. 2014. Species identification of archaeological skin objects from Danish bogs: comparison between mass spectrometry-based peptide sequencing and microscopy-based methods. *PloS ONE* 9(9): 1–10.

Brink, J. & Lee-Thorp, J. 1992. The feeding niche of an extinct springbok, Antidorcas bondi (Antilopini, Bovidae), and its palaeoenvironmental meaning. *South African Journal of Science* 88: 227–229.

Brink, J.S. 1987. The archaeozoology of Florisbad, Orange Free State. *National Museum of Bloemfontein* 24: 1–151.

Brink, J.S. 1999. Preliminary report on a caprine from the Cape mountains, South Africa. *Archaeozoologia* 10(1–2): 11–25.

Brink, J.S. 2005. The evolution of the black wildebeest, Connochaetes gnou, and modern large mammal faunas in central Southern Africa. Unpublished PhD thesis. Stellenbosch: University of Stellenbosch.

Brink, J.S. 2016. Faunal evidence for mid- and late Quaternary environmental change in southern Africa. In: Knight, J. & Grab, S.W. (eds) *Quaternary Environmental Change in Southern Africa: Physical and Human Dimensions* 286–307. Cambridge: Cambridge University Press.

Britton, K.H. 2010. Multi-isotope analysis and the reconstruction of prey species palaeomigrations and palaeoecology. Unpublished DPhil dissertation. United Kingdom: Durham University.

Brook, G.A., Cowart, J.B. & Brandt, S.A. 1998. Comparison of Quaternary environmental change in eastern and southern Africa using cave speleothem, tufa and rock shelter sediment data. In: Alsharan, A.S., Glennie, K.W., Whittle, G.L. & Kendall, C.G.S.C. (eds) *Quaternary Deserts and Climate Change*: 239–250. Rotterdam: Balkema.

Brook, G.A., Cowart, J.B., Brandt, S.A. & Scott, L. 1997. Quaternary climatic change in southern and eastern Africa during the last 300 ka: the evidence from caves in Somalia and the Transvaal region of South Africa. *Zeitschrift für Geomorphologie* 108: 15–48.

Brook, G.A., Scott, L., Railsback, L.B. & Goddard, E.A. 2010. A 35ka pollen and isotope record of environmental change along the southern margin of the Kalahari from a stalagmite and animal dung deposits in Wonderwerk Cave, South Africa. *Journal of Arid Environments* 74(7): 870–884.

Brown, S., Higham, T., Slon, V., Pääbo, S., Meyer, M., Douka, K., Brock, F., Comeskey, D., Procopio, N., Shunkov, M. & Derevianko, A. 2016. Identification of a new hominin bone from Denisova Cave, Siberia using collagen fingerprinting and mitochondrial DNA analysis. *Scientific Reports* 6: 1–8.

Brown, T.A. & Brown, K.A. 1992. Ancient DNA and the archaeologist. *Antiquity* 66(250): 10–23.

Buckley, M. & Cheylan, M. 2020. Collagen fingerprinting for the species identification of archaeological amphibian remains. *Boreas* 49: 709–717.

Buckley, M. & Collins, M.J. 2011. Collagen survival and its use for species identification in Holocene-lower Pleistocene bone fragments from British archaeological and paleontological sites. *Antiqua* 1(1): 1–7.

Buckley, M. & Herman, J. 2019. Species identification of Late Pleistocene bat bones using collagen fingerprinting. *International Journal of Osteoarchaeology* 29(6): 1051–1059.

Buckley, M. & Kansa, S.W. 2011. Collagen fingerprinting of archaeological bone and teeth remains from Domuztepe, South Eastern Turkey. *Archaeological and Anthropological Sciences* 3(3): 271–280.

Buckley, M. & Wadsworth, C. 2014. Proteome degradation in ancient bone: diagenesis and phylogenetic potential. *Palaeogeography, Palaeoclimatology, Palaeoecology* 416: 69–79.

Buckley, M. 2013. A molecular phylogeny of Plesiorycteropus reassigns the extinct mammalian order 'Bibymalagasia'. *PloS ONE* 8(3): 1–8.

Buckley, M. 2016. Species identification of bovine, ovine and porcine type 1 collagen; comparing peptide mass fingerprinting and LC-based proteomics methods. *International Journal of Molecular Sciences* 17(445): 1–17.

Buckley, M. 2018. Zooarchaeology by mass spectrometry (ZooMS) collagen fingerprinting for the species identification of archaeological bone fragments. In: Giovas, C.M. & LeFebvre, M.J. (eds) *Zooarchaeology in Practice*: 227–247. Cham: Springer.

Buckley, M., Anderung, C., Penkman, K., Raney, B.J., Götherström, A., Thomas-Oates, J. & Collins, M.J. 2008a. Comparing the survival of osteocalcin and mtDNA in archaeological bone from four European sites. *Journal of Archaeological Science* 35(6): 1756–1764.

Buckley, M., Collins, M. & Thomas-Oates, J. 2008b. A method of isolating the collagen (I) α2 chain carboxytelopeptide for species identification in bone fragments. *Analytical Biochemistry* 374(2): 325–334.

Buckley, M., Collins, M., Thomas-Oates, J. & Wilson, J.C. 2009. Species identification by analysis of bone collagen using matrix-assisted laser desorption/ionisation time-of-flight mass spectrometry. *Rapid Communications in Mass Spectrometry: An International Journal Devoted to the Rapid Dissemination of Up-to-the-Minute Research in Mass Spectrometry* 23(23): 3843–3854.

Buckley, M., Fariña, R.A., Lawless, C., Tambusso, P.S., Varela, L., Carlini, A.A., Powell, J.E. & Martinez, J.G. 2015. Collagen sequence analysis of the extinct giant ground sloths Lestodon and Megatherium. *PloS ONE* 10(11): 1–11.

Buckley, M., Fraser, S., Herman, J., Melton, N.D., Mulville, J. & Pálsdóttir, A.H. 2014. Species identification of archaeological marine mammals using collagen fingerprinting. *Journal of Archaeological Science* 41: 631–641.

Buckley, M., Gu, M., Shameer, S., Patel, S. & Chamberlain, A.T. 2016. High-throughput collagen fingerprinting of intact microfaunal remains; a low-cost method for distinguishing between murine rodent bones. *Rapid Communications in Mass Spectrometry* 30(7): 805–812.

Buckley, M., Harvey, V.L. & Chamberlain, A.T. 2017. Species identification and decay assessment of Late Pleistocene fragmentary vertebrate remains from Pin Hole Cave (Creswell Crags, UK) using collagen fingerprinting. *Boreas* 46(3): 402–411.

Buckley, M., Kansa, S.W., Howard, S., Campbell, S., Thomas-Oates, J. & Collins, M. 2010. Distinguishing between archaeological sheep and goat bones using a single collagen peptide. *Journal of Archaeological Science* 37(1): 13–20.

Buckley, M., Larkin, N. & Collins, M. 2011. Mammoth and Mastodon collagen sequences; survival and utility. *Geochimica et Cosmochimica Acta* 75(7): 2007–2016.

Buckley, M., Walker, A., Ho, S. Y., Yang, Y., Smith, C., Ashton, P., Thomas-Oates, J., Cappellini, E., Koon, H., Penkman, K., Elsworth, B., Ashford, D., Solazzo, C., Andrews, P., Strahler, J., Shapiro, B., Ostrom, P., Gandhi, H., Miller, W., Raney, B., Zylber, M. I., Gilbert, M. T., Prigodich, R. V., Ryan, M., Rijsdijk, K. F., Janoo, A. & Collins, M. J. 2008c. Comment on “Protein sequences from mastodon and Tyrannosaurus rex revealed by mass spectrometry”. *Science* 319(5859): 33.

Buitenwerf, R., Bond, W.J., Stevens, N. & Trollope, W. 2012. Increased tree densities in South African savannas: >50 years of data suggests CO_2 as a driver. *Global Change Biology* 18(2): 675–684.

Burrough, S.L. & Thomas, D.S. 2013. Central southern Africa at the time of the African Humid Period: a new analysis of Holocene palaeoenvironmental and palaeoclimate data. *Quaternary Science Reviews* 80: 29–46.

Burrough, S.L., Breman, E. & Dodd, C. 2012. Can phytoliths provide an insight into past vegetation of the Middle Kalahari palaeolakes during the late Quaternary? *Journal of Arid Environments* 82: 156–164.

Butzer, K.W. 1984a. Late Quaternary environments in South Africa. In: Vogel, J.C. (ed) *Late Cainozoic Paleoclimates of the Southern Hemisphere* 235–264. Rotterdam: Balkema.

Butzer, K.W. 1984b. Archeogeology and Quaternary environment in the interior of southern Africa. In: Klein, R.G. (ed) *Southern African Prehistory and Paleoenvironments*: 1–64. Rotterdam: Balkema.

Butzer, K.W., Stuckenrath, R., Bruzewicz, A.J. & Helgren, D.M. 1978. Late Cenozoic paleoclimates of the Gaap Escarpment, Kalahari margin, South Africa. *Quaternary Research* 10(3): 310–339.

Campana, M.G., Bower, M.A. & Crabtree, P.J. 2013. Ancient DNA for the archaeologist: the future of African research. *African Archaeological Review* 30(1): 21–37.

Cappellini, E., Jensen, L.J., Szklarczyk, D., Ginolhac, A., da Fonseca, R.A., Stafford Jr, T.W., Holen, S.R., Collins, M.J., Orlando, L., Willerslev, E. & Gilbert, M.T.P. 2012. Proteomic analysis of a Pleistocene mammoth femur reveals more than one hundred ancient bone proteins. *Journal of Proteome Research* 11(2): 917–926.

Carr, A.S., Boom, A., Chase, B.M., Meadows, M.E. & Grimes, H.L. 2015. Holocene sea level and environmental change on the west coast of South Africa: evidence from plant biomarkers, stable isotopes and pollen. *Journal of Paleolimnology* 53(4): 415–432.

Carr, A.S., Boom, A., Chase, B.M., Roberts, D.L. & Roberts, Z.E. 2010. Molecular fingerprinting of wetland organic matter using pyrolysis-GC/MS: an example from the southern Cape coastline of South Africa. *Journal of Paleolimnology* 44(4): 947–961.

Carr, A.S., Thomas, D.S., Bateman, M.D., Meadows, M.E. & Chase, B. 2006. Late Quaternary palaeoenvironments of the winter-rainfall zone of southern Africa: palynological and sedimentological evidence from the Agulhas Plain. *Palaeogeography, Palaeoclimatology, Palaeoecology* 239(1–2): 147–165.

Carter, P.L. 1976. The effects of climatic change on settlement in eastern Lesotho during the Middle and Later Stone Age. *World Archaeology* 8(2): 197–206.

Cartwright, C. & Parkington, J. 1997. The wood charcoal assemblages from Elands Bay Cave, southwestern Cape: principles, procedures and preliminary interpretation. *The South African Archaeological Bulletin* 52: 59–72.

Cassidy, L.M., Teasdale, M.D., Carolan, S., Enright, R., Werner, R., Bradley, D.G., Finlay, E.K. & Mattiangeli, V. 2017. Capturing goats: documenting two hundred years of mitochondrial DNA diversity among goat populations from Britain and Ireland. *Biology Letters* 13(3): 1–6.

Castelló, J.R. 2016. *Bovids of the World: Antelopes, Gazelles, Cattle, Goats, Sheep, and Relatives.* United Kingdom: Princeton University Press.

Castro, D.J. & Bell, F.G. 1995. An engineering geological appraisal of the sandstones of the Clarens Formation, Lesotho, in relation to tunnelling. *Geotechnical & Geological Engineering* 13(3): 117–142.

Cattaneo, C., Gelsthorpe, K., Phillips, P. & Sokol, R.J. 1992. Reliable identification of human albumin in ancient bone using ELISA and monoclonal antibodies. *American Journal of Physical Anthropology* 87(3): 365–372.

Caut, S., Angulo, E. & Courchamp, F. 2008. Discrimination factors ($\Delta^{15}N$ and $\Delta^{13}C$) in an omnivorous consumer: effect of diet isotopic ratio. *Functional Ecology* 22(2): 255–263.

Caut, S., Angulo, E. & Courchamp, F. 2009. Variation in discrimination factors ($\Delta^{15}N$ and $\Delta^{13}C$): the effect of diet isotopic values and applications for diet reconstruction. *Journal of Applied Ecology* 46(2): 443–453.

Cerling, T.E. & Harris, J.M. 1999. Carbon isotope fractionation between diet and bioapatite in ungulate mammals and implications for ecological and paleoecological studies. *Oecologia* 120(3): 347–363.

Cerling, T.E., Harris, J.M. & Passey, B.H. 2003. Diets of East African Bovidae based on stable isotope analysis. *Journal of Mammalogy* 84(2): 456–470.

Cerling, T.E., Harris, J.M., MacFadden, B.J., Leakey, M.G., Quade, J., Eisenmann, V. & Ehleringer, J.R. 1997. Global vegetation change through the Miocene/Pliocene boundary. *Nature* 389(6647): 153–158.

Cernusak, L.A., Ubierna, N., Winter, K., Holtum, J.A., Marshall, J.D. & Farquhar, G.D. 2013. Environmental and physiological determinants of carbon isotope discrimination in terrestrial plants. *New Phytologist* 200(4): 950–965.

Chafetz, H.S. & Buczynski, C. 1992. Bacterially induced lithification of microbial mats. *PALAIOS* 7: 277–293.

Chase, B.M. & Meadows, M.E. 2007. Late Quaternary dynamics of southern Africa's winter rainfall zone. *Earth-Science Reviews* 84(3–4): 103–138.

Chase, B.M. & Thomas, D.S. 2006. Late Quaternary dune accumulation along the western margin of South Africa: distinguishing forcing mechanisms through the analysis of migratory dune forms. *Earth and Planetary Science Letters* 251(3–4): 318–333.

Chase, B.M. 2021. Orbital forcing in southern Africa: towards a conceptual model for predicting deep time environmental change from an incomplete proxy record. *Quaternary Science Reviews* 265: 1–14.

Chase, B.M., Boom, A., Carr, A.S., Carré, M., Chevalier, M., Meadows, M.E., Pedro, J.B., Stager, J.C. & Reimer, P.J. 2015a. Evolving southwest African response to abrupt deglacial North Atlantic climate change events. *Quaternary Science Reviews* 121: 132–136.

Chase, B.M., Boom, A., Carr, A.S., Meadows, M.E. & Reimer, P.J. 2013. Holocene climate change in southernmost South Africa: rock hyrax middens record shifts in the southern westerlies. *Quaternary Science Reviews* 82: 199–205.

Chase, B.M., Chevalier, M., Boom, A. & Carr, A.S. 2017. The dynamic relationship between temperate and tropical circulation systems across South Africa since the last glacial maximum. *Quaternary Science Reviews* 174: 54–62.

Chase, B.M., Lim, S., Chevalier, M., Boom, A., Carr, A.S., Meadows, M.E. & Reimer, P.J. 2015b. Influence of tropical easterlies in southern Africa's winter rainfall zone during the Holocene. *Quaternary Science Reviews* 107: 138–148.

Chase, B.M., Meadows, M.E., Carr, A.S. & Reimer, P.J. 2010. Evidence for progressive Holocene aridification in southern Africa recorded in Namibian hyrax middens: Implications for African Monsoon dynamics and the ‘‘African Humid Period’’. *Quaternary Research* 74(1): 36–45.

Chase, B.M., Meadows, M.E., Scott, L., Thomas, D.S.G., Marais, E., Sealy, J. & Reimer, P.J. 2009. A record of rapid Holocene climate change preserved in hyrax middens from southwestern Africa. *Geology* 37(8): 703–706.

Chase, B.M., Quick, L.J., Meadows, M.E., Scott, L., Thomas, D.S. & Reimer, P.J. 2011. Late glacial interhemispheric climate dynamics revealed in South African hyrax middens. *Geology* 39(1): 19–22.

Chase, B.M., Scott, L., Meadows, M.E., Gil-Romera, G., Boom, A., Carr, A.S., Reimer, P.J., Truc, L., Valsecchi, V. & Quick, L.J. 2012. Rock hyrax middens: a palaeoenvironmental archive for southern African drylands. *Quaternary Science Reviews* 56: 107–125.

Chevalier, M. & Chase, B.M. 2015. Southeast African records reveal a coherent shift from high-to low-latitude forcing mechanisms along the east African margin across last glacial–interglacial transition. *Quaternary Science Reviews* 125: 117–130.

Chevalier, M. & Chase, B.M. 2016. Determining the drivers of long-term aridity variability: a southern African case study. *Journal of Quaternary Science* 31(2): 143–151.

Chowdhury, M.P., Choudhury, K.D., Bouchard, G.P., Riel-Salvatore, J., Negrino, F., Benazzi, S., Slimak, L., Frasier, B., Szabo, V., Harrison, R. & Hambrecht, G. 2021. Machine learning ATR-FTIR spectroscopy data for the screening of collagen for ZooMS analysis and mtDNA in archaeological bone. *Journal of Archaeological Science* 126: 1–13.

Chu, M.L., De Wet, W., Bernard, M., Ding, J.F., Morabito, M., Myers, J., Williams, C. & Ramirez, F. 1984. Human pro α 1 (I) collagen gene structure reveals evolutionary conservation of a pattern of introns and exons. *Nature* 310(5975): 337–340.

Clark, A.M.B. 1997. The final Middle Stone Age at Rose Cottage Cave: a distinct industry in the Basutolian ecozone. *South African Journal of Science* 93: 449–458.

Clark, J.L. & Kandel, A.W. 2013. The evolutionary implications of variation in human hunting strategies and diet breadth during the Middle Stone Age of southern Africa. *Current Anthropology* 54(S8): S269–S287.

Clark, J.L. 2017. The Howieson's Poort fauna from Sibudu cave: documenting continuity and change within Middle Stone Age industries. *Journal of Human Evolution* 107: 49–70.

Cockcroft, M.J., Wilkinson, M.J. & Tyson, P.D. 1987. The application of a present-day climatic model to the late Quaternary in southern Africa. *Climatic Change* 10(2): 161–181.

Codron, D. & Brink, J.S. 2007. Trophic ecology of two savanna grazers, blue wildebeest Connochaetes taurinus and black wildebeest Connochaetes gnou. *European Journal of Wildlife Research* 53(2): 90–99.

Codron, D. & Codron, J. 2009. Reliability of $\delta^{13}C$ and $\delta^{15}N$ in faeces for reconstructing savanna herbivore diet. *Mammalian Biology* 74(1): 36–48.

Codron, D., Brink, J.S., Rossouw, L. & Clauss, M. 2008. The evolution of ecological specialization in southern African ungulates: competition-or physical environmental turnover? *Oikos* 117(3): 344–353.

Codron, D., Codron, J., Lee-Thorp, J.A., Sponheimer, M., De Ruiter, D., Sealy, J., Grant, R. & Fourie, N. 2007b. Diets of savanna ungulates from stable carbon isotope composition of faeces. *Journal of Zoology* 273(1): 21–29.

Codron, D., Lee-Thorp, J.A., Sponheimer, M. & Codron, J. 2007a. Nutritional content of savanna plant foods: implications for browser/grazer models of ungulate diversification. *European Journal of Wildlife Research* 53(2): 100–111.

Codron, D., Lee-Thorp, J.A., Sponheimer, M., de Ruiter, D. & Codron, J. 2006. Inter-and intrahabitat dietary variability of chacma baboons (*Papio ursinus*) in South African savannas based on fecal $\delta^{13}C$, $\delta^{15}N$, and %N. *American Journal of Physical Anthropology: The Official Publication of the American Association of Physical Anthropologists* 129(2): 204–214.

Codron, D., Sponheimer, M., Codron, J., Hammer, S., Tschuor, A., Braun, U., Bernasconi, S.M. & Clauss, M. 2012. Tracking the fate of digesta ^{13}C and ^{15}N compositions along the ruminant gastrointestinal tract: Does digestion influence the relationship between diet and faeces? *European Journal of Wildlife Research* 58(1): 303–313.

Codron, J., Lee-Thorp, J.A., Sponheimer, M. & Codron, D. 2013. Plant stable isotope composition across habitat gradients in a semi-arid savanna: implications for environmental reconstruction. *Journal of Quaternary Science* 28(3): 301–310.

Coetzee, J.A. 1967. Pollen analytical studies in East and Southern Africa. *Paleoecology Africa* 3: 1–146.

Cohen, A.L. & Tyson, P.D. 1995. Sea-surface temperature fluctuations during the Holocene off the south coast of Africa: implications for terrestrial climate and rainfall. *The Holocene* 5(3): 304–312.

Cohen, A.L., Parkington, J.E., Brundrit, G.B. & van der Merwe, N.J. 1992. A Holocene marine climate record in mollusc shells from the southwest African coast. *Quaternary Research* 38(3): 379–385.

Collins, B.R., Wilkins, J. & Ames, C.J. 2017. Revisiting the Holocene occupations at Grassridge Rockshelter, Eastern Cape, South Africa. *The South African Archaeological Bulletin* 72(206): 162–170.

Collins, B.R., Wojcieszak, M., Nowell, A., Hodgskiss, T. & Ames, C.J. 2020. Beads and bead residues as windows to past behaviours and taphonomy: a case study from Grassridge

Rockshelter, Eastern Cape, South Africa. *Archaeological and Anthropological Sciences* 12(8): 1–20.

Collins, J.A., Schefuß, E., Heslop, D., Mulitza, S., Prange, M., Zabel, M., Tjallingii, R., Dokken, T.M., Huang, E., Mackensen, A. & Schulz, M. 2011. Interhemispheric symmetry of the tropical African rainbelt over the past 23,000 years. *Nature Geoscience* 4(1): 42–45.

Collins, M.J, Buckley, M., Grundy, H.H., Thomas-Oates, J., Wilson, J. & van Doorn, N. 2010. ZooMS: the collagen barcode and fingerprints. *Spectroscopy Europe* 22(2): 6–10.

Collins, M.J., Child, A.M., van Duin, A.T.C. & Vermeer, C. 1998. Ancient osteocalcin: the most stable bone protein. *Ancient Biomolecules* 2: 223–238.

Collins, M.J., Nielsen–Marsh, C.M., Hiller, J., Smith, C.I., Roberts, J.P., Prigodich, R.V., Wess, T.J., Csapo, J., Millard, A.R. & Turner–Walker, G. 2002. The survival of organic matter in bone: a review. *Archaeometry* 44(3): 383–394.

Conard, N., Porraz G. & Wadley, L. 2012. What is in a name? Characterising the 'post-Howieson's Poort' at Sibudu. *The South African Archaeological Bulletin* 67: 180–199.

Cooper, R.G., Horbańczuk, J.O., Villegas-Vizcaíno, R., Kennou Sebei, S., Faki Mohammed, A.E. & Mahrose, K. 2010. Wild ostrich (Struthio camelus) ecology and physiology. *Tropical Animal Health and Production* 42(3): 363–373.

Cooper, R.G., Mahrose, K., Horbańczuk, J.O., Villegas-Vizcaíno, R., Kennou Sebei, S. & Faki Mohammed, A.E. 2009. The wild ostrich (Struthio camelus): a review. *Tropical Animal Health and Production* 41(8): 1669–1678.

Cordova, C. & Avery, G. 2017. African savanna elephants and their vegetation associations in the Cape Region, South Africa: Opal phytoliths from dental calculus on prehistoric, historic and reserve elephants. *Quaternary International* 443: 189–211.

Cormie, A.B. & Schwarcz, H.P. 1996. Effects of climate on deer bone $\delta^{15}N$ and $\delta^{13}C$: lack of precipitation effects on $\delta^{15}N$ for animals consuming low amounts of C_4 plants. *Geochimica et Cosmochimica Acta* 60(21): 4161–4166.

Cotrufo, M.F., Ineson, P. & Scott, A. 1998. Elevated CO_2 reduces the nitrogen concentration of plant tissues. *Global Change Biology* 4(1): 43–54.

Coutu, A.N., Taurozzi, A.J., Mackie, M., Jensen, T.Z.T., Collins, M.J. & Sealy, J. 2021. Palaeoproteomics confirm earliest domesticated sheep in southern Africa ca. 2000 BP. *Scientific Reports* 11(1): 1–11.

Coutu, A.N., Whitelaw, G., le Roux, P. & Sealy, J. 2016. Earliest evidence for the ivory trade in southern Africa: Isotopic and ZooMS analysis of seventh–tenth century AD ivory from KwaZulu-Natal. *African Archaeological Review* 33(4): 411–435.

Cowling, R.M., Cartwright, C.R., Parkington, J.E. & Allsopp, J.C. 1999. Fossil wood charcoal assemblages from Elands Bay Cave, South Africa: implications for Late Quaternary vegetation and climates in the winter-rainfall fynbos biome. *Journal of Biogeography* 26(2): 367–378.

Craig, C., Collins, B.R., Nowell, A. & Ames, C.J. 2020. The effects of heating ostrich eggshell on bead manufacturing: An experimental approach. *Journal of Archaeological Science: Reports* 31: 1–9.

Craine, J.M., Elmore, A.J., Aidar, M.P., Bustamante, M., Dawson, T.E., Hobbie, E.A., Kahmen, A., Mack, M.C., McLauchlan, K.K., Michelsen, A. & Nardoto, G.B. 2009. Global patterns of foliar nitrogen isotopes and their relationships with climate, mycorrhizal fungi, foliar nutrient concentrations, and nitrogen availability. *New Phytologist* 183(4): 980–992.

Cremaschi, M. 2002. Late Pleistocene and Holocene climatic changes in the central Sahara: the case study of the southwestern Fezzan, Libya. In: Hassan, F.A. (ed) *Droughts, Food and Culture*: 65–82. New York: Plenum Publishers.

Cruz-Uribe, K., Klein, R.G., Avery, G., Avery, M., Halkett, D., Hart, T., Milo, R.G., Sampson, C.G. & Volman, T.P. 2003. Excavation of buried late Acheulean (mid-quaternary) land surfaces at Duinefontein 2, Western Cape Province, South Africa. *Journal of Archaeological Science* 30(5): 559–575.

Cuijpers, S. & Lauwerier, R.C. 2008. Differentiating between bone fragments from horses and cattle: a histological identification method for archaeology. *Environmental Archaeology* 13(2): 165–179.

Culley, C. 2021. Coastal caprines: using ZooMS to trace the spread of domesticates in coastal Eastern Africa. Unpublished master's dissertation. Queensland: The University of Queensland.

Culley, C., Janzen, A., Brown, S., Prendergast, M.E., Shipton, C., Ndiema, E., Petraglia, M.D., Boivin, N. & Crowther, A. 2021a. Iron Age hunting and herding in coastal eastern Africa: ZooMS identification of domesticates and wild bovids at Panga ya Saidi, Kenya. *Journal of Archaeological Science* 130: 1–13.

Culley, C., Janzen, A., Brown, S., Prendergast, M.E., Wolfhagen, J., Abderemane, B., Ali, A.K., Haji, O., Horton, M.C., Shipton, C. & Swift, J. 2021b. Collagen fingerprinting traces the introduction of caprines to island Eastern Africa. *Royal Society Open Science* 8(7): 1–18.

d'Errico, F., Backwell, L., Villa, P., Degano, I., Lucejko, J.J., Bamford, M.K., Higham, T.F., Colombini, M.P. & Beaumont, P.B. 2012. Early evidence of San material culture represented by organic artifacts from Border Cave, South Africa. *Proceedings of the National Academy of Sciences* 109(33): 13214–13219.

d'Errico, F., Martí, A.P., Shipton, C., Le Vraux, E., Ndiema, E., Goldstein, S., Petraglia, M.D. & Boivin, N. 2020. Trajectories of cultural innovation from the Middle to Later Stone Age in Eastern Africa: Personal ornaments, bone artifacts, and ochre from Panga ya Saidi, Kenya. *Journal of Human Evolution* 141: 1–25.

David, B., Roberts, R.G., Magee, J., Mialanes, J., Turney, C., Bird, M., White, C., Fifield, L.K. & Tibby, J. 2007. Sediment mixing at Nonda Rock: investigations of stratigraphic integrity at an early archaeological site in northern Australia and implications for the human colonisation of the continent. *Journal of Quaternary Science: Published for the Quaternary Research Association* 22(5): 449–479.

Dawson, T.E. & Siegwolf, R.T.W. 2007. Using stable isotopes as indicators, tracers, and recorders of ecological change: some context and background. In: Dawson, T.E. & Siegwolf, R.T.W (eds) *Stable Isotopes as Indicators of Ecological Change*: 3–18. Amsterdam: Elsevier.

Dayet, L., Erasmus, R., Val, A., Feyfant, L. & Porraz G. 2017. Beads, pigments and early Holocene ornamental traditions at Bushman Rock Shelter, South Africa. *Journal of Archaeological Science: Reports* 13: 635–651.

de Graaf, G., Schultz, K.C.A. & van der Waet, P.T. 1973. Notes on rumen contents of Cape buffalo Syncerus caffer in the Addo Elephant National Park. *Koedoe* 16(1): 45–58.

de Sousa, D.V., Ker, J.C., Prous, A., Schaefer, C.E., Rodet, M.J., Oliveira, F.S. & Silva, R.C. 2017. Archaeoanthrosol formation and evolution of the "Santana do Riacho"

archaeological shelter: an old burial site in South America. *Geoarchaeology* 32(6): 678–693.

Deacon, H.J. & Thackeray, J.F. 1984. Late Pleistocene environmental changes and implications for the archaeological record in southern Africa. In: Vogel, J.C. (ed) *Late Cainozoic Palaeoclimates of the Southern Hemisphere*: 375–390. Rotterdam: Balkema.

Deacon, H.J. 1976. *Where Hunters Gathered: A Study of Holocene Stone Age People in the Eastern Cape.* Claremont: South African Archaeological Society Monograph Series Vol. 1.

Deacon, H.J. 1979. Excavations at Boomplaas Cave: a sequence through the Upper Pleistocene and Holocene in South Africa. *World Archaeology* 10: 241–257.

Deacon, H.J. 1995. Two late Pleistocene-Holocene archaeological depositories from the southern Cape, South Africa. *The South African Archaeological Bulletin* 50(162): 121–131.

Deacon, H.J., Deacon, J., Scholtz, A., Thackeray, J.F. & Brink, J.S. 1984. Correlation of palaeoenvironmental data from the Late Pleistocene and Holocene deposits at Boomplaas Cave, southern Cape. In: Vogel, J.C (ed) *Late Cainozic Palaeoclimates of the Southern Hemisphere* 339–351. Rotterdam: Balkema.

Deacon, J. & Lancaster, N. 1988. *Late Quaternary Palaeoenvironments of Southern Africa*. Oxford: Oxford University Press.

Deacon, J. 1978. Changing patterns in the Late Pleistocene/Early Holocene prehistory of southern Africa as seen from the Nelson Bay Cave stone artifact sequence. *Quaternary Research* 10: 84–111.

Deacon, J. 1984. *The Later Stone Age of Southernmost Africa*. Oxford: British Archaeological Reports International Series 213.

deMenocal, P., Ortiz, J., Guilderson, T., Adkins, J., Sarnthein, M., Baker, L. & Yarusinsky, M. 2000. Abrupt onset and termination of the African Humid Period: rapid climate responses to gradual insolation forcing. *Quaternary Science Reviews* 19(1–5): 347–361.

DeNiro, M.J. & Epstein, S. 1977. Mechanism of carbon isotope fractionation associated with lipid synthesis. *Science* 197(4300): 261–263.

DeNiro, M.J. & Epstein, S. 1978. Influence of diet on the distribution of carbon isotopes in animals. *Geochimica et Cosmochimica Acta* 42(5): 495–506.

DeNiro, M.J. & Epstein, S. 1981. Influence of diet on the distribution of nitrogen isotopes in animals. *Geochimica et Cosmochimica Acta* 45(3): 341–351.

DeNiro, M.J. 1987. Stable isotopy and archaeology. *American Scientist* 75(2): 182–191.

DeNiro, M.J., Schoeninger, M.J. & Hastorf, C.A. 1985. Effect of heating on the stable carbon and nitrogen isotope ratios of bone collagen. *Journal of Archaeological Science* 12(1): 1–7.

Dercon, G., Clymans, E., Diels, J., Merckx, R. & Deckers, J. 2006. Differential ^{13}C isotopic discrimination in maize at varying water stress and at low to high nitrogen availability. *Plant and Soil* 282(1): 313–326.

Desmond, A., Barton, N., Bouzouggar, A., Douka, K., Fernandez, P., Humphrey, L., Morales, J., Turner, E. & Buckley, M. 2018. ZooMS identification of bone tools from the North African Later Stone Age. *Journal of Archaeological Science* 98: 149–157.

Dewar, G.I. 2007. The archaeology of the coastal desert of Namaqualand, South Africa: a regional synthesis. Unpublished DPhil dissertation. Cape Town: University of Cape Town.

Diefendorf, A.F., Mueller, K.E., Wing, S.L., Koch, P.L. & Freeman, K.H. 2010. Global patterns in leaf ^{13}C discrimination and implications for studies of past and future climate. *Proceedings of the National Academy of Sciences* 107(13): 5738–5743.

Driver, J.C. 1992. Identification, classification and zooarchaeology. *Circaea* 9: 35–47.

Drucker, D. & Bocherens, H. 2004. Carbon and nitrogen stable isotopes as tracers of change in diet breadth during Middle and Upper Palaeolithic in Europe. *International Journal of Osteoarchaeology* 14(3-4): 162–177.

Dupont, L.M., Caley, T., Kim, J.H., Castañeda, I., Malaizé, B. & Giraudeau, J. 2011. Glacial-interglacial vegetation dynamics in South Eastern Africa coupled to sea surface temperature variations in the Western Indian Ocean. *Climate of the Past* 7(4): 1209–1224.

Dupont, L.M., Kim, J.H., Schneider, R.R. & Shi, N. 2004. Southwest African climate independent of Atlantic sea surface temperatures during the Younger Dryas. *Quaternary Research* 61(3): 318–324.

Ecker, M., Brink, J., Horwitz, L.K., Scott, L. & Lee-Thorp, J.A. 2018. A 12,000-year record of changes in herbivore niche separation and palaeoclimate (Wonderwerk Cave, South Africa). *Quaternary Science Reviews* 180: 132–144.

Edwards, E.J., Osborne, C.P., Strömberg, C.A., Smith, S.A., C_4 Grasses Consortium, Bond, W.J., Christin, P.A., Cousins, A.B., Duvall, M.R., Fox, D.L. & Freckleton, R.P. 2010. The origins of C_4 grasslands: integrating evolutionary and ecosystem science. *Science* 328(5978): 587–591.

Ehleringer, J.R. & Cerling, T.E. 2002. C_3 and C_4 photosynthesis. In: Mooney, H.A. & Canadell, J.G. (eds) *Encyclopaedia of Global Environmental Change*: 186–190. Chichester: John Wiley & Sons Ltd.

Ehleringer, J.R. & Monson, R.K. 1993. Evolutionary and ecological aspects of photosynthetic pathway variation. *Annual Review of Ecology and Systematics* 24(1): 411–439.

Ehleringer, J.R., Cerling, T.E. & Helliker, B.R. 1997. C_4 photosynthesis, atmospheric CO_2, and climate. *Oecologia* 112(3): 285–299.

Engelbrecht, C.J., Landman, W.A., Engelbrecht, F.A. & Malherbe, J. 2015. A synoptic decomposition of rainfall over the Cape south coast of South Africa. *Climate Dynamics* 44(9–10): 2589–2607.

Engelbrecht, F.A., Marean, C.W., Cowling, R.M., Engelbrecht, C.J., Neumann, F.H., Scott, L., Nkoana, R., O'Neal, D., Fisher, E., Shook, E. & Franklin, J. 2019. Downscaling last glacial maximum climate over southern Africa. *Quaternary Science Reviews* 226: 1–28.

Esterhuysen, A.B. & Mitchell, P.J. 1997. Palaeoenvironmental and archaeological implications of charcoal assemblages from Holocene sites in western Lesotho, southern Africa. *Palaeoecology of Africa* 24*:* 203–232.

Esterhuysen, A.B. & Smith, J. 2003. A comparison of charcoal and stable carbon isotope results for the Caledon River Valley, southern Africa, for the period 13 500–5000 yr BP. *The South African Archaeological Bulletin* 58(177): 1–5.

Esterhuysen, A.B. 1996. Palaeoenvironmental reconstruction from Pleistocene to present: an analysis of charcoal from sites in the eastern Free State and Lesotho. Unpublished PhD thesis. Johannesburg: University of the Witwatersrand.

Esterhuysen, A.B., Mitchell, P.J. & Thackeray, J.F. 1999. Climatic change across the Pleistocene/Holocene boundary in the Caledon River southern Africa: Results of a factor analysis of charcoal assemblages. *Southern African Field Archaeology* 8: 28–34.

Evans, R.D. & Ehleringer, J.R. 1993. A break in the nitrogen cycle in aridlands? Evidence from $\delta^{15}N$ of soils. *Oecologia* 94(3): 314–317.

Fagan, B.M.1967. Iron Age Cultures in Zambia (Vol. 1). London: Chatto and Windus.

Faith, J.T. & Behrensmeyer, A.K. 2013. Climate change and faunal turnover: testing the mechanics of the turnover-pulse hypothesis with South African fossil data. *Paleobiology* 39(4): 609–627.

Faith, J.T. 2011a. Ungulate community richness, grazer extinctions, and human subsistence behavior in southern Africa's Cape Floral Region. *Palaeogeography, Palaeoclimatology, Palaeoecology* 306(3–4): 219–227.

Faith, J.T. 2011b. Late Pleistocene climate change, nutrient cycling, and the megafaunal extinctions in North America. *Quaternary Science Reviews* 30(13–14): 1675–1680.

Faith, J.T. 2012. Late Quaternary megafaunal extinctions in Southern Africa's Cape Floral Region. Unpublished PhD Thesis. Washington: The George Washington University.

Faith, J.T. 2013a. Taphonomic and paleoecological change in the large mammal sequence from Boomplaas Cave, Western Cape, South Africa. *Journal of Human Evolution* 65: 715–730.

Faith, J.T. 2013b. Ungulate diversity and precipitation history since the Last Glacial Maximum in the Western Cape, South Africa. *Quaternary Science Reviews 68:* 191–199.

Faith, J.T. 2014. Late Pleistocene and Holocene mammal extinctions on continental Africa. *Earth-Science Reviews* 128: 105–121.

Faith, J.T., Chase, B.M. & Avery, D.M. 2019. Late Quaternary micromammals and the precipitation history of the southern Cape, South Africa. *Quaternary Research* 91(2): 848–860.

Farmer, E.C., deMenocal, P.B. & Marchitto, T.M. 2005. Holocene and deglacial ocean temperature variability in the Benguela upwelling region: Implications for low-latitude atmospheric circulation. *Paleoceanography* 20(2): 1–16.

Farquhar, G.D., Ehleringer, J.R. & Hubick, K.T. 1989. Carbon isotope discrimination and photosynthesis. *Annual Review of Plant Biology* 40(1): 503–537.

Faure, G. 1986. *Principles of Isotope Geology*. New York: John Wiley & Sons Ltd.

Fernandez-Jalvo, Y. & Andrews, P. 2016. *Atlas of Taphonomic Identifications: 1001+ Images of Fossil and Recent Mammal Bone Modification*. Dordrecht: Springer.

Fiddyment, S., Holsinger, B., Ruzzier, C., Devine, A., Binois, A., Albarella, U., Fischer, R., Nichols, E., Curtis, A., Cheese, E. & Teasdale, M.D. 2015. Animal origin of 13th-century uterine vellum revealed using non-invasive peptide fingerprinting. *Proceedings of the National Academy of Sciences* 112(49): 15066–15071.

Finch, J.M. & Hill, T.R. 2008. A late Quaternary pollen sequence from Mfabeni Peatland, South Africa: Reconstructing forest history in Maputaland. *Quaternary Research* 70(3): 442–450.

Finné, M., Norström, E., Risberg, J. & Scott, L. 2010. Siliceous microfossils as late-Quaternary paleo-environmental indicators at Braamhoek wetland, South Africa. *The Holocene* 20(5): 747–760.

Fischer, H., Fundel, F., Ruth, U., Twarloh, B., Wegner, A., Udisti, R., Becagli, S., Castellano, E., Morganti, A., Severi, M. & Wolff, E. 2007. Reconstruction of millennial changes in dust emission, transport and regional sea ice coverage using the deep EPICA ice cores from the Atlantic and Indian Ocean sector of Antarctica. *Earth and Planetary Science Letters* 260(1–2): 340–354.

Fisher, E.C., Cawthra, H.C., Esteban, I., Jerardino, A., Neumann, F.H., Oertle, A., Pargeter, J., Saktura, R.B., Szabó, K., Winkler, S. & Zohar, I. 2020. Coastal occupation and foraging during the last glacial maximum and early Holocene at Waterfall Bluff, eastern Pondoland, South Africa. *Quaternary Research*, 97: 1–41.

Fitchett, J.M. & Bamford, M.K. 2017. The validity of the Asteraceae: Poaceae fossil pollen ratio in discrimination of the southern African summer-and winter-rainfall zones. *Quaternary Science Reviews* 160: 85–95.

Fitchett, J.M. 2019. The Holocene Climates of South Africa. In: Knight, J. & Rogerson, C.M. (eds) *The Geography of South Africa*: 47–56. Cham: Springer.

Fitchett, J.M. 2019. The Holocene Climates of South Africa. In: Knight, J. & Rogerson, C.M. (eds) *The Geography of South Africa*: 47–56. Cham: Springer.

Fitchett, J.M., Grab, S.W., Bamford, M.K. & Mackay, A.W. 2017a. Late Quaternary research in southern Africa: progress, challenges and future trajectories. *Transactions of the Royal Society of South Africa* 72(3): 280–293.

Fitchett, J.M., Mackay, A.W., Grab, S.W. & Bamford, M.K. 2017b. Holocene climatic variability indicated by a multi-proxy record from southern Africa's highest wetland. *The Holocene* 27(5): 638–650.

Fletcher, S.M., Dolton, P. & Harris-Smith, P.W. 1984. Species identification of blood and saliva stains by enzyme-linked immunoassay (ELISA) using monoclonal antibody. *Journal of Forensic Science* 29(1): 67–74.

Freytet, P. & Verrecchia, E. 1995. Discovery of Ca oxalate crystals associated with fungi in moss travertines (bryoherms, freshwater heterogeneous stromatolites). *Geomicrobiology Journal* 13: 117–127.

Fry, B. 2006. *Stable Isotope Ecology*. New York: Springer.

Fuller, B.T., Fuller, J.L., Sage, N.E., Harris, D.A., O'Connell, T.C. & Hedges, R.E. 2005. Nitrogen balance and $\delta^{15}N$: why you're not what you eat during nutritional stress. *Rapid Communications in Mass Spectrometry: An International Journal Devoted to the Rapid Dissemination of Up-to-the-Minute Research in Mass Spectrometry* 19(18): 2497–2506.

Gagnon, M. & Chew, A.E. 2000. Dietary preferences in extant African Bovidae. *Journal of Mammalogy* 81(2): 490–511.

Gasse, F. & van Campo, E. 1998. A 40,000-yr pollen and diatom record from Lake Tritrivakely, Madagascar, in the southern tropics. *Quaternary Research* 49(3): 299–311.

Gasse, F. 2000. Hydrological changes in the African tropics since the Last Glacial Maximum. *Quaternary Science Reviews* 19(1–5): 189–211.

Geoghegan, N. 2019. Working smarter, not harder: the taphonomy and skeletal element representation of bovid remains at Grassridge Rock Shelter, Eastern Cape. Unpublished honours dissertation. Johannesburg: University of the Witwatersrand.

Ghannoum, O., Von Caemmerer, S. & Conroy, J.P. 2002. The effect of drought on plant water use efficiency of nine NAD–ME and nine NADP–ME Australian C_4 grasses. *Functional Plant Biology* 29(11): 1337–1348.

Gifford-Gonzalez, D. 2018. *An Introduction to Zooarchaeology*. Cham: Springer.

Goldberg, P. & Bar-Yosef, O. 2002. Site formation processes in Kebara and Hayonim Caves and their significance in Levantine prehistoric caves. In: Akazawa, T., Aoki, K. & Bar-Yosef, O. (eds) *Neandertals and Modern Humans in Western Asia*: 107–125. New York: Plenum Press.

Gordon, C.C. & Buikstra, J.E. 1981. Soil pH, bone preservation, and sampling bias at mortuary sites. *American Antiquity* 46(3): 566–571.

Grab, S. 2015. Sandstone landforms of the Karoo Basin: Naturally sculpted rock. In: Grab, S. & Knight, J. (eds) *Landscapes and Landforms of South Africa*: 11–21. Cham: Springer.

Grab, S., Scott, L., Rossouw, L. & Meyer, S. 2005. Holocene palaeoenvironments inferred from a sedimentary sequence in the Tsoaing River Basin, western Lesotho. *Catena* 61(1): 49–62.

Grab, S.W. & Mills, S.C. 2011. Quaternary slope processes and morphologies in the upper Sehonghong Valley, eastern Lesotho. *Proceedings of the Geologists' Association* 122(1): 179–186.

Green, H., Pickering, R., Drysdale, R., Johnson, B.C., Hellstrom, J. & Wallace, M. 2015. Evidence for global teleconnections in a late Pleistocene speleothem record of water balance and vegetation change at Sudwala Cave, South Africa. *Quaternary Science Reviews 110*: 114–130.

Greenlee, D.M. & Dunnell, R.C. 2010. Identification of fragmentary bone from the Pacific. *Journal of Archaeological Science* 37(5): 957–970.

Gröcke, D.R., Bocherens, H. & Mariotti, A. 1997. Annual rainfall and nitrogen-isotope correlation in macropod collagen: application as a palaeoprecipitation indicator. *Earth and Planetary Science Letters* 153(3–4): 279–285.

Gu, X. & Li, W.H. 1992. Higher rates of amino acid substitution in rodents than in humans. *Molecular Phylogenetics and Evolution* 1(3): 211–214.

Guiry, E.J. & Szpak, P. 2021. Improved quality control criteria for stable carbon and nitrogen isotope measurements of ancient bone collagen. *Journal of Archaeological Science* 132: 1–15.

Haberzettl, T., Baade, J., Compton, J., Daut, G., Dupont, L., Finch, J., Frenzel, P., Green, A., Hahn, A., Hebbeln, D., Helmschrot, J., Humphries, M. Kasper, T., Kirsten, K., Mäusbacher, R., Meadows, M., Meschner, S., Quick, L., Schefuβ, E., Wündsch, M. & Zabel, M. 2014. Paleoenvironmental investigations using a combination of terrestrial and marine sediments from South Africa-The RAIN (Regional Archives for Integrated iNvestigations) approach. *Zentralblatt für Geologie und Paläontologie* 1: 55–73.

Haile, J., Holdaway, R., Oliver, K., Bunce, M., Gilbert, M.T.P., Nielsen, R., Munch, K., Ho, S.Y., Shapiro, B. & Willerslev, E. 2007. Ancient DNA chronology within sediment deposits: Are paleobiological reconstructions possible and is DNA leaching a factor? *Molecular Biology and Evolution* 24(4): 982–989.

Handley, L.L., Austin, A.T., Robinson, D., Scrimgeour, C.M., Raven, J.A., Heaton, T.H.E., Schmidt, S. & Stewart, G.R. 1999. The ^{15}N natural abundance ($\delta^{15}N$) of ecosystem samples reflects measures of water availability. *Australian Journal of Plant Physiology* 26(2): 185–199.

Harsanyi, L. 1993. Differential diagnosis of human and animal bone. In: Grupe, G. & Garland, A.N. (eds) *Histology of Ancient Human Bone: Methods and Diagnosis*: 79–94. Berlin: Springer.

Hartman, G. & Danin, A. 2010. Isotopic values of plants in relation to water availability in the Eastern Mediterranean region. *Oecologia* 162(4): 837–852.

Hartman, G. 2011. Are elevated $\delta^{15}N$ values in herbivores in hot and arid environments caused by diet or animal physiology? *Functional Ecology* 25(1): 122–131.

Harvey, V.L., Daugnora, L. & Buckley, M. 2018. Species identification of ancient Lithuanian fish remains using collagen fingerprinting. *Journal of Archaeological Science* 98: 102–111.

Harvey, V.L., Egerton, V.M., Chamberlain, A.T., Manning, P.L. & Buckley, M. 2016. Collagen fingerprinting: a new screening technique for radiocarbon dating ancient bone. *PloS ONE* 11(3): 1–15.

Harvey, V.L., LeFebvre, M.J., Defrance, S.D., Toftgaard, C., Drosou, K., Kitchener, A.C. & Buckley, M. 2019. Preserved collagen reveals species identity in archaeological marine turtle bones from Caribbean and Florida sites. *Royal Society Open Science* 6(10): 1–16.

Hatch K.A. 2012. The use and application of stable isotope analysis to the study of starvation, fasting, and nutritional stress in animals. In: McCue, M. (ed) *Comparative Physiology of Fasting, Starvation, and Food Limitation*: 337–364. Berlin: Springer.

Hatch, K.A., Crawford, M.A., Kunz, A.W., Thomsen, S.R., Eggett, D.L., Nelson, S.T. & Roeder, B.L. 2006. An objective means of diagnosing anorexia nervosa and bulimia nervosa using $^{15}N/^{14}N$ and $^{13}C/^{12}C$ ratios in hair. *Rapid Communications in Mass Spectrometry* 20(22): 3367–3373.

Hayes, J.M. 1993. Factors controlling ^{13}C contents of sedimentary organic compounds: principles and evidence. *Marine Geology* 113: 111–125.

Hayward, M.W., White, R.M., Mabandla, K.M. & Bukeye, P. 2005. Mammalian fauna of indigenous forest in the Transkei region of South Africa: an overdue survey. South African *Journal of Wildlife Research* 35(2): 117–124.

Heaton, T.H.E. 1986. Isotopic studies of nitrogen pollution in the hydrosphere and atmosphere: a review. *Chemical Geology: Isotope Geoscience Section* 59: 87–102.

Heaton, T.H.E. 1987. The $^{15}N/^{14}N$ ratios of plants in South Africa and Namibia: relationship to climate and coastal/saline environments. *Oecologia* 74: 236–246.

Heaton, T.H.E. 1999. Spatial, species, and temporal variations in the $^{13}C/^{12}C$ ratios of C_3 plants: implications for palaeodiet studies. *Journal of Archaeological Science* 26(6): 637–649.

Heaton, T.H.E., Talma, A.S. & Vogel, J.C. 1986b. Dissolved gas paleotemperatures and ^{18}O variations derived from groundwater near Uitenhage, South Africa. *Quaternary Research* 25(1): 79–88.

Heaton, T.H.E., Vogel, J.C., von La Chevallerie, G. & Collett, G. 1986a. Climatic influence on the isotopic composition of bone nitrogen. *Nature* 322: 822–823.

Hedges, R.E.M., Stevens, R.E. & Richards, M.P. 2004. Bone as a stable isotope archive for local climatic information. *Quaternary Science Reviews* 23(7–8): 959–965.

Heine, K. 1982. The main stages of the late Quaternary evolution of the Kalahari region, southern Africa. *Palaeoecology of Africa and the Surrounding Islands* 15: 53–76.

Hemming, S.R. 2004. Heinrich events: massive late Pleistocene detritus layers of the North Atlantic and their global climate imprint. *Reviews of Geophysics* 42(1): 1–43.

Hempson, G.P., Archibald, S. & Bond, W.J. 2015. A continent-wide assessment of the form and intensity of large mammal herbivory in Africa. *Science* 350(6264): 1056–1061.

Hendy, J. 2021. Ancient protein analysis in archaeology. *Science Advances* 7(3): 1–11.

Henriksen, K. & Karsdal, M.A. 2016. Type I collagen. In: Karsdal, M.A. (ed) *Biochemistry of Collagens, Laminins and Elastin*: *Structure, Function and Biomarkers*: 1–11. Amsterdam: Academic Press.

Hillier, M.L. & Bell, L.S. 2007. Differentiating human bone from animal bone: a review of histological methods. *Journal of Forensic Sciences* 52(2): 249–263.

Hjeljord, O. & Histøl, T. 1999. Range-body mass interactions of a northern ungulate: a test of hypothesis. *Oecologia* 119(3): 326–339.

Hoare, D.B. & Bredenkamp, G.J. 2001. Syntaxonomy and environmental gradients of the grasslands of the Stormberg/Drakensberg mountain region of the Eastern Cape, South Africa. *South African Journal of Botany* 67(4): 595–608.

Hobbie, E.A. & Högberg, P. 2012. Nitrogen isotopes link mycorrhizal fungi and plants to nitrogen dynamics. *New Phytologist* 196(2): 367–382.

Hobson, K.A. & Clark, R.G. 1992. Assessing avian diets using stable isotopes II: factors influencing diet-tissue fractionation. *The Condor* 94(1): 189–197.

Hobson, K.A., Alisauskas, R.T. & Clark, R.G. 1993. Stable-nitrogen isotope enrichment in avian tissues due to fasting and nutritional stress: implications for isotopic analyses of diet. *The Condor* 95(2): 388–394.

Hodgkins, J., Marean, C.W., Venter, J.A., Richardson, L., Roberts, P., Zech, J., Difford, M., Copeland, S.R., Orr, C.M., Keller, H.M. & Fahey, B.P. 2020. An isotopic test of the seasonal migration hypothesis for large grazing ungulates inhabiting the Palaeo-Agulhas Plain. *Quaternary Science Reviews* 235: 1–18.

Hoefs, J. 2004. *Stable Isotope Geochemistry*. Berlin: Springer.

Hofmann, R.R. 1989. Evolutionary steps of ecophysiological adaptation and diversification of ruminants: a comparative view of their digestive system. *Oecologia* 78(4): 443–457.

Hollemeyer, K., Altmeyer, W. & Heinzle, E. 2002. Identification and quantification of feathers, down, and hair of avian and mammalian origin using matrix-assisted laser desorption/ionization time-of-flight mass spectrometry. *Analytical Chemistry* 74(23): 5960–5968.

Hollmann, J.C. 2001. 'Big pictures': insights into southern African San rock paintings of ostriches. *The South African Archaeological Bulletin* 56(173–174): 62–75.

Hollmann, J.C. 2003. Indigenous knowledge and paintings of human-animal combinations: ostriches, swifts and religion in Bushman rock-art, Western Cape Province, South Africa. Unpublished PhD dissertation. Johannesburg: University of the Witwatersrand.

Holmes, K.M., Brown, K.A.R., Oates, W.P. & Collins, M.J. 2005. Assessing the distribution of African Palaeolithic sites: a predictive model of collagen degradation. *Journal of Archaeological Science* 32(2): 157–166.

Holmgren, K., Karlén, W. & Shaw, P.A. 1995. Paleoclimatic significance of the stable isotopic composition and petrology of a Late Pleistocene stalagmite from Botswana. *Quaternary Research* 43(3): 320–328.

Holmgren, K., Karlén, W., Lauritzen, S.E., Lee-Thorp, J.A., Partridge, T.C., Piketh, S., Repinski, P., Stevenson, C., Svanered, O. & Tyson, P.D. 1999. A 3000-year high-

resolution stalagmite based record of palaeoclimate for northeastern South Africa. *The Holocene* 9(3): 295–309.

Holmgren, K., Lee-Thorp, J.A., Cooper, G.R., Lundblad, K., Partridge, T.C., Scott, L., Sithaldeen, R., Talma, A.S. & Tyson, P.D. 2003. Persistent millennial-scale climatic variability over the past 25,000 years in Southern Africa. *Quaternary Science Reviews* 22: 2311–2326.

Holzkämper, S., Holmgren, K., Lee-Thorp, J., Talma, S., Mangini, A. & Partridge, T. 2009. Late Pleistocene stalagmite growth in Wolkberg cave, South Africa. *Earth and Planetary Science Letters* 282(1–4): 212–221.

Hopper, C., Sealy, J.C. & Dewar, G. 2018. Little Ice Age drought reconstructed from isotopic analysis of archaeological springbok (Antidorcas marsupialis) teeth. *Palaeogeography, Palaeoclimatology, Palaeoecology* 495: 105-112.

Horbańczuk, J.O., Cooper, R.G., Jóźwik, A., Klewiec, J., Krzyżewski, J., Malecki, I., Chyliński, W., Wójcik, A. & Kawka, M. 2003. Cholesterol content and fatty acid composition of fat from culled breeding ostriches (Struthio camelus). *Animal Science Papers and Reports* 21(4): 271–275.

Horsburgh, K.A. & Moreno-Mayar, J.V. 2015. Molecular identification of sheep at Blydefontein Rock Shelter, South Africa. *Southern African Humanities* 27(1): 65–80.

Horsburgh, K.A., Orton, J. & Klein, R.G. 2016. Beware the springbok in sheep's clothing: how secure are the faunal identifications upon which we build our models? *African Archaeological Review* 33(4): 353–361.

Horwitz, L.K. & Chazan, M. 2015. Past and present at Wonderwerk Cave (Northern Cape Province, South Africa). *African Archaeological Review* 32: 595–612.

Hungate, B.A., Stiling, P.D., Dijkstra, P., Johnson, D.W., Ketterer, M.E., Hymus, G.J., Hinkle, C.R. & Drake, B.G. 2004. CO_2 elicits long-term decline in nitrogen fixation. *Science* 304(5675): 1291–1291.

Irving, S.J.E. 1998. Late Quaternary Paleoenvironments at Vankervelsvlei, Near Knysna, South Africa. Unpublished MSc Thesis. Cape Town: University of Cape Town.

Jacobs, Z., Roberts, R.G., Galbraith, R.F., Deacon, H.J., Grün, R., Mackay, A., Mitchell, P.J., Vogelsang, R. & Wadley, L. 2008. Ages for the Middle Stone Age of southern Africa: implications for human behavior and dispersal. *Science* 322: 733–735.

Janz, L., Elston, R.G. & Burr, G.S. 2009. Dating North Asian surface assemblages with ostrich eggshell: implications for palaeoecology and extirpation. *Journal of Archaeological Science* 36(9): 1982–1989.

Janzen, A., Richter, K.K., Mwebi, O., Brown, S., Onduso, V., Gatwiri, F., Ndiema, E., Katongo, M., Goldstein, S.T., Douka, K. & Boivin, N. 2021. Distinguishing African bovids using Zooarchaeology by Mass Spectrometry (ZooMS): new peptide markers and insights into Iron Age economies in Zambia. *PloS ONE* 16(5): 1–36.

Johnson, B.J., Miller, G.H., Fogel, M.L. & Beaumont, P.B. 1997. The determination of late Quaternary paleoenvironments at Equus Cave, South Africa, using stable isotopes and amino acid racemization in ostrich eggshell. *Palaeogeography, Palaeoclimatology, Palaeoecology* 136(1–4): 121–137.

Johnson, T.C., Brown, E.T., McManus, J., Barry, S., Barker, P. & Gasse, F. 2002. A high-resolution paleoclimate record spanning the past 25,000 years in southern East Africa. *Science* 296(5565): 113–132.

Jones, A.M., O'Connell, T.C., Young, E.D., Scott, K., Buckingham, C.M., Iacumin, P. & Brasier, M.D. 2001. Biogeochemical data from well preserved 200 ka collagen and skeletal remains. *Earth and Planetary Science Letters* 193(1–2): 143–149.

Jones, P.D. & Mann, M.E. 2004. Climate over past millennia. *Reviews of Geophysics* 42(2): 1–42.

Jousse, H. & Escarguel, G. 2006. The use of Holocene bovid fossils to infer palaeoenvironment in Africa. *Quaternary Science Reviews* 25(7–8): 763–783.

Kahila Bar-Gal, G., Khalaily, H., Mader, O., Ducos, P. & Horwitz, L.K. 2002. Ancient DNA evidence for the transition from wild to domestic status in Neolithic goats: a case study from the site of Abu Gosh, Israel. *Ancient Biomolecules* 4(1): 9–17.

Kang'ethe, E.K. & Gathuma, J.M. 1987. Species identification of autoclaved meat samples using antisera to thermostable muscle antigens in an enzyme immunoassay. *Meat Science* 19(4): 265–270.

Katzenberg, M.A. 2008. Stable isotope analysis: a tool for studying past diet, demography, and life history. In: Katzenberg, M.A. & Saunders, S.R. (eds) *Biological Anthropology of the Human Skeleton*: 413–441. New Jersey: John Wiley & Sons Inc.

Kaye, T.G., Gaugler, G. & Sawlowicz, Z. 2008. Dinosaurian soft tissues interpreted as bacterial biofilms. *PloS ONE* 3(7): 1–7.

Keeling, R.F., Graven, H.D., Welp, L.R., Resplandy, L., Bi, J., Piper, S.C., Sun, Y., Bollenbacher, A. & Meijer, H.A. 2017. Atmospheric evidence for a global secular increase in carbon isotopic discrimination of land photosynthesis. *Proceedings of the National Academy of Sciences* 114(39): 10361–10366.

Kellner, C.M. & Schoeninger, M.J. 2007. A simple carbon isotope model for reconstructing prehistoric human diet. *American Journal of Physical Anthropology* 133(4): 1112–1127.

Kelly, J.F. 2000. Stable isotopes of carbon and nitrogen in the study of avian and mammalian trophic ecology. *Canadian Journal of Zoology* 78(1): 1–27.

Kempster, B., Zanette, L., Longstaffe, F.J., MacDougall-Shackleton, S.A., Wingfield, J.C. & Clinchy, M. 2007. Do stable isotopes reflect nutritional stress? Results from a laboratory experiment on song sparrows. *Oecologia* 151(3): 365–371.

Kendall, C., Eriksen, A.M.H., Kontopoulos, I., Collins, M.J. & Turner-Walker, G. 2018. Diagenesis of archaeological bone and tooth. *Palaeogeography, Palaeoclimatology, Palaeoecology* 491: 21–37.

Kirby, D.P., Buckley, M., Promise, E., Trauger, S.A. & Holdcraft, T.R. 2013. Identification of collagen-based materials in cultural heritage. *Analyst* 138(17): 4849–4858.

Kirby, D.P., Manick, A. & Newman, R. 2020. Minimally invasive sampling of surface coatings for protein identification by peptide mass fingerprinting: a case study with photographs. *Journal of the American Institute for Conservation* 59(3–4): 235–245.

Kistler, L., Ware, R., Smith, O., Collins, M. & Allaby, R.G. 2017. A new model for ancient DNA decay based on paleogenomic meta-analysis. *Nucleic Acids Research* 45(11): 6310–6320.

Kitching, J.W. & Raath, M.A. 1984. Fossils from the Elliot and Clarens Formations (Karoo Sequence) of the northeastern Cape, Orange Free State and Lesotho, and a suggested biozonation based on tetrapods. *Palaeontologica Africana* 25: 111–125.

Klein, R.G. & Cruz-Uribe, K. 1984. *The Analysis of Animal Bones from Archaeological Sites*. Chicago: University of Chicago Press.

Klein, R.G. & Cruz-Uribe, K. 1987. Large mammal and tortoise bones from Eland's Bay Cave and nearby sites, Western Cape Province, South Africa. *Papers in the Prehistory of the Western Cape, South Africa* 1: 132–163.

Klein, R.G. & Cruz-Uribe, K. 2016. Large mammal and tortoise bones from Elands Bay Cave (South Africa): implications for Later Stone Age environment and ecology. *Southern African Humanities* 29: 259–282.

Klein, R.G. 1972. The late Quaternary mammalian fauna of Nelson Bay Cave (Cape Province, South Africa): its implications for megafaunal extinctions and environmental and cultural change. *Quaternary Research* 2(2): 135–142.

Klein, R.G. 1974. Environment and subsistence of prehistoric man in the southern Cape Province, South Africa. *World Archaeology* 5(3): 249–284.

Klein, R.G. 1976. The mammalian fauna of the Klasies River mouth sites, southern Cape Province, South Africa. *The South African Archaeological Bulletin* 31: 75–98.

Klein, R.G. 1978. A preliminary report on the larger mammals from the Boomplaas Stone Age cave site, Cango Valley, Oudtshoorn District, South Africa. *The South African Archaeological Bulletin* 33(127): 66–75.

Klein, R.G. 1980. Environmental and ecological implications of large mammals from Upper Pleistocene and Holocene sites in southern Africa. *Annals of the South African Museum* 81(7): 223–283.

Klein, R.G. 1983. Palaeoenvironmental implications of Quaternary large mammals in the fynbos region. In: Deacon, H.J., Hendey, Q.B. & Lambrechts, J.J.N (eds) *Fynbos Palaeoecology: A Preliminary Synthesis*: 116–138. South African National Scientific Programmes Report No *75.* Pretoria: CSIR.

Klein, R.G. 1984. Mammalian extinctions and Stone Age people in Africa. In: Martin, P.S. & Klein, R.G. (eds) *Quaternary Extinctions: A Prehistoric Revolution* 553–573. Tucson: University of Arizona Press.

Klein, R.G. 1991. Size variation in the Cape dune molerat (*Bathyergus suillus*) and Late Quaternary climatic change in the southwestern Cape Province, South Africa. *Quaternary Research* 36(3): 243–256.

Klinken, G.J.V. 1991. Dating aand dietary reconstruction by isotopic analysis of amino acids in fossil bone collagen-with special reference to the caribbean. University of Groningen.

Koch, P.L. 2007. Isotopic study of the biology of modern and fossil vertebrates. In: Michener, R.H. & Lajtha, K. (eds) *Stable Isotopes in Ecology and Environmental Science*: 99–154. United States: Blackwell Publishing Ltd.

Kohn, M.J. 2010. Carbon isotope compositions of terrestrial C_3 plants as indicators of (paleo) ecology and (paleo) climate. *Proceedings of the National Academy of Sciences* 107(46): 19691–19695.

Kontopoulos, I., Penkman, K., Mullin, V.E., Winkelbach, L., Unterländer, M., Scheu, A., Kreutzer, S., Hansen, H.B., Margaryan, A., Teasdale, M.D. & Gehlen, B. 2020. Screening archaeological bone for palaeogenetic and palaeoproteomic studies. *PloS ONE* 15(6): 1–17.

Kreitler, C.W. 1975. *Determining the Source of Nitrate in Ground Water by Nitrogen Isotope Studies*. Texas: Bureau of Economic Geology.

Kristen, I., Fuhrmann, A., Thorpe, J., Rohl, U., Wilkes, H. & Oberhansli, H. 2007. Hydrological changes in southern Africa over the last 200 Ka as recorded in lake sediments from the Tswaing impact crater. *South African Journal of Geology* 110(2–3): 311–326.

Kristen, I., Wilkes, H., Vieth, A., Zink, K.G., Plessen, B., Thorpe, J., Partridge, T.C. & Oberhänsli, H. 2010. Biomarker and stable carbon isotope analyses of sedimentary organic matter from Lake Tswaing: evidence for deglacial wetness and early Holocene drought from South Africa. *Journal of Paleolimnology* 44(1) 143–160.

Kuitems, M., van Kolfschoten, T. & van der Plicht, J. 2015. Elevated $\delta^{15}N$ values in mammoths: a comparison with modern elephants. *Archaeological and Anthropological Sciences* 7(3): 289–295.

Kuper, J. 2015. Filling a gap: Early Holocene evidence from Central Libya. In: Kabacinski, J., Chlodnicki, M. & Kobusiewicz, M. (eds) *Hunter-gatherers and Early Food Producing Societies in Northeastern Africa*: 337–350. Poznan: Poznan Archaeological Museum.

Kutzbach, J.E. & Street-Perrott, F.A. 1985. Milankovitch forcing of fluctuations in the level of tropical lakes from 18 to 0 kyr BP. *Nature* 317(6033): 130–134.

Kutzbach, J.E. 1981. Monsoon climate of the early Holocene: climate experiment with the earth's orbital parameters for 9000 years ago. *Science* 214(4516): 59–61.

Kylander, M.E., Holm, M., Fitchett, J., Grab, S., Martinez Cortizas, A., Norström, E. & Bindler, R. 2021. Late glacial (17,060–13,400 cal yr BP) sedimentary and paleoenvironmental evolution of the Sekhokong Range (Drakensberg), southern Africa. *PloS ONE* 16(3): 1–29.

Langer, P. 1984. Anatomical and nutritional adaptation in wild herbivores. In: Gilchrist, F.M.C. & Mackie, P.I. (eds) *Herbivore Nutrition in the Subtropics and Tropics*: 185–203. South Africa: The Science Press.

Langer, P. 2002. The digestive tract and life history of small mammals. *Mammal Review* 32(2): 107–131.

Lario, J., Sanchez-Moral, S., Fernandez, V., Jimeno, A. & Menendez, M. 1997. Palaeoenvironmental evolution of the Blue Nile (Central Sudan) during the Early and Mid-Holocene (Mesolithic-Neolithic transition). *Quaternary Science Reviews* 16(6): 583–588.

Lawson, D. 1989. The food habits of suni antelopes (Neotragus moschatus) (Mammalia: Artiodactyla). *Journal of Zoology* 217(3): 441–448.

Le Meillour, L., Zazzo, A., Lesur, J., Cersoy, S., Marie, A., Lebon, M., Pleurdeau, D. & Zirah, S. 2018. Identification of degraded bone and tooth splinters from arid environments using palaeoproteomics. *Palaeogeography, Palaeoclimatology, Palaeoecology* 511: 472–482.

Le Meillour, L., Zirah, S., Zazzo, A., Cersoy, S., Détroit, F., Imalwa, E., Lebon, M., Nankela, A., Tombret, O., Pleurdeau, D. & Lesur, J. 2020. Palaeoproteomics gives new insight into early southern African pastoralism. *Scientific Reports* 10(1) 1–11.

Lebrasseur, O., Ryan, H. & Abbona, C. 2018. Bridging archaeology and genetics. In: Pişkin, E., Marciniak, A. & Bartkowiak, M. (eds) *Environmental Archaeology: Current Theoretical and Methodological Approaches*: 111–132. Cham: Springer.

Lee, R.B. 1972. !Kung spatial organization: an ecological and historical perspective. *Human Ecology* 1(2): 125–147.

Lee-Thorp, J. & van der Merwe, N.J. 1987. Carbon isotope analysis of fossil bone apatite. *South African Journal of Science* 83(11): 712–715.

Lee-Thorp, J.A. & Beaumont, P.B. 1995. Vegetation and seasonality shifts during the late Quaternary deduced from $^{13}C/^{12}C$ ratios of grazers at Equus Cave, South Africa. *Quaternary Research* 43(3): 426–432.

Lee-Thorp, J.A. & Ecker, M. 2015. Holocene environmental change at Wonderwerk Cave, South Africa: Insights from stable light isotopes in ostrich eggshell. *African Archaeological Review* 32(4): 793–811.

Lee-Thorp, J.A. & Sponheimer, M. 2006. Contribution of stable light isotopes to paleoenvironmental reconstruction. In: Henke, W. & Tattersall, I. (eds) *Handbook of Paleoanthropology*: 289–310. Verlag: Springer.

Lee-Thorp, J.A. & Talma, A.S. 2000. Stable light isotopes and environments in the southern African Quaternary and Late Pliocene. *Oxford Monographs on Geology and Geophysics* 40: 236–251.

Lee-Thorp, J.A. 1989. Stable carbon isotopes in deep time: the diets of fossil fauna and hominids. Unpublished PhD thesis. Cape Town: University of Cape Town.

Lee-Thorp, J.A. 2008. On isotopes and old bones. *Archaeometry* 50(6): 925–950.

Lee-Thorp, J.A., Holmgren, K., Lauritzen, S.E., Linge, H., Moberg, A., Partridge, T.C., Stevenson, C. & Tyson, P.D. 2001. Rapid climate shifts in the southern African interior throughout the mid to late Holocene. *Geophysical Research Letters* 28(23): 4507–4510.

Lee-Thorp, J.A., Sealy, J.C. & Van Der Merwe, N.J. 1989. Stable carbon isotope ratio differences between bone collagen and bone apatite, and their relationship to diet. *Journal of Archaeological Science* 16(6): 585–599.

Lee-Thorp, J.A., Sponheimer, M. & Luyt, J. 2007. Tracking changing environments using stable carbon isotopes in fossil tooth enamel: an example from the South African hominin sites. *Journal of Human Evolution* 53(5): 595–601.

LeFebvre, M.J. & Sharpe, A.E. 2018. Contemporary challenges in zooarchaeological specimen identification. In: Giovas, C.M. & LeFebvre, M.J. (eds) *Zooarchaeology in Practice*: 35–57. Cham: Springer.

Lehmann, D., Mfune, J.K.E., Gewers, E., Brain, C. & Voigt, C.C. 2015. Individual variation of isotopic niches in grazing and browsing desert ungulates. *Oecologia* 179(1): 75–88.

Lehmann, D., Mfune, J.K.E., Gewers, E., Cloete, J., Brain, C. & Voigt, C.C. 2013. Dietary plasticity of generalist and specialist ungulates in the Namibian desert: a stable isotopes approach. *PLoS ONE* 8(8): 1–10.

Leonard, J.A., Shanks, O., Hofreiter, M., Kreuz, E., Hodges, L., Ream, W., Wayne, R.K. & Fleischer, R.C. 2007. Animal DNA in PCR reagents plagues ancient DNA research. *Journal of Archaeological Science* 34(9): 1361–1366.

Lewis, C.A. & Illgner, P.M. 2001. Late Quaternary glaciation in southern Africa: moraine ridges and glacial deposits at Mount Enterprise in the Drakensberg of the Eastern Cape Province, South Africa. *Journal of Quaternary Science: Published for the Quaternary Research Association* 16(4): 365–374.

Lewis, C.A. 2008. Late Quaternary climatic changes, and associated human responses, during the last ~45 000yr in the Eastern and adjoining Western Cape, South Africa. *Earth-Science Reviews* 88(3–4): 167–187.

Lewis, C.A. 2011. Late Quaternary environmental phases in the Eastern Cape and adjacent Plettenberg Bay-Knysna region and Little Karoo, South Africa. *Proceedings of the Geologists' Association* 122(1): 187–200.

Librado, P., Gamba, C., Gaunitz, C., Der Sarkissian, C., Pruvost, M., Albrechtsen, A., Fages, A., Khan, N., Schubert, M., Jagannathan, V. & Serres-Armero, A. 2017. Ancient genomic changes associated with domestication of the horse. *Science* 356(6336): 442–445.

Lightfoot, E., Przelomska, N., Craven, M., O′ Connell, T.C., He, L., Hunt, H.V. & Jones, M.K. 2016. Intraspecific carbon and nitrogen isotopic variability in foxtail millet (Setaria italica). *Rapid Communications in Mass Spectrometry* 30(13): 1475–1487.

Lightfoot, E., Ustunkaya, M.C., Przelomska, N., O'Connell, T.C., Hunt, H.V., Jones, M.K. & Petrie, C.A. 2020. Carbon and nitrogen isotopic variability in foxtail millet (Setaria italica*)* with watering regime. *Rapid Communications in Mass Spectrometry* 34(6): 1–14.

Lindsay, W.L. 1979. *Chemical Equilibria in Soils*. New York: John Wiley and Sons Ltd.

Lister, A.M. 2013. The role of behaviour in adaptive morphological evolution of African proboscideans. *Nature* 500(7462): 331–334.

Livingstone, D.A. & Clayton, W.D. 1980. An altitudinal cline in tropical African grass floras and its paleoecological significance. *Quaternary Research* 13(3): 392–402.

Loftus, E., Pargeter, J., Mackay, A., Stewart, B.A. & Mitchell, P.J. 2019. Late Pleistocene human occupation in the Maloti-Drakensberg region of southern Africa: new radiocarbon dates from Rose Cottage Cave and inter-site comparisons. *Journal of Anthropological Archaeology* 56: 1–17.

Loftus, E., Roberts, P. & Lee-Thorp, J.A. 2016a. An isotopic generation: four decades of stable isotope analysis in African archaeology. *Azania: Archaeological Research in Africa* 51(1): 88–114.

Loftus, E., Sealy, J. & Lee-Thorp, J. 2016b. New Radiocarbon dates and Bayesian Models for Nelson Bay Cave and Byneskranskop 1: implications for the South African Later Stone Age sequence. *Radiocarbon* 58(2): 365–381.

Loftus, E., Stewart, B.A., Dewar, G. & Lee-Thorp, J. 2015. Stable isotope evidence of late MIS 3 to middle Holocene palaeoenvironments from Sehonghong Rockshelter, eastern Lesotho. *Journal of Quaternary Science* 30(8): 805–816.

Lombard, M., Wadley, L., Deacon, J., Wurz, S., Parsons, I., Mohapi, M., Swart, J. & Mitchell, P.J. 2012. South African and Lesotho stone age sequence updated. *The South African Archaeological Bulletin* 67: 123–144.

Longin, R. 1971. New method of collagen extraction for radiocarbon dating. *Nature* 230(5291): 241–242.

Lovegrove, B. 2003. *The Living Deserts of Southern Africa*. Cape Town: Fernwood Press.

Low, A.B. & Rebelo, A.G. 1996. *Vegetation of South Africa, Lesotho and Swaziland.* Pretoria: Department of Environmental Affairs and Tourism.

Low, C. 2009. Birds in the life of KhoeSan; with particular reference to healing and ostriches. *Alternation* 16(2): 64–90.

Low, C. 2011. Birds and KhoeSān: linking spirits and healing with day-to-day life. *Africa* 81(2): 295–313.

Lowe, K.M., Mentzer, S.M., Wallis, L.A. & Shulmeister, J. 2018. A multi-proxy study of anthropogenic sedimentation and human occupation of Gledswood Shelter 1: exploring an interior sandstone rockshelter in Northern Australia. *Archaeological and Anthropological Sciences* 10(2): 279–304.

Lowenstein, J.M., Reuther, J.D., Hood, D.G., Scheuenstuhl, G., Gerlach, S.C. & Ubelaker, D.H. 2006. Identification of animal species by protein radioimmunoassay of bone fragments and bloodstained stone tools. *Forensic Science International* 159(2–3): 182–188.

Lukich, V., Cowling, S. & Chazan, M. 2020. Palaeoenvironmental reconstruction of Kathu Pan, South Africa, based on sedimentological data. *Quaternary Science Reviews* 230: 1–18.

Luo, Y., Su, B.O., Currie, W.S., Dukes, J.S., Finzi, A., Hartwig, U., Hungate, B., McMurtrie, R.E., Oren, R.A.M., Parton, W.J. & Pataki, D.E. 2004. Progressive nitrogen

limitation of ecosystem responses to rising atmospheric carbon dioxide. *Bioscience* 54(8): 731–739.

Lutjeharms, J.R.E., Monteiro, P.M., Tyson, P.D. & Obura, D. 2001. The oceans around southern Africa and regional effects of global change: START Regional Syntheses. *South African Journal of Science* 97(3): 119–130.

Luyt, J. 2001. Revisiting the palaeoenvironments of the South African hominid-bearing Plio-Pleistocene sites: new isotopic evidence from Sterkfontein. Unpublished MSc dissertation. Cape Town: University of Cape Town.

Luyt, J. 2017. Stable light isotopes in fauna as environmental proxies in the Southern African winter and year-round rainfall zones. Unpublished PhD dissertation. Cape Town: University of Cape Town.

Luyt, J., Hare, V.J. & Sealy, J. 2019. The relationship of ungulate $\delta^{13}C$ and environment in the temperate biome of southern Africa, and its palaeoclimatic application. *Palaeogeography, Palaeoclimatology, Palaeoecology* 514: 282–291.

Lyman, R.L. 1994. *Vertebrate Taphonomy*. Cambridge: Cambridge University Press.

Lyman, R.L. 2010. Paleozoology's dependence on natural history collections. *Journal of Ethnobiology* 30(1): 126–136.

Lyman, R.L. 2017. Paleoenvironmental reconstruction from faunal remains: ecological basics and analytical assumptions. *Journal of Archaeological Research* 25(4): 315–371.

Mackay, A., Stewart, B.A. & Chase, B.M. 2014. Coalescence and fragmentation in the late Pleistocene archaeology of southernmost Africa. *Journal of Human Evolution* 72: 26–51.

Makarewicz, C.A. & Sealy, J. 2015. Dietary reconstruction, mobility, and the analysis of ancient skeletal tissues: expanding the prospects of stable isotope research in archaeology. *Journal of Archaeological Science* 56: 146–158.

Makarewicz, C.A. 2014. Winter pasturing practices and variable fodder provisioning detected in nitrogen ($\delta^{15}N$) and carbon ($\delta^{13}C$) isotopes in sheep dentinal collagen. *Journal of Archaeological Science* 41: 502–510.

Makarewicz, C.A. 2016. Toward an integrated isotope zooarchaeology. In: Grupe, G. & McGlynn, G.C. (eds) *Isotopic Landscapes in Bioarchaeology*: 189–209. Berlin: Springer.

Marean, C.W., Abe, Y., Nilssen, P.J. & Stone, E.C. 2001. Estimating the minimum number of skeletal elements (MNE) in zooarchaeology: a review and a new image-analysis GIS approach. *American Antiquity* 66(2): 333–348.

Marean, C.W., Rodrigo, M.D. & Pickering, T.R. 2004. Skeletal element equifinality in Zooarchaeology begins with method: the evolution and status of the" shaft critique". *Journal of Taphonomy* 2(1): 69–98.

Marino, B.D. & McElroy, M.B. 1991. Isotopic composition of atmospheric CO_2 inferred from carbon in C_4 plant cellulose. *Nature* 349(6305): 127–131.

Marshall, J.D., Brooks, J.R. & Lajtha, K. 2007. Sources of variation in the stable isotopic composition of plants. In: Michener, R. H. & Lajtha, K. (eds) *Stable Isotopes in Ecology and Environmental Science:* 22–60. United States: Blackwell Publishing Ltd.

Martin, A.R.H. 1968. Pollen analysis of Groenvlei lake sediments, Knysna (South Africa). *Review of Palaeobotany and Palynology* 7(2): 107–144.

Martínez, G.A., Mazzanti, D.L., Quintana, C., Zucol, A.F., de los Milagros Colobig, M., Hassan, G.S., Brea, M. & Passeggi, E. 2013. Geoarchaeological and Paleoenvironmental context of the human settlement in the Eastern Tandilia Range, Argentina. *Quaternary International* 299: 23–37.

Martisius, N.L., Welker, F., Dogandžić, T., Grote, M.N., Rendu, W., Sinet-Mathiot, V., Wilcke, A., Mcpherron, S.J., Soressi, M. & Steele, T.E. 2020. Non-destructive ZooMS identification reveals strategic bone tool raw material selection by Neandertals. *Scientific Reports* 10(1): 1–12.

Matisoo-Smith, E. 2018. Ancient DNA in zooarchaeology: new methods, new questions and settling old debates in Pacific commensal studies. In: Giovas, C.M. & LeFebvre, M.J. (eds) *Zooarchaeology in Practice*: 209–225. Cham: Springer.

Mayewski, P.A., Rohling, E.E., Stager, J.C., Karlén, W., Maasch, K.A., Meeker, L.D., Meyerson, E.A., Gasse, F., van Kreveld, S., Holmgren, K., Lee-Thorp, J., Rosqvist, G., Rack, F., Staubwasser, M., Schneider, R.R. & Steig, E.J. 2004. Holocene climate variability. *Quaternary Research* 62(3): 243–255.

McCarthy, T.S., Ellery, W.N., Backwell, L., Marren, P., De Klerk, B., Tooth, S., Brandt, D. & Woodborne, S. 2010. The character, origin and palaeoenvironmental significance of the Wonderkrater spring mound, South Africa. *Journal of African Earth Sciences* 58(1): 115–126.

McGrath, K., Rowsell, K., St-Pierre, C.G., Tedder, A., Foody, G., Roberts, C., Speller, C. & Collins, M. 2019. Identifying archaeological bone via non-destructive ZooMS and the materiality of symbolic expression: examples from Iroquoian bone points. *Scientific Reports* 9(1): 1–10.

McManus, J.F., Francois, R., Gherardi, J.M., Keigwin, L.D. & Brown-Leger, S. 2004. Collapse and rapid resumption of Atlantic meridional circulation linked to deglacial climate changes. N*ature* 428(6985): 834–837.

Meadows, M.E. & Baxter, A.J. 1999. Late Quaternary palaeoenvironments of the southwestern Cape, South Africa: a regional synthesis. *Quaternary International* 57: 193–206.

Meadows, M.E. & Baxter, A.J. 2001. Holocene vegetation history and palaeoenvironments at Klaarfontein Springs, Western Cape, South Africa. *The Holocene* 11(6): 699–706.

Meadows, M.E. 2014. Recent methodological advances in Quaternary palaeoecological proxies. *Progress in Physical Geography* 38(6): 807–817.

Meadows, M.E., Chase, B.M. & Seliane, M. 2010. Holocene palaeoenvironments of the Cederberg and Swartruggens mountains, Western Cape, South Africa: pollen and stable isotope evidence from hyrax dung middens. *Journal of Arid Environments* 74(7): 786–793.

Meignen, L., Goldberg, P. & Bar-Yosef, O. 2007. The hearths at Kebara Cave and their role in site formation processes. In: Bar-Yosef, O. & Meignen, L. (eds) *Kebara Cave, Mt Carmel, Israel, Part I: The Middle and Upper Paleolithic Archaeology*: 91–122. Cambridge: Peabody Museum Press.

Mekota, A., Grupe, G., Ufer, S. & Cuntz, U. 2006. Serial analysis of stable nitrogen and carbon isotopes in hair: monitoring starvation and recovery phases of patients suffering from anorexia nervosa. *Rapid Communications in Mass Spectrometry* 20(10): 1604–1610.

Merzoug, S. 2011. Faunal remains from Medjez II (Epipalaeolithic, Algeria): evidence of ostrich consumption and interpretation of Capsian subsistence behaviors. In: Jousse, H. & Lesur, J. (eds) *People and Animals in Holocene Africa: Recent Advances in Archaeozoology*: 123–131. Frankfurt: Africa Magna Verlag.

Metwally, A.A., Scott, L., Neumann, F.H., Bamford, M.K. & Oberhänsli, H. 2014. Holocene palynology and palaeoenvironments in the Savanna Biome at Tswaing Crater, central South Africa. *Palaeogeography, Palaeoclimatology, Palaeoecology* 402: 125–135.

Miller, J.M. 2019. Variability in ostrich eggshell beads from the Middle and Later Stone Age of Africa. Unpublished PhD dissertation. Alberta: University of Alberta.

Mills, S.C., Barrows, T.T., Telfer, M.W. & Fifield, L.K. 2017. The cold climate geomorphology of the Eastern Cape Drakensberg: a re-evaluation of past climatic conditions during the last glacial cycle in Southern Africa. *Geomorphology* 278: 184–194.

Mills, S.C., Grab, S.W. & Carr, S.J. 2009a. Recognition and palaeoclimatic implications of late Quaternary niche glaciation in eastern Lesotho. *Journal of Quaternary Science: Published for the Quaternary Research Association* 24(7): 647–663.

Mills, S.C., Grab, S.W. & Carr, S.J. 2009b. Late quaternary moraines along the Sekhokong range, eastern Lesotho: contrasting the geomorphic history of north-and south-facing slopes. *Geografiska Annaler: Series A, Physical Geography* 91(2): 121–140.

Mills, S.C., Grab, S.W., Rea, B.R., Carr, S.J. & Farrow, A. 2012. Shifting westerlies and precipitation patterns during the Late Pleistocene in southern Africa determined using glacier reconstruction and mass balance modelling. *Quaternary Science Reviews* 55: 145–159.

Minagawa, M. & Wada, E. 1984. Stepwise enrichment of ^{15}N along food chains: further evidence and the relation between $\delta^{15}N$ and animal age. *Geochimica et Cosmochimica Acta* 48(5): 1135–1140.

Mitchell, P.J. & Arthur, C. 2014. Ha Makotoko: Later Stone Age occupation across the Pleistocene/Holocene transition in western Lesotho. *Journal of African Archaeology* 12(2): 205–232.

Mitchell, P.J. & Steinberg, J.M. 1992. Ntloana Tšoana: a Middle Stone Age sequence from Western Lesotho. *The South African Archaeological Bulletin* 47: 26–33.

Mitchell, P.J. & Vogel, J.C. 1994. New radiocarbon dates from Sehonghong Rock Shelter, Lesotho. *South African Journal of Science* 90: 284–288.

Mitchell, P.J. 1990. Preliminary report on the Later Stone Age sequence from Tloutle Rock Shelter, Western Lesotho. *The South African Archaeological Bulletin* 45: 100–105.

Mitchell, P.J. 1993. The archaeology of Tloutle rock-shelter, Maseru District, Lesotho. *Research Reports of the National Museum (Bloemfontein)* 9: 77–132.

Mitchell, P.J. 1994. Understanding the MSA/LSA transition: the pre-20 000 BP assemblages from new excavations at Sehonghong Rockshelter, Lesotho. *Southern African Field Archaeology* 3: 15–25.

Mitchell, P.J. 1995. Revisiting the Robberg: new results and a revision of old ideas at Sehonghong Rock Shelter, Lesotho. *The South African Archaeological Bulletin* 50(161): 28–38.

Mitchell, P.J. 1996a. The late Quaternary of the Lesotho Highlands, southern Africa: Preliminary results and future potential of ongoing research at Sehonghong shelter. *Quaternary International* 33: 35–43.

Mitchell, P.J. 1996b. Filling a gap: the early and middle Holocene assemblages from new excavations at Sehonghong Rock Shelter, Lesotho. *Southern African Field Archaeology* 5: 17–27.

Mitchell, P.J. 1997. Holocene Later Stone Age hunter-gatherers south of the Limpopo River, c. 10,000–2000 BP. *Journal of World Prehistory* 11(4): 359–424.

Mitchell, P.J. 2002. *The Archaeology of Southern Africa*. Cambridge: Cambridge University Press.

Mitchell, P.J. 2008. Developing the archaeology of Marine Isotope Stage 3. *Goodwin Series* 10: 52–65.

Mitchell, P.J. 2013. Southern African hunter-gatherers of the last 25,000 years. In: Mitchell P.J. & Lane P.J. (eds) *The Oxford Handbook of African Archaeology*: 473–489. Oxford: Oxford University Press.

Monnin, E., Indermuhle, A., Dallenbach, A., Fluckiger, J., Stauffer, B., Stocker, T.F., Raynaud, D. & Barnola, J.M. 2001. Atmospheric CO_2 concentrations over the last glacial termination. *Science* 291(5501): 112–114.

Morley, M.W., Goldberg, P., Sutikna, T., Tocheri, M.W., Prinsloo, L.C., Saptomo, E.W., Wasisto, S. & Roberts, R.G. 2017. Initial micromorphological results from Liang Bua, Flores (Indonesia): Site formation processes and hominin activities at the type locality of Homo floresiensis. *Journal of Archaeological Science* 77: 125–142.

Mucina, L. & Rutherford, M.C. 2006. *The Vegetation of South Africa, Lesotho and Swaziland*. Pretoria: South African National Biodiversity Institute.

Murphy, B.P. & Bowman, D.M. 2006. Kangaroo metabolism does not cause the relationship between bone collagen $\delta^{15}N$ and water availability. *Functional Ecology* 20(6): 1062–1069.

Murphy, B.P. & Bowman, D.M. 2009. The carbon and nitrogen isotope composition of Australian grasses in relation to climate. *Functional Ecology* 23(6): 1040–1049.

Neumann, F.H., Botha, G.A. & Scott, L. 2014. 18,000 years of grassland evolution in the summer rainfall region of South Africa: evidence from Mahwaqa Mountain, KwaZulu-Natal. *Vegetation History and Archaeobotany* 23(6): 665–681.

Neumann, F.H., Scott, L., Bousman, C.B. & Van As, L. 2010. A Holocene sequence of vegetation change at Lake Eteza, coastal KwaZulu-Natal, South Africa. *Review of Palaeobotany and Palynology* 162(1): 39–53.

Neumann, F.H., Stager, J.C., Scott, L., Venter, H.J. & Weyhenmeyer, C. 2008. Holocene vegetation and climate records from lake Sibaya, KwaZulu-Natal (South Africa). *Review of Palaeobotany and Palynology* 152(3–4): 113–128.

Nicholson, S.E. 1986. The nature of rainfall variability in Africa south of the equator. *Journal of Climatology* 6(5): 515–530.

Nielsen-Marsh, C., Gernaey, A., Turner-Walker, G., Hedges, R., Pike, A. & Collins, M. 2000. The chemical degradation of bone. In: Cox, M. & Mays, S. (eds) *Human Osteology: In Archaeology and Forensic Science:* 439–454. Cambridge: Cambridge University Press.

Nielsen-Marsh, C.M. & Hedges, R.E. 2000. Patterns of diagenesis in bone I: the effects of site environments. *Journal of Archaeological Science* 27(12): 1139–1150.

Norström, E., Neumann, F.H., Scott, L., Smittenberg, R.H., Holmstrand, H., Lundqvist, S., Snowball, I., Sundqvist, H.S., Risberg, J. & Bamford, M. 2014. Late Quaternary vegetation dynamics and hydro-climate in the Drakensberg, South Africa. *Quaternary Science Reviews* 105: 48–65.

Norström, E., Scott, L., Partridge, T.C., Risberg, J. & Holmgren, K. 2009. Reconstruction of environmental and climate changes at Braamhoek wetland, eastern escarpment South Africa, during the last 16,000 years with emphasis on the Pleistocene–Holocene transition. *Palaeogeography, Palaeoclimatology, Palaeoecology* 271(3–4): 240–258.

Northup, D.E. & Lavoie, KH. 2001. Geomicrobiology of Caves: A Review. *Geomicrobiology Journal* 18: 199–222.

O’Connor, T. 2000. *The Archaeology of Animal Bones*. Stroud: Sutton Publishing Limited.

O’Sullivan, N.J., Teasdale, M.D., Mattiangeli, V., Maixner, F., Pinhasi, R., Bradley, D.G. & Zink, A. 2016. A whole mitochondria analysis of the Tyrolean Iceman’s leather provides insights into the animal sources of Copper Age clothing. *Scientific Reports* 6: 1–9.

O'Connell, T.C., Kneale, C.J., Tasevska, N. & Kuhnle, G.G. 2012. The diet-body offset in human nitrogen isotopic values: A controlled dietary study. *American Journal of Physical Anthropology* 149(3): 426–434.

O'Connor, T.G., Puttick, J.R. & Hoffman, M.T. 2014. Bush encroachment in southern Africa: changes and causes. *African Journal of Range & Forage Science* 31(2): 67–88.

Oelbermann, K. & Scheu, S. 2002. Stable isotope enrichment ($\delta^{15}N$ and $\delta^{13}C$) in a generalist predator (Pardosa lugubris, Araneae: Lycosidae): effects of prey quality. *Oecologia* 130(3): 337–344.

O'Leary, M.H. 1981. Carbon isotope fractionation in plants. *Phytochemistry* 20(4): 553–567.

O'Leary, M.H. 1988. Carbon isotopes in photosynthesis. *BioScience* 38(5): 328–336.

O'Leary, M.H. 1995. Environmental effects on carbon isotope fractionation in terrestrial plants. In: Wada, E., Yoneyama, T., Minagawa, M., Ando, T. & Fry, B.D. (eds) *Stable Isotopes in the Biosphere*: 78–91. Kyoto: Kyoto University Press.

Olff, H., Ritchie, M.E. & Prins, H.H. 2002. Global environmental controls of diversity in large herbivores. *Nature* 415(6874): 901–904.

Opperman, H. & Heydenrych, B. 1990. A 22000-year-old Middle Stone Age camp site with plant food remains from the north-eastern Cape. *The South African Archaeological Bulletin* 45(152): 93–99.

Opperman, H. 1982. Some research results of excavations in the Colwinton rock shelter, northeastern Cape. *The South African Archaeological Bulletin* 37: 51–66.

Opperman, H. 1984. A report on excavations at Grassridge Rock Shelter, Sterkstroom District, Cape Province. *Fort Hare Papers* 7: 391–406.

Opperman, H. 1987. *The Later Stone Age of the Drakensberg Range and its Foothills*. Oxford: British Archaeological Reports International Series 339.

Opperman, H. 1988. An excavation of a Middle Stone Age deposit in Grassridge Rockshelter, Sterkstroom District, Cape Province. *Fort Hare Papers* 9: 51–61.

Opperman, H. 1992. A report on the results of a test pit in Strathalan Cave B, Maclear district, north-eastern Cape. *Southern African Field Archaeology* 1(2): 98–102.

Opperman, H. 1996. Strathalan Cave B, north-eastern Cape Province, South Africa: evidence for human behaviour 29,000–26,000 years ago. *Quaternary International* 33: 45–53.

Orton, J., Klein, R.G., Mackay, A., Schwortz, S. & Steele, T.E. 2011. Two Holocene rock shelter deposits from the Knersvlakte, southern Namaqualand, South Africa. *Southern African Humanities* 23(1): 109–150.

Ostrom, P.H., Gandhi, H., Strahler, J.R., Walker, A.K., Andrews, P.C., Leykam, J., Stafford, T.W., Kelly, R.L., Walker, D.N., Buckley, M. & Humpula, J. 2006. Unravelling the sequence and structure of the protein osteocalcin from a 42 ka fossil horse. *Geochimica et Cosmochimica Acta* 70(8): 2034–2044.

Ostrom, P.H., Schall, M., Gandhi, H., Shen, T.L., Hauschka, P.V., Strahler, J.R. & Gage, D.A. 2000. New strategies for characterizing ancient proteins using matrix-assisted laser desorption ionization mass spectrometry. *Geochimica et Cosmochimica Acta* 64(6): 1043–1050.

Outram, A.K. 2001. A new approach to identifying bone marrow and grease exploitation: why the "indeterminate" fragments should not be ignored. *Journal of Archaeological Science* 28(4): 401–410.

Owen-Smith, N. 2008. The comparative population dynamics of browsing and grazing ungulates. In: Gordon, I.J. & Prins, H.H.T. (eds) *The Ecology of Browsing and Grazing*: 149–177. Berlin: Springer.

Owen-Smith, N., Le Roux, E. & Macandza, V. 2013. Are relatively rare antelope narrowly selective feeders? A sable antelope and zebra comparison. *Journal of Zoology* 291(3): 163–170.

Pargeter, J., Loftus, E. & Mitchell, P.J. 2017. New ages from Sehonghong Rockshelter: implications for the late Pleistocene occupation of highland Lesotho. *Journal of Archaeological Science: Reports* 12: 307–315.

Pargeter, J., Loftus, E., Mackay, A., Mitchell, P.J. & Stewart, B. 2018. New ages from Boomplaas Cave, South Africa, provide increased resolution on late/terminal Pleistocene human behavioural variability. *Azania: Archaeological Research in Africa* 53(2): 156–184.

Pargeter, J., MacKay, A., Mitchell, P., Shea, J. & Stewart, B.A. 2016. Primordialism and the 'Pleistocene San' of southern Africa. *Antiquity* 90(352): 1072–1079.

Parker, K.L., Barboza, P.S. & Stephenson, T.R. 2005. Protein conservation in female caribou (*Rangifer tarandus*): effects of decreasing diet quality during winter. *Journal of Mammalogy* 86(3): 610–622.

Parkington, J., Cartwright, C., Cowling, R.M, Baxter, A. & Meadows, M. 2000. Palaeovegetation at the last glacial maximum in the western Cape, South Africa: wood charcoal and pollen evidence from Elands Bay Cave. *South African Journal of Science* 96(11–12): 543–546.

Partridge, T.C., Avery, D.M., Botha, G.A., Brink, J.S., Deacon, J., Herbert, R.S., Aar, R.R., Scholtz, A., Scott, L., Talma, A.S. & Vogel, J.C. 1990. Late Pleistocene and Holocene climatic-change in Southern Africa. *South African Journal of Science* 86(7–10): 302–306.

Partridge, T.C., deMenocal, P.B., Lorentz, S.A., Paiker, M.J. & Vogel, J.C. 1997. Orbital forcing of climate over South Africa: a 200,000-year rainfall record from the Pretoria Saltpan. *Quaternary Science Reviews* 16(10): 1125–1133.

Passey, B.H., Robinson, T.F., Ayliffe, L.K., Cerling, T.E., Sponheimer, M., Dearing, M.D., Roeder, B.L. & Ehleringer, J.R. 2005. Carbon isotope fractionation between diet, breath CO_2, and bioapatite in different mammals. *Journal of Archaeological Science* 32(10): 1459–1470.

Pastor, J. 2006. The roles of large herbivores in ecosystem nutrient cycles. In: Kjell, D., Duncan, P., Bergstrom, R. & Pastor, J. (eds) *Large Herbivore Ecology, Ecosystem Dynamics and Conservation*: 289–325. Cambridge: Cambridge University Press.

Pate, F.D. & Anson, T.J. 2008. Stable nitrogen isotope values in arid-land kangaroos correlated with mean annual rainfall: potential as a palaeoclimatic indicator. *International Journal of Osteoarchaeology* 18(3): 317–326.

Pate, F.D. 1997. Bone collagen diagenesis at Roonka Flat, South Australia: implications for isotopic analysis. *Archaeology in Oceania* 32(2): 170–175.

Pedro, J.B., Bostock, H.C., Bitz, C.M., He, F., Vandergoes, M.J., Steig, E.J., Chase, B.M., Krause, C.E., Rasmussen, S.O., Markle, B.R. & Cortese, G. 2016. The spatial extent and dynamics of the Antarctic Cold Reversal. *Nature Geoscience* 9(1): 51–55.

Peisker, M. & Henderson, S.A. 1992. Carbon: terrestrial C_4 plants. *Plant, Cell & Environment* 15(9): 987–1004.

Pestle, W.J. & Colvard, M. 2012. Bone collagen preservation in the tropics: a case study from ancient Puerto Rico. *Journal of Archaeological Science* 39(7): 2079–2090.

Peters, C., Richter, K.K., Manne, T., Dortch, J., Paterson, A., Travouillon, K., Louys, J., Price, G.J., Petraglia, M., Crowther, A. & Boivin, N. 2021. Species identification of Australian marsupials using collagen fingerprinting. *Royal Society Open Science* 8(10): 1–18.

Peterson, B.J. & Fry, B. 1987. Stable isotopes in ecosystem studies. *Annual Review of Ecology and Systematics* 18(1): 293–320.

Pilaar Birch, S.E., Scheu, A., Buckley, M. & Çakırlar, C. 2019. Combined osteomorphological, isotopic, aDNA, and ZooMS analyses of sheep and goat remains from Neolithic Ulucak, Turkey. *Archaeological and Anthropological Sciences* 11(5): 1669–1681.

Plug, I. & Engela, R. 1992. The macrofaunal remains from recent excavations at Rose Cottage Cave, Orange Free State. *The South African Archaeological Bulletin* 47: 16–25.

Plug, I. & Mitchell, P.J. 2008. Fishing in the Lesotho highlands: 26,000 years of fish exploitation, with special reference to Sehonghong Shelter. *Journal of African Archaeology* 6(1): 33–55.

Plug, I. 1993. The macrofaunal and molluscan remains from Tloutle, a Later Stone Age site in Lesotho. *Southern African Field Archaeology* 2(1): 44–48.

Plug, I. 1997. Late Pleistocene and Holocene hunter–gatherers in the eastern highlands of South Africa and Lesotho: a faunal interpretation. *Journal of Archaeological Science* 24(8): 715–727.

Plummer, T.W. & Bishop, L.C. 1994. Hominid paleoecology at Olduvai Gorge, Tanzania as indicated by antelope remains. *Journal of Human Evolution* 27(1-3): 47–75.

Prendergast, M.E., Buckley, M., Crowther, A., Frantz, L., Eager, H., Lebrasseur, O., Hutterer, R., Hulme-Beaman, A., Van Neer, W., Douka, K. & Veall, M.A. 2017. Reconstructing Asian faunal introductions to eastern Africa from multi-proxy biomolecular and archaeological datasets. *PloS ONE* 12(8): 1–20.

Prendergast, M.E., Janzen, A., Buckley, M. & Grillo, K.M. 2019. Sorting the sheep from the goats in the Pastoral Neolithic: morphological and biomolecular approaches at Luxmanda, Tanzania. *Archaeological and Anthropological Sciences* 11(6): 3047–3062.

Presslee, S., Wilson, J., Woolley, J., Best, J., Russell, D., Radini, A., Fischer, R., Kessler, B., Boano, R., Collins, M. & Demarchi, B. 2018. The identification of archaeological eggshell using peptide markers. *STAR: Science & Technology of Archaeological Research* 3(1): 89–99.

Quick, L.J., Carr, A.S., Meadows, M.E., Boom, A., Bateman, M.D., Roberts, D.L., Reimer, P.J. & Chase, B.M. 2015. A late Pleistocene–Holocene multi-proxy record of palaeoenvironmental change from Still Bay, southern Cape Coast, South Africa. *Journal of Quaternary Science* 30(8): 870–885.

Quick, L.J., Chase, B.M., Meadows, M.E., Scott, L. & Reimer, P.J. 2011. A 19.5 kyr vegetation history from the central Cederberg Mountains, South Africa: palynological evidence from rock hyrax middens. *Palaeogeography, Palaeoclimatology, Palaeoecology* 309(3–4): 253–270.

Reidsma, F.H., Sifogeorgaki, I., Dinckal, A., Huisman, H., Sier, M.J., van Os, B. & Dusseldorp, G.L. 2021. Making the invisible stratigraphy visible: a grid-based, multi-proxy geoarchaeological study of Umhlatuzana Rockshelter, South Africa. *Frontiers in Earth Science* 9: 1–21.

Reitsema, L.J. 2013. Beyond diet reconstruction: stable isotope applications to human physiology, health, and nutrition. *American Journal of Human Biology* 25(4): 445–456.

Reitz, E.J. & Wing, E.S. 2008. *Zooarchaeology*. Cambridge: Cambridge University Press.

Reitz, E.J., Newsom, L.A., Scudder, S.J. & Scarry, C.M. 2012. Introduction to environmental archaeology. In: Reitz, E.J. & Shackley, M. (eds) *Manuals in Archaeological Method, Theory, and Technique*: 1–39. New York: Springer.

Richter, J. 1986. Experimental study of heat induced morphological changes in fish bone collagen. *Journal of Archaeological Science* 13(5): 477–481.

Richter, K.K., McGrath, K., Masson-MacLean, E., Hickinbotham, S., Tedder, A., Britton, K., Bottomley, Z., Dobney, K., Hulme-Beaman, A., Zona, M. & Fischer, R. 2020. What's the catch? Archaeological application of rapid collagen-based species identification for Pacific Salmon. *Journal of Archaeological Science* 116: 1–16.

Richter, K.K., Wilson, J., Jones, A.K., Buckley, M., van Doorn, N. & Collins, M.J. 2011. Fish ’n chips: ZooMS peptide mass fingerprinting in a 96 well plate format to identify fish bone fragments. *Journal of Archaeological Science* 38(7): 1502–1510.

Riding, R. 2000. Microbial carbonates: the geological record of calcified bacterial-algal mats and biofilms. *Sedimentology* 47(1): 179–214.

Robbins, C.T., Felicetti, L.A. & Florin, S.T. 2010. The impact of protein quality on stable nitrogen isotope ratio discrimination and assimilated diet estimation. *Oecologia* 162(3): 571–579.

Robbins, C.T., Felicetti, L.A. & Sponheimer, M. 2005. The effect of dietary protein quality on nitrogen isotope discrimination in mammals and birds. *Oecologia* 144(4): 534–540.

Roberts, P., Lee-Thorp, J.A., Mitchell, P.J. & Arthur, C. 2013. Stable carbon isotopic evidence for climate change across the late Pleistocene to early Holocene from Lesotho, southern Africa. *Journal of Quaternary Science* 28(4): 360–369.

Roberts, P., Prendergast, M.E., Janzen, A., Shipton, C., Blinkhorn, J., Zech, J., Crowther, A., Sawchuk, E.A., Stewart, M., Ndiema, E. & Petraglia, M. 2020. Late Pleistocene to Holocene human palaeoecology in the tropical environments of coastal eastern Africa. *Palaeogeography, Palaeoclimatology, Palaeoecology* 537: 1–18.

Robertshaw, P.T. 1984. Excavations at Fairview Rockshelter: a contribution to the prehistory of the Eastern Cape Province, South Africa. *Annals of the Cape Provincial Museums* 1(3): 55–92.

Robinson, J.R. & Wadley, L. 2018. Stable isotope evidence for (mostly) stable local environments during the South African Middle Stone Age from Sibudu, KwaZulu-Natal. *Journal of Archaeological Science* 100: 32–44.

Rossouw, L., Stynder, D.D. & Haarhof, P. 2009. Evidence for opal phytolith preservation in the Langebaanweg 'E'Quarry Varswater Formation and its potential for palaeohabitat reconstruction. *South African Journal of Science* 105(5–6): 223–227.

Rudakova, T.E. & Zaikov, G.E. 1987. Degradation of collagen and its possible applications in medicine. *Polymer Degradation and Stability* 18(4): 271–291.

Ryano, K.P., Wurz, S., van Niekerk, K.L. & Henshilwood, C.S. 2017. The technology of the early Oakhurst lithic techno-complex from Klipdrift Cave, Southern Cape, South Africa. *African Archaeological Review* 34(1): 93–119.

Rybczynski, N., Gosse, J.C., Harington, C.R., Wogelius, R.A., Hidy, A.J. & Buckley, M. 2013. Mid-Pliocene warm-period deposits in the High Arctic yield insight into camel evolution. *Nature Communications* 4(1): 1–9.

Sakalauskaite, J., Marin, F., Pergolizzi, B. & Demarchi, B. 2020. Shell palaeoproteomics: First application of peptide mass fingerprinting for the rapid identification of mollusc shells in archaeology. *Journal of Proteomics* 227: 1–10.

Sampson, C.G. 1968. *The Middle Stone Age Industries of the Orange River Scheme Area*. Bloemfontein, South Africa: National Museum.

Sampson, C.G. 1970. *The Smithfield Industrial Complex: Further Field Results*. Bloemfontein, South Africa: National Museum.

Sampson, C.G. 1972. *The Stone Age Industries of the Orange River Scheme and South Africa*. Bloemfontein, South Africa: National Museum.

Sampson, C.G. 1974. *The Stone Age Archaeology of Southern Africa*. New York: Academic Press.

San Antonio, J.D., Schweitzer, M.H., Jensen, S.T., Kalluri, R., Buckley, M. &Orgel, J.P. 2011. Dinosaur peptides suggest mechanisms of protein survival. *PloS ONE* 6(6): 1–7.

Sanborn, L.H., Reid, R.E., Bradley, A.S. & Liu, X. 2021. The effect of water availability on the carbon and nitrogen isotope composition of a C_4 plant (pearl millet, Pennisetum glaucum). *Journal of Archaeological Science: Reports* 38: 1–9.

Schefuß, E., Schouten, S., Jansen, J.F. & Damsté, J.S.S. 2003. African vegetation controlled by tropical sea surface temperatures in the mid-Pleistocene period. *Nature* 422(6930): 418–421.

Schleser, G.H. 1995. Parameters determining carbon isotope ratios in plants. In: Frenzel, B., Stauffer, B. & Weib, M. (eds*) Problems of Stable Isotopes in Tree-Rings, Lake Sediments and Peat-Bogs as Climatic Evidence for the Holocene:* 71–96. Stuttgart: Fischer Verlag.

Schoeninger, M.J. & DeNiro, M.J. 1984. Nitrogen and carbon isotopic composition of bone collagen from marine and terrestrial animals. *Geochimica et Cosmochimica acta* 48(4): 625–639.

Schoeninger, M.J. 1989. Reconstructing prehistoric human diet. In: Price, T.D. (ed) *The Chemistry of Prehistoric Human Bone*: 38–67. Cambridge: University Press Cambridge.

Schoeninger, M.J., DeNiro, M.J. & Tauber, H. 1983. Stable nitrogen isotope ratios of bone collagen reflect marine and terrestrial components of prehistoric human diet. *Science* 220(4604): 1381–1383.

Scholtz, A. 1986. Palynological and palaeobotanical studies in the Southern Cao. Unpublished MSc dissertation. Stellenbosch: University of Stellenbosch.

Schulze, E.D., Ellis, R., Schulze, W., Trimborn, P. & Ziegler, H. 1996. Diversity, metabolic types and $\delta^{13}C$ carbon isotope ratios in the grass flora of Namibia in relation to growth form, precipitation and habitat conditions. *Oecologia* 106(3): 352–369.

Schulze, E.D., Williams, R.J., Farquhar, G.D., Schulze, W., Langridge, J., Miller, J.M. & Walker, B.H. 1998. Carbon and nitrogen isotope discrimination and nitrogen nutrition of trees along a rainfall gradient in northern Australia. *Functional Plant Biology* 25(4): 413–425.

Schwarcz, H.P., Dupras, T.L. & Fairgrieve, S.I. 1999. ^{15}N enrichment in the Sahara: in search of a global relationship. *Journal of Archaeological Science* 26(6): 629–636.

Schweitzer, M.H., Zheng, W., Organ, C.L., Avci, R., Suo, Z., Freimark, L.M., Lebleu, V.S., Duncan, M.B., Vander Heiden, M.G., Neveu, J.M. & Lane, W.S. 2009. Biomolecular characterization and protein sequences of the Campanian hadrosaur B. canadensis. *Science* 324(5927): 626–631.

Scott, K. & Plug, I. 2016. Osteomorphology and osteometry versus aDNA in taxonomic identification of fragmentary sheep and sheep/goat bones from archaeological deposits: Blydefontein Shelter, Karoo, South Africa. *Southern African Humanities* 28: 61–79.

Scott, L. & Lee-Thorp, J.A. 2004. Holocene climatic trends and rhythms in southern Africa. In: Battarbee, R.W., Gasse, F & Stickley, C.E. (eds) *Past Climate Variability through Europe and Africa*: 69–91. Dordrecht: Springer.

Scott, L. & Nyakale, M. 2002. Pollen indications of Holocene palaeoenvironments at Florisbad spring in the central Free State, South Africa. *The Holocene* 12(4): 497–503.

Scott, L. & Thackeray, J.F. 1987. Multivariate analysis of late Pleistocene and Holocene pollen spectra from Wonderkrater, Transvaal, South Africa. *South African Journal of Science* 83(2): 93–97.

Scott, L. & Thackeray, J.F. 2015. Palynology of Holocene deposits in excavation 1 at Wonderwerk cave, northern Cape (South Africa). *African Archaeological Review* 32(4): 839–855.

Scott, L. & Woodborne, S. 2007a. Pollen analysis and dating of Late Quaternary faecal deposits (hyraceum) in the Cederberg, Western Cape, South Africa. *Review of Palaeobotany and Palynology* 144(3–4): 123–134.

Scott, L. & Woodborne, S. 2007b. Vegetation history inferred from pollen in Late Quaternary faecal deposits (hyraceum) in the Cape winter-rain region and its bearing on past climates in South Africa. *Quaternary Science Reviews* 26(7–8): 941–953.

Scott, L. 1976. Preliminary palynological results from the Alexandersfontein Basin near Kimberly. *Annals of the South African Museum* 71: 73–189.

Scott, L. 1982a. A late Quaternary pollen record from the Transvaal bushveld, South Africa. *Quaternary Research* 17(3): 339–370.

Scott, L. 1982b. Late Quaternary fossil pollen grains from the Transvaal, South Africa. *Review of Palaeobotany and Palynology* 36(3–4): 241–278.

Scott, L. 1986. Pollen analysis and palaeoenvironmental interpretation of late Quaternary sediment exposures in the eastern Orange Free State, South Africa. *Palaeoecology of Africa* 17: 113–170.

Scott, L. 1987. Late Quaternary forest history in Venda, southern Africa. *Review of Palaeobotany and Palynology* 53(1–2): 1–10.

Scott, L. 1989. Climatic conditions in southern Africa since the last glacial maximum, inferred from pollen analysis. *Palaeogeography, Palaeoclimatology, Palaeoecology* 70(4): 345–353.

Scott, L. 1993. Palynological evidence for late Quaternary warming episodes in Southern Africa. *Palaeogeography, Palaeoclimatology, Palaeoecology* 101(3–4): 229–235.

Scott, L. 1999a. Palynological analysis of the Pretoria Saltpan (Tswaing Crater) sediments and vegetation history in the bushveld savanna biome, South Africa. In: Partridge, T.C. (ed) *Tswaing, Investigations into the Origin, Age and Palaeoenvironments of the Pretoria Saltpan*: 143–166. Pretoria: Council of Geoscience.

Scott, L. 1999b. Vegetation history and climate in the Savanna biome South Africa since 190,000 ka: a comparison of pollen data from the Tswaing Crater (the Pretoria Saltpan) and Wonderkrater. *Quaternary International* 57: 215–223.

Scott, L. 2016. Fluctuations of vegetation and climate over the last 75 000 years in the Savanna Biome, South Africa: Tswaing Crater and Wonderkrater pollen sequences reviewed. *Quaternary Science Reviews* 145: 117–133.

Scott, L., Bousman, C.B. & Nyakale, M. 2005. Holocene pollen from swamp, cave and hyrax dung deposits at Blydefontein (Kikvorsberge), Karoo, South Africa. *Quaternary International* 129(1): 49–59.

Scott, L., Holmgren, K. & Partridge, T.C. 2008. Reconciliation of vegetation and climatic interpretations of pollen profiles and other regional records from the last 60 thousand years in the Savanna Biome of Southern Africa. *Palaeogeography, Palaeoclimatology, Palaeoecology* 257(1–2): 198–206.

Scott, L., Holmgren, K., Talma, A.S., Woodborne, S. & Vogel, J.C. 2003. Age interpretation of the Wonderkrater spring sediments and vegetation change in the Savanna Biome, Limpopo province, South Africa. *South African Journal of Science* 99(9–10): 484–488.

Scott, L., Marais, E. & Brook, G.A. 2004. Fossil hyrax dung and evidence of Late Pleistocene and Holocene vegetation types in the Namib Desert. *Journal of Quaternary Science: Published for the Quaternary Research Association* 19(8): 829–832.

Scott, L., Neumann, F.H., Brook, G.A., Bousman, C.B., Norström, E. & Metwally, A.A. 2012. Terrestrial fossil-pollen evidence of climate change during the last 26 thousand years in Southern Africa. *Quaternary Science Reviews* 32: 100–118.

Scott, L., Steenkamp, M. & Beaumont, P.B. 1995. Palaeoenvironmental conditions in South Africa at the Pleistocene-Holocene transition. *Quaternary Science Reviews* 14(9): 937–947.

Sealy, J.C., Johnson, M., Richards, M. & Nehlich, O. 2014. Comparison of two methods of extracting bone collagen for stable carbon and nitrogen isotope analysis: comparing whole bone demineralization with gelatinization and ultrafiltration. *Journal of Archaeological Science* 47: 64–69.

Sealy, J.C., Lee-Thorp, J.A., Loftus, E., Faith, J.T. & Marean, C.W. 2016. Late Quaternary environmental change in the Southern Cape, South Africa, from stable carbon and oxygen isotopes in faunal tooth enamel from Boomplaas Cave. *Journal of Quaternary Science* 31(8): 919–927.

Sealy, J.C., Naidoo, N., Hare, V.J., Brunton, S. & Faith, J.T. 2020. Climate and ecology of the palaeo-Agulhas Plain from stable carbon and oxygen isotopes in bovid tooth enamel from Nelson Bay Cave, South Africa. *Quaternary Science Reviews* 235: 1–14.

Sealy, J.C., van der Merwe, N.J., Lee-Thorp, J.A. & Lanham, J.L. 1987. Nitrogen isotopic ecology in southern Africa: implications for environmental and dietary tracing. *Geochimica et Cosmochimica Acta* 51(10): 2707–2717.

Sharp, Z. 2017. *Principles of Stable Isotope Geochemistry (2nd ed.)*. New Jersey: Pearson Prentice Hall.

Shoulders, M.D. & Raines, R.T. 2009. Collagen structure and stability. *Annual Review of Biochemistry* 78: 929–958.

Simon, M.H., Ziegler, M., Bosmans, J., Barker, S., Reason, C.J. & Hall, I.R. 2015. Eastern South African hydroclimate over the past 270,000 years. *Scientific Reports* 5(1): 1–10.

Sinclair, I., Hockey, P., Tarboton, W., Perrins, N., Rollinson, D. & Ryan, P. 2020. *Sasol Birds of Southern Africa*. South Africa: Penguin Random House.

Sinet-Mathiot, V., Smith, G.M., Romandini, M., Wilcke, A., Peresani, M., Hublin, J.J. & Welker, F. 2019. Combining ZooMS and zooarchaeology to study Late Pleistocene hominin behaviour at Fumane (Italy). *Scientific Reports* 9(1): 1–13.

Skinner, J.D. & Chimimba, C.T. 2005. *The Mammals of the Southern African Sub-region*. Cambridge: Cambridge University Press.

Smith, A.B. 2006. *Excavations at Kasteelberg and the Origins of the Khoekhoen in the Western Cape, South Africa*. Oxford: British Archaeological Reports International Series 1537.

Smith, B.N. & Epstein, S. 1971. Two categories of $^{13}C/^{12}C$ ratios for higher plants. *Plant Physiology* 47(3): 380–384.

Smith, B.N. 1972. Natural abundance of the stable isotopes of carbon in biological systems. *BioScience* 22(4): 226–231.

Smith, C.I., Chamberlain, A.T., Riley, M.S., Stringer, C. & Collins, M.J. 2003. The thermal history of human fossils and the likelihood of successful DNA amplification. *Journal of Human Evolution*: 45(3): 203–217.

Smith, J.M., Lee-Thorp, J.A. & Sealy, J.C. 2002. Stable carbon and oxygen isotopic evidence for late Pleistocene to middle Holocene climatic fluctuations in the interior of

southern Africa. *Journal of Quaternary Science: Published for the Quaternary Research Association* 17(7): 683–695.

Smith, R.M.H. 1990. A review of stratigraphy and sedimentary environments of the Karoo Basin of South Africa. *Journal of African Earth Sciences (and the Middle East)* 10(1–2): 117–137.

Solazzo, C., Heald, S., Ballard, M.W., Ashford, D.A., DePriest, P.T., Koestler, R.J. & Collins, M.J. 2011. Proteomics and coast Salish blankets: a tale of shaggy dogs? *Antiquity* 85: 1418–1432.

Soriano, S., Villa, P. & Wadley, L. 2007. Blade technology and tool forms in the Middle Stone Age of South Africa: the Howiesons Poort and post-Howiesons Poort at Rose Cottage Cave. *Journal of Archaeological Science* 34(5): 681–703.

Sponheimer, M. & Cerling, T.E. 2014. Investigating ancient diets using stable isotopes in bioapatites. In: Holland, H.D. & Turekian, K.K. (eds) *Treatise on Geochemistry*: 341–355. Amsterdam: Elsevier Ltd.

Sponheimer, M., Codron, D., Passey, B.H., de Ruiter, D.J., Cerling, T.E. & Lee-Thorp, J.A. 2009. Using carbon isotopes to track dietary change in modern, historical, and ancient primates. *American Journal of Physical Anthropology: The Official Publication of the American Association of Physical Anthropologists* 140(4): 661–670.

Sponheimer, M., Lee-Thorp, J.A., DeRuiter, D.J., Smith, J.M., Van Der Merwe, N.J., Reed, K., Grant, C.C., Ayliffe, L.K., Robinson, T.F., Heidelberger, C. & Marcus, W. 2003a. Diets of southern African Bovidae: stable isotope evidence. *Journal of Mammalogy* 84(2): 471–479.

Sponheimer, M., Robinson, T.F., Roeder, B.L., Passey, B.H., Ayliffe, L.K., Cerling, T.E., Dearing, M.D. & Ehleringer, J.R. 2003b. An experimental study of nitrogen flux in llamas: is ^{14}N preferentially excreted? *Journal of Archaeological Science* 30(12): 1649–1655.

Spriggs, A.C. & Dakora, F.D. 2009. Field assessment of symbiotic N_2 fixation in wild and cultivated Cyclopia species in the South African fynbos by ^{15}N natural abundance. *Tree Physiology* 29(2): 239–247.

Stager, J.C. & Mayewski, P.A. 1997. Abrupt early to mid-Holocene climatic transition registered at the equator and the poles. *Science* 276(5320): 1834–1836.

Stager, J.C., Cumming, B.F. & Meeker, L.D. 2003. A 10,000-year high-resolution diatom record from Pilkington Bay, Lake Victoria, East Africa. *Quaternary Research* 59(2): 172–181.

Stager, J.C., Mayewski, P.A., White, J., Chase, B.M., Neumann, F.H., Meadows, M.E., King, C.D. & Dixon, D.A. 2012. Precipitation variability in the winter rainfall zone of South Africa during the last 1400 yr linked to the austral westerlies. *Climate of the Past* 8(4): 877–887.

Stager, J.C., Ryves, D.B., King, C., Madson, J., Hazzard, M., Neumann, F.H. & Maud, R. 2013. Late Holocene precipitation variability in the summer rainfall region of South Africa. *Quaternary Science Reviews* 67: 105–120.

Steele, T.E. 2015. The contributions of animal bones from archaeological sites: the past and future of zooarchaeology. *Journal of Archaeological Science* 56: 168–176.

Steele, T.E., Mackay, A., Fitzsimmons, K.E., Igreja, M., Marwick, B., Orton, J., Schwortz, S. & Stahlschmidt, M.C. 2016. Varsche Rivier 003: a Middle and Later Stone Age site with Still Bay and Howiesons Poort assemblages in southern Namaqualand, South Africa. *PaleoAnthropology* 2016: 100–163.

Steig, E.J., Morse, D.L., Waddington, E.D., Stuiver, M., Grootes, P.M., Mayewski, P.A., Twickler, M.S. & Whitlow, S.I. 2000. Wisconsinan and Holocene climate history from an ice core at Taylor Dome, western Ross Embayment, Antarctica. *Geografiska Annaler: Series A, Physical Geography* 82(2–3): 213–235.

Stewart, B.A. & Mitchell, P.J. 2018. Late Quaternary palaeoclimates and human-environment dynamics of the Maloti-Drakensberg region, southern Africa. *Quaternary Science Reviews* 196: 1–20.

Stewart, B.A., Dewar, G.I., Morley, M.W., Inglis, R.H., Wheeler, M., Jacobs, Z. & Roberts, R.G. 2012. Afromontane foragers of the Late Pleistocene: site formation, chronology and occupational pulsing at Melikane Rockshelter, Lesotho. *Quaternary International* 270: 40–60.

Stewart, B.A., Parker, A.G., Dewar, G.I., Morley, M.W. & Allott, L.F. 2016. Follow the Senqu: Maloti-Drakensberg paleoenvironments and implications for early human dispersals into mountain systems. In: Jones, S.C. & Stewart, B.A. (eds) *Africa from MIS 6–2: Population Dynamics and Paleoenvironments*: 247–271. Dordrecht: Springer.

Stewart, B.A., Zhao, Y., Mitchell, P.J., Dewar, G., Gleason, J.D. & Blum, J.D. 2020. Ostrich eggshell bead strontium isotopes reveal persistent macroscale social networking across late Quaternary southern Africa. *Proceedings of the National Academy of Sciences* 117(12): 6453–6462.

Stewart, G.R., Turnbull, M.H., Schmidt, S. & Erskine, P.D. 1995. ^{13}C natural abundance in plant communities along a rainfall gradient: a biological integrator of water availability. *Functional Plant Biology* 22(1): 51–55.

Stewart, J.R., Allen, R.B., Jones, A.K., Penkman, K.E. & Collins, M.J. 2013. ZooMS: making eggshell visible in the archaeological record. *Journal of Archaeological Science* 40(4): 1797–1804.

Still, C.J., Berry, J.A., Collatz, G.J. & DeFries, R.S. 2003. Global distribution of C_3 and C_4 vegetation: carbon cycle implications. *Global Biogeochemical Cycles* 17(1): 1–14.

Stiner, M.C., Kuhn, S.L., Weiner, S. & Bar-Yosef, O. 1995. Differential burning, recrystallization, and fragmentation of archaeological bone. *Journal of Archaeological Science* 22(2): 223–237.

Stokes, S., Thomas, D.S. & Washington, R. 1997. Multiple episodes of aridity in southern Africa since the last interglacial period. *Nature* 388(6638): 154–158.

Stone, A.E.C. 2014. Last Glacial Maximum conditions in southern Africa: are we any closer to understanding the climate of this time period? *Progress in Physical Geography* 38(5): 519–542.

Stowe, M.J. & Sealy, J. 2016. Terminal Pleistocene and Holocene dynamics of southern Africa's winter rainfall zone based on carbon and oxygen isotope analysis of bovid tooth enamel from Elands Bay Cave. *Quaternary International* 404: 57–67.

Strachan, K.L., Finch, J.M., Hill, T. & Barnett, R.L. 2014. A late Holocene sea-level curve for the east coast of South Africa. *South African Journal of Science* 110(1–2): 1–9.

Strachan, K.L., Finch, J.M., Hill, T.R., Barnett, R.L., Morris, C.D. & Frenzel, P. 2016. Environmental controls on the distribution of salt-marsh foraminifera from the southern coastline of South Africa. *Journal of Biogeography* 43(5): 887–898.

Strachan, K.L., Hill, T.R., Finch, J.M. & Barnett, R.L. 2015. Vertical zonation of foraminifera assemblages in Galpins salt marsh, South Africa. *The Journal of Foraminiferal Research* 45(1): 29–41.

Stratford, D., Braun, K. & Morrissey, P. 2021. Cave and rock shelter sediments of southern Africa: a review of the chronostratigraphic and palaeoenvironmental record from Marine Isotope Stage 6 to 1. *South African Journal of Geology 2021* 124(4): 879–914.

Strauss, T. 2015. Cape Mountain zebra (Equus zebra zebra) habitat use and diet in the Bontebok National Park, South Africa. Unpublished PhD thesis. Port Elizabeth: Nelson Mandela Metropolitan University.

Street-Perrott, A.F. & Perrott, R.A. 1993. Holocene vegetation, lake levels, and climate of Africa. In: Wright, H.E., Kutzbach, J.E., Webb, T., Ruddiman, W.E., Street, F.A. & Bartlein, P.J. (eds) *Global Climates since the Last Glacial Maximum* 318–356. Minneapolis: University of Minnesota Press.

Stuut, J.B.W., Crosta, X., van der Borg, K. & Schneider, R. 2004. Relationship between Antarctic sea ice and southwest African climate during the late Quaternary. *Geology* 32(10): 909–912.

Sulzman, E.W. 2007. Stable isotope chemistry and measurement: a primer. In: Michener, R. H. & Lajtha, K. (eds) *Stable Isotopes in Ecology and Environmental Science*: 1–21. United States: Blackwell Publishing Ltd.

Sundqvist, H.S., Holmgren, K., Fohlmeister, J., Zhang, Q., Matthews, M.B., Spötl, C. & Körnich, H. 2013. Evidence of a large cooling between 1690 and 1740 AD in southern Africa. *Scientific Reports 3*: 1–6.

Swap, R.J., Aranibar, J.N., Dowty, P.R., Gilhooly III, W.P. & Macko, S.A. 2004. Natural abundance of ^{13}C and ^{15}N in C_3 and C_4 vegetation of southern Africa: patterns and implications. *Global Change Biology* 10(3): 350–358.

Szpak, P. 2014. Complexities of nitrogen isotope biogeochemistry in plant-soil systems: implications for the study of ancient agricultural and animal management practices. *Frontiers in Plant Science* 5: 1–19.

Szpak, P., Orchard, T.J., McKechnie, I. & Gröcke, D.R. 2012. Historical ecology of late Holocene sea otters (*Enhydra lutris*) from northern British Columbia: isotopic and zooarchaeological perspectives. *Journal of Archaeological Science* 39(5): 1553–1571.

Szpak, P., White, C.D., Longstaffe, F.J., Millaire, J.F. & Sánchez, V.F.V. 2013. Carbon and nitrogen isotopic survey of northern Peruvian plants: baselines for paleodietary and paleoecological studies. *PloS ONE* 8(1): 1–28.

Talbot, M.R., Filippi, M.L., Jensen, N.B. & Tiercelin, J.J. 2007. An abrupt change in the African monsoon at the end of the Younger Dryas. *Geochemistry, Geophysics, Geosystems* 8(3): 1–16.

Talma, A.S. & Vogel, J.C. 1992. Late Quaternary paleotemperatures derived from a speleothem from Cango caves, Cape province, South Africa. *Quaternary Research* 37(2): 203–213.

Taylor, R.E., Hare, P.E. & White, T.D. 1995. Geochemical criteria for thermal alteration of bone. *Journal of Archaeological Science* 22(1): 115–119.

Termine, J.D. 1993. Bone matrix proteins and the mineralisation process. In: Christakos, S. & Favus, M.J. (eds) *Primer on the Metabolic Bone Diseases and Disorders of Mineral Metabolism*: 21–25. New York: Raven Press.

Thackeray, J.F. & Fitchett, J.M. 2016. Rainfall seasonality captured in micromammalian fauna in Late Quaternary contexts, South Africa. *Palaeontologica Africana* 51: 1–9.

Thackeray, J.F. & Lee-Thorp, J.A. 1992. Isotopic analysis of equid teeth from Wonderwerk Cave, northern Cape Province, South Africa. *Palaeogeography, Palaeoclimatology, Palaeoecology* 99(1–2): 141–150.

Thackeray, J.F. & Scott, L. 2006. The Younger Dryas in the Wonderkrater sequence, South Africa? *Annals of the Transvaal Museum* 43: 111–112.

Thackeray, J.F. 1980. New approaches in interpreting archaeological faunal assemblages with examples from southern Africa. South African. *Journal of Science* 76(5): 216–223.

Thackeray, J.F. 1983. Disguises, animal behaviour and concepts of control in relation to rock art of southern Africa. *Goodwin Series* 4: 38–43.

Thackeray, J.F. 1984. Man, animals and extinctions: the analysis of Holocene faunal remains from Wonderwerk Cave, South Africa. Unpublished PhD thesis. New Haven: Yale University.

Thackeray, J.F. 1987. Late Quaternary environmental changes inferred from small mammalian fauna, southern Africa. *Climatic Change* 10(3): 285–305.

Thackeray, J.F. 1990. Temperature indices from late Quaternary sequences in South Africa: comparisons with the Vostok core. *South African Geographical Journal* 72(2): 47–49.

Thackeray, J.F. 2015. Faunal remains from Holocene deposits, excavation 1, Wonderwerk cave, South Africa. *African Archaeological Review* 32(4): 729–750.

Thackeray, J.F. 2018. A temperature index in a Late Quaternary sequence at Wonderkrater, South Africa. *South African Journal of Science* 114(5–6): 1–2.

Thackeray, J.F., Scott, L. & Pieterse, P. 2019. The Younger Dryas interval at Wonderkrater (South Africa) in the context of a platinum anomaly. *Palaeontologia Africana* 54: 30–35.

Thomas, R. & Miller, H. 2018. Zooarchaeology and stable isotopes. In: Lopez Varela, S.L. (ed) *The Encyclopedia of Archaeological Sciences*: 1–6. New Jersey: John Wiley and Sons Inc.

Thompson, L.G., Mosley-Thompson, E., Davis, M.E., Henderson, K.A., Brecher, H.H., Zagorodnov, V.S., Mashiotta, T.A., Lin, P.N., Mikhalenko, V.N., Hardy, D.R. & Beer, J. 2002. Kilimanjaro ice core records: evidence of Holocene climate change in tropical Africa. *Science* 298(5593): 589–593.

Thompson, L.G., Mosley-Thompson, E., Davis, M.E., Lin, P.N., Henderson, K.A., Cole-Dai, J., Bolzan, J.F. & Liu, K.B. 1995. Late glacial stage and Holocene tropical ice core records from Huascaran, Peru. *Science* 269(5220): 46–50.

Tieszen, L.L. 1991. Natural variations in the carbon isotope values of plants: implications for archaeology, ecology, and paleoecology. *Journal of Archaeological Science* 18(3): 227–248.

Tieszen, L.L., Boutton, T.W., Tesdahl, K.G. & Slade, N.A. 1983. Fractionation and turnover of stable carbon isotopes in animal tissues: implications for $\delta^{13}C$ analysis of diet. *Oecologia* 57(1–2): 32–37.

Tieszen, L.L., Hein, D., Qvortrup, S.A., Troughton, J.H. & Imbamba, S.K. 1979b. Use of $\delta^{13}C$ values to determine vegetation selectivity in East African herbivores. *Oecologia* 37(3): 351–359.

Tieszen, L.L., Senyimba, M.M., Imbamba, S.K. & Troughton, J.H. 1979a. The distribution of C_3 and C_4 grasses and carbon isotope discrimination along an altitudinal and moisture gradient in Kenya. *Oecologia* 37(3): 337–350.

Toffolo, M.B., Brink, J.S., van Huyssteen, C. & Berna, F. 2017. A microstratigraphic re-evaluation of the Florisbad spring site, Free State Province, South Africa: formation processes and paleoenvironment. *Geoarchaeology* 32(4): 456–478.

Trollope, W.S.W., Trollope, L.A. & Hartnett, D.C. 2002. Fire behaviour a key factor in the fire ecology of African grasslands and savannas. In: Viegas, D.X (ed) *Forest Fire Research and Wildland Fire Safety*: 1–15. Rotterdam: Millpress.

Truc, L., Chevalier, M., Favier, C., Cheddadi, R., Meadows, M.E., Scott, L., Carr, A.S., Smith, G.F. & Chase, B.M. 2013. Quantification of climate change for the last 20,000 years from Wonderkrater, South Africa: implications for the long-term dynamics of the Intertropical Convergence Zone. *Palaeogeography, Palaeoclimatology, Palaeoecology* 386: 575–587.

Trueman, C.N., Behrensmeyer, A.K., Tuross, N. & Weiner, S. 2004. Mineralogical and compositional changes in bones exposed on soil surfaces in Amboseli National Park, Kenya: diagenetic mechanisms and the role of sediment pore fluids. *Journal of Archaeological Science* 31(6): 721–739.

Turner-Walker, G. 2008. The chemical and microbial degradation of bones and teeth. In: Pinhasi, R. & Mays, S. (eds) *Advances in Human Palaeopathology*: 3–29. England: John Wiley & Sons Ltd.

Tusenius, M.L. 1989. Charcoal analytical studies in the north-eastern Cape, South Africa. *Goodwin Series* 6: 77–83.

Tyson, P.D. & Preston-Whyte, R.A. 2000. *Weather and Climate of Southern Africa*. Cape Town: Oxford University Press.

Tyson, P.D. 1986. *Climatic Change and Variability in Southern Africa*. Cape Town: Oxford University Press.

Valsecchi, V., Chase, B.M., Slingsby, J.A., Carr, A.S., Quick, L.J., Meadows, M.E., Cheddadi, R. & Reimer, P.J. 2013. A high resolution 15,600-year pollen and microcharcoal record from the Cederberg Mountains, South Africa. *Palaeogeography, Palaeoclimatology, Palaeoecology* 387: 6–16.

Van der Merwe, N.J. & Medina, E. 1991. The canopy effect, carbon isotope ratios and foodwebs in Amazonia. *Journal of Archaeological Science* 18(3): 249–259.

Van der Merwe, N.J. & Vogel, J.C. 1978. ^{13}C content of human collagen as a measure of prehistoric diet in Woodland North America. *Nature* 276(5690): 815–816.

Van der Merwe, N.J. & Vogel, J.C. 1983. Recent carbon isotope research and its implications for African archaeology. *African Archaeological Review* 1(1): 33–56.

Van der Merwe, N.J. 1982. Carbon isotopes, photosynthesis, and archaeology: different pathways of photosynthesis cause characteristic changes in carbon isotope ratios that make possible the study of prehistoric human diets. *American Scientist* 70(6): 596–606.

Van der Sluis, L.G., Hollund, H.I., Buckley, M., De Louw, P.G., Rijsdijk, K.F. & Kars, H. 2014. Combining histology, stable isotope analysis and ZooMS collagen fingerprinting to investigate the taphonomic history and dietary behaviour of extinct giant tortoises from the Mare aux Songes deposit on Mauritius. *Palaeogeography, Palaeoclimatology, Palaeoecology* 416: 80–91.

Van Doorn, N.L., Hollund, H. & Collins, M.J. 2011. A novel and non-destructive approach for ZooMS analysis: ammonium bicarbonate buffer extraction. *Archaeological and Anthropological Sciences* 3(3): 281–289.

Van Zinderen Bakker, E.M. & Coetzee, J.A. 1988. A review of Late Quaternary pollen studies in East, Central and Southern Africa. *Review of Palaeobotany and Palynology* 55(1–3): 155–174.

Van Zinderen Bakker, E.M. 1962. Botanical evidence for quaternary climates in Africa. *Annals of the Cape Provincial Museums* 2: 16–31.

Van Zinderen Bakker, E.M. 1967. Upper Pleistocene and Holocene stratigraphy and ecology on the basis of vegetation changes in sub-Saharan Africa. In: Bishop, W.W. & Clark, J.D. (eds) *Background to Evolution in Africa*: 125–147. Chicago: University of Chicago Press.

Van Zinderen Bakker, E.M. 1976. The evolution of late Quaternary palaeoclimates of southern Africa. *Palaeoecology of Africa* 9: 160–202.

Varela, J.L., Ortega, A., la Gándara, F. & Medina, A. 2015. Effects of starvation on $\delta^{15}N$ and $\delta^{13}C$ in Atlantic bonito, Sarda sarda (Bloch, 1793). *Aquaculture Research* 8(46): 2043–2047.

Venter, J.A. & Kalule-Sabiti, M.J. 2016. Diet composition of the large herbivores in Mkambati nature reserve, eastern cape, South Africa. *African Journal of Wildlife Research* 46(1): 49–56.

Venter, J.A., Brooke, C.F., Marean, C.W., Fritz, H. & Helm, C.W. 2020. Large mammals of the Palaeo-Agulhas Plain showed resilience to extreme climate change but vulnerability to modern human impacts. *Quaternary Science Reviews* 235: 1–13.

Vermeulen, M.M. 2018. Exploring feeding ecology and population growth rate responses of ungulates in southern African arid biomes. Unpublished PhD thesis. Port Elizabeth: Nelson Mandela Metropolitan University.

Villa, P., Soriano, S., Tsanova, T., Degano, I., Higham, T.F., d'Errico, F., Backwell, L., Lucejko, J.J., Colombini, M.P. & Beaumont, P.B. 2012. Border Cave and the beginning of the Later Stone Age in South Africa. *Proceedings of the National Academy of Sciences* 109(33): 13208–13213.

Virginia, R.A. & Delwiche, C.C. 1982. Natural ^{15}N abundance of presumed N_2-fixing and non-N_2-fixing plants from selected ecosystems. *Oecologia* 54(3): 317–325.

Vogel, J.C. & van der Merwe, N.J. 1977. Isotopic evidence for early maize cultivation in New York State. *American Antiquity* 42(2): 238–242.

Vogel, J.C. 1978. Isotopic assessment of the dietary habits of ungulates. *South African Journal of Science* 74(8): 298–301.

Vogel, J.C. 1983. Isotopic evidence for the past climates and vegetation of southern Africa. *Bothalia* 14(3–4): 391–394.

Vogel, J.C., Fuls, A. & Ellis, R.P. 1978. The geographical distribution of Kranz-grasses in South Africa. *South African Journal of Science* 74: 209–219.

Voigt, E.A. 1982. The molluscan fauna. In: Singer, R. & Wymer, J. (eds) *The Middle Stone Age at Klasies River Mouth in South Africa:* 155–186. Chicago: Chicago University Press.

Von Holstein, I.C., Ashby, S.P., van Doorn, N.L., Sachs, S.M., Buckley, M., Meiri, M., Barnes, I., Brundle, A. & Collins, M.J. 2014. Searching for Scandinavians in pre-Viking Scotland: molecular fingerprinting of Early Medieval combs. *Journal of Archaeological Science* 41: 1–6.

Vrba, E.S. 1980. The significance of bovid remains as indicators of environment and predation patterns. In: Behrensmeyer, A.K. & Hill, A.P. (eds) *Fossils in the Making: Vertebrate Taphonomy and Paleoecology:* 247–271. Chicago: University of Chicago Press.

Vrba, E.S. 1985. Environment and evolution: alternative causes of the temporal distribution of evolutionary events. *South African Journal of Science* 81(5): 229–236.

Vrba, E.S. 1995. The fossil record of African antelopes (Mammalia, Bovidae) in relation to human evolution and paleoclimate. In: Vrba, E.S., Denton, G.H., Partridge, T.C. &

Burckle, L.H. (eds) *Paleoclimate and Evolution, with Emphasis on Human Origins*: 385–424. New Haven: Yale University Press.

Wadley, L. 1993. The Pleistocene Later Stone Age south of the Limpopo River. *Journal of World Prehistory* 7(3): 243–296.

Wadley, L. 1995. Review of dated Stone Age sites recently excavated in the eastern Free State, South Africa. *South African Journal of Science* 91(11–12): 574–579.

Wadley, L. 1996. The Robberg Industry of Rose Cottage Cave, eastern Free State: the technology, spatial patterns and environment. *The South African Archaeological Bulletin* 51(164): 64–74.

Wadley, L. 1997. Rose Cottage Cave: archaeological work 1987 to 1997. *South African Journal of Science* 93: 439–444.

Wadley, L. 2000a. The Early Holocene layers of Rose Cottage Cave, eastern Free State: technology, spatial patterns and environment. *The South African Archaeological Bulletin* 55: 18–31.

Wadley, L. 2000b. The Wilton and pre-ceramic post-classic Wilton industries at Rose Cottage Cave and their context in the South African sequence. *The South African Archaeological Bulletin* 55: 90–106.

Wadley, L. 2004. Late Middle Stone Age spatial patterns in Rose Cottage Cave, South Africa. In: Conard, N.J. (ed) *Settlement Dynamics of the Middle Paleolithic and Middle Stone Age II*: 23–36. Tübingen: Kerns Verlag.

Wadley, L. 2015. Those marvellous millennia: the Middle Stone Age of southern Africa. *Azania: Archaeological Research in Africa* 50(2): 155–226.

Wadley, L., Esterhuysen, A. & Jeannerat, C. 1992. Later Pleistocene and Holocene environments at Rose Cottage Cave: the evidence from charcoal studies. *South African Journal of Science* 88: 558–563.

Wadley, L., Sievers, C., Bamford, M., Goldberg, P., Berna, F. & Miller, C. 2011. Middle Stone Age bedding construction and settlement patterns at Sibudu, South Africa. *Science* 334: 1388–1391.

Wadsworth, C. & Buckley, M. 2014. Proteome degradation in fossils: investigating the longevity of protein survival in ancient bone. *Rapid Communications in Mass Spectrometry* 28(6): 605–615.

Wagner, A., Richter, K.K., Ludes, E., Arbogast, R.M., Carita, D., Guidez, A., Soussoko, S., Boivin, N.L., Marche, J.C., Wandhammer, M.D. & Meister, M. 2020. Whale bone puzzles: reconstructing and identifying historical whale skeletons using archive records, osteology, and zooarchaeology by Mass Spectrometry (ZooMS). *Journal of Conservation & Museum Studies* 18(1): 1–12.

Wakeling, J.L., Cramer, M.D. & Bond, W.J. 2012. The savanna-grassland 'treeline': why don't savanna trees occur in upland grasslands? *Journal of Ecology* 100(2): 381–391.

Wang, S.Y., Cappellini, E. & Zhang, H.Y. 2012. Why collagens best survived in fossils? Clues from amino acid thermal stability. *Biochemical and Biophysical Research Communications* 422(1): 5–7.

Wanner, H., Mercolli, L., Grosjean, M. & Ritz, S.P. 2015. Holocene climate variability and change: a data-based review. *Journal of the Geological Society* 172(2): 254–263.

Weiguo, L., Xiahong, F., Youfeng, N., Qingle, Z., Yunning, C. & Zhisheng, A.N. 2005. $\delta^{13}C$ variation of C_3 and C_4 plants across an Asian monsoon rainfall gradient in arid northwestern China. *Global Change Biology* 11(7): 1094–1100.

Weldeab, S., Stuut, J.B., Schneider, R.R. & Siebel, W. 2013. Holocene climate variability in the winter rainfall zone of South Africa. *Climate of the Past* 9(5): 2347–2364.

Welker, F. 2017. The palaeoproteomic identification of Pleistocene hominin skeletal remains: towards a biological understanding of the middle to upper Palaeolithic transition. Unpublished PhD dissertation. Leipzig: Max Planck Institute for Evolutionary Anthropology.

Welker, F., Hajdinjak, M., Talamo, S., Jaouen, K., Dannemann, M., David, F., Julien, M., Meyer, M., Kelso, J., Barnes, I. & Brace, S. 2016. Palaeoproteomic evidence identifies archaic hominins associated with the Châtelperronian at the Grotte du Renne. *Proceedings of the National Academy of Sciences* 113(40): 11162–11167.

Welker, F., Soressi, M., Rendu, W., Hublin, J.J. & Collins, M. 2015. Using ZooMS to identify fragmentary bone from the late Middle/Early Upper Palaeolithic sequence of Les Cottés, France. *Journal of Archaeological Science* 54: 279–286.

White, E.M. & Hannus, L.A. 1983. Chemical weathering of bone in archaeological soils. *American Antiquity* 48(2): 316–322.

White, T.D. 1992. *Prehistoric Cannibalism at Mancos 5MTURMR-2346*. New Jersey: Princeton University Press.

Wingler, A., Lea, P.J., Quick, W.P. & Leegood, R.C. 2000. Photorespiration: metabolic pathways and their role in stress protection. *Philosophical Transactions of the Royal Society of London B* 355(1402): 1517–1529.

Winter, R.M., de Kock, W., Palsbøll, P.J. & Çakirlar, C. 2021. Potential applications of biomolecular archaeology to the ecohistory of sea turtles and groupers in Levant coastal antiquity. *Journal of Archaeological Science: Reports* 36: 1–6.

Wolverton, S. 2013. Data quality in zooarchaeological faunal identification. *Journal of Archaeological Method and Theory* 20(3): 381–396.

Wurz, S. 2013. Technological trends in the Middle Stone Age of South Africa between MIS 7 and MIS 3. *Current Anthropology* 54(S8): S305–S319.

Wurz, S. 2019. Human evolution, archaeology and the South African stone age landscape during the last 100,000 years. In: Knight, J. & Rogerson, C.M. (eds) *The Geography of South Africa*: 125–132. Cham: Springer.

Yin, X. 1993. Variation in foliar nitrogen concentration by forest type and climatic gradients in North America. *Canadian Journal of Forest Research* 23(8): 1587–1602.

Zhao, X., Dupont, L., Meadows, M.E. & Wefer, G. 2016a. Pollen distribution in the marine surface sediments of the mudbelt along the west coast of South Africa. *Quaternary International* 404: 44–56.

Zhao, X., Dupont, L., Schefuß, E., Meadows, M.E., Hahn, A. & Wefer, G. 2016b. Holocene vegetation and climate variability in the winter and summer rainfall zones of South Africa. *The Holocene* 26(6): 843–857.

Zhu, M.R.M.W, 2016. Reconstructing the diets of southern African farmers: comparing stable isotopes across body tissues. Unpublished master's dissertation. Cape Town: University of Cape Town.

APPENDIX 1

Taphonomy for GRS faunal assemblage (abbreviations are found below)

Appendix 1.A: Taphonomic data from GRS faunal remains, abbreviations and scoring found below. Fauna from the MH are highlighted in green, TP are orange, and LP are yellow.

No.	Layer	Unit	Breakage	Age	Burn	CM	CMd	PM	PMd	TM	TMd	GM	RE	Weathering	Encrusted	Surface Condition	A/S	Trampling	Colour	Preservation	Length (mm)	Cortical Thickness (mm)	Manganese
001	B4NW	1000B:3	S-S	A	Br	~	~	1	N	~	~	~	~	1	1	S	~	~	LB/DB	3	118,9	4,3	~
002	B4NW	1003:1	S-S	A	~	~	~	~	~	~	~	~	1	1	1	S	~	~	LB	3	87,9	5,2	~
003	B4NW	1003:1	S-S	A	~	1	Sl	2	N/M	~	~	~	2	1	1	S	~	~	LB	3	118,0	5,2	~
004	B4NW	1003:2	S-S	A	Br Local	~	~	1	M	~	~	~	1	1	1	S	~	~	LB	3	131,2	3,6	~
005	B4NW	1003:2	S-S	A	~	~	~	1	M	1	S	~	1	1	1	S	1	~	LB	3	49,1	3,6	~
006	B4NW	1007:1	S-S	J	~	~	~	~	~	~	~	~	1	1	1	P	~	~	LB	3	84,0	3,8	1
007	B4NW	1007:1	S-S	A	RB Local	~	~	1	N/M	~	~	~	1	1	1	S	1	~	LB	3	70,3	3,7	~
008	B4NW	1007:1	S-S	J	~	~	~	1	M	~	~	~	1	1	1	P	1	~	LB	3	61,3	4,5	1
009	B4NW	1007:2	S-S	J	Br Possible	1	Sl	1	M	~	~	~	1	1	1	P	1	~	Br	3	108,2	7,2	1
010	B4NW	1010:1	S-S	A	~	~	~	1	M	~	~	~	1	1	1	S	1	~	Be	3	64,7	3,0	~
011	B4NW	1010:1	S-S	J	~	1	Sl	~	~	~	~	~	1	1	1	P	1	~	LB	3	72,5	3,6	~
012	B4NW	1010:1	S-S	A	Br Local	~	~	1	N	~	~	~	1	1	1	S	1	~	LB	3	75,9	4,7	~
013	B4NW	1012:2	S-S	A	~	1	Sl	1	N/M	~	~	~	1	1	1	S	1	1	LB	3	63,3	4,1	~
014	B4NW	1012:2	S-S	J	~	~	~	~	~	~	~	~	1	1	~	P	1	~	LB	3	50,7	4,4	~
015	B4NW	1012:2	S-S	J	~	~	~	2	M	~	~	~	1	1	1	P	1	~	Be	3	69,7	5,7	~

No.	Layer	Unit	Breakage	Age	Burn	CM	CMd	PM	PMd	TM	TMd	GM	RE	Weathering	Encrusted	Surface Condition	A/S	Trampling	Colour	Preservation	Length (mm)	Cortical Thickness (mm)	Manganese
016	B4NW	1012:2	S-S	J	~	~	~	~	~	~	~	~	~	1	1	P	~	~	Be	3	74,6	4,9	~
017	B4NW	1018:1	S-S	A	Br Local	~	~	1	M	~	~	~	~	1	1	S	1	~	LB	3	48,2	4,2	~
018	B4NW	1018:1	S-S	?	~	~	~	~	~	~	~	~	1	1	1	R	1	1	LB	2	47,5	10,2	1
019	B4NW	1018:1	S-S	A	Br Local	~	~	~	~	~	~	~	2	1	1	S	1	1	LB	3	59,5	5,1	~
020	B4NW	1018:1	S-S	?	~	~	~	~	~	~	~	~	1	1	2	S	~	1	LB	2	60,4	10,9	
021	B4NW	1018:1	S-S	A	Br/Bl Local	~	~	~	~	~	~	~	1	1	2	S	~	~	RB	2	55,2	5,8	1
022	B4NW	1018:1	S-S	?	~	~	~	1	M	~	~	~	1	1	1	P	~	~	LB	3	33,0	5,6	1
023	B4NW	1018:2	S-S	A	~	~	~	~	~	~	~	~	1	1	1	S	~	~	LB	3	51,1	7,2	2
024	B4NW	1018:2	S-S	A	~	~	~	~	~	~	~	~	1	1	1	S	~	1	LB	3	45,1	7,4	2
025	B4NW	1018:3	S-S	A	~	~	~	~	~	~	~	~	2	1	1	S	~	~	LB	3	68,2	8,0	1
026	B4NW	1018:3	S-S	A	RB Local	~	~	~	~	~	~	~	1	1	1	S	~	~	LB	3	34,3	5,8	1
027	B4SW	1000B:1	S-S	A	~	~	~	~	~	2	S	~	1	1	1	S	~	~	Be	3	69,6	4,6	1
028	B4SW	1000B:1	S-S	J	~	~	~	1	M	~	~	~	1	1	1	P	1	~	LB	3	57,4	5,7	1
029	B4SW	1000B:1	S-S	A	~	~	~	1	M	~	~	~	1	1	1	S	1	~	LB/RB	3	43,4	4,4	1
030	B4SW	1003:2	S-S	A	~	~	~	~	~	~	~	~	1	1	1	S	1	~	LB	3	50,4	3,6	1
031	B4SW	1003:2	S-S	A	~	~	~	~	~	~	~	~	1	1	1	S	1	~	LB	3	34,9	4,1	2
032	B4SW	1003:2	S-S	J	Br Local	~	~	~	~	~	~	~	1	1	~	P	~	~	Br	3	40,1	2,5	1
033	B4SW	1003:2	S-S	J	DB Local	~	~	~	~	~	~	~	1	2	~	P	~	~	LB	2	48,1	3,3	1
034	B4SW	1003:2	S-S	A	~	1	Sl	1	M	~	~	~	1	1	1	S	1	~	LB	3	39,3	4,7	1
035	B4SW	1003:2	S-S	J	~	~	~	~	~	2	S	~	1	1	1	P	1	~	LB	2	79,4	7,2	~

No.	Layer	Unit	Breakage	Age	Burn	CM	CMd	PM	PMd	TM	TMd	GM	RE	Weathering	Encrusted	Surface Condition	A/S	Trampling	Colour	Preservation	Length (mm)	Cortical Thickness (mm)	Manganese
036	B4SW	1003:2	S-S	A	~	~	~	1	M	~	~	~	1	1	1	S	1	~	Be	3	82,0	3,9	~
037	B4SW	1003:2	S-S	A	~	~	~	~	~	2	S	~	1	1	1	S	1	~	Br	3	55,8	6,4	1
038	B4SW	1003:2	S-S	A	~	~	~	~	~	~	~	~	1	1	1	S	1	~	Be	3	80,1	4,2	1
039	B4SW	1003:2	S-S	J	~	~	~	1	M	~	~	~	1	1	1	P	1	1	LB	3	105,7	4,8	1
040	B4SW	1003:2	S-S	A	~	~	~	~	~	~	~	~	1	1	1	S	1	~	Be	3	111,8	8,7	~
041	B4SW	1004A:2	S-S	A	~	~	~	~	~	2	S	~	~	1	1	S	1	1	Be	3	82,3	4,5	~
042	B4SW	1004A:2	S-S	A	~	~	~	~	~	~	~	~	1	1	1	S	1	1	Br/RB	3	41,0	2,9	1
043	B4SW	1012:3	S-S	A	RB	~	~	~	~	~	~	~	1	1	1	S	1	1	LB/RB	2	43,7	4,6	1
044	B4SW	1012:3	S-S	A	~	~	~	~	~	2	S	~	1	1	~	S	1	~	Be	3	39,5	4,7	1
045	B4SW	1012:3	S-S	J	~	~	~	1	M	~	~	~	1	1	1	P	1	~	Be	2	46,0	5,0	2
046	B4 Wall	~	S-S	A	RB	~	~	~	~	~	~	~	~	4	1	S	1	1	RB	2	101,5	9,3	~
047	B4SW	1017:1	S-S	A	~	~	~	~	~	1	S	~	1	1	~	S	1	1	Be	3	43,0	4,6	1
048	B4SW	1017:1	S-S	A	RB/DB	~	~	~	~	~	~	~	1	2	1	S	1	~	Br/DB	2	73,6	11,6	1
049	B4SW	1017:2	S-S	A	~	~	~	1	N/M	~	~	~	1	1	1	S	~	~	LB	2	60,2	4,3	2
050	B4SW	1017:2	S-S	A	~	~	~	~	~	~	~	~	1	1	~	S	~	1	Be	3	51,0	3,5	1
051	B4SW	1017:2	S-S	A	~	~	~	1	M	~	~	~	1	1	1	S	~	~	Be	2	34,4	4,3	2
052	B4SW	1017:2	S-S	A	~	~	~	~	~	~	~	~	1	1	~	S	1	~	Be	3	32,8	6,9	~
053	B4SW	1018:1	S-S	J	~	~	~	~	~	~	~	~	~	2	1	P	~	~	RB	2	43,4	9,5	~
054	B4SW	1018:1	S-S	J	~	~	~	1	M	~	~	~	1	2	1	P	~	~	RB	2	60,1	3,9	1
055	B4SW	1018A:1	S-S	A	~	~	~	1	M	~	~	~	1	1	~	S	1	~	LB	3	34,1	3,5	1
056	B4SW	1018A:1	S-S	J	~	~	~	~	~	~	~	1	1	2	1	P	~	~	LB	2	59,5	3,9	1
057	C5NW	3005:1	S-S	A	~	1	C	2	M	1	S	~	1	1	1	A	~	1	Br	3	106,6	5,9	1
058	C5NW	3005:1	S-S	A	~	~	~	2	M	1	S	~	1	2	1	A	~	~	Br	2	85,0	4,9	1
059	C5NW	3005:1	S-S	A	LB/RB	1	C	~	~	~	~	~	1	1	1	S	~	~	LB	3	94,7	3,7	~

No.	Layer	Unit	Breakage	Age	Burn	CM	CMd	PM	PMd	TM	TMd	GM	RE	Weathering	Encrusted	Surface Condition	A/S	Trampling	Colour	Preservation	Length (mm)	Cortical Thickness (mm)	Manganese
					Local																		
060	C5NW	3005:1	S-S	A	LB to RB	~	~	1	M	~	~	~	2	1	1	S	1	1	LB	3	75,1	5,5	1
061	C5NW	3005:2	S-S	A	~	~	~	~	~	~	~	~	1	1	2	S	~	~	Br	2	82,0	5,5	1
062	C5NW	3006:1	S-S	?	LB/RB	~	~	~	~	~	~	~	1	2	2	A	~	~	Br	1	95,1	3,7	~
063	C5NW	3006:1	S-S	A	~	~	~	~	~	2	S	1	1	1	1	S	~	~	LB	3	136,3	10,5	1
064	C5NW	3006:1	S-S	J	~	~	~	1	M	~	~	~	1	1	1	P	~	~	Br	1	108,2	4,3	1
065	C5NW	3006:1	S-S	J	~	~	~	1	M	~	~	~	1	1	2	P	~	~	Br	2	136,3	5,2	1
066	C5NW	3007:1	S-S	A	~	~	~	1	M	~	~	~	1	1	1	S	~	~	Br	3	99,7	7,1	1
067	C5NW	3007:1	S-S	A	RB Local	~	~	~	~	~	~	~	1	1	1	S	1	~	Br/RB	2	80,0	6,8	1
068	C5NW	3021:1	S-S	A	~	1	Sl	1	M	~	~	~	1	1	1	S	~	~	LB	1	61,1	9,9	1
069	C5NW	3024:2	S-S	J	RB	~	~	~	~	~	~	~	1	2	2	P	~	~	Br/RB	2	98,1	10,1	1
070	C5NE	4003:1	S-S	?	RB	~	~	1	M	1	S	~	~	1	1	S	~	~	RB/Br	2	88,1	9,4	1
071	C5NE	4003:1	S-S	J	~	~	~	1	M	~	~	~	1	2	1	P	~	1	Br	2	52,9	6,6	1
072	C5NE	4004:1	S-S	J	~	1	Sl	1	M	~	~	~	1	1	1	P	~	~	LB	3	154,0	9,1	1
073	C5NE	4004:1	S-S	J	~	~	~	1	M	~	~	~	1	1	1	P	~	~	LB	3	63,6	4,1	1
074	C5NE	4006:1	S-S	A	~	~	~	~	~	~	~	~	1	1	1	S	1	1	Be	3	48,2	3,6	~
075	C5NE	4006:1	S-S	A	Br Local	~	~	2	M	2	S	~	1	1	~	S	1	~	LB/Br	2	71,2	5,9	1
076	C5NE	4015:2	S-S	A	Br Local	~	~	1	M	~	~	~	1	1	1	S	~	~	LB	3	40,2	4,3	1
077	C5NE	4015:2	S-S	A	DB Local	~	~	2	M	~	~	~	1	1	1	S	~	~	LB	3	109,4	6,6	1
078	C5NE	4015:4	S-S	A	~	~	~	~	~	~	~	~	1	1	1	S	1	1	LB	3	100,9	3,9	1
079	C5NE	4015:4	S-S	J	~	~	~	~	~	~	~	~	1	2	1	P	~	~	Br	2	67,2	3,2	1

No.	Layer	Unit	Breakage	Age	Burn	CM	CMd	PM	PMd	TM	TMd	GM	RE	Weathering	Encrusted	Surface Condition	A/S	Trampling	Colour	Preservation	Length (mm)	Cortical Thickness (mm)	Manganese
080	C4NE	2001B:1	S-S	J	RB Local	~	~	1	M	~	~	~	1	1	1	P	~	~	Br	3	33,5	4,4	1
081	C4NE	2001B: 1	S-S	A	RB	~	~	2	M	~	~	~	1	1	1	S	1	~	LB/RB	3	35,6	3,1	~
082	C4NE	2002:1	S-S	J	~	~	~	1	M	~	~	~	1	2	1	P	1	~	Br/LB	3	46,0	5,6	1
083	C4NE	2002:1	S-S	A	~	~	~	1	M	~	~	~	1	1	1	S	1	1	LB/RB	3	51,3	3,4	~
084	C4NE	2002:1	S-S	A	~	~	~	~	~	~	~	~	1	1	1	S	1	~	LB	3	38,6	3,1	1
085	C4NE	2002:1	S-S	A	DB	~	~	2	M	~	~	~	1	1	1	S	1	1	LB/DB	3	48,2	3,2	1
086	C4NE	2004E:1	S-S	A	~	1	Sl	1	M	~	~	~	1	1	1	S	1	1	LB	3	68,5	5,1	~
087	C4NE	2007:1	S-S	J	~	~	~	1	M	~	~	1	1	1	1	P	1	~	LB	2	57,2	9,9	1
088	C4NE	2011:1	S-S	J	~	~	~	~	~	1	S	~	1	1	1	P	1	1	Br	3	44,6	4,2	1
089	C4NE	2011:2	S-S	A	RB	~	~	1	M	~	~	~	1	1	1	S	1	1	LB/RB	3	86,3	4,8	1
090	B4NE	1021:1	S-S	A	DB	~	~	~	~	~	~	~	~	2	~	S	1	1	DB	2	19,6	2,0	~
091	B4NE	1021:1	S-T	A	DB/RB	~	~	~	~	~	~	~	1	2	2	S	~	~	DB/RB	2	21,4	2,3	~
092	B4SW	1023:1	S-S	A	~	~	~	~	~	~	~	~	~	1	3	S	1	~	LB/Be	1	41,0	4,8	~
093	B4NW	1018D:1	S-S	A	~	~	~	~	~	~	~	~	~	1	1	S	1	~	Be	3	21,3	~	1
094	B4NW	1018D:1	S-S	A	~	~	~	~	~	~	~	~	1	1	1	S	1	~	LB	3	28,1	~	1
095	B4NW	1018D:1	S-S	A	~	~	~	~	~	~	~	~	~	1	1	S	1	~	LB	3	16,2	~	1
096	B4NW	1018D:1	S-S	A	~	~	~	~	~	~	~	~	1	1	1	S	1	~	LB	2	16,8	~	1
097	B4NE	1031:1	S-S	J	DB Local	~	~	~	~	~	~	~	2	3	1	P	~	~	Br/DB	2	36,2	~	~
098	B4NE	1031:1	S-S	?	RB Local	~	~	~	~	~	~	~	~	2	~	S/R	~	~	LB/RB	2	23,5	~	~
099	B4NE	1031:1	S-S	A	Br	~	~	~	~	~	~	~	2	2	1	S	~	~	Br	2	20,9	~	~
100	B4SW	1012:3	S-S	A	~	~	~	2	M	1	S/P	~	1	1	1	S	2	~	LB	3	48,9	2,4	1

Breakage [1], [2]

S = Spiral Fracture, T = Transverse Fracture

Age

J = Juvenile, A = Adult

Burn (colour)

Be = Beige, LB = Light Brown, RB = Red Brown, DB = Dark Brown, Br = Brown, Bl = Black

Cut Mark (CM)[3]

1 = Present but mild (< 30% of surface affected), 2 = Moderate (30-60%), 3 = Severe (> 60%)

Cut Mark details (CMd)[3]

Sc = Scrape-mark, Sl = Slice-mark, C = Chop-mark

Percussion (PM)[3]

1 = Present but mild (< 30% of surface affected), 2 = Moderate (30-60%), 3 = Severe (> 60%)

Percussion Mark details (PMd)[3]

M = Percussion mark, N = Percussion notch

Tooth Mark (TM)[3]

1 = Mild, 2 = Moderate, 3 = Severe

Tooth Mark details (TMd)[3]

P = Pit, S = Score

Gnaw Mark (GM)[4]

1 = Mild, 2 = Moderate, 3 = Severe

Root Etching (RE)[4]

1 = Mild, 2 = Moderate, 3 = Severe

Weathering[5]

0 = Greasy bone, no cracking on surface, 1 = Some longitudinal cracking, 2 = Longitudinal and split line cracking present and some flaking/exfoliation, 4 = Crack edges are rounded. Extreme flaking/exfoliation. Flaking or exfoliation occurs during movement or handling, 5 = Falls apart in situ and is very fragile[6]

Encrusted[4]

1 = < ½, 2 = ½ - ¾, 3 = > ¾

Surface Condition[4]

A = Abraded, P = Porous, R = Rough, S = Smooth

Abrasion/Sheen (A/S)[4]

1 = Light sheen (< 30% of surface affected), 2 = Moderate sheen (30-60%), 3 = Heavy sheen (> 60%)

Trampling[4]

1 = Mild, 2 = Moderate, 3 = Severe

Colour

Be = Beige, LB = Light Brown, RB = Red Brown, DB = Dark Brown, Br = Brown, Bl = Black

Preservation[4]

1 = < ¼ of total cortical surface is well preserved, 2 = ¼ - ½, 3 = ½ - ¾, 4 = ≥ ¾

Manganese[4]

1 = Spots, 2 = Patches, 3 = Completely Covered

---

[1] Villa, P.& Mahieu, E. 1991. Breakage patterns of human long bones. *Journal of Human Evolution* 21(1): 27–48.

[2] Driver, J.C. 2005. Manual for description of vertebrate remains. Unpublished manual. Crow Canyon Archaeological Center: Cortez.

[3] Blumenschine, R.J., Marean, C.W. & Capaldo, S.D. 1996. Blind tests of inter-analyst correspondence and accuracy in the identification of cut marks, percussion marks, and carnivore tooth marks on bone surfaces. *Journal of Archaeological Science* 23(4): 493–507.

[4] Fernandez-Jalvo, Y. & Andrews, P. 2016. *Atlas of Taphonomic Identifications: 1001+ Images of Fossil and Recent Mammal Bone Modification.* Dordrecht: Springer.

[5] Behrensmeyer, A.K. 1978. Taphonomic and ecologic information from bone weathering. *Paleobiology* 4(2): 150–162.

APPENDIX 2

Stable carbon and nitrogen isotope ratios for GRS faunal assemblage

Appendix 2.A: $\delta^{13}C$ and $\delta^{15}N$ values with collagen quality indicators including %N, %C and C:N ratio elemental.

No.	$\delta^{13}C$ corr (‰)	%C	$\delta^{15}N$ corr (‰)	%N	C/N
001	-18,9	43,5	8,3	15,8	3,2
002	-5,6	41,4	3,2	14,9	3,2
003	-19,8	43,3	4,6	16,0	3,2
004	-18,9	45,8	3,8	16,7	3,2
005	-16,4	46,5	7,0	16,9	3,2
006	-19,1	44,7	4,9	16,4	3,2
007	-20,0	47,0	5,5	17,1	3,2
008	-18,8	45,7	9,4	16,8	3,2
009	-13,8	47,2	6,2	17,3	3,2
010	-19,8	43,9	5,8	16,0	3,2
011	-19,9	40,1	6,0	14,2	3,3
012	-19,0	46,4	4,2	17,1	3,2
013	-19,6	36,2	5,6	12,8	3,3
014	-13,2	42,0	7,6	15,3	3,2
015	-	-	-	-	-
016	-13,2	39,8	6,9	14,5	3,2
017	-5,5	43,5	5,8	16,1	3,2
018	-18,4	42,7	11,2	15,6	3,2
019	-6,1	43,9	5,8	16,0	3,2
020	-9,6	43,5	6,3	15,9	3,2
021	-7,9	45,7	6,0	16,8	3,2
022	-13,3	43,1	8,2	15,9	3,2
023	-6,4	45,0	12,0	16,5	3,2
024	-7,5	46,1	12,7	16,9	3,2
025	-9,8	44,2	6,3	16,2	3,2
026	-7,0	42,7	12,8	15,6	3,2
027	-19,5	42,0	4,4	15,3	3,2
028	-7,8	43,0	4,0	15,9	3,2
029	-18,0	42,5	3,1	15,7	3,2
030	-19,2	45,4	4,8	16,6	3,2
031	-20,0	42,2	5,8	15,6	3,2
032	-10,9	43,2	3,7	15,6	3,2
033	-19,7	45,7	4,7	16,7	3,2
034	-19,9	43,9	4,0	16,3	3,2
035	-17,5	46,2	6,1	17,0	3,2
036	-11,1	46,8	4,3	17,1	3,2

No.	$\delta^{13}C$ corr (‰)	%C	$\delta^{15}N$ corr (‰)	%N	C/N
037	-19,9	35,8	3,8	13,0	3,2
038	-20,3	45,5	4,7	16,7	3,2
039	-5,3	42,7	2,8	15,6	3,2
040	-18,7	46,2	5,7	17,1	3,2
041	-19,2	33,6	5,4	12,0	3,3
042	-19,2	31,5	4,7	11,2	3,3
043	-19,4	44,1	4,9	16,0	3,2
044	-6,1	45,6	3,1	16,7	3,2
045	-11,8	45,2	7,5	16,5	3,2
046	-7,4	40,3	11,7	14,4	3,3
047	-18,9	43,2	6,2	15,8	3,2
048	-6,8	41,8	6,1	15,1	3,2
049	-17,5	43,6	12,0	15,8	3,2
050	-17,5	42,9	5,4	15,8	3,2
051	-17,6	43,3	12,0	15,6	3,2
052	-6,2	47,6	10,2	17,5	3,2
053	-19,9	45,4	8,5	16,5	3,2
054	-6,2	42,7	13,1	15,6	3,2
055	-18,9	44,6	8,2	16,2	3,2
056	-6,5	45,8	10,7	16,6	3,2
057	-19,4	44,4	3,7	14,3	3,6
058	-19,3	42,6	4,8	15,4	3,2
059	-19,3	44,4	4,9	16,3	3,2
060	-6,7	41,0	6,0	15,1	3,2
061	-19,5	41,8	5,0	15,2	3,2
062	-19,5	46,8	5,3	17,1	3,2
063	-17,9	42,7	4,7	15,8	3,2
064	-19,6	46,3	5,3	17,0	3,2
065	-20,7	42,7	4,2	15,8	3,2
066	-20,3	42,6	5,2	15,3	3,3
067	-6,0	46,0	7,6	16,7	3,2
068	-9,5	24,6	3,2	8,7	3,3
069	-	-	-	-	-
070	-18,3	43,4	7,0	15,9	3,2
071	-19,6	43,7	7,5	15,3	3,3
072	-12,2	45,1	4,3	16,6	3,2
073	-19,8	43,2	4,6	15,9	3,2
074	-20,8	43,7	5,3	15,3	3,3
075	-9,0	37,3	7,0	13,4	3,2
076	-6,9	45,0	2,3	16,6	3,2
077	-10,5	46,0	3,7	16,9	3,2
078	-20,0	41,4	6,2	14,9	3,2

No.	$\delta^{13}C$ corr (‰)	%C	$\delta^{15}N$ corr (‰)	%N	C/N
079	-19,6	39,7	4,2	14,5	3,2
080	-13,4	42,7	5,3	15,7	3,2
081	-19,8	44,9	5,1	16,4	3,2
082	-19,4	41,2	4,6	15,0	3,2
083	-20,2	44,8	4,0	16,4	3,2
084	-19,3	46,5	4,3	16,8	3,2
085	-7,4	43,7	3,2	16,1	3,2
086	-6,0	44,5	3,6	16,3	3,2
087	-6,7	46,8	8,7	17,2	3,2
088	-18,7	45,1	4,0	16,5	3,2
089	-20,0	46,3	4,6	16,8	3,2
100	-19,6	45,2	8,5	16,1	3,3

APPENDIX 3

Summary statistics of current study

Appendix 3.A: Summary statistics for $\delta^{13}C$ and $\delta^{15}N$ values from browser, grazer, intermediate feeder, water-dependent, and water-independent taxa in the TP and MH.

$\delta^{13}C$	**Browser**		**Grazer**		**Water-dependent**		**Water-independent**	
	MH	**TP**	**MH**	**TP**	**MH**	**TP**	**MH**	**TP**
N	44	7	16	10	8	9	41	5
Min	-20,8	-19,9	-13,8	-9,6	-13,8	-9,6	-20,8	-19,9
Max	-16,4	-17,5	-5,3	-5,5	-6,0	-5,5	-16,4	-17,6
Mean	-19,4	-18,4	-9,1	-6,8	-10,6	-6,9	-19,3	-18,7
SD	0,8	0,9	3,1	1,1	3,5	1,2	0,8	0,8
Median	-19,5	-18,4	-8,4	-6,5	-12,5	-6,5	-19,5	-18,9
Range	4,4	2,4	8,5	4,1	7,8	4,1	4,4	2,3
$\delta^{15}N$	**Browser**		**Grazer**		**Water-dependent**		**Water-independent**	
	MH	**TP**	**MH**	**TP**	**MH**	**TP**	**MH**	**TP**
N	44	7	16	10	8	9	41	5
Min	3,1	5,4	2,3	5,8	3,6	5,8	3,1	6,2
Max	9,4	12,0	8,7	13,1	8,7	13,1	9,4	12,0
Mean	5,2	9,1	5,1	9,6	6,5	10,0	5,1	9,2
SD	1,2	2,7	2,1	3,2	1,6	3,1	1,2	2,4
Median	4,9	8,5	4,7	10,5	6,6	10,7	4,8	8,5
Range	6,3	6,6	6,4	7,3	5,1	7,3	6,3	5,8

Appendix 3.B: Outcome of Shapiro-Wilk tests for normality, significant results in green.

Sample	**N**	**$\delta^{13}C$**		**$\delta^{15}N$**	
		Shapiro-Wilk	**p-value**	**Shapiro-Wilk**	**p-value**
TP Browser	7	0,88	0,24	0,89	0,28
MH Browser	44	0,89	< 0,001	0,89	< 0,001
MH grey rhebok	33	0,97	0,43	0,99	0,94
MH Other Browser	11	0,93	0,39	0,97	0,89
TP Grazer	10	0,81	0,02	0,81	0,02
MH Grazer	16	0,88	0,03	0,91	0,13
TP Water-independent	5	0,97	0,86	0,94	0,66
MH Water-independent	41	0,90	0,002	0,89	< 0,001
TP Water-dependent	9	0,84	0,05	0,83	0,04
MH Water-dependent	8	0,77	0,01	0,97	0,93

Appendix 3.C: Outcome of chi-square test for success of ZooMS at GRS. Expected values smaller than five in orange.

Success ZooMS			
	MH	TP	LP
No ID/low resolution	9	3	3
ID (at least Tribe)	61	17	7
Expected Values			
	MH	TP	LP
No ID/low resolution	10,5	3	1,5
ID (at least Tribe)	59,5	17	8,5
χ^2 = 2,01; df = 2; p = 0,36			

Appendix 3.D: Outcome of chi-square test for success of ZooMS vs surface preservation and heating at GRS. Expected values smaller than five in orange.

Success ZooMS vs Surface Preservation			**Success ZooMS vs Heating**		
	ID (to tribe)	No-ID		ID (to tribe)	No-ID
Below Average	26	8	Heated	27	5
Good	59	7	Not Heated	58	10
Expected Values			Expected Values		
	ID (to tribe)	No-ID		ID (to tribe)	No-ID
Below Average	28,9	5,1	Below Average	27,2	4,8
Good	56,1	9,9	Good	57,8	10,2
χ^2 = 2,94; df = 1; p = 0,09			χ^2 = 0,01; df = 1; p = 0,90		

Appendix 3.E: Outcome of chi-square test for browsers vs grazers through time. Expected values and adjusted residuals are included when necessary. Expected values smaller than five are highlighted in orange, significant values in green.

Browser vs Grazer			
	MH	TP	LP
Browser	44	7	1
Grazer	17	10	6
Expected Values			
	MH	TP	LP
Browser	37,3	10,4	4,3
Grazer	23,7	6,6	2,7
χ^2 = 12,43; df = 2; p = 0,002			
Adjusted Residuals			

	MH	TP	LP
Browser	3,30	-1,89	-2,66
Grazer	-3,30	1,89	2,66

MH vs TP		
	MH	TP
Browser	44	7
Grazer	17	10
Expected Values		
	MH	TP
Browser	39,9	11,1
Grazer	21,1	5,9
$\chi^2 = 5,63$; df = 1; p = 0,02		
Adjusted Residuals		
	MH	TP
Browser	2,37	-2,37
Grazer	-2,37	2,37

TP vs LP		
	TP	LP
Browser	7	1
Grazer	10	6
Expected Values		
	TP	LP
Browser	5,7	2,3
Grazer	11,3	4,7
$\chi^2 = 1,61$; df = 1; p = 0,20		

Appendix 3.F: Outcome of chi-square test for water-dependent vs water-independent through time. Expected values and adjusted residuals are included when necessary. Expected values smaller than five are highlighted in orange, significant values in green.

WD vs WI			
	MH	TP	LP
WD	8	9	6
WI	41	5	0
Expected Values			
	MH	TP	LP
Browser	16,3	4,7	2,0
Grazer	32,7	9,3	4,0
Adjusted Residuals			
	MH	TP	LP
Browser	-4,69	2,75	3,63
Grazer	4,69	-2,75	-3,63
$\chi^2 = 24,41$; df = 2; p < 0,001			

MH vs TP		
	MH	TP
WD	8	9
WI	41	5
Expected Values		

TP vs LP		
	TP	LP
WD	9	6
WI	6	0
Expected Values		

	MH	TP		TP	LP
WD	13,2	3,8	WD	10,5	4,5
WI	35,8	10,2	WI	3,5	1,5
χ^2 = 12,71; df = 1; p = 0,002			χ^2 = 2,86; df = 1; p = 0,09		
Adjusted Residuals					
	MH	TP			
WD	-3,57	3,57			
WI	3,57	-3,57			

Appendix 3.G: Outcome of Mann-Whitney U-Test, significant differences in green.

Sample	**$\delta^{13}C$**			**$\delta^{15}N$**		
	MW	**z**	**p-value**	**MW**	**z**	**p-value**
MH Browser vs Grazer	0	5,88	< 0,001	319,5	0,54	0,59
TP Browser vs Grazer	0	3,37	< 0,001	30	0,44	0,66
Browser MH vs TP	61,5	2,52	0,01	22,5	3,59	< 0,001
Grazer MH vs TP	50,5	-1,53	0,13	25	-2,87	0,004
MH vs TP taxa				91,5	-5,14	< 0,001
Springbok vs Browser	41,5	-0,91	0,36			
Unknown Antilopinae 2 vs Browser	31	-0,46	0,65			
Unknown Antilopinae 1 vs Grazer	39	1,56	0,12			
Reduncini Browser vs Grazer	0	-3,56	< 0,001	40,5	-1,90	0,057
WD MH vs TP	16	-1,88	0,06	15	-1,97	0,049
WI MH vs TP	56,5	-1,61	0,11	6	-3,39	0,001
MH WD vs WI				70,5	-2,52	0,01
TP WD vs WI				18,5	-0,47	0,64
MH migratory vs non-migratory	8	0,37	0,71			
Migratory TP vs MH	8	1,28	0,20			

APPENDIX 4

Combined results

Appendix 4.A: Opperman's fauna were combined with the fauna from this study. Outcome of chi-square test for browsers vs grazers through time. Expected values and adjusted residuals are included when necessary. Expected values smaller than five in orange, significant values in green.

Browser vs Grazer			
	MH	TP	LP
Browser	129	15	1
Grazer	48	19	13
Expected Values			
	MH	TP	LP
Browser	114,1	21,9	9,0
Grazer	62,9	12,1	5,0
χ^2 = 31,69; df = 2; p < 0,001			
Adjusted Residuals			
	MH	TP	LP
Browser	5,08	-2,69	-4,63
Grazer	-5,08	2,69	4,63

MH vs TP			**TP vs LP**		
	MH	TP		TP	LP
Browser	129	15	Browser	15	1
Grazer	48	19	Grazer	19	13
Expected Values			Expected Values		
	MH	TP		TP	LP
Browser	120,8	23,2	Browser	11,3	4,7
Grazer	56,2	10,8	Grazer	22,7	9,3
χ^2 = 10,89; df = 1; p = 0,001			χ^2 = 6,10; df = 1; p = 0,01		
Adjusted Residuals			Adjusted Residuals		
	MH	TP		TP	LP
Browser	3,3	-3,3	Browser	2,5	-2,5
Grazer	-3,3	3,3	Grazer	-2,5	2,5

Appendix 4.B: Opperman's fauna were combined with the fauna from this study. Outcome of chi-square test for water-dependent vs water-independent through time. Expected values and adjusted residuals are included when necessary. Expected values smaller than five in orange, significant values in green.

WD vs WI			
	MH	TP	LP
WD	36	18	13
WI	126	13	0
Expected Values			
	MH	TP	LP
WD	52,7	10,1	4,2
WI	109,3	20,9	8,8
χ^2 = 44,02; df = 2; p < 0,001			
Adjusted Residuals			
	MH	TP	LP
WD	-6,06	3,29	5,37
WI	6,06	-3,29	-5,37

MH vs TP			**TP vs LP**		
	MH	TP		TP	LP
WD	36	18	WD	18	13
WI	126	13	WI	13	0
Expected Values			Expected Values		
	MH	TP		TP	LP
WD	45,3	8,7	WD	21,8	9,2
WI	116,7	22,3	WI	9,2	3,8
χ^2 = 16,59; df = 1; p < 0,001			χ^2 = 7,74; df = 1; p = 0,01		
Adjusted Residuals			Adjusted Residuals		
	MH	TP		TP	LP
WD	-4,07	4,07	WD	-2,78	2,78
WI	4,07	-4,07	WI	2,78	-2,78

APPENDIX 5

ZooMS for GRS faunal assemblage

Appendix 5.A: ZooMS results for GRS fauna. Collagen peptide markers included. Collagen markers from Bradfield et al. (2021) used to identify fauna.

No.	ID	A	B	C	X2	D	X3	F	G	X4
001	No collagen									
002	Unknown - Antilopinae 1	1166,5840	1427,6809	1550,7117		2103,1000	2567,1892	2883,3541	3033,4224	
003	Reduncini	1166,5846	1427,6804	1550,7117		2131,0531	2568,1155	2883,3527	3033,4188	
004	Reduncini	1166,5864	1427,6966	1550,7134		2131,0906	2567,1868	2883,3993	3033,4789	
005	Antelopini - Springbok	1196,5980	1427,7088	1550,7471		2131,0913	2554,1502	2883,4191	3033,4215	
006	Reduncini	1166,5891	1427,6814	1550,7058		2131,0411	2567,1210	2883,3398	3034,3967	
007	Reduncini	1166,6111	1427,7122	1550,7390		2131,1048	2567,2105	2883,4268	3033,4881	
008	Antelopini - Springbok	1196,6125	1427,6921	1550,7198		2131,0803	2554,1445	2883,3713	3033,4300	
009	Alcelaphini	1196,6057	1427,6951	1550,7193		2131,0712		2883,3807	3033,4384	3201,4361
010	Reduncini	1166,6198	1427,7329	1550,7638		2131,1355	2568,2320	2883,4900	3033,5173	
011	Reduncini	1166,6385	1427,7487	1550,7820		2131,1489	2567,2464	2883,4712	3033,4964	
012	Reduncini	1166,5970	1427,6970	1550,7205		2131,0719	2568,1129	2883,3774	3033,4453	
013	Reduncini	1166,6041	1427,7056	1550,7336		2131,0991	2568,1807	2883,4028	3033,4611	
014	Reduncini	1166,6113	1427,7066	1550,7276		2131,0847	2567,8408	2883,3847	3033,4410	
015	Warthog	1196,6181	1453,7246	1548,7549	1832,8277 1848,1361	2131,0818	2579,1244	2883,3893	3033,4524	
016	Reduncini	1166,6000	1427,7037	1550,7475		2131,0663	2568,1534	2883,3486	3033,4222	
017	Reduncini	1166,4633	1427,7156	1550,7414		2133,9474		2884,3832	3033,4478	
018	Tragelaphini - Common eland	1208,6558	1427,7095	1580,7268		2131,0796	2624,1864	2883,3665		
019	Unknown - Antilopinae 1	1166,6141	1427,6958	1550,7343		2103,1000			3033,4173	
020	Equid	1182	1427,7052	1550,7348		2145,0968		2883,3902	2999,4	
021	Antilopinae - low resolution	1196,6138	1427,6968	1550,7337		2131,0741		2883,3844	3034,4171	

No.	ID	A	B	C	X2	D	X3	F	G	X4
022	Antilopinae - low resolution	1196,6113	1427,6973	1550,7236		2131,0628		2883,3521	3034,3987	
023	Alcelaphini	1196,6286	1427,7153	1550,7416		2131,0855		2883,3675	3033,4474	3202,4806
024	Alcelaphini	1196,6293	1427,7181	1550,7431		2131,0999	2581,2148	2883,4043	3033,4721	3201,4842
025	Neotragini - Suni	1196,5973	1427,6891	1580,7255		2131,0719	2581,1901	2883,3749	3033,4355	3227,5186
026	Alcelaphini	1196,6034	1427,6839	1550,7101		2131,0574	2582,1326	2883,3385	3033,4220	3202,4327
027	Reduncini	1166,5700	1427,6957	1550,7603		2131,0730	2567,0000	2883,3776	3034,4311	
028	Unknown - Antilopinae 1	1166,5747	1427,7019	1550,7325		2103,1000	2568,1929	2883,3985	3033,4667	
029	Reduncini	1166,5907	1427,6929	1550,7212		2131,0604	2568,1424	2883,3643	3033,4285	
030	Reduncini	1166,6128	1427,7089	1550,7344		2131,0911	2567,1986	2883,4040	3033,4700	
031	Antelopini - Springbok	1196,6330	1427,7185	1550,7464		2131,1065	2553,2024	2883,4249	3033,4789	
032	Aepycerotini/Antilopini/Neotragini	1196,6070	1427,7103	1550,7241		2131,0958	2582,5790	2883,3962	3033,4463	3228,4404
033	Reduncini	1166,6124	1427,7105	1550,7341		2131,1011	2568,1848	2883,3846	3033,4524	
034	Reduncini	1166,6015	1427,7029	1550,7343		2131,0647	2567,1608	2883,3659	3033,4387	
035	Cephalophini - Blue duiker	1208,6479	1427,7078	1580,7344		2131,0928		2883,4180	3059,4606	
036	Aepycerotini/Antilopini/Neotragini	1196,6358	1427,7247	1550,7465		2131,1108	2581,2206	2883,4199	3033,4973	3227,5387
037	Reduncini	1166,6013	1427,7100	1550,7364		2131,0934	2568,1961	2883,3976	3033,4608	
038	Reduncini	1166,6162	1427,7163	1550,7440		2131,1065	2567,1828	2883,4054	3033,4596	
039	Unknown - Antilopinae 1	1166,6217	1427,7269	1550,7495		2103,1000	2567,2157	2883,4247	3033,4953	
040	Tragelaphini - Common eland	1208,6624	1427,7168	1580,7534		2131,0930	2623,2164	2883,3937		
041	Reduncini	1166,6205	1427,7264	1550,7519		2131,1109	2567,2093	2883,4229	3033,4888	
042	Reduncini	1166,6129	1427,7070	1550,7476		2131,0936	2567,1834	2883,3857	3033,4465	
043	Reduncini	1166,6444	1427,7583	1550,7879		2131,1619	2567,2399	2883,4909	3033,4660	
044	Unknown - Antilopinae 1	1166,6142	1427,7142	1550,7492		2103,1000		2883,3636	3033,4476	
045	Reduncini	1166,6159	1427,7262	1550,7529		2131,1213	2568,1662	2883,4003	3033,4439	
046	Antilopinae - low resolution	1196,9687	1427,7012	1550,7293		2131,0768		2883,3524		
047	Reduncini	1166,6243	1427,7245	1550,7496		2131,1047	2567,1949	2883,4057	3033,4693	
048	Alcelaphini	1196,6466	1427,7431	1550,7681		2131,1446	2582,2183	2883,4472	3033,4996	3201,7572
049	Aepycerotini/Antilopini/Neotragini	1196,5867	1427,6858	1550,7180		2131,0523		2883,3594	3033,4165	3228,4377

No.	ID	A	B	C	X2	D	X3	F	G	X4
050	Unknown - Antilopinae 2	1208,6505	1427,7150	1550,7429		2131,1069	2581,2010	2883,4210	3033,5272	3227,5272
051	Antelopini - Springbok	1196,6451	1427,7285	1550,7677		2131,1230	2553,2229	2883,4406	3033,5090	3228,5484
052	Alcelaphini	1196,6230	1427,7222	1550,7520		2131,1131	2581,2527	2883,4233	3033,4913	3201,4878
053	Tragelaphini - Common eland	1208,6581	1427,7103	1580,7402		2131,0847	2625,1848	2883,3691		
054	Alcelaphini	1196,6301	1427,7079	1550,7346		2131,0841	2582,1981	2883,3827	3033,4524	3201,4263
055	Reduncini	1166,6228	1427,7262	1550,7599		2131,1095	2567,2084	2883,4103	3033,4864	
056	Alcelaphini	1196,6424	1427,7392	1550,7690		2131,1316	2581,2253	2883,4550	3033,5191	3201,5130
057	Reduncini	1166,6175	1427,7252	1550,7562		2131,1162	2567,2320	2883,4369	3033,5111	
058	Reduncini	1166,6151	1427,7137	1550,7408		2131,0956	2568,1687	2883,3836	3033,4575	
059	Reduncini	1166,6138	1427,7199	1550,7430		2131,1079	2568,1985	2883,4045	3033,4806	
060	Alcelaphini	1196,6333	1427,7272	1550,7571		2131,1144	2581,2314	2883,4219	3033,4865	3201,5021
061	Reduncini	1167,6278	1427,7270			2131,0965	2567,2352	2883,4120	3033,4650	
062	Reduncini	1166,6202	1427,7400	1550,7603		2131,1130	2567,2024	2883,4285	3033,5160	
063	Tragelaphini - Common eland	1208,7225	1427,7497	1580,7901		2131,1471	2624,2333	2883,3933		
064	Reduncini	1166,6194	1427,7265	1550,7548		2131,0995		2883,3810	3033,4868	
065	Reduncini	1166,6297	1427,7384	1550,7626		2131,1259	2567,2377	2883,4386	3033,4805	
066	Ostrich					2149,1000		2879,4000	2927,5000	
067	No collagen									
068	Hippotragini	1196,6416	1427,7402	1580,7801		2131,1311	2582,2357	2883,4461	3059,5154	
069	Antilopinae - low resolution		1427,7324	1550,7492				2883,3942		3227,5096
070	Tragelaphini - Common eland	1208,6844	1427,7409	1580,7759		2131,1260	2624,2527	2883,4363		
071	Tragelaphini - Common eland	1208,6689	1427,7290	1580,7525		2131,1013	2624,2404	2883,4067		
072	Antilopinae - low resolution		1427,7317	1550,7667		2131,1142	2581,2377	2883,4245	3033,4940	
073	Reduncini	1166,6017	1427,7193	1550,7417		2131,1020	2567,1874	2883,4202	3033,4854	
074	Reduncini	1166,6069	1427,7102	1550,7377		2131,1036	2568,1854	2883,1854	3033,4822	
075	Warthog	1196,6413	1453,7485	1548,7835	1832,8732 1848,8745	2131,1199	2580,2403	2883,4363	3033,4697	

No.	ID	A	B	C	X2	D	X3	F	G	X4
076	Unknown - Antilopinae 1	1166,6281	1427,3510	1550,7665		2103,1000	2567,2453	2883,4588	3033,5259	
077	Unknown - Antilopinae 1	1166,6315	1427,7310	1550,7646		2103,1000	2568,2162	2883,4338	3033,4992	
078	Unknown - Antilopinae 2	1208,6745	1427,7311	1550,7626		2131,1228	2581,2255	2883,4420	3033,5073	3227,5385
079	Reduncini	1167,6286	1427,7261	1550,7198		2131,1085	2568,1950	2883,4466	3033,4899	
080	Alcelaphini	1196,6481	1427,7322	1550,7646		2311,1253	2581,2341	2883,4411	3033,5020	3201,5246
081	Reduncini	1166,6349	1427,7511	1550,7828		2131,1494	2567,2522	2883,4766	3033,5241	
082	Reduncini	1167,6197	1427,7280	1550,7453		2131,1112	2568,1978	2883,4082	3033,4813	
083	Reduncini	1166,6225	1427,7351	1550,7532		2131,1389		2883,4551	3034,5290	
084	Unknown - Antilopinae 2	1208,6793	1427,7400	1550,7592		2131,1317	2581,2418	2883,4369	3033,5244	3227,5862
085	Little collagen		1427,7340	1550,8332						
086	Reduncini	1166,6182	1427,7204	1550,7422		2131,9740				
087	Alcelaphini		1427,7156	1550,8012		2131,0982		2883,3875	3033,4841	3201,4804
088	Reduncini	1166,6278	1427,7337	1550,7618		2131,1227	2567,2250	2883,4303	3033,4953	
089	Reduncini	1166,6192	1427,7390	1550,7600		2131,1315		2883,4552	3034,5454	
090	Antilopinae - low resolution	1196,8407	1427,7416							
091	Antilopinae - low resolution	1197,2149	1427,7336							
092	Alcelaphini	1196,6453	1427,7299	1550,7585		2131,1057	2582,2226	2883,3938	3033,4827	3202,5063
093	Alcelaphini	1197,6425	1427,7333	1550,7702		2131,1097	2582,2111	2883,4016	3033,4821	3202,4920
094	Equid	1182,6000	1427,7474	1550,7737		2145,1		2883,4000		
095	Alcelaphini	1196,556	1427,7454	1550,7357		2131,1		2883,3844	3033,4466	3201,4775
096	Unknown - Antilopinae 2	1208,6744	1427,7339	1551,3768		2131,1304		2884,4269		
097	Antilopinae - low resolution		1427,7008	1550,7460				2883,4160	3033,5698	3228,5533
098	Alcelaphini	1197,6272	1427,7187	1550,7527		2131,1079	2583,2637	2883,4143	3033,4884	3202,4537
099	Alcelaphini		1427,7255	1550,7533		2131,1138	2582,2365	2883,4103	3033,5171	3202,4820
100	Aepycerotini/Antilopini/Neotragini	1196,6462	1427,7400	1550,7641		2131,1369	2582,2504	2883,4654	3033,5386	3228,5411

APPENDIX 6

Opperman faunal results

Appendix 6.A: Outcome of chi-square test for browsers vs grazers through time. Expected values and adjusted residuals are included when necessary. Expected values smaller than five in orange, significant values in green.

Browser vs Grazer			
	MH	TP	LP
Browser	85	8	0
Grazer	31	9	7
Expected Values			
	MH	TP	LP
Browser	77,1	11,3	4,7
Grazer	38,9	5,7	2,4
χ^2 = 19,15; df = 2; p < 0,001			
Adjusted Residuals			
	MH	TP	LP
Browser	3,8	-1,8	-3,8
Grazer	-3,8	1,8	3,8

MH vs TP			**TP vs LP**		
	MH	TP		TP	LP
Browser	85	8	Browser	8	0
Grazer	31	9	Grazer	9	7
Expected Values			Expected Values		
	MH	TP		TP	LP
Browser	81,1	11,9	Browser	5,7	2,3
Grazer	34,9	5,1	Grazer	11,3	4,7
χ^2 = 4,85; df = 1; p = 0,03			χ^2 = 4,94; df = 1; p = 0,03		
Adjusted Residuals			Adjusted Residuals		
	TP	LP		TP	LP
Browser	2,2	-2,2	Browser	2,2	-2,2
Grazer	-2,2	2,2	Grazer	-2,2	2,2

Appendix 6.B: Outcome of chi-square test for water-dependent vs water-independent through time. Expected values and adjusted residuals are included when necessary. Expected values smaller than five in orange, significant values in green.

WD vs WI			
	MH	TP	LP
WD	28	9	7
WI	85	8	0
Expected Values			
	MH	TP	LP
Browser	36,3	5,5	2,2
Grazer	76,7	11,5	4,8
χ^2 = 20,97; df = 2; p < 0,001			
Adjusted Residuals			
	MH	TP	LP
Browser	-3,99	1,96	3,95
Grazer	3,99	-1,96	-3,95

MH vs TP			**TP vs LP**		
	MH	TP		TP	LP
WD	28	9	WD	9	7
WI	85	8	WI	8	0
Expected Values			Expected Values		
	MH	TP		TP	LP
WD	32,2	4,8	WD	11,3	4,7
WI	80,8	12,2	WI	5,7	2,3
χ^2 = 5,76; df = 1; p = 0,02			χ^2 = 4,94; df = 1; p = 0,03		
Adjusted Residuals			Adjusted Residuals		
	MH	TP		TP	LP
WD	-2,40	2,40	WD	-2,22	2,22
WI	2,40	-2,40	WI	2,22	-2,22

APPENDIX 7

Beard Results

Appendix 7.A: Outcome of chi-square test for browsers vs grazers through time. Expected values and adjusted residuals are included when necessary. Expected values smaller than five in orange, significant values in green.

MH vs TP		
	MH	TP
Browser	122	7
Grazer	114	4
Expected Values		
	MH	TP
Browser	123,3	5,7
Grazer	112,7	5,3
χ^2 = 0,60; df = 1; p = 0,44		

Appendix 7.B: Outcome of chi-square tests for bovid size classes through time. This was done for both Beard's and Opperman's faunal assemblages. Expected values and adjusted residuals are included when necessary. Expected values smaller than five in orange, significant values in green.

Beard			**Opperman**		
	MH	TP		MH	TP
Bovid Size 1	46	2	Bovid Size 1	34	3
Bovid Size 2	226	5	Bovid Size 2	72	8
Bovid 3/4	17	10	Bovid 3/4	7	4
Expected Values			Expected Values		
	MH	TP		MH	TP
Bovid Size 1	45,3	2,7	Bovid Size 1	32,7	4,3
Bovid Size 2	218,2	12,8	Bovid Size 2	70,6	9,4
Bovid 3/4	25,5	1,5	Bovid 3/4	9,7	1,3
Adjusted Residuals			Adjusted Residuals		
	MH	TP		MH	TP
Bovid Size 1	0,46	-0,46	Bovid Size 1	0,81	-0,81
Bovid Size 2	4,54	-4,54	Bovid Size 2	0,78	-0,78
Bovid 3/4	-7,5	7,5	Bovid 3/4	-2,66	2,66
χ^2 = 56,24; df = 2; p < 0,001			χ^2 = 7,15; df = 2; p = 0,03		